2004-05-01

Synthesis, Characterisation and Biological Activity of Transition Metal Complexes of Thiabendazole

Rachel Kelly
Technological University Dublin

Synthesis, Characterisation and Biological Activity of Transition Metal complexes of Thiabendazole

Rachel Kelly

A thesis presented to Dublin Institute of Technology for the degree of Master of Philosophy

May 2004

School of Food Science and Environmental Health,
Dublin Institute of Technology, Marlborough St., Dublin 1.

Research supervisor: Dr. Michael Devereux
Head of School (Acting): Dr. Seamus Cassidy

ABSTRACT

A series of transition metal complexes of 2-(4'-thiazolyl)benzimidazole {thiabendazole}(TBZH) have been prepared and their ability to prevent the growth of the fungal pathogen *Candida albicans* has been assessed.

The compounds were synthesised using the Chloride, Nitrate, Sulfate and Acetate salts of Mn(II), Fe(II), Fe(III),Co(II), Ni(II), Zn(II) and Ag(I) resulting in the formation of 29 metal complexes. The complexes were formulated on the basis of their physico-chemical data. Reaction of $Fe(NO_3)_3.9H_2O$ with TBZH yielded the unusual nitrate salt $[TBZH_2NO_3]$, a compound which could not be generated using simple acid-base chemistry. The X-ray crystal structure of $[TBZH_2NO_3]$ was determined.

TBZH, $[TBZH_2NO_3]$, the 29 complexes and the simple salt starting materials were all tested, over a range of concentrations, for their anti-*Candida* activity. At a concentration of $100\mu g/cm^{-3}$ all of the non-silver complexes exhibit good to moderate activity but as the concentration drops their efficacy diminishes significantly. The silver compounds examined during this study have excellent biological activity.

DECLARATION

I certify that this thesis which I now submit for examination for the award of Masters of Philosophy, is entirely my own work and has not been taken from the work of others save and to the extent that such work has been cited and acknowledged within the text of my work.

This thesis was prepared according to the regulations for postgraduate study by research of the Dublin Institute of Technology and has not been submitted in whole or in part for an award in any other Institute or University.

The work reported on in this thesis conforms to the principles and requirements of the Institute's guidelines for ethics in research.

The Institute has permission to keep, to lend or to copy this thesis in whole or in part, on condition that any such use of the material of the thesis be duly acknowledged.

Signature _____ Date 27/9/04

ACKNOWLEDGEMENTS

I would like to thank my supervisor Dr. Michael Devereux for his guidance and support which he has given during the course of the work. I wish to thank Dr. Seamus Cassidy (Acting head of School) and FOCAS (Dublin Institute of Technology, Kevin Street) for financial support and allowing me access to the facilities of their respective departments.

Thank you so much to all the Staff and Postgrads in the 04 school for the help and advice and for making Marlborough St an enjoyable place to work.

Finally a heartfelt thanks to my parents, sister and all my friends for their very much appreciated support and encouragement throughout.

SYMBOLS AND ABBREVIATIONS

BZDH	Benzimidazole
EtOH	Ethanol
TBZH	Thiabendazole
RNA	Ribo Nucleic Acid
DNA	Deoxyribonucleic acid
HIV	Human Immunodeficiency Virus
14DM	14α demethylase
ATP	Adenine triphosphate
ABC transporters	ATP-binding cassettes
IR	Infrared
NMR	Nuclear magnetic resonance
HCl	Hydrochloric acid
IDA	Iminodiacetato
Sac^-	Saccharinate
MeOH	Methanol
Me_2BBZ	Dimethyl bisbenzimidazole
UV	Ultraviolet
DMSO	Dimethyl sulphoxide
DMF	Dimethylformamide
μ_{eff}	Effective magnetic moment
B.M.	Bohr magnetons
Λ_M	Molar conductivity (Scm^2mol^{-1})
ca.	Circa
Bipy	2,2 bipyridine
Phen	Phenanthroline
Sym, asym	Symmetric, asymmetric
Å	Armstrong
°	Degrees
°C	Degrees Celsius

TABLE OF CONTENTS

INTRODUCTION

EXPERIMENTAL

CONCLUSION

REFERENCES

APPENDIX

FIGURES, TABLES AND SCHEMES CONTAINED WITHIN THE THESIS

FIGURES

TABLES

SCHEMES

INTRODUCTION

I.1 INTRODUCTION TO ANTIFUNGAL TREATMENT

I.1.1 *Candida and Candidosis*[1]

During the last two decades the frequency and types of life-threatening fungal infections has increased dramatically. This has been as a result of changes in both medical practice and in the diseases to which humans are exposed.

The yeast *Candida albicans,* is considered to be the most opportunistic pathogen as it presents itself in immunocompromised patients, and over 75% of women suffer from vaginal candidosis at some stage in their lifetime. *Candida* infections are diverse in their manifestations, varying from superficial skin problems, chronic infection of the nails, mouth, throat or vagina to frequently fatal systemic diseases that involve the lungs, heart, gastrointestinal tract, central nervous system and other organs. These infections are considered to be opportunistic in nature since some aspect of the host's defence system is impaired in some way.

Many of the current antifungal agents that are used in therapy are generating resistance or have adverse side effects. For example, the anti-*Candida* agent, fluconazole can cause nausea, headache or provoke liver damage[2]. As a result of this increase in resistance, infections caused by other *Candida* species such as *Candida glabrata, Candida kreusi* and *Candida dublineinsis* are becoming more common.

Due to these problems with the current antifungal drugs it is necessary to develop drugs which work by a different mode of action and therefore do not encounter the problem of resistance.

I.1.2 Nomenclature

C. albicans is a dimorphic yeast, existing in a yeast phase (blastospore) and having the ability to form germ tubes that elongate into hyphae (hyphal phase). The definitions of the two phases are given below.

I.1.2.1 Blastospore.

A blastospore is defined as the unicellular form of the fungus, the yeast cell. It is distinguished by a specific process of mitotic cell division known as budding (*Figure 1)*. Budding involves the growth of new cellular material from selected sites on the blastospore surface. The new bud grows for a period of time until it is one third the size of the parent blastospore, and then stops. Nuclear division follows and a septum is laid down between the parent and the daughter cell. The two cell units separate and form two blastospores[3].

Figure 1: A yeast cell budding

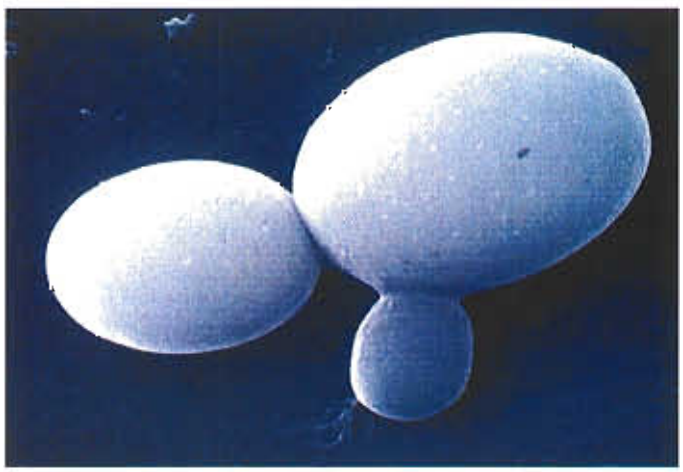

I.1.2.2 Germ tube/germination.

In mycology, germination refers to a process in which a hardy dominant spore undergoes a complex set of metabolic rearrangements and cell wall alterations to generate a new hyphal cell. This cell emerges through a pore in the wall of the spore as a germ tube of different molecular architecture from the spore. This nomenclature is being used in all studies of *C. albicans* to define a process where a novel hypha emerges by a simple evagination of the cell wall. Septae are laid down along the extending hyphae. The term "germ tube" is used to refer to newly evaginating hypha up to the time that the first septum is laid down.

Figure 2 : Yeast cells, pseudohyphal cells and true hyphal cells[3]

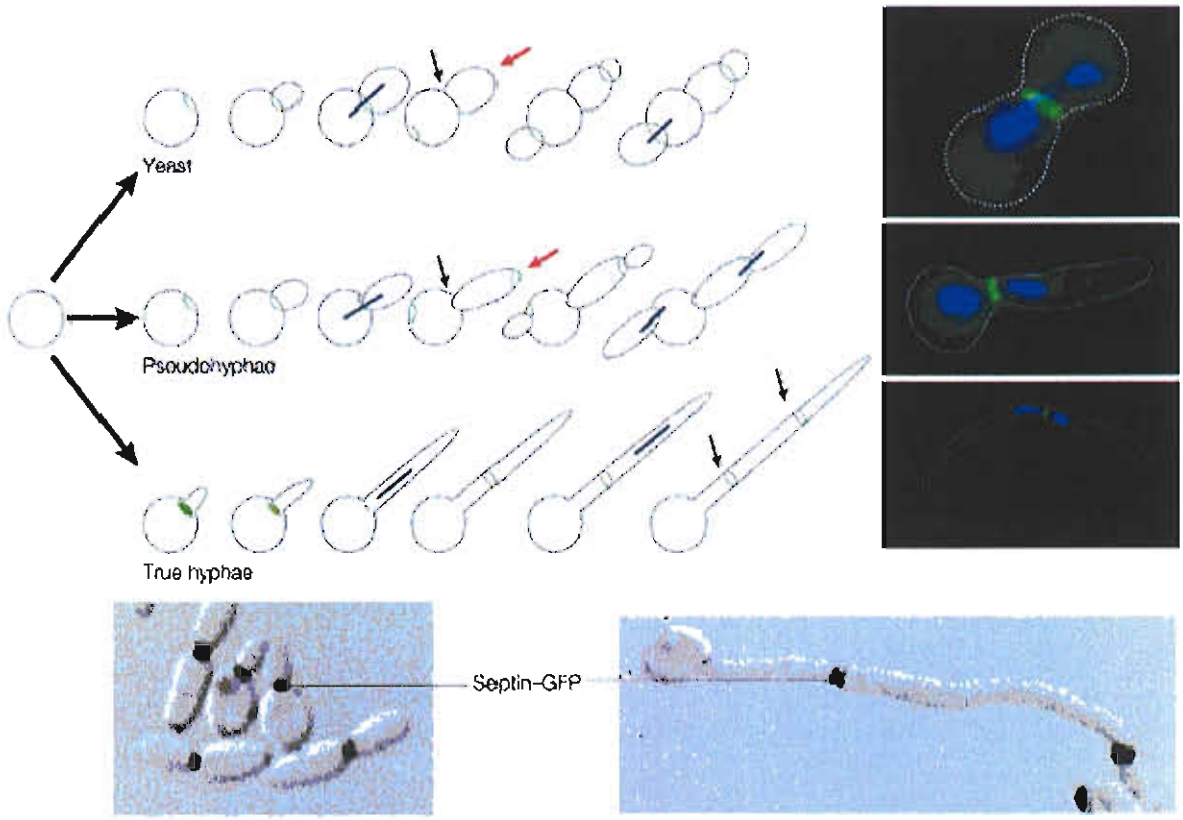

Candida albicans can exist in three forms that have distinct shapes: yeast cells (also known as blastospores), pseudohyphal cells and true hyphal cells (*Figure 2*). Yeast cells are round to ovoid in shape and separate readily from each other. Pseudohyphae resemble elongated, ellipsoid yeast cells that remain attached to one another at the constricted septation site and usually grow in a branching pattern that is thought to facilitate foraging for nutrients away from the parental cell and colony. True hyphal cells are long and highly polarized, with parallel sides and no obvious constrictions between cells. All three cell types have a single nucleus per cell before mitosis. Important differences between yeast, pseudohyphal and true hyphal cells include the degree of polarized growth, the positioning of the septin ring (green in *Figure 2* and micrographs, and black in light microscope images) and of the true septum relative to the mother cell, the movement of the nucleus (blue line in *Figure 2* and in micrographs) relative to the mother cell and the degree to which daughter cells are able to separate into individuals

I.1.3 State of the art antifungal drugs[4]

Treatment of deeply invasive fungal infections has consistently lagged behind bacterial chemotherapy. One reason for the slow progress is that, like mammalian cells, fungi are eukaryotes, and thus, drugs that inhibit protein, RNA or DNA biosynthesis in the yeast have greater potential for toxicity to the host. A second reason is that, until recently, the incidence of life-threatening fungal infections was perceived as being too low to warrant aggressive research by the pharmaceutical industry. In the past two decades, however, there has been a major expansion in the number of antifungal drugs available.

I.1.3.1 Antifungal agents in clinical use.

There are four major classes of systemic antifungal compounds currently in clinical use: the polyene antibiotics, the azole derivatives, the allyamines and thiocarbamates, and the morpholines (*Figures 3,4,5,7,8 and 9* and *Table 2*). The first three are targeted against ergosterol, the major fungal sterol in the plasma membrane. Echinocandins (a recent discovery) are successors to cilofungin, which was abandoned in the 1980s. The echinocandins inhibit synthesis of fungal β-1,3 glucan, and this represents the first novel target in 20 years of antifungal drug discovery in terms of clinically useful drugs[5].

Of these the polyene antibiotics and the azole derivatives are the most effective. *Table 1* shows a treatment schedule for the treatment of candidasis in HIV-positive patients with these drugs[6].

I.1.3.2 The Polyenes[4]

The polyene antibiotics, produced by *Streptomyces species*, are fungicidal (kills cells) and have the broadest spectrum of activity of any clinically useful compound. The polyenes complex with ergosterol in the plasma membrane, causing membrane disruption, increased permeability, leakage of cytoplasmic contents and cell death (*Figure 6*).

The first polyene was discovered by Rachel Brown and Elizabeth Hazen at the New York city branch of the New York State Division of Laboratories and Research. They called the drug Nystatin (*Figure 3*) after the state which employed them. Nystatin was isolated from a soil actinomycete and was found to have profound anti-*Candida* activity. It is highly toxic when administered parenterally and is, therefore, not suitable for systemic *Candida* infections.

Table 1. A treatment schedule for the treatment of Candidasis in HIV-positive patients.

Compound	**Administration**	**Dosage** (per day)	**Duration**
Non-absorbable			
Nystatin	Topical	205 mg x 5	2-3 weeks
Amphotericin B	Topical	200-400 mg x 5	2-3 weeks
Clotrimazole	Troches	10 mg x 3-5	2-3 weeks
Miconazole	Buccal gel	2.5 ml x 3-5	2-3 weeks
Systemic			
Ketoconazole	Orally	200-400 mg	10-15 days
Fluconazole	Orally	50-100 mg	10-15 days
Itraconazole	Orally	200 mg	10-15 days
Amphotericin	I.V	15-20 mg	10-15 days

In 1956 scientists at E.R. Squibb and Sons discovered Amphotericin B (*Figure 3*) in soil taken from Venezuela. This compound was found to be extremely active against candidosis and is still considered to be the "gold standard" for the treatment of most severe invasive fungal infections. Due to its lack of absorbance Amphotericin B is usually used topically for oral candidosis.

Amphotericin B

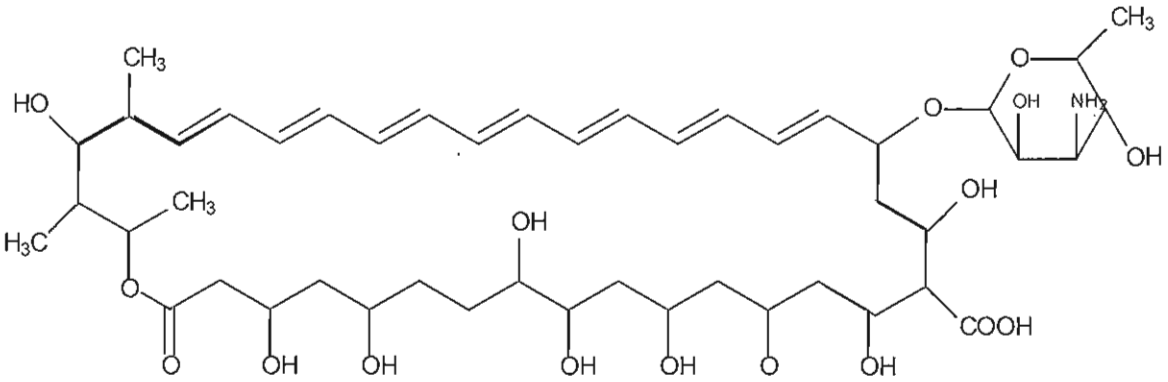

Nystatin

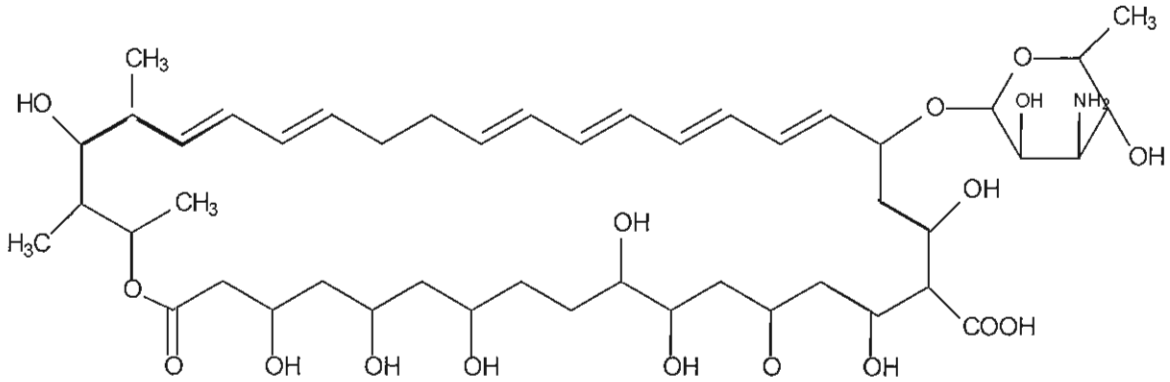

Figure 3 **:** The structure of Amphotericin B and Nystatin.

I.1.3.3 The Azoles[4]

The azole derivatives were discovered in the late 1960's and are totally synthetic. They are classified as imidazoles or triazoles (*Figure 4*) on the basis of having either two or three nitrogens in the five-membered azole ring. Azole antifungal agents have

fungistatic (inhibits cell growth) broad-spectrum activity that includes most yeasts and filamentous fungi.

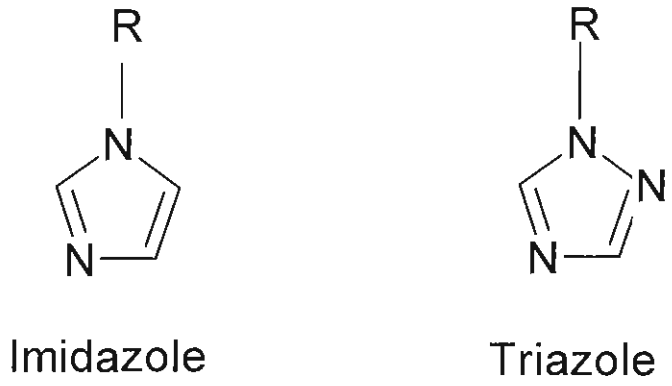

***Figure 4*:** Structure of Imidazole and Triazole

Clotrimazole (*Figure 5*) was the first imidazole to be marketed and it showed a broad spectrum of antifungal activity *in vitro*. Clotrimazole has been effectively used for the treatment of oral candidosis although side effects such as nausea, vomiting and skin irritation have been reported.

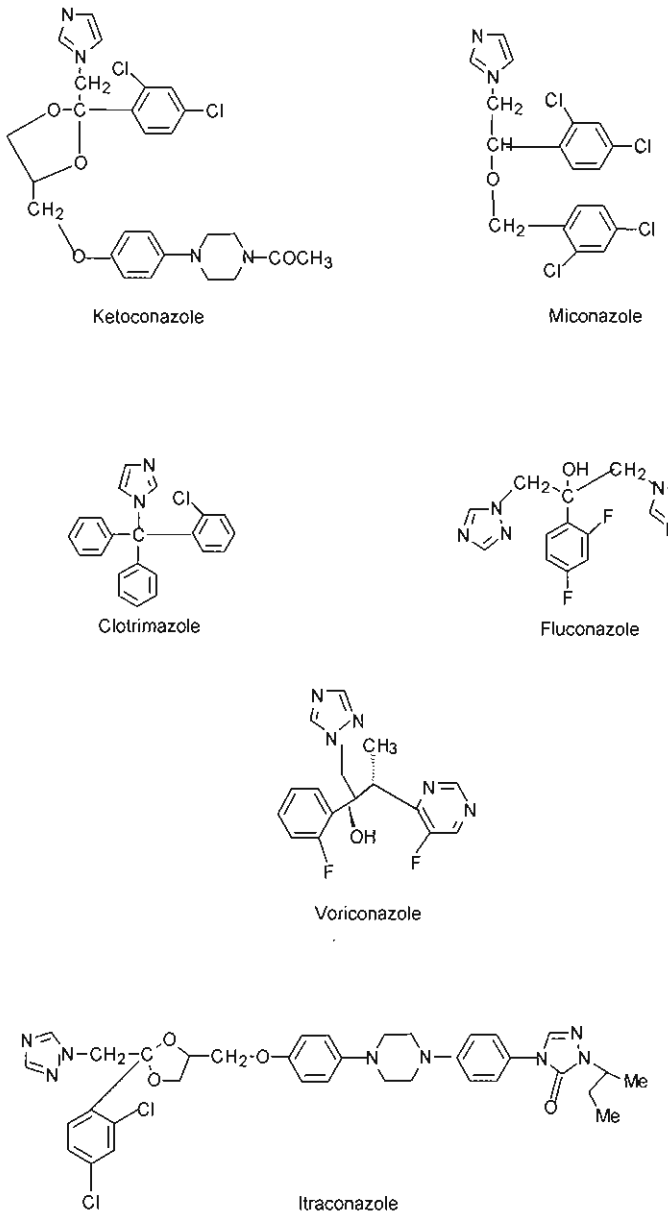

Figure 5: Some current azole antifungal drugs

Other azole derivatives such as miconazole (*Figure 5*) were discovered but it was not until the discovery of ketoconazole that a breakthrough in treatment of deep mycoses came.

The azoles had been used as topical drugs for the treatment of superficial mycoses, but good oral absorption, low toxicity and a broad spectrum of activity made ketoconazole the standard against which subsequent azoles would be measured.

In recent years other azoles have been synthesised such as fluconazole (*Figure 5*) and itraconazole (*Figure 5*). Fluconazole, in particular, has become a much used drug due to the fact it is efficiently absorbed from the gastrointestinal tract.

Posaconazole, ravuconazole and voriconazole are new triazole compounds, a subset of the azoles which are the most successful antifungal class in the clinic since the late 1960s, have just reached, or are approaching, the clinic.

Voriconazole (*Figure 5)*, which is the first to be approved and so far the most fully characterised of the three new triazole, enjoys a very broad spectrum of target fungal species and like itraconazole, is even fungicidal against some isolates of the filamentous species[5].

I.1.3.4 Mode of action of polyenes and azoles

Both major classes of the commonly used antifungal drugs, the azoles and polyenes, target ergosterol in the fungal plasma membrane (see *Figure 6 and Table 2*). Azole drugs inhibit a key enzyme in the biosynthetic pathway for ergosterol, the major sterol component of the fungal plasma membrane and a chemical relative of cholesterol, which is a component of mammalian plasma membranes. The target yeast enzyme, lanosterol 14α demethylase (14DM), is a cytochrome P-450 enzyme containing a heme

cofactor in the catalytic site, to which the azole drugs bind. When the azoles are present, this enzyme produces less of its normal ergosterol end product. Leading to sterol precursors being introduced to the plasma membrane, thereby disrupting several of its functions and reducing the effectiveness of several membrane associated enzymes. Azole drugs bind preferentially to the fungal rather than the comparable mammalian enzyme, meaning there is little if any disruption of host cell membrane. Amphotericin B and other polyene drugs are amphipathic molecules that bind preferentially to membrane containing ergosterol. In yeast cells, these drugs form channels in the plasma membrane, causing essential cytosolic components to leak from cells. Amphotericin B can also interact with mammalian membranes, which can lead to toxicity, especially in the kidneys.

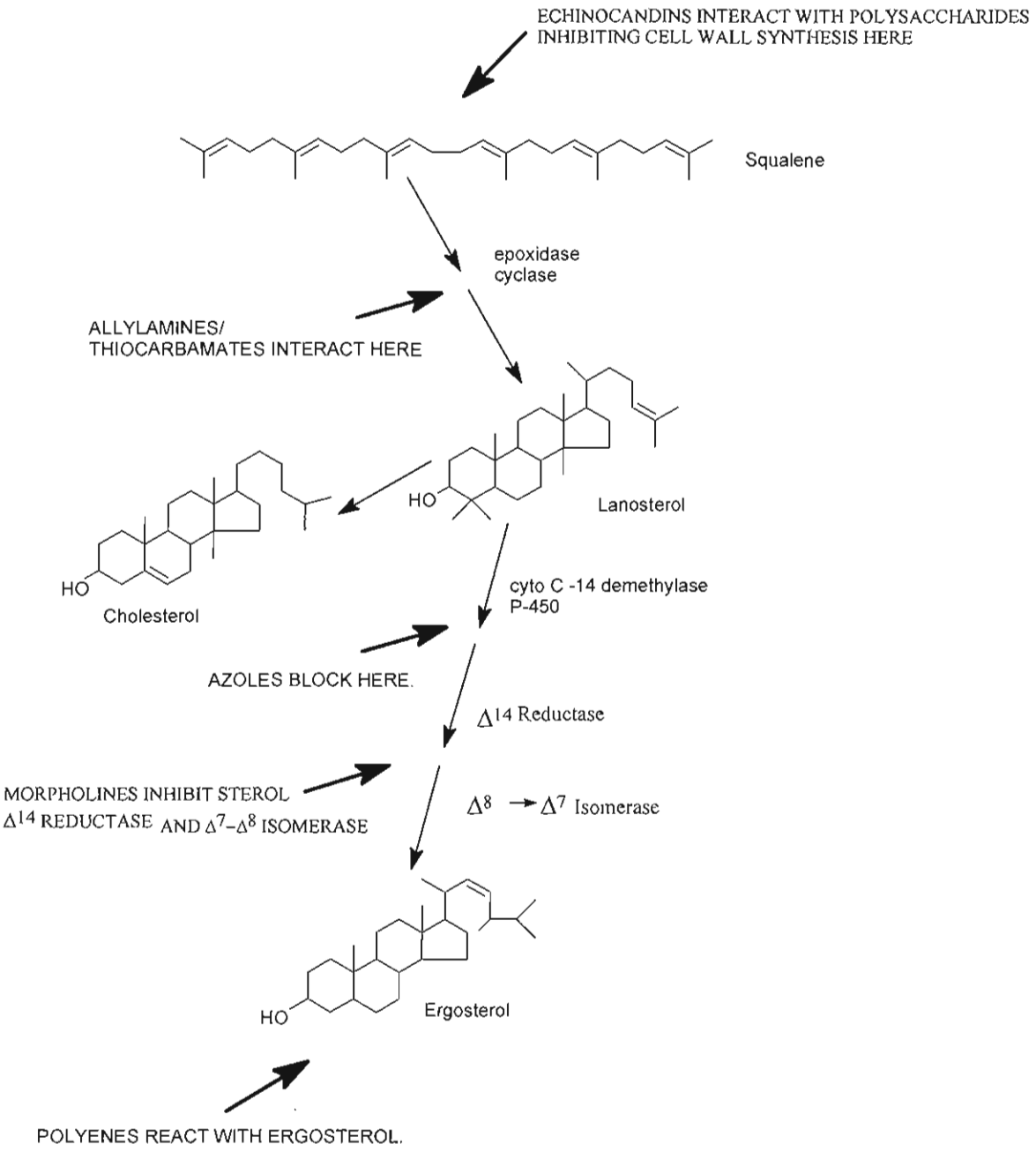

Figure 6 : Mode of action of Anti-fungal agents

I.1.3.5 Other sterol synthesis inhibitors: allylamines and morpholines[5]

The ergosterol biosynthetic pathway is the target for two other classes of antifungal agent. The allylamines, notably terbinafine (*Figure 7*), inhibit squalene epoxidase, an

early step in the pathway, with fungicidal consequences in susceptible species. These include many filamentous fungi but few pathogenic yeasts. Although terbinafine is not approved for treatment of visceral mycoses, there is interest in the possibility of combining terbinafine with other ergosterol synthesis inhibitors to achieve synergistic inhibitory effects. The phenylmorpholine class, of which amorolfine (*Figure 7*) is the sole representative in human medicine, affects two targets late in the ergosterol pathway: Erg24p, the Δ^{14} reductase enzyme, and Erg2p, the Δ^{8}-Δ^{7} isomerase enzyme. Amorolfine can be used only for topical treatment of superficial mycoses, and neither of its targets has attracted recent research interest.

Terbinafine

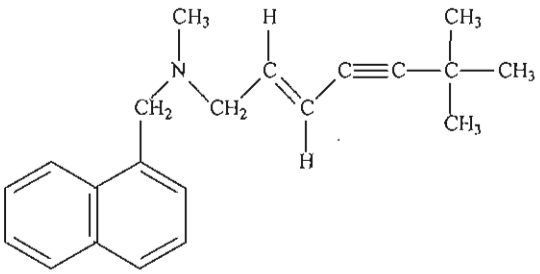

Amorolfine

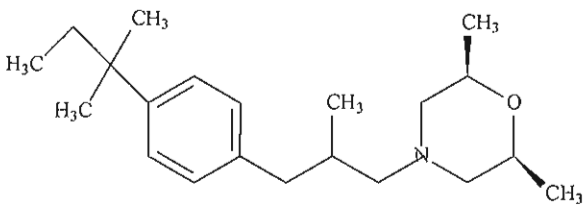

Figure 7: Structure of terbinafine and amorolfine

I.1.3.6 Echinocandins[5]

The echinocandins are fungal secondary metabolites comprising a cyclic hexapeptide core with a lipid sidechain responsible for antifungal activity (*Figure 8*). Antifungal activity in the prototypes, echinocandin B and aculeacin A, was discovered by random screening in the 1970s.

In the late 1990s, three echinocandin-class compounds, anidulafungin, caspofungin and micafungin all entered clinical development.

The target for the echinocandins is the complex of proteins responsible for synthesis of cell wall β-1,3 glucan polysaccharides.

Caspofungin was approved by the USA Federal Drug Agency in 2001 for therapy of aspergillosis unresponsive to other agents, and approval for treatment of disseminated *Candida* infections is imminent.

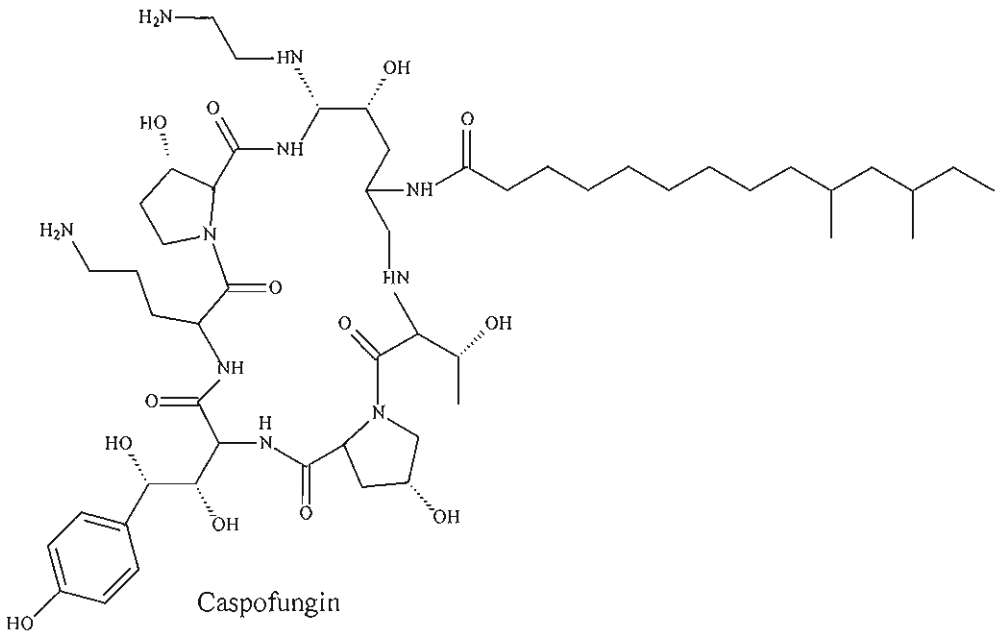

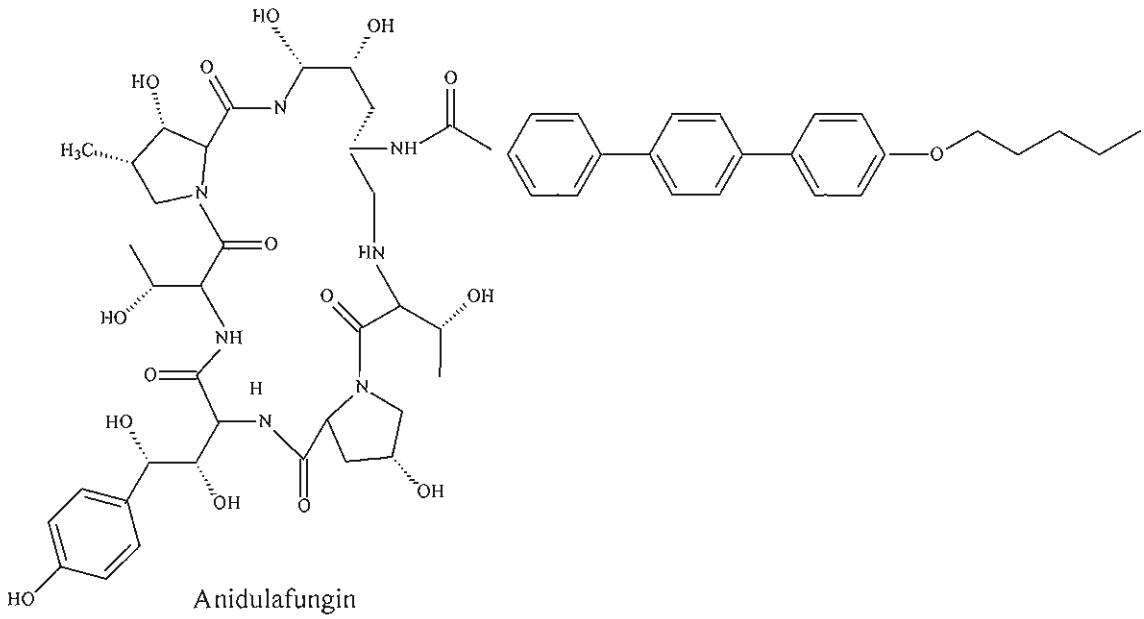

Figure 8: Structure of anidulafungin and caspofungin

I.1.3.7 Sordarins[5]

The sordarin antifungal class, although not developed for clinical use, merits mention among the new mechanisms of action. Sordarins (*Figure 9*) inhibit protein synthesis by blocking the function of fungal translation Elongation Factor 2 (EF2). The class was discovered by routine screening but was abandoned in the early 1970s. Interest in sordarins was re-awakened as a result of a prospective screen for inhibitors of *C. albicans* protein synthesis *in vitro*, which pinpointed the nature of the sordarin antifungal effect.

Figure 9: Structure of GM193663 and GM531920

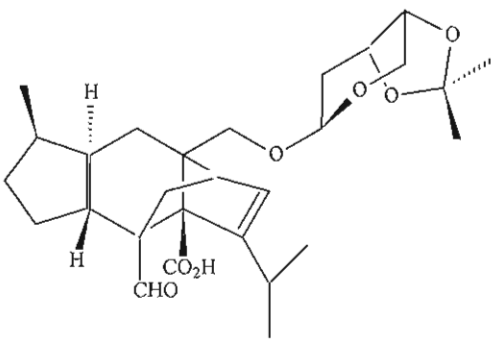

GM193663

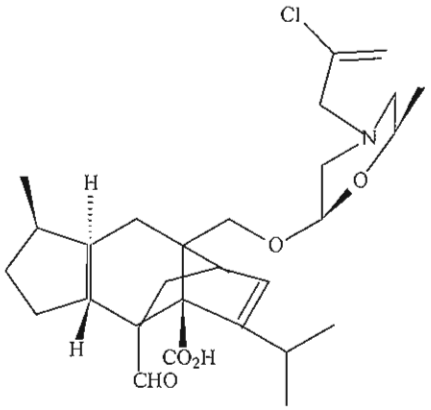

GM531920

Table 2. Mechanisms of action of some antifungal agents used clinically[6]

Class and compound	Route of administration	Mechanism of action
Polyenes		Interact with ergosterol, thereby disrupting the cytoplasmic membrane
Amphotericin B	Systemic	
Nystatin	Topical	
Azoles		Interact with cytochrome P-450; inhibit C-14 demethylation of lanosterol, thereby causing ergosterol depletion and accumulation of aberrant sterols in the membrane
Miconazole	Topical	
Ketoconazole	Systemic	
Itraconazole	Systemic	
Fluconazole	Systemic	
Voriconazole	Systemic	
Allyamines		Inhibit oxidosqualene cyclase, thereby causing ergosterol depletion and accumulation of squalene oxides in the membrane
Naftifine	Topical	
Terbinafine	Systemic	
Morpholines		Inhibit sterol Δ^{14} reductase and Δ^{7}- Δ^{8} isomerase
Amorolfine	Topical	
Echinocandins		Inhibit synthesis of fungal cell wall polysaccharides
Anidulafungin	Systemic	
Caspofungin	Systemic	

I.1.4 Why the need for new antifungals?

There are two main reasons for developing new antifungal drugs. The first is that most of the drugs in use at present have adverse side effects (*Table 3*) and secondly, in recent times resistance to azoles has emerged in *C. albicans*.

***Table 3*:** Typical side effects of prescription *anti Candida* drugs

DRUG	SIDE EFFECTS
Amphotericin B	Blindness
	Pulmonary toxicity
Nystatin	Nausea
	Vomiting
	Diarrhoea
Fluconazole	Nausea
	Headache
	Skin rash
	Abdominal pain
	Diarrhoea
Ketoconazole	Nausea
	Vomiting
	Diarrhoea
	Abdominal pain

I.1.4.1 Resistance to azoles[1,7].

Resistance to azoles, particularly fluconazole, is emerging in *C. albicans* after long-term suppressive therapy. This resistance is due to altered or overproduced target enzyme or by an active efflux process.

The target enzyme for the azoles in the *Candida* cell is usually the 14 DM enzyme. Once the antifungal molecules enter a cell, their interaction with the target enzyme can be modified in at least two ways. First, certain point mutations in the gene for 14 DM make the enzyme less sensitive to azole drugs. In addition to point mutations, enzyme overexpression, which leads to more of the azole target molecule per cell, necessitates higher doses of drug to achieve inhibitory effects comparable to those seen in susceptible cells.

Efflux mechanisms, which reduce the cytoplasmic concentration of drugs and other small molecules, are a major factor affecting a cell's susceptibility to azoles. There are two classes of efflux systems in *C. albicans*, the ABC transporters and major facilitators. ABC transporters are associated with drug resistance in a wide variety of organisms besides yeasts, including mammals. The genes of the ABC transporters encode several components, including a transmembrane pore composed of several segments and two ATP-binding cassettes (ABC), which are situated on the cytosolic side of the membrane and provide metabolic energy for the pump.

The major facilitators are also associated with drug resistance, but so far seem to be active in prokaryotic systems. The genes of this system encode a transmembrane pore

composed of several segments. Instead of an ABC system for metabolic energy, the major facilitators use membrane potential.

Whatever the mechanism of resistance is, strains of *Candida* are becoming more resistant to the azoles. This, together with the toxicity of the polyenes, makes the development of new antifungal drugs so important.

I.2 BENZIMIDAZOLES

I.2.1 General Background to Benzimidazole[8]

Imidazole is one of a class of organic heterocyclic compounds of five-membered diunsaturated ring structure, composed of three carbon atoms and two nitrogen atoms at nonadjacent positions. The simplest member of the imidazole family is imidazole itself, *Figure 10*.

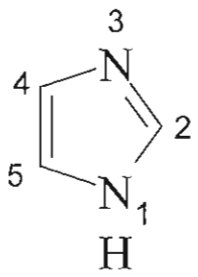

Figure 10: Structure and numbering system of Imidazole

The imidazole nucleus is found in a number of important natural products such as histidine and purines, while 5,6-dimethyl-1-(α-D-ribofuranosyl)benzimidazole is an integral part of the structure of vitamin B_{12}. Benzimidazoles contain a phenyl ring fused to an imidazole ring as indicated in *Figure 11*.

Figure 11: Structure of benzimidazole (BZDH) and the numbering system indicated

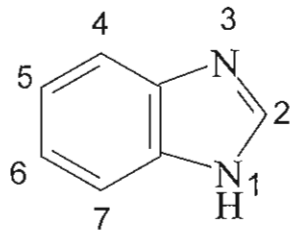

Benzimidazoles with the imide nitrogen (i.e., hydrogen in the 1-position) are usually more soluble in polar solvents and less soluble in organic solvents. With the introduction of other non-polar substituents in various positions of the benzimidazole ring, the solubility in non-polar solvents is increased. Conversely, the introduction of polar groupings into the molecule increases solubility in polar solvents. Benzimidazoles are weakly basic, being somewhat less basic than the imidazoles. Accordingly, they are, in general, soluble in dilute acids, the pK_a values have been determined for benzimidazole to be pK_{a1}= 5.30 and pK_{a2}= 12.3. Benzimidazoles are also sufficiently acidic and so generally soluble in aqueous alkali. The acidic properties of the benzimidazole like those of the imidazoles seem to be due to stabilization of the ion by resonance.

Benzimidazoles which contain a hydrogen atom attached to nitrogen in the 1-position readily tautomerize (*Figure 12*)[8].

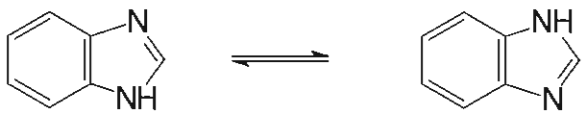

Figure 12: The tautomerization of benzimidazole.

This tautomerization is analogous to that found in the imidazole and amidines, the benzimidazoles may be considered as cyclic analogs of the amidines. Because of this tautomerism in benzimidazole certain derivatives which appear at first to be isomers are in reality tautomers, although two non-equivalent structures can be written, only one

compound is known. This may be illustrated with 5(or 6)-methylbenzimidazole (*Figure 13*).

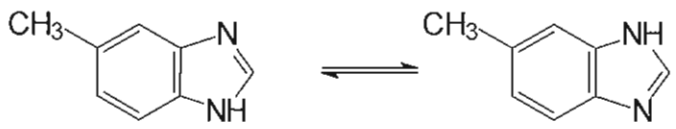

***Figure 13*:** Two non-equivalent structures can be drawn for 5(or 6)-methylbenzimidazole, only one compound is known.

When the group attached to the nitrogen in the 1-position is larger than hydrogen, such tautomerism is not indicated and isomeric forms exist.

The structure and names of some common benzimidazole derivatives are shown in *Figure 14*[9].

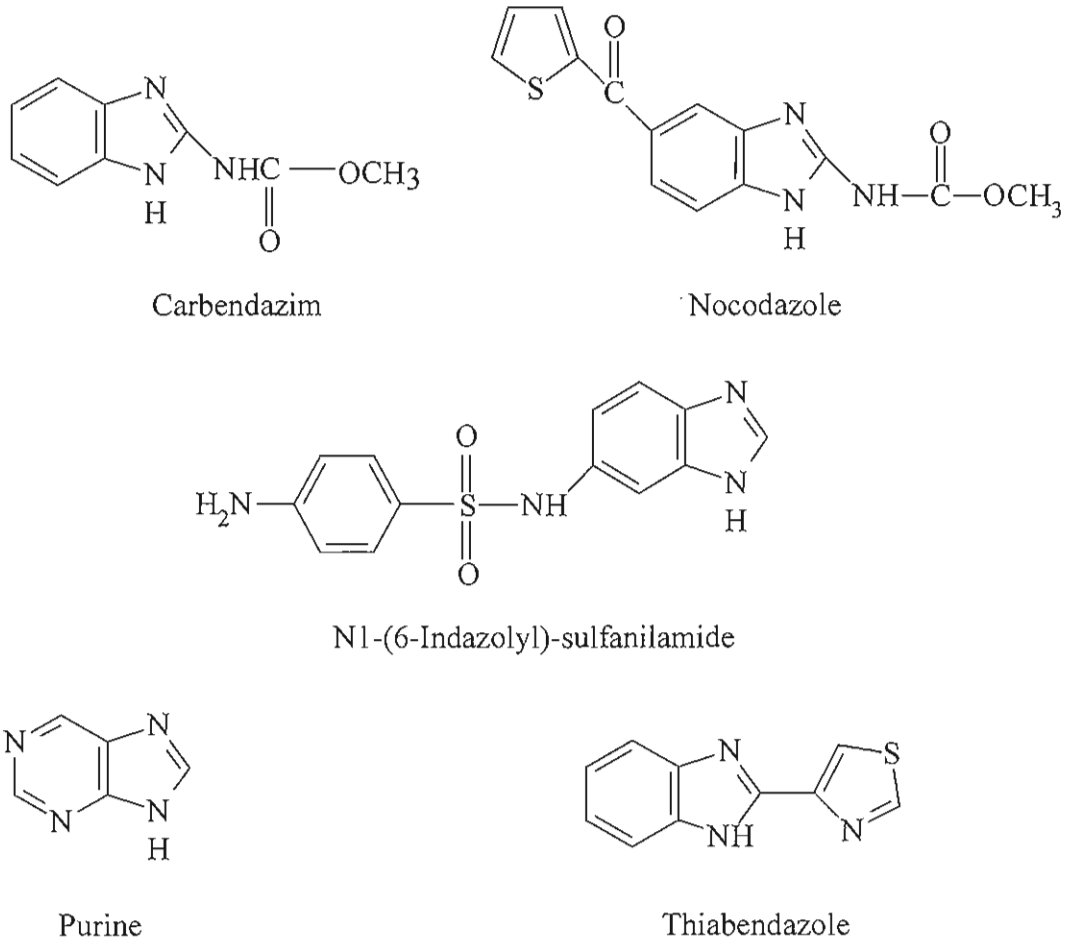

Figure 14: Structures of some common BZDH derivatives

I.2.2 Synthesis of Benzimidazole

One of the most common methods,(the Phillips method [10]), of preparing benzimidazoles involves the reaction of *ortho* – phenylenediamine with a carboxylic acid:

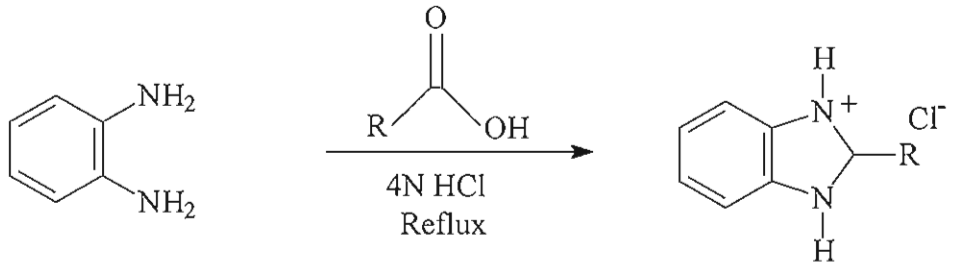

I.3 THIABENDAZOLE

I 3.1 Structure of Thiabendazole

The compound 2-(4'-thiazoly)benzimidazole, also called thiabendazole (TBZH), is a well known and widely used anthelmintic. Its discovery was reported by Brown et al[11], who stated that's its potency coupled with the absence of activity toward other microrganisms and negligible mammalian toxicity suggests a unique interference with a metabolic pathway essential to a variety of helminths.

Figure 15: The crystal structure of Thiabendazole[12]

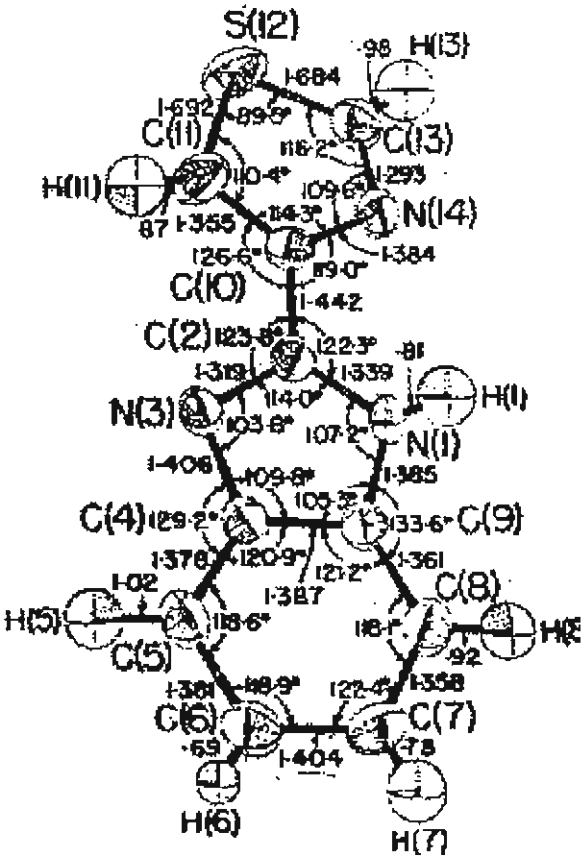

The crystal structure of thiabendazole was reported by Trust et al[12]. The thiazolyl and benzimidazole ring systems are each closely planar. They are twisted about the the C(2)-C(10) bond, by 10° relative to one another, the C(2)-C(10) bond length of 1.442 Å suggests appreciable delocalisation across the bond. The protonated nitrogen atom, N(1), is cis to N(14) of the thiazolyl ring. This conformation may be stabilised by a weak electrostatic interaction H(1)-N(14) and a trans conformation would result in steric interference between H(1) and H(11).

I.3.2 Synthesis of Thiabendazole[13]

Two different routes exist for the synthesis of thiabendazole.

The compound can be obtained by condensation of *o*-phenylenediamine with thiazole-4-carboxylic acid.

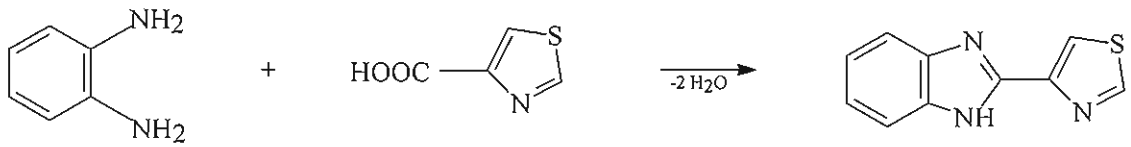

o-phenylenediamine thiazole-4-carboxylic acid thiabendazole

The second process involves reacting 4-cyanothiazole with aniline in HCl which results in the formation of the corresponding amidine. On treatment with hypochlorite it is cyclized via the intermediate *N*-chloro compound to thiabendazole,:

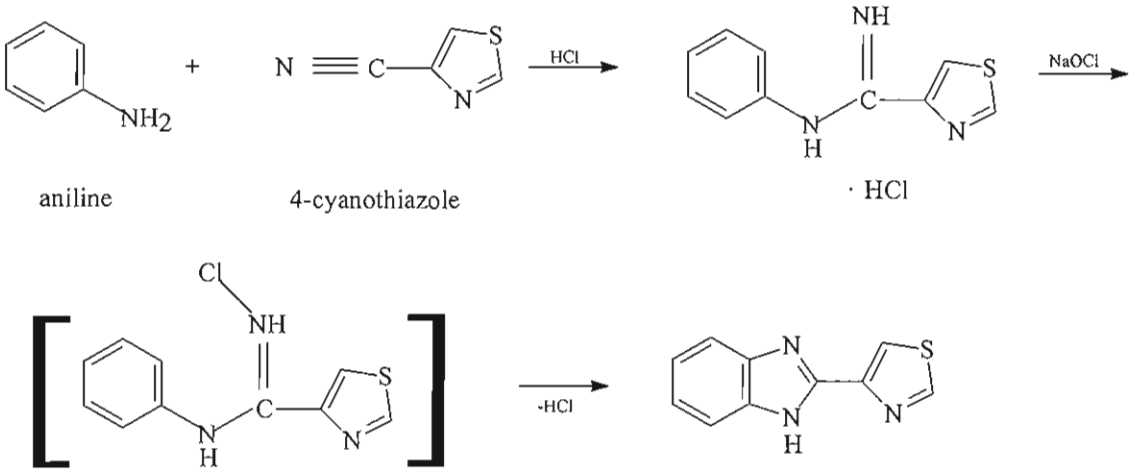

aniline 4-cyanothiazole

thiabendazole

I.4 ANTIFUNGAL ACTIVITY OF BENZIMIDAZOLE AND ITS DERIVATIVES.

Benzimidazole and many of its derivatives exhibit a variety of biological actions, including antibacterial, antiviral, anticancer and antifungal activity. There has been wide interest in the antifungal activity of benzimidazole since Woolley et al linked its activity to purine competition[14]. Woolley proposed that the mode of action of benzimidazole was due to its close structural similarity to the vitamin B complex biotin. However, while the growth of the microgranisms was shown to be inhibited by benzimidazole and some of its derivatives, this effect was not overcome by addition of biotin. The close structural similarity of benzimidazole to purine was then investigated and results showed that the effect on growth was overcome by the addition of adenine. Addition of other purines, such as aminopurines, adenine and guanine also showed reversal of inhibitory effects.

Certain structural features were necessary in benzimidazoles in order for them to have growth inhibiting powers for yeast. Studies have shown that when the hydrogen atom of position 2 was replaced by a side chain or by an hydroxyl group, activity was destroyed or greatly diminished[14]. Since the substitution of an amino group in position 4 would result in a compound more analogous to adenine and the substitution of an amino group in position 5 would yield one more analogous to guanine, it was hoped that such amino compounds would be more active than unsubstituted benzimidazole. However, 4-aminobenzimidazole and 4-nitrobenzimidazole had approximately the same potency as benzimidazole when judged on a molecular basis. 5-Aminobenzimidazole was somewhat less than half as active.

The reversal of benzimidazole action on microorganisms by purines suggested the hypothesis that benzimidazole owed its pharmacological properties to its competition in the animal with aminopurines.

Due to these findings numerous benzimidazole derivatives have been analysed for their antifungal activity with varying success. Goker et al reported the synthesis and antifungal evaluation of 5-ethoxycarbonyl-2-(substituted-benzyl or phenoxymethyl)benzimidazoles (*Figure 16*)[15]. Preliminary results showed that the compounds showed no antifungal activity at the concentration of 100 μg/ml against a number of fungal strains.

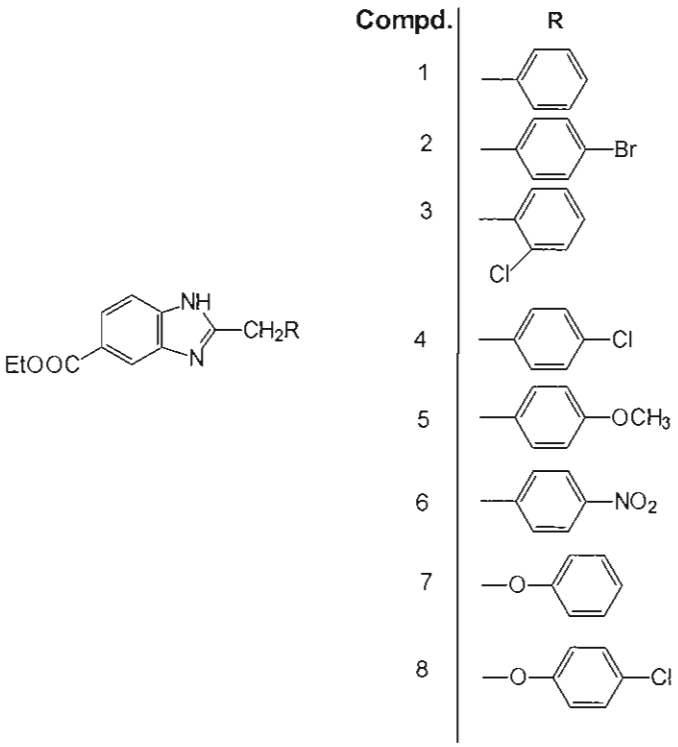

Figure 16: Structure of 5-ethoxycarbonyl-2-(substituted-benzyl or phenoxymethyl)benzimidazoles compounds reported by Goker et al[15].

In 1992 Gunes et al[16] reported a number of 1H-benzimidazole-2-propanoic acid derivatives which had been synthesised using the Phillips method. The chemical structures of the compounds were elucidated by spectroscopic and elemental analysis. Of the compounds tested only N-hydroxy-3-(1H-benzimidazol-2yl)-propionamide (*Figure 17*) showed considerable activity against *Candida albicans* and *Candida tropicalis* at extremely high concentrations of 800-1000 μg/ml.

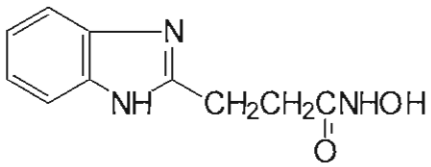

Figure 17: Structure of N-hydroxy-3-(1H-benzimidazol-2yl)-propionamide.

Rida et al reported the synthesis and antifungal behaviour of a number of thiazolylbenzimidazoles and benzimidazolylthiazolo[3,2-a]pyridines[17]. The thiazolylbenzimidazole 2-[(4-oxo-4,5-dihydrothiazol-2-yl)methyl]-1H-benzimidazole (*Figure 16*) was prepared through the reaction of 2-cyanomethyl-1H-benzimidazole with thioglycolic acid. The synthesis of its arylidene and diazo-coupled compounds and the cyclization of 2-[(4-oxo-4,5-dihydrothiazol-2-yl)methyl]-1H-benzimidazole to benzimidazolythiazolo[3,2-a]pyridines were also performed. The compounds showed good antifungal activity in the range of 25-50 μg/ml.

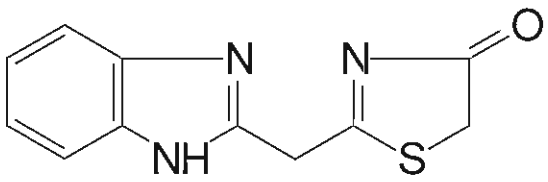

Figure 18: Structure of 2-[(4-oxo-4,5-dihydrothiazol-2-yl)methyl]-1H-benzimidazole.

In 1995 Demirayak et al reported the synthesis of some 2-aryl-4-hydroxypyridol[1,2-a]benzimidazole and 1-substituted 3-arylpyrazino-[1,2-a]benzimidazole derivatives which were synthesised using 1-(2-arylethan-2-on)-2-acylbenzimidazole as starting materials[18]. No considerable antifungal effect was found, however some of the compounds showed reasonable activity at 62.5 μg/ml.

Goker et al[19] reported the synthesis of a series of 1,2,5(6)-Trisubstituted Benzimidazoles and all of the compounds were evaluated *in vitro* for antimicrobial activity. The compounds were prepared by firstly synthesising 2-chloromethyl-5(6)-substituted-1H-benzimidazole, which was then substituted at C-2 with several piperazine or piperidine derivatives. Of the compounds only 2-(4-methylpiperidin-1-yl)methyl-5(6)-chloro-1H-benzimidazole (*Figure 19*) exhibited good activity and in order to clarify the effect of the substituents at C-1 on the activity, benzimidazole derivatives having ethyl, ally, benzyl and p-fluorobenzyl substituents at C-1 were prepared and slightly increased activity was seen.

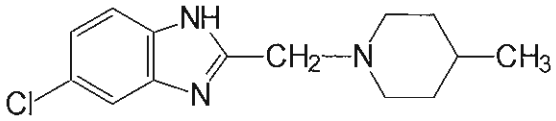

Figure 19: Structure of 2-(4-methylpiperidin-1-yl)methyl-5(6)-chloro-1H-benzimidazole

In 1996 Goker et al[20] reported the synthesis of a series of 14, N'-(N,N-dialkylaminoethyl)-benzimidazole-5(6) or 5-carboxyamides, having several substituents on the azole and benzene nuclei, and the evaluation of their antimicrobial activity.

The precursor benzimidazolecarboxcylic acids were prepared via oxidative condensation of diaminobenzoic acids and several aldehydes with Cu(II) and the carboxamides were prepared from the corresponding acids and N,N-dialkylenediamine (*Figure 20*).

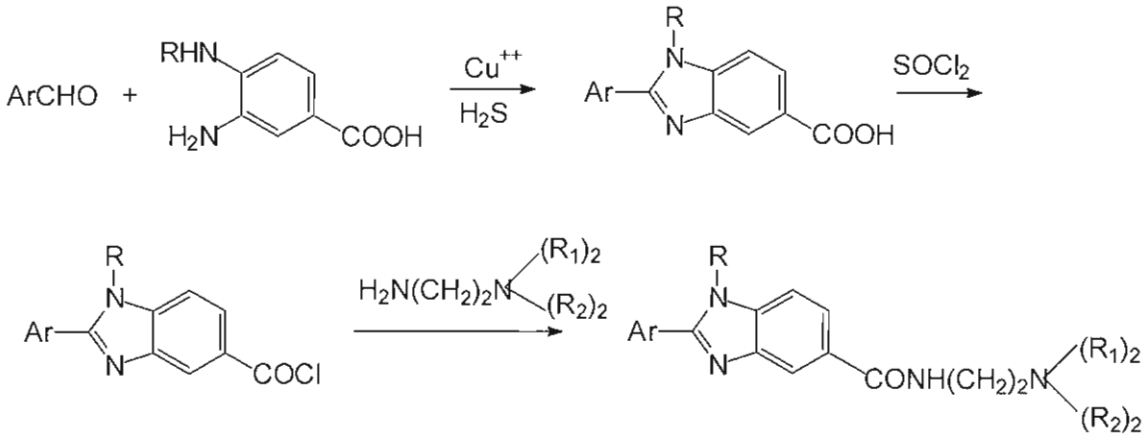

Figure 20: Synthetic route to carboxamides where R= H, benzyl or p-chlorobenzyl , $R_1 = R_2 =$ -CH_3 or –CH_2CH_3.

Goker et al reported the synthesis and antimicrobial activity of a series of 2-(4-methylpiperidin-1-yl)-1,5(6)-disubstituted-1H-benzimidazoles[21]. The compounds were prepared in a multistep procedure through the reaction of 2-chloro (or 2-chloromethyl)-1H-benzimidazole derivatives with 4-methylpiperidine. All the compounds were evaluated for their in vitro antimicrobial activity, they were found to be essentially ineffective against C. *albicans* with exception of those shown in *Figure 21* which showed moderate activity.

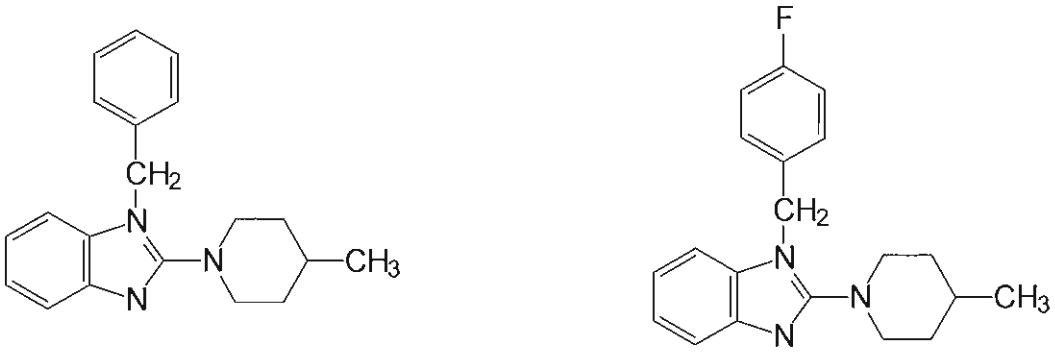

Figure 21.: Structure of carboxamides reported by Goker et al, which showed moderate anti-*candida* activity

Ersan et al reported the synthesis of β-[(2-benzimidazoly)thio]- β-benzoyl styrene derivatives by reacting 2-(phenacetylthio)benzimidazole and substituted benzaldehydes in piperdine/dry benzene[22]. The structures were characterised by IR and NMR spectroscopy and microanalysis. Of the compounds tested for antimicrobial activity only β-[(2-benzimidazoly)thio]- β-benzoyl-4-chloro styrene, β-[(2-benzimidazoly)thio]- β-benzoyl-4-nitro styrene and β-[(2-benzimidazoly)thio]- β-benzoyl-4-acetylamino styrene showed favourable activity (*Figure 22*).

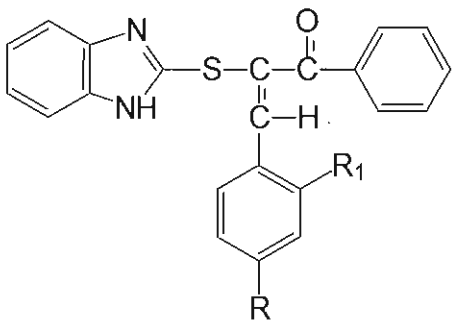

Figure 22 : Structure of β-[(2-benzimidazoly)thio]- β-benzoyl styrene derivatives.

Oren et al reported the synthesis and microbiological activity of 5(or6)-Methyl-2-substituted benzimidazole and benzoxazole derivatives[25]. The compounds were prepared by the heating of carboxylic acids with appropriate *o*-substituted anilines in the presence of HCl which acts as a condensation reagent. While the benzoxazole showed some activity against *C. albicans* the benzimidazole derivatives were less potent in their antifungal activity.

I.5 ANTIFUNGAL ACTIVITY OF THIABENDAZOLE

As well as its anthelmintic properties, Thiabendazole, a 2-(4-thiazolyl)-benzimidazole (TBZH), is a systemic benzimidazole fungicide used to control fruit and vegetable diseases such as mold, rot, blight and stain. It is also active against storage diseases and Dutch Elm disease[26]. Thiabendazole is also used as an anti-fungal agent for the treatment of Fusarium and Aspergillus infections of the eye[27]. Thiabendazole is also used medicinally in chelation therapy[26].

An especially notable aspect of thiabendazole as an antifungal is the systemic distribution of this compound in plants which permit a more efficient use as a general disease control agent[27]. The antifungal spectrum of thiabendazole is broad yet selective, and several pathogens are resistant to it[29]. Thiabendazole controls a variety of plant diseases such as *Cercospora beticola* leaf spot beets[30,31], pear scab [32], crown rust of rye [33], verticillium wilt of cotton [34] and some transport and storage diseases of fruit [26].

I.5.1 Mode of Action

An inhibition of protein synthesis by thiabendazole was observed by Staron et al.[28], who believed that the fungicide interfered with the transfer of amino acids for peptide synthesis. They also attributed part of the growth inhibition to a decrease in the transaminating properties of the thiabendazole-treated cells because the inhibiting effect could be partially offset by the addition of pyrodoxine and biotin. This type of reversal was not found in studies carried out by Allen and Gottlieb[29], so decreases in protein synthesis may not be primary effects of thiabendazole.

A study on the mechanism of action of thiabendazole in 1970 by Allen and Gottlieb found that the limitation of growth of fungi by thiabendazole could be ascribed to an interference with many cellular metabolic activities. They concluded that the inhibition of the terminal electron transport system of the mitochondria probably was the primary site of action of thiabendazole, and decreases in other metabolic function are secondary and follow from the unavailability of energy.

I.6 METAL COMPLEXES OF THIABENDAZOLE

I.6.1 Benzimidazole as a Ligand

Benzimidazole can act as an acid and deprotonation leads to an anionic group (*Figure 24*).

***Figure 24*:** Deprotonation of benzimidazole

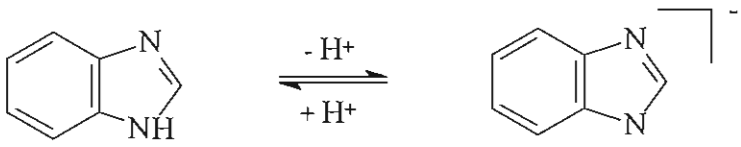

Complexation of Benzimidazole with metals can either involve it acting as a neutral[35] or an anionic[36] ligand. Whereas the neutral BZDH acts as a monodentate ligand, BZD^- invariably bridges the metal centre to give a polymeric complex (see *figure* below).

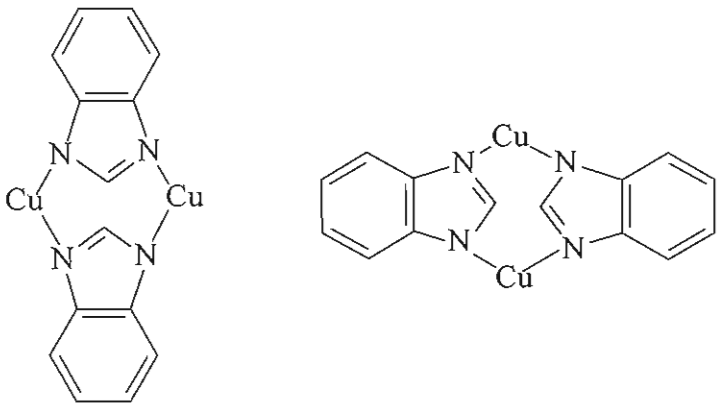

I.6.2 Thiabendazole as a ligand.

In general, with respect to metal ion coordination, thiabendazole can coordinate through either of its nitrogen atoms. Coordination through its imide nitrogen occurs with the loss of the proton, leaving the thiabendazole to act as an anion in any complex formed. Thiabendazole can also coordinate through its non imide nitrogen due to its strong electron donor. Further interest is derived from TBZH as it can act as both an acid and a base (in accordance with *Figure 25*) making it possible to generate inorganic compounds in which it can be neutral, anionic or cationic[37].

Figure 25.:

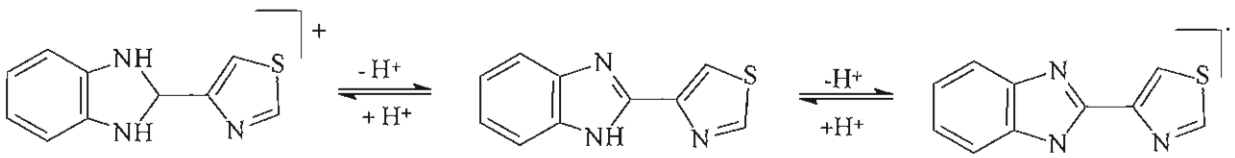

In 1971 Kowala[38] et al reported the crystal and molecular structure of hydrated dichlorodithiabendazolecobalt(II), $[Co(TBZH)_2Cl_2.xH_2O]$. The complex was found to have both thiabendazole ligand molecules coordinated to the cobalt atom through their trigonal nitrogen atoms to form two 5 membered bidentate rings in cis configuratuion. The two chlorine atoms complete the octaherdal coordination which is distorted by displacements of the nitrogen atoms, especially those of the thiazole rings, from their expected positions. These displacements are a consequence of the angle adjustments required to form the 5 membered chelate ring angles. Both ligand molecules are virtually planar as would be expected from the many limiting resonance forms resulting

from the transfer into the molecule of lone pair electrons from the sulphur or secondary nitrogen atoms.

Landschoot et al[39] further investigated the coordination of thiabendazole and agreed that thiabendazole also acted as a strong chelate ligand, yielding compounds with one, two or three ligands per metal centre. For compounds with 3 thiabendazole ligands pseudo-octahedral geometry is found around the metal ion, while compounds with 2 ligands exhibit a square planar structure. It was also observed that compounds contain rather firmly bound water or ethanol or both, probably due to their zeolitic nature.

Grevy et al[40] investigated coordination compounds derived from thiabendazole using main group and transition metals. They reported that in solution and in solid state the ligand coordinates to the metal ions through the imidazolic and thiazole nitrogen atoms regardless of the nature of the metal ion, and that in all cases, the heterocyclic sulpher does not coordinate or interact with the metal ions due to its weak Lewis base nature.

I.6.3 METAL COMPLEXES OF BENZIMIDAZOLE TYPE LIGANDS

In 1995 Mishra et al[41] reported the synthesis and antimicrobial activity of Fe(II)/Fe(III) complexes containing 1,3-diacetyl-2H-benzimidazole-2-thione along with derivatives of 1,2,4-triazol, 1,3,4-oxadiazole and 1,3,4-thiadiazole as co-ligands. The antifungal activity of the complexes, the free heterocyles and $FeCl_3$ were investigated. At higher concentrations, 500 and 1000 μg/ml, almost all compounds showed significant acitivity. However activity is related to the type of fungi being investigated, *Curvularia lunata* showed higher activity than *Alternaria alternata* and *Helminthosporium oryzae*. At lower concentrations the chloro bridged complexes derived from oxadiazole derivatives showed the highest activity againtst all fungi. Correlation of activity with structure of the complexes could not be generalized again since the activities of the free benzothiazole and free $FeCl_3$ even at lowest concentration (250 μg/ml) are found to be significant.

Matthews et al[42] investigated the co-ordinating environments provided by a selection of bis(benzimidazole) ligands. The ligands used were 1-(5,6-dimethylbenzimidazolyl)-3-benzimidazolyl-2-thiapropane **1**, 1-(5,6-dimethylbenzimidazolyl)-3-benzimidazolyl-2-oxopropane **2**, 1-(N-methyl)benzimidazolyl-3-benzimidazolyl-2-oxopropane **3**, and 1,7-bis(benzimidazol-2-yl)-2,6-dithiaheptane **4.** Crystal structures for the following complexes were determined $[Zn(\mathbf{1})Cl_2].CH_3OH$,(*Figure 26*), $[Zn(\mathbf{3})(H_2O)(CH_3CN)(ClO_4)_2]$, (*Figure 27.*), $[Hg(\mathbf{1})Br_2]CH_3OH$ (*Figure 28*) and $[Ag(\mathbf{4})](NO_3)$.

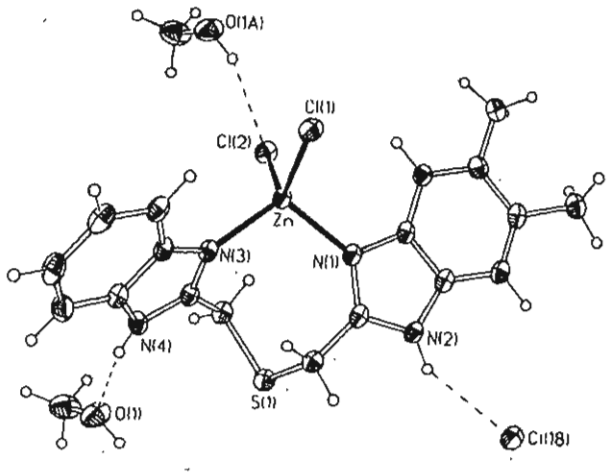

Figure 26: Structure of $[Zn(\mathbf{1})Cl_2].CH_3OH$, $[Hg(\mathbf{1})Br_2]$

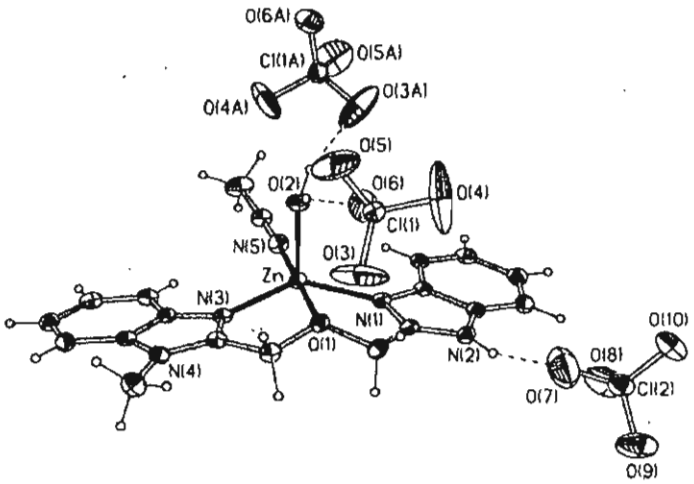

Figure 27: Structure of $[Zn(\mathbf{3})(H_2O)(CH_3CN)(ClO_4)_2]$

Ligand **3** provided the expected N_2O donor set to Zn(II) forming part of a pseudotrigonal bipyramidal coordinating enviroment, which has been tentatively extrapolated to the Zn(II), Cd(II) and Hg(II) complexes of ligand **2** from ^1H NMR studies. The thioether-bridged ligands (**1** and **4**) displayed a strikingly different coordinating mode, in none of these structures was the thioether found to be coordinated to the central metal ion, resulting in pseudotetrahedral structures for the Zn(II) and Hg(II) complexes (*Figure 28*) of ligand **1** and a bis(chloro)-bridged dimeric five-coordinate complex of Cd(II) with ligand **1**, and a near linear coordination mode for the Ag(I) complex of ligand **4**.

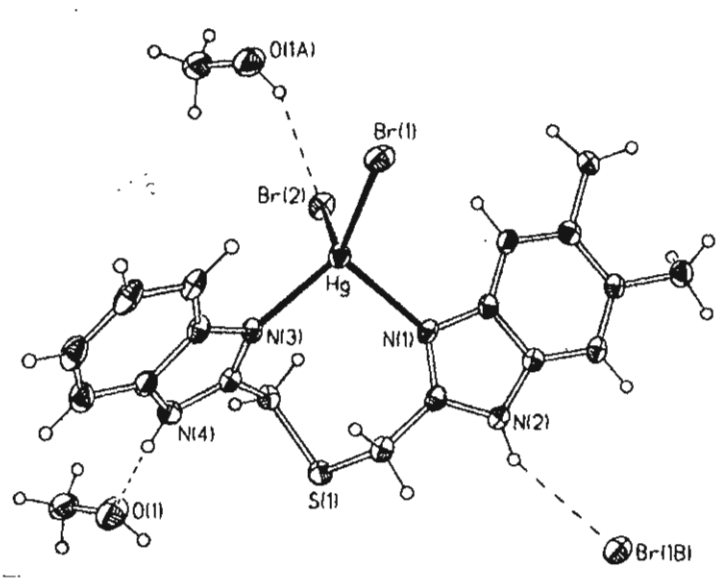

Figure 28: Structure of [Hg(**1**)Br_2] CH_3OH with hydrogen-bonding interactions to solvent molecules and one neighbouring Br ligand.

Matthews et al[43] also reported the crystal structures of a copper(II) and nickel(II) complexes of 4-(benzimidazol-2-yl)-3-thiabutanoic acid which provides a benzimidazole, a thioether and a carboxyl donor group. The crystal structure of the copper complex (*Figure 29*) indicates that the two oxygen and two nitrogen donors form square planar co-ordination around the central copper ion, with a slight tetrahedral distortion. Each oxygen is trans to nitrogen and cis to the other oxygen, the two sulphurs are approximately axial to the copper centre. The structure is a dihydrate, the water molecules providing a link between metal complexes by a three dimensional hydrogen bonding network involving the water molecules, the coordinated and uncoordinated oxygen of each carboxyl and the benzimidazole N-H groups.

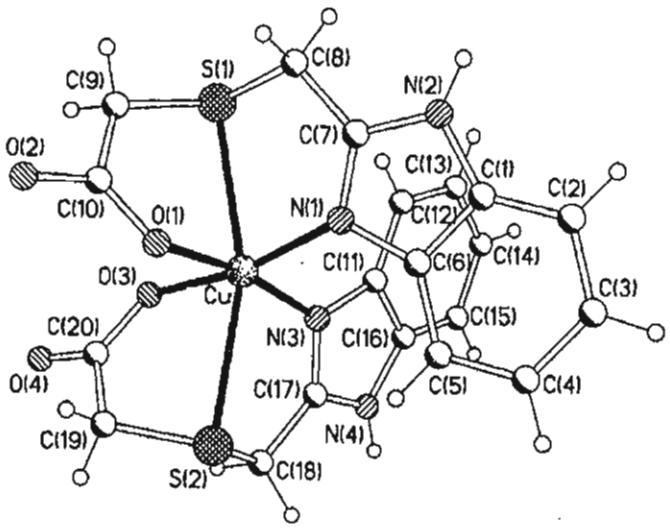

***Figure 29*:** Structure of the [Cu(4-(benzimidazol-2-yl)-3-thiabutanoic acid)$_2$] complex

The crystal structure of the brilliant turquoise nickel complex (*Figure 30*) contains two crystallographically independent molecules of the nickel chelate. Molecule 1 has two sulphurs cis, the nitrogens cis and the oxygens cis. One sulphur is trans to oxygen and the other to nitrogen. The second molecule is the same positional isomer, with slightly

different angles, having cis sulphurs, cis oxygens, cis nitrogens and essentially the same bond lenghts. The molecules are linked by a complex two dimensional hydrogen bonding network involving the six crystallographically independent molecules of methanol of crystallisation, the uncoordinated and half the coordinated carboxylate oxygen atoms and the benzimidazole N-H groups.

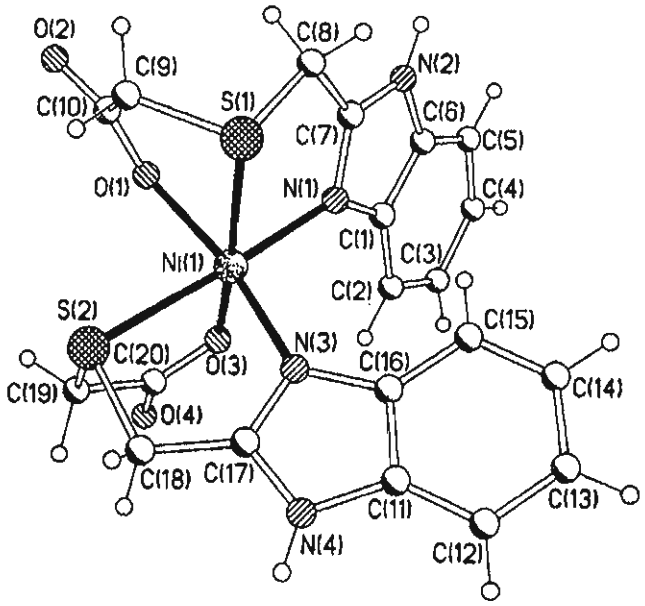

Figure 30: One of the crystallographically independent molecules of the [Ni(4-(benzimidazol-2-yl)-3-thiabutanoic acid)$_2$] complex.

Roman-Alpiste[44] reported the synthesis and crystal structure of the mixed ligand compound [Cu(IDA)(BZDH)(H_2O)] (IDA=iminodiacetato) (*Figure 31*). The complex was prepared by the reaction of $Cu_2CO_3(OH)_2$ and H_2IDA in water and stirring under reduced pressure followed by the addition of BZDH, from which yielded blue prismatic crystals. The crystal structure of this compound consists of complex units of [Cu(IDA)(BZDH)(H_2O)] linked in a three dimensional hydrogen bonding network where all polar N-H and O-H groups are involved. The copper(II) ion has a distorted

square base pyramidal co-ordination rather common in related mixed ligand Cu(II) complexes of BZDH or $BZDH^-$. The O(1), O(7) and N(4) donor atoms from the terdentate IDA ligand and N(8) pyridine like donor atom of BZDH define the square base. A long Cu-O bond completes the elongated square pyramidal Cu(II) co-ordination.

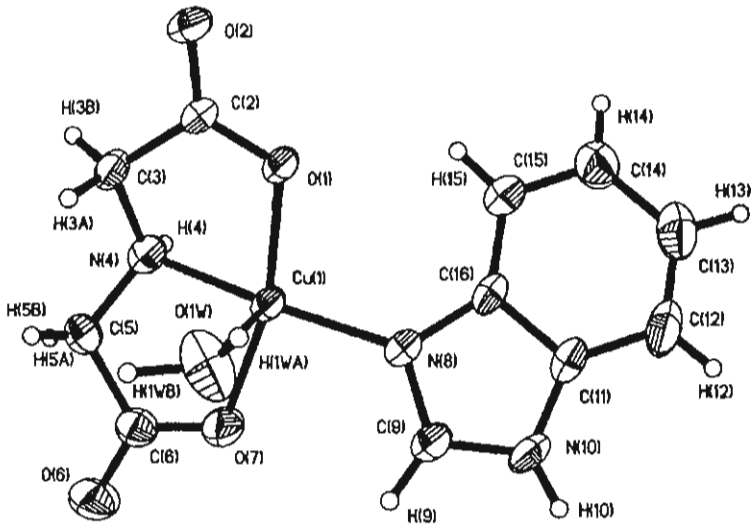

Figure 31: Molecular structure of [Cu(IDA)(BZDH)(H_2O)].

Beyer et al[45] reported the synthesis and molecular structure of bis(2-benzoylimino-benzimidazolinato)copper(II)-dimethylformamide complex (*Figure 32*). The complex was prepared by the reaction of 2-Benzoylimino-benzimidazoline with [$Cu(CH_3COO)_2.H_2O$] in ethanol, crystals suited for X-ray structure analysis were obtained by dissolving the complex in dimethylformamide and slow evaporation of the solvent at room temperature. The complex is a chelate with two bidentate ligands bonding through N and O. The coordination geometry is tetrahedrally distorted square

planar with trans arrangement of the ligands. The crystal structure contains molecules of the solvent dimethylformamide.

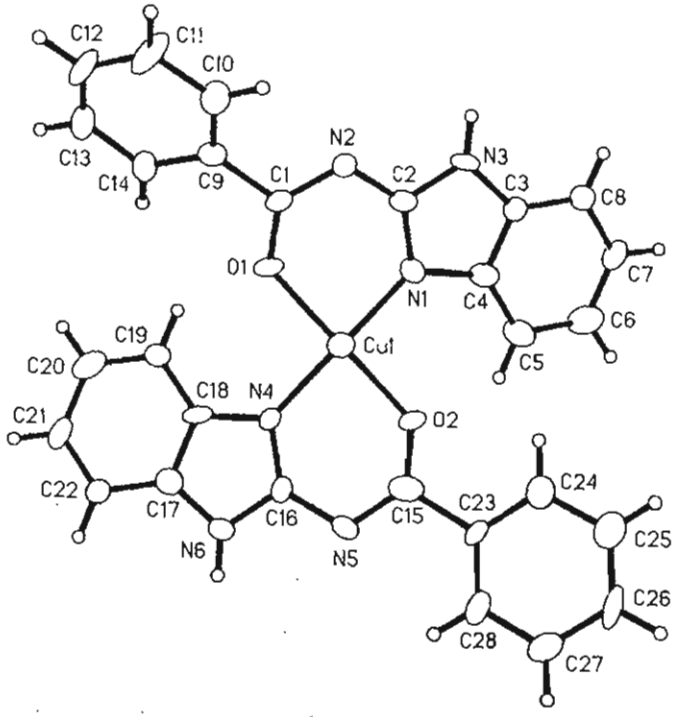

Figure 32: Molecular structure of bis(2-benzoylimino-benzimidazolinato)copper(II)-dimethylformamide complex.

Williams et al[46] reported the characterization of two copper(II) complexes with saccharinate and benzimidazole ligands. The complexes were prepared by the addition of $[Cu(sac)_2(H_2O)_4].2H_2O$ (sac^- = saccharinate) to hot aqueous or ethanolic solutions of benzimidazole, the resulting solutions produced crystals of x-ray crystallographic quality. The first complex $[Cu(sac)_2(BZDH)_2.H_2O]$ (*Figure 33*) contains the Cu(II) at the centre of a square base centre of an elongated pyramidal environment, equatorially trans-coordinated to two saccharinate anions and two benzimidazole molecules. The axial ligand at the pyramidal apex is a water molecule, with the Cu(II) ion slightly out of the mean N_4 plane towards this water molecule. The second complex

$[Cu(sac)_2(BZDH)(H_2O)(EtOH)].2EtOH$ (EtOH = ethanol) (*Figure 34*) also has the Cu(II) at the square base centre of an elongated pyramidal environment, equatorially trans-coordinated to two saccharinate anions and one benzimidazole molecule and a water molecule. The axial position is occupied by the oxygen atom of an ethanol molecule. The crystal also contains a network of relatively weak and bent interdimer ligand EtOH-O bonds involving one oxygen atom of one saccharinate sulphony group.

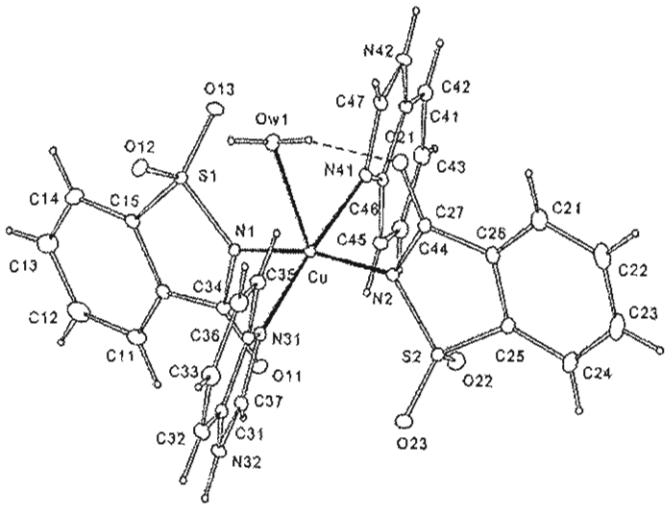

Figure 33: Structure of $[Cu(sac)_2(BZDH)_2.H_2O]$

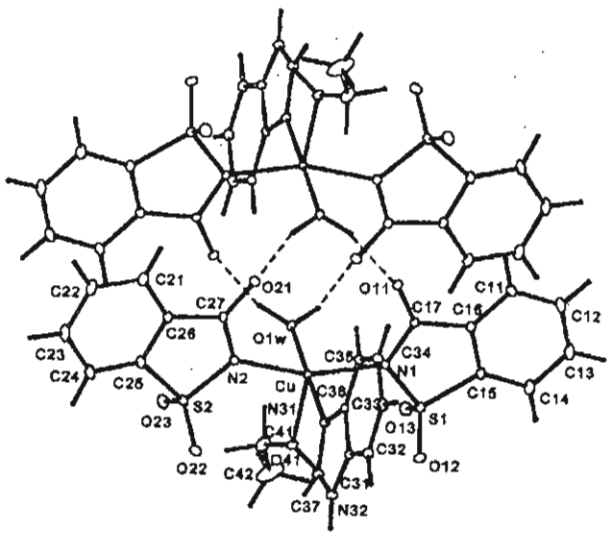

Figure 34: Structure of [$Cu(sac)_2(BZDH)(H_2O)(EtOH)$].2EtOH

Kwok et al[47] reported the synthesis and characterization of a manganese complex of dimethyl-substituted bisbenzimidazole. The complex, [$Mn(Me_2BBZ)Cl$]Cl, (Me_2BBZ = dimethyl bisbenzimidazole), was prepared by refluxing the Me_2BBZ ligand with $MnCl_2.4H_2O$ in CH_3CN from which an orange solid was obtained. Crystals suitable for x-ray analysis were obtained by evaporation from CH_3CN. The divalent manganese ion was found to be five-coordinate and has a distorted square pyramidal geometry. One of the chlorides serves as the axial ligand of the manganese ion and like the diprotonated Me_2BBZ ligand the Mn-Me_2BBZ complex is nonplanar. The general features of the Mn-Me_2BBZ complex are similar to manganese tetrapyroles. Both manganese (II) porphyrins bisbenzimidazoles favour a five coordinate square pyramidal geometry and bind the metal around the equatorial plane.

I.6.4 METAL COMPLEXES OF THIABENDAZOLE

In 1972 Kowala[38] et al reported the crystal and molecular structure of hydrated dichlorodithiabendazolecobalt(II), $Co(TBZH)_2Cl_2.xH_2O$ (*Figure 35*). The complex was found to have both thiabendazole ligand molecules coordinated to the cobalt atom through their trigonal nitrogen atoms to form two 5 membered bidentate rings in cis configuratuion. The two chlorine atoms complete the octahedral coordination which is distorted by displacements of the nitrogen atoms, especially those of the thiazole rings, from their expected positions. These displacements are a consequence of the angle adjustments required to form the 5 membered chelate ring angles. Both ligand molecules are virtually planar as would be expected from the many limiting resonance forms resulting from the transfer into the molecule of lone pair electrons from the sulphur or secondary nitrogen atoms.

Figure 35: The structure of $Co(TBZH)_2Cl_2.xH_2O$

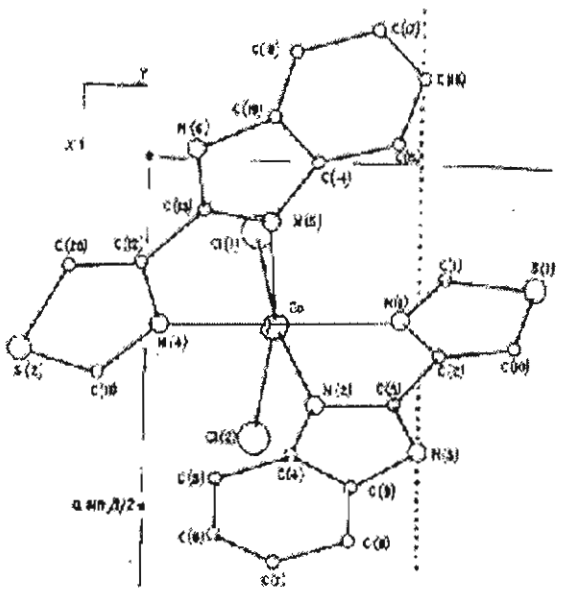

In 1976, Landschoot et al[39] further investigated the coordination of thiabendazole with a selection of transition metals. They also found that thiabendazole acted as a strong chelate ligand, yielding compounds with one, two or three ligands per metal centre. For compounds with 3 thiabendazole ligands pseudo-octahedral geometry is proposed around the metal ion, while compounds with 2 ligands exhibit a square planar structure. It was also observed that compounds contain rather firmly bound water or ethanol or both, probably due to their zeolitic nature.

Udupa et al[48] reported the crystal and molecular structure of chlorodithiabendazolecopper(II) chloride dihydrate. The crystal structure consists of $[CuCl(thiabendazole)_2]^+$ (*Figure 36)* units linked through hydrogen bonds involving the protonated nitrogen atoms of the benzimidazole rings, water molecules and the chlorine atoms. Both the ligand molecules are bonded to the copper atom through a nitrogen atom of the thiazolyl ring and one of the nitrogen atoms of the benzimidazole in *cis* configuration to form two 5-membered bidentate chelate rings. One of the chlorine atoms completes the 5-coordinated geometrical arrangement around the copper. The coordination polyhedron of copper may be described as a distorted trigonal bipyramid.

Figure 36: Chlorodithiabendazolecopper(II) cation with atom numbering

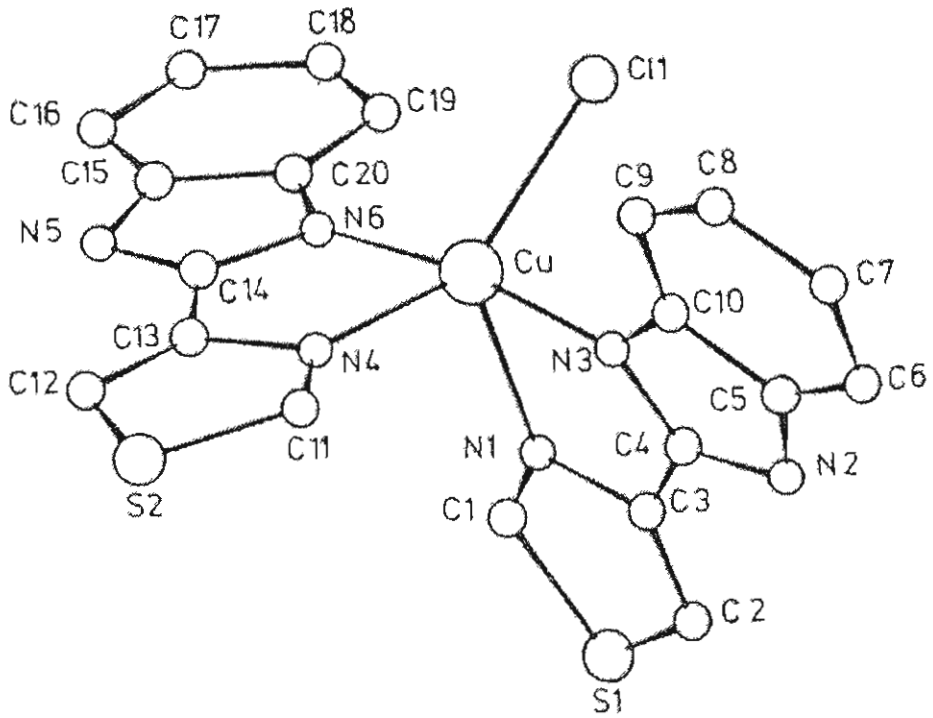

In 2001, Wisniewski et al[49] reported complexes of thiabendazole with Co(II), Ni(II) and Cu(II) all with the general formula of $ML_2(NO_3)_2.H_2O$ and complexes of Pd(II) and Pt(II) of the general formula $ML_2Cl_2.H_2O$. The complexes were characterised by elemental analysis, infrared spectroscopy and magnetic studies. The x-ray structure of $[Cu(TBZH)_2(NO_3)_2H_2O]$ was also reported (*Figure 37*). The *in vitro* cell proliferation inhibitory activity of these compounds was examined against human cancer cell lines A549 (lung carcinoma), HCV-29 (urinary bladder carcinoma), MCF-7 (breast cancer), T47D breast cancer), MES-SA (uterine carcinoma) and HL-60 (promyelocytic leukemia).

Figure 37: $[Cu(TBZH)_2(NO_3)_2H_2O]$

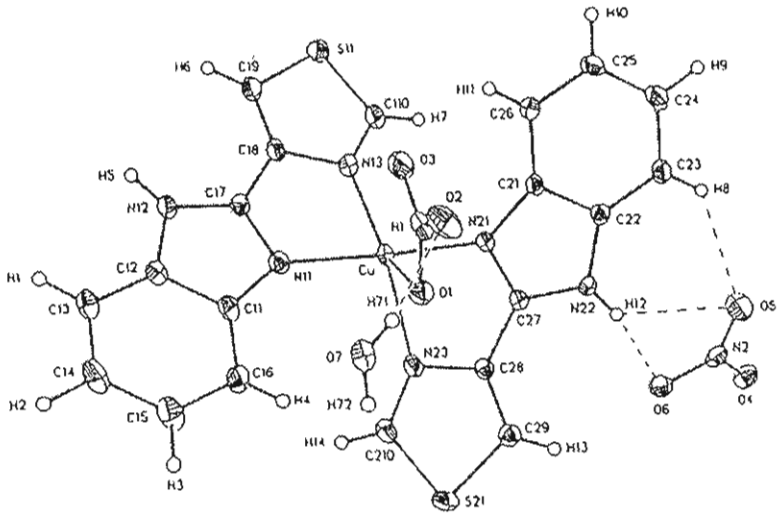

In 2002, Grevy et al[50] reported metal coordination compounds derived from thiabendazole, using Li^I, Na^I, K^I, Pb^{II}, Co^{II}, Ni^{II}, Cu^{II}, Zn^{II}, Cd^{II} and Hg^{II}. The compounds were charachterised by analytical and spectroscopic techniques. X-ray diffraction analysis of Na^I, Pb^{II}, Co^{II}, Ni^{II}, Cu^{II} and Cd^{II} complexes showed that thiabendazole stabilises bis- and tris- chelated coordination compounds. In solution and in solid state the ligand coordinates to the metal ions through the imidazole and thiazole nitrogen atoms, and they remain planar due to its conjugated character.

In 2004, Mothilal et al[51] reported the synthesis and characterisation of four nitrate complexes of Co^{2+}, Cu^{2+}, Ni^{2+} and Zn^{2+} incorporating the TBZH ligand. The structure of $[Co(TBZH)_2(NO_3)(H_2O)](NO_3)$ was determined crystallographically. The geometry of the $[Co(TBZH)_2(NO_3)(H_2O)]^+$ cation (*Figure 38*) is best described as a distorted octrahedral and the Co^{2+} is coordinated by two TBZH ligands through two nitrogen

atoms, each resulting in two 5-membered bidentate chelate rings in *cis*-configuration, and by two oxygen atoms, one from each of the coordinated nitrate and water groups. Both the nickel and zinc complexes were found to exhibit very promising antimicrobial activity against *B.subtilis* and *E.coli* and the yeast *A.flavues*.

Figure 38: $[Co(TBZH)_2(NO_3)(H_2O)]^+$ cation

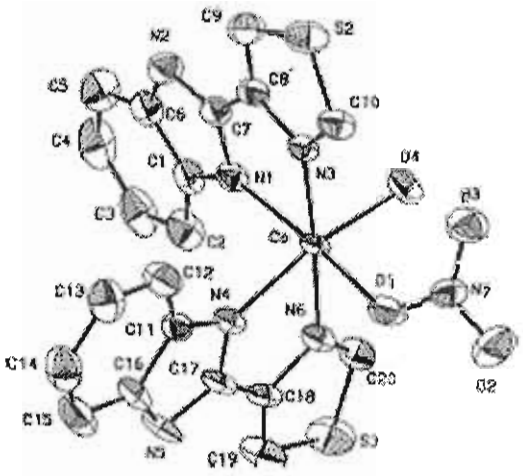

I.7.1 NOVEL METAL-PHENANTHROLINE ANTI-*CANDIDA* DRUGS

The problems associated with the state-of-the-art polyene and azole drugs (resistance and unwanted side effects) have resulted in a search for possible alternative anti-fungal agents. The strategy for the development of new anti-*candida* agents must involve compounds which act on the *candida* via an alternative mode of action to that of the current, purely organic, therapeutics. Due to the possibility of a difference in mode of anti-fungal activity metal-based drugs may represent a novel group of anti-mycotic agents which could have potential applications as pharmaceuticals.

Recently, in this laboratory, it has been shown that a range of carboxylate and dicarboxylate complexes incorporating transition metal centres and including the N,N'-donor ligand 1,10-phenanthroline(phen) {*Figure 39*(a)} are potent *in-vitro* inhibitors of the growth of *Candida albicans*.

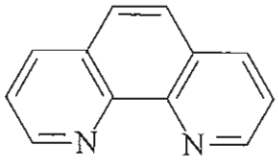

(a) 1,10 Phenanthrolin

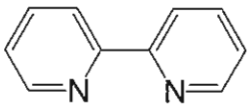

(b) 2,2'-bipyridine

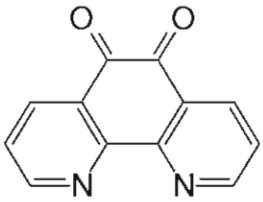

(c) 1,10 phenanthroline-5,6 dione

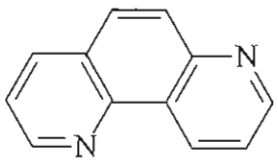

(d) 1, 7 phenanthroline

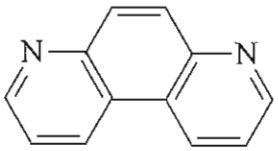

(e) 4,7 phenanthroline

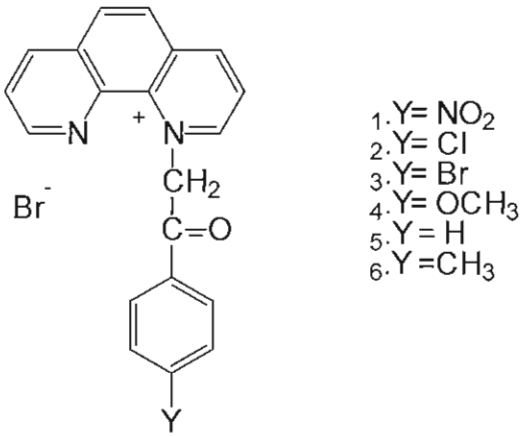

(f) Organic derivatives of 1,10 Phenanthroline

***Figure 39*:** The structures of (a) 1,10-phenanthroline; (b) 2,2'-bypyridine; (c) 1,10-phenantroline-5,6-dione;(d) 1,7-phenanthroline; (e) 4,7-phenanthroline; (f) Organic derivatives of 1,10-phenanthroline

Furthermore, the group has shown that by changing the structural nature of the chelating phenanthroline molecules to include ketonic carbonyl groups (*Figure 39*) it is possible to generate complexes that are very active at much lower concentrations[52]. Experiments with 1,7-phenanthroline and 4,7-phenanthroline (*Figure 39*(d).(e)) demonstrated that ligands with chelating ability appeared to be desirable for anti-fungal activity[53]. However, when the 1,10-phenanthroline is replaced by the structurally similar N,N'-donor ligand 2,2'-bipyridine(bipy) (*Figure 39*(b)) complexes devoid of anti-*candida* activity are obtained[54]. Significantly, when the so called 'metal free' 1,10-phenantroline and the 1,10-phenantroline-5,6-dione are tested against the *candida* they generally exhibit superior activity to that of the metal complexes and activity comparable to the prescription drugs. Other workers have recently reported very good anti-*candida* activity for several new organic 1,10-phenanthroline derivatives (*Figure 39*(f))[55]. It is believed that the so called "metal free" 1,10-phenanthrolines are probably coordinating to metal ions, that are present in trace amounts in the growth medium, and that it is these resulting metal-phenanthroline complexes that are responsible for the high anti-Candida activity.

I.7.2 The mode of action of the Phenanthrolines and their metal complexes

The mode of action of 1,10-phenanthroline and a number of the potent anti-*candida* metal complexes{M = Cu(II), Mn(II) or Ag(I)}, previously reported by this group[56], was examined. The phen and its metal complexes had minimum inhibitory concentrations (MIC's) in the range 1.25-5μg/ml and at concentration of 10μg/ml they displayed some fungicidal activity. Yeast cells exposed to these drugs showed a diminished ability to reduce 2,3,5-triphenyltetrazolium chloride (TTC), indicating a

reduction in respiratory function. Treating exponential and stationary phase yeast cells with phen and the Cu(II) and Mn(II) complexes caused a dramatic increase in oxygen consumption. All of the drugs promoted reduction in levels of cytochrome b and c in the cells, whilst the Ag(I) complex also lowered the level of cytochrome aa. Cells treated with phen and the Cu(II) and Ag(I) species showed reduced levels of ergosterol whilst the Mn(II) complex induced an increase in the sterol concentration. The general conclusion was that phen and its Cu(II), Mn(II) and Ag(I) complexes damage mitochondrial function and uncouple respiration. The fact that these drugs were not uniformly active suggests that their biological activity has a degree of metal-ion dependency.

The effect of these drugs on the structure of yeast and mammalian cell organelles and the integrity of cellular DNA was also studied[57]. The conclusion was that phen and the metal-phen complexes have the potential to induce apoptosis in fungal and mammalian cells.

This group has concluded that selected 1,10-phenanthrolines and their metal complexes represent a novel set of highly active anti-fungal agents whose mode of action is significantly different to that of the state-of-the-art polyene and azole prescription drugs. However the fact that these compounds may also be deleterious to mammalian cells has prompted this group to search for possible, less toxic, metal complexes containing alternative N,N-donor ligands.

In an effort to extend this class of novel metal based drugs workers in this laboratory have been studying metal complexes containing benzimidazole based ligands[58].

Benzimidazole and many of its derivatives exhibit a variety of biological actions, including antibacterial, antiviral, anticancer and antifungal activity[59]. Furthermore their toxicology is well established.

2-(4'-thiazolyl)benzimidazole {Thiabendazole(TBZH)} (*Figure 15*) is known to be non-toxic to humans[60] and has applications in both agriculture and medicine as an anti-fungal agent. A series of copper complexes of TBZH were synthesised and the anti-*candida* activity of the free TBZH was compared to that of the metal derivatives (*Table 4*)[37].

Table 4: Anti-*Candida* activity* of TBZH and some of its copper derivatives

Test Compound	**%Cell Growth**
Control	100
Ketoconazole	20
1,10-phenanthroline	15
$CuCl_2$	95
$CuNO_3$	98
$Cu(OAc)_2$	94
$HO_2C\text{-}CH_2CH_2\text{-}CO_2H$	98
$[Cu(O_2C\text{-}CH_2CH_2\text{-}CO_2)]$	95
TBZH	76
$[Cu(TBZ)_2(H_2O)_2]$ (**1**)	54
$[Cu(TBZH)_2Cl]Cl.H_2O.EtOH$ (**2**)	29
$[Cu(NO_3)_2(TBZH)_2]$ (**3**)	30
$[Cu(TBZH)(O_2C\text{-}CH_2CH_2\text{-}CO_2)]$ (**4**)	19

* The compounds were tested at concentrations of 10μg/ ml of aqueous RPMI medium. Yeast cells were grown for 24h at 37°C. Results are presented as % cell growth and the effectiveness of the compounds are compared to the growth of the control (no drug added).

The copper free neutral TBZH was found to be a very poor inhibitor of the growth of the pathogen. The copper complexes (**1**) in which the ligand is found in its anionic state is a moderate anti-*Candida* agent. Significantly when the neutral TBZH is coordinated to a copper center(complexes (**2**)-(**4**)) very potent anti-*Candida* drugs are produced. Complex (**4**) exhibits the greatest fungitoxic activity and indeed is comparable to the prescription drug Ketoconazole at this concentration. Preliminary studies on the mode of action of the copper TBZH complexes have revealed that they cause a reduction in the ergosterol content of the fungal cells[61] which was also found to be the case for the phenanthroline complexes previously reported[56].

The cytotoxic activity of TBZH and the DMSO soluble complexes (**2**) and (**3**) on two human epithelial derived cancer model cell lines was determined by calculation of IC_{50}. Calculation of this value allows a direct comparison of the cytotoxicity of each of the test agents. The values were obtained for each compound, and in each cell line (*Table 5*).

Table 5: The Chemotherapeutic potential of TBZH, (**2**) and (**3**)

	Toxicities (IC_{50} μM)	
	CAL-27	*SK-MEL-31*
Test Compound	*Mean ± S.D.*	*Mean ± S.D.*
TBZH	676.7 ± 12.0	453.3 ± 66.0
$[Cu(TBZH)_2Cl]Cl.H_2O.EtOH$ (**3**)	55.0 ± 0.0	49.5 ± 7.7
$[Cu(NO_3)_2(TBZH)_2]$ (**4**)	54.0 ± 2.5	46.7 ± 5.0

The cancer chemotherapeutic potential of complexes (**2**) and (**3**) along with metal free TBZH in CAL-27 and SK-MEL-31, following continuous incubation for 96 hr in the concentration range of 0.1-1000 μM was determined using MTT assay. A graph of viability as % of solvent treated control verses drug concentration was used to calculate IC_{50} values (μM), (Mean ± S.D.; n= 5).

TBZH was capable of killing both cancer derived mammalian cell lines only at higher concentrations with IC_{50} values of 453 and 677 μM (equivalent to 91.7 and 136.9 μg/ml), for the tongue and skin cell line, respectively. In the case of compounds **2** and **3** the IC_{50} values were very similar across the two human model cell lines. They had almost identical IC_{50} values of 55 and 54 μM (equivalent to 33.1 and 31.9 μg/ml), respectively in the CAL-27 cell line and 50 and 47 μM (equivalent to 39.1 and 30.7 μg/ml), respectively in the SK-MEL-31 cell line. These results demonstrate the non toxic nature of TBZH towards mammalian cells. Furthermore, although the activity of TBZH is increased significantly upon coordination to a copper center in **2** and **3** the complexes are not nearly as cytotoxic as the phenanthrolines (IC_{50} values as low as 0.008μg/ml)[57].

The current project seeks to study the effects of changing the nature of the metal centre in the TBZH based complexes. Thus evaluating the contribution of different types of transition metals to any enhancement of anti-*candida* activity of the TBZH. Furthermore, the affect of changing the counterion present has also been studied. Evidence from the literature suggests that the type of counterion present is critical to Metal Based Drug activity[37].

I.8 THE GENERAL CHEMISTRY OF THE TRANSITION METALS USED IN THIS STUDY[62]

I.8.1 General Chemistry of Manganese

Manganese has the electron configuration $[Ar]4s^2 3d^5$ and shows the widest range of electron states of all the elements, ranging from (-III) to (+VII). Coordination complexes of manganese (II), (III), and (IV) are generally octahedral while those of manganese (VI) and (VII) are generally tetrahedral. Manganese (V) is little known except in the bright blue "hypomanganates" that are formed by the reduction of permanganate with an excess of sulphite. Almost all manganese compounds are coloured. Hydrated manganese (II) ions are pale pink and MnO_2 is black, both because of *d-d* spectra. Manganese (VII) has a d^0 electronic configuration and would be expected to be colourless. However permanganates containing manganese (VII) are intensely coloured because of charge-transfer spectra.

I.8.1.1 The Manganese (II) Oxidation State

Manganese (II) is the most stable and common oxidation state, with the half-filled $3d^5$ electronic configuration. Most manganese complexes are high spin with five unpaired electrons. In octahedral fields this configuration gives spin-forbidden as well as parity-forbidden transitions, thus accounting for the extremely pale colour of such compounds. In tetrahedral environments, the transitions are still spin-forbidden but no longer parity-forbidden; these transitions are therefore ~100 times stronger and the compound have a noticeable pale yellow-green colour.

I.8.2 General Chemistry of Iron

Iron is the second most abundant metal after Aluminium and the fourth most abundant element in the earths crust. The earths core is believed to consist mainly of iron and nickel, and the occurrence of iron meteorites suggests that it is abundant throughout the solar system. Iron is also an essential element for all forms of life. It is a white, lustrous metal. It is not particularly hard, and it is quite reactive.

Iron has an electron configuration $[Ar]3d^6 4s^2$.

I.8.2.1 The Iron(II) Oxidation State

Iron (II) has the electron configuration $[Ar]3d^6$. The coordination numbers for Iron(II) are usually four, five, six and eight, with the octahedral shape being the most common. Iron (II) halides and other salts absorb NH_3 in excess giving the $[Fe(NH_3)_6]^{2+}$. Ligands like phen, bipy and others supplying imine nitrogen donor atoms give stable low spin (i.e. dimagnetic), octahedral, or distorted octahedral complexes.

I.8.2.2 The Iron(III) Oxidation State

Iron (III) has an electron configuration of $[Ar]3d^5$. The coordination numbers are usually three, four, five, six and seven. Iron (III) oxides are generally red-brown gels and are a major constituent of soils.

I.8.3 General Cobalt Chemistry

Cobalt always occurs in nature in association with Nickel and usually also with arsenic and is a hard, bluish-white metal. The name is derived from the German 'Kobald', meaning goblin. Cobalt has the electron configuration $[Ar]3d^7 4s^2$. It can be magnetised like iron and so can be used to make magnets, as well as ceramics and paints. The radioactive isotope cobalt-60 is used in medical treatment and in some countries to irradiate food to preserve it. Cobalt is an essential element for humans since it is part of vitamin B12.

I.8.3.1 The Cobalt (II) oxidation state

Cobalt (II) has the electron configuration $[Ar]3d^7$.

Cobalt (II) forms an extensive group of simple and hydrated salts. They are usually red or pink and contain the $[Co(H_2O_6)]^{2+}$ ion or other octrahedrally coordinated ions.

Cobalt (II) forms numerous complexes, mostly either octrahedral or tetrahedral. There are more terahedral complexes of Cobalt(II) than for other transition metal ions. This is in accordance with the fact that for a d^7 ion, ligand field stabilisation energies disfavour the tetrahedral configuration relative to the octahedral one to the smaller extent for any other d^n configuration.

I.8.4 General Nickel Chemistry

Nickel occurs in nature mainly in combination with arsenic, antimony and sulphur. Elemental nickel is also found alloyed with iron in many meteors, and the central regions of earth are believed to contain considerable quantities. The name is a shortened version of the German 'Kupfernickel', meaning devils copper or St.Nicholas's copper.

Nickel has the electron configuration $[Ar]3d^8 4s^2$.

I.8.4.1 The Nickel (II) oxidation state

Nickel (II) has the electronic configuration $[Ar]3d^8$. It forms a large number of complexes with coordination numbers three to six. A particular characteristic is the existence of complicated equilibria, commonly temperature and concentration dependent, involving different structural types.

I.8.5 General Chemistry of Zinc

Zinc was known in India and China before 1500AD and to the Greeks and Romans before 20BC as the copper –zinc alloy brass. It is a grey metal with a blue tinge. World production exceeds seven million tonnes a year, and it is used to galvanise iron to prevent rusting. It is also employed in alloys and batteries, and as zinc oxide to stabilise rubber and plastic. Zinc is one of the three most important trace elements in the human body along with iron and copper. Zinc has an electron configuration $[Ar]\ 3d^{10}4s^2$.

I.8.5.1 The Zinc(II) Oxidation State

The most common oxidation state of zinc is +2 with the electron configuration *[Ar] $3d^{10}$*. The coordination numbers for Zinc (II) are usually four, five and six, with the tetrahedral structure being the most common.

Zinc (II) is functionally active in synaptic transmission and is a contributory factor in neurological disorders including epilepsy and Alzheimer's disease.

I.8.6 General Chemistry of Silver

Silver, one of the "coinage metals" was almost certainly one of the three first metals known to man, along with the other "coinage metals", gold and copper. Silver has the electron configuration *[Kr] $4d^{10}5s^{1}$*.

I.8.6.1 The Silver(I) Oxidation State

The +1 state is by far the best known oxidation state of silver, with the electron configuration *[Kr] $4d^{10}$*. The most common coordination number of silver (I) is two, but the complexes of coordination number three, four and six are also found, with linear, trigonal planar, tetrahedral, square planar and octahedral structures commonly found.

EXPERIMENTAL

E.1 INSTRUMENTATION

Infrared (IR) spectra were recorded in the region 4000-400 cm^{-1} on a Nicolet FT-IR 400 Impact spectrometer. Solid samples were prepared in a KBr matrix.

Room temperature magnetic susceptibility measurements were carried out using a Sherwood Scientific Magnetic Susceptibility Balance. $Hg[Co(SCN)_4]$ was used as a reference standard.

Conductivity measurements were made using a Jenway Conductivity Meter 4310.

Electronic spectra were obtained in $1cm^{-1}$ UV grade disposable cuvettes on a Genesys 5 Milton Roy spectrometer.

Measurement of drug minimum inhibitory concentrations (MIC's) was carried out using an Anthos bt 3 plate reader.

Elemental analyses were carried out by the Microanalytical Laboratory, University College Cork, Ireland.

X-ray crystallographic work was carried out by Dr. Vickie McKee, Chemistry Department, Loughborough University, Loughborough, Leics., LE11 3TU, UK.

E.2 CHEMICALS

All chemicals were purchased from commercial sources and were generally used without further purification.

E.3 SYNTHESIS OF TRANSITION METAL COMPLEXES OF THIABENDAZOLE

E.4 Reactions of Thiabendazole (TBZH) with Metal Chlorides

E.4.1 $[Mn(TBZH)_2Cl_2].3H_2O.0.5EtOH$ (1)

To a solution of $MnCl_2.4H_2O$ (0.5 g, 2.52 mmol) in ethanol (100 cm^3) (clear/yellow solution), was added thiabendazole (1.014g, 5.04 mmol), the suspension turned white. The resulting suspension was refluxed for 3 hours. The colourless solid which deposited was filtered off, washed with water and ethanol, and then air-dried.

Yield: 0.93g, 61.18%

% Calc: 41.62%C; 3.79%H; 13.87%N,

% Found: 41.14%C; 2.24%H; 14.04%N,

IR (KBr): 3645.42, 3191.82, 3089.02, 2748.45, 1927.84, 1772.64, 1680.62, 1622.66, 1587.52, 1501.25, 1472.86, 1453.50, 1432.52, 1322.21, 1293.96, 1271.75, 1256.94, 1224.48, 1198.15, 1148.05, 1113.66, 1008.70, 990.40, 921.49, 901.73, 878.44, 841.15, 789.61, 762.16, 739.68, 685.54, 659.31, 638.46, 569.18, 545.38, 486.51, 434.49.

Solubility: insoluble in water, ethanol, methanol, acetone and DMSO

μ_{eff}: 6.87BM

E.4.1A $[Mn(TBZH)_3Cl_2].0.5EtOH$ (2)

To a solution of $MnCl_2.4H_2O$ (0.5 g, 2.52 mmol) in ethanol (100 cm^3) (clear/yellow solution), was added thiabendazole (2.02g, 10.08 mmol), the suspension turned white.

The resulting suspension was refluxed for 3 hours. The colourless solid which deposited was filtered off, washed with water and ethanol, and then air-dried.

Yield: 1.73g, 91%

% Calc: 49.42%C; 3.18%H; 16.74%N,

% Found: 49.05%C; 2.79%H; 16.81%N,

IR (KBr): 3435.76, 3084.87, 3065.94, 3021.81, 2970.85, 2904.81, 2868.49, 2814.05, 2749.08, 2666.11, 2510.51, 1926.48, 1889.83, 1772.40, 1670.75, 1621.57, 1579.40, 1498.60, 1473.07, 1454.16, 1420.23, 1414.17, 1404.61, 1357.41, 1323.15, 1305.95, 1295.53, 1272.32, 1256.53, 1227.92, 1196.93, 1147.51, 1117.98, 1095.15, 1073.60, 1046.88, 1008.30, 988.93, 919.89, 902.20, 878.08, 841.00, 788.44, 763.81, 740.25, 660.22, 648.20, 623.20, 570.05, 545.14, 537.08, 488.34, 433.32.

Solubility: insoluble in water, ethanol, methanol, acetone and DMSO

μ_{eff}: 5.56BM

E.4.2 $[Fe(TBZH)_2Cl_3.H_2O]0.5EtOH$ (3)

To a solution of anhydrous $FeCl_3$ (0.5 g, 3 mmol) in ethanol (100 cm^3) (yellow solution), was added thiabendazole (1.24g, 6 mmol), the solution turned orange/red, then a brown suspension appeared. The resulting suspension was refluxed for 3 hours. The brown solid which deposited was filtered off, washed with water and ethanol, and then air-dried.

Yield: 1.5g, 82.41%

% Calc: 41.65%C; 3.14%H; 13.88%N,

% Found: 41.4%C; 2.925%H; 13.59%N,

IR (KBr): 3676.29, 3650.45, 3328.95, 3066.82, 2966.56, 2818.50, 2759.04, 2360.64, 2342.50, 1620.75, 1593.53, 1509.64, 1481.74, 1454.10, 1426.02, 1380.95, 1326.07, 1299.24, 1276.31, 1227.01, 1187.60, 1043.91, 1015.42, 999.68, 932.89, 877.31, 835.59, 759.53, 750.52, 668.20, 631.44, 629.82, 556.04, 485.99.

Solubility: soluble in water, ethanol, methanol, acetone and DMSO

μ_{eff}: 5.86BM

Λ_M **(H_2O):** 499.39 cm^2mol^{-1}

λmax (H_2O): 322nm

E.4.3 $[Co(TBZH)_2Cl_2]0.5H_2O.\ 0.5EtOH$ (4)

To a solution of $CoCl_2.6H_2O$(0.5 g, 2.1 mmol) in ethanol (100 cm^3) (blue solution), was added thiabendazole (0.8 g, 4.2 mmol). The resulting purple solution was refluxed for 3 hours, after which time a purple powder precipitated. The product was filtered off, washed with water and ethanol, and then air-dried.

Yield: 0.9g, 75%

% Calc: 44.65%C; 3.19%H; 14.88%N,

% Found: 44.43%C; 2.705%H; 14.7%N,

IR (KBr): 3430.17, 3068.20, 2968.49, 2868.28, 2749.93, 2359.86, 2341.52, 1619.84, 1586.95, 1503.78, 1473.04, 1455.49, 1433.60, 1323.55, 1295.78, 1272.01, 1257.45, 1224.51, 1193.84, 1073.61, 1009.41, 991.30, 923.65, 876.57, 839.88, 787.75, 763.36, 740.82, 651.54, 488.13.

Solubility: soluble in water, ethanol, methanol and DMSO

μ_{eff}: 5.19BM

Λ_M (H_2O): 206.89cm^2mol^{-1}

λmax (H_2O): 310nm

E.4.3A $[Co(TBZH)_3Cl_2]0.5ETOH$ (5)

To a solution of $CoCl_2.6H_2O$ (0.5 g, 2.1 mmol) in ethanol (100 cm^3) (blue solution), was added, thiabendazole (1.68 g, 8.4mmol). The resulting orange solution was refluxed for 3 hours, after which time an orange powder precipitated. The product was filtered off, washed with water and ethanol, and then air-dried.

Yield: 1.19g, 74.89%

% Calc: 49.16%C; 3.17%H; 16.65%N,

% Found: 49.01%C; 3.33%H; 17.05%N,

IR (KBr): 3356.69, 3063.17, 17.69.61, 1621.52, 1590.19, 1505.06, 1476.87, 1453.41, 1427.16, 1357.99, 1323.76, 1301.23, 1277.23, 1228.95, 1195.22, 1149.53, 1093.54, 1047.04, 1009.96, 991.96, 927.70, 901.74, 873.84, 834.74, 744.23, 653.17, 627.59, 570.74, 552.42, 535.92, 487.98, 432.52.

Solubility: soluble in water, ethanol, methanol and DMSO

μ_{eff}: 4.51

Λ_M (H_2O): 120.56 cm^2mol^{-1}

λmax (H_2O): 316nm

E.4.4 $[Ni(TBZH)_2Cl_2]0.5ETOH$ (6)

To a solution of $NiCl_2.6H_2O$(0.5 g, 2 mmol) in ethanol (100 cm^3) (green solution), was added thiabendazole (0.8g, 4 mmol) yielding a purple/blue solution. The solution was refluxed for 3 hours, after which time a green powder precipitated. The product was

filtered off, washed with water and ethanol, and then air-dried. The green/blue solution was left to stand.

Yield: 0.8g, 72.07%

% Calc: 45.43%C; 3.07%H; 15.13%N,

% Found: 44.55%C; 2.985%H; 15.26%N,

IR (KBr): 3426.11, 3066.90, 2967.16, 2868.48, 2751.24, 2633.37, 1618.82, 1587.98, 1503.07, 1474.69, 1457.93, 1436.01, 1324.43, 1296.84, 1273.14, 1257.98, 1224.71, 1191.42, 1074.04, 1010.59, 993.04, 926.04, 875.30, 839.35, 789.14, 763.13, 740.83, 652.84, 626.46, 488.44.

Solubility: soluble in water, ethanol, methanol, acetone, trichloromethane and DMSO

μ_{eff}: 3.29BM

Λ_M (H_2O): 215.55 cm^2mol^{-1}

λmax (H_2O): 307nm

E.4.5 [Zn(TBZH)Cl_2] (7)

To a colourless solution of $ZnCl_2$(0.5 g, 3.6 mmol) in ethanol (100 cm^3), was added thiabendazole (1.5g, 7 mmol) resulting no colour change. The resulting solution was refluxed for 3 hours, after which time a colourless powder precipitated. The product was filtered off, washed with water and ethanol, and then air-dried.

Yield: 1g, 82.28%

% Calc: 35.54%C; 2.07%H; 12.44%N,

% Found: 35.475%C; 2.05%H; 12.62%N,

IR (KBr): 3189.79, 3095.60, 1623.82, 1590.91, 1506.50, 1478.60, 1458.09, 1441.96, 1422.58, 1321.72, 1296.17, 1229.12, 1195.29,

1143.04, 1120.95, 1105.53, 1011.37, 995.41, 938.02, 906.35, 880.11, 839.99, 787.81, 761.81, 748.82, 670.77, 667.78, 643.96, 627.03, 570.96, 548.50, 484.39, 435.60.

Solubility: soluble in water, methanol, acetone, trichloromethane and DMSO

Λ_M (H_2O): 231.41cm^2mol^{-1}

λmax (H_2O): 343nm

E.5 Reactions of Thiabendazole with Metal Nitrates

E.5.1 Attempted Reaction of TBZH with Manganese (II) Nitrate

To a solution of $Mn(NO_3)_2.4H_2O$ (0.5 g, 1.99 mmol) in ethanol (100 cm^3) (clear/yellow solution), was added thiabendazole (0.8g, 3.98 mmol), the solution remained clear and was refluxed for 3 hours. Upon standing, a colourless solid which deposited was filtered off, washed with water and ethanol, and then air-dried. IR spectroscopy confirmed this to be unreacted TBZH.

E.5.1A $[Mn(TBZH)_2(NO_3)](NO_3).H_2O$ (8)

To a solution of $Mn(NO_3)_2.4H_2O$ (0.5 g, 1.99 mmol) in ethanol (100 cm^3) (clear/yellow solution), was added thiabendazole (1.6g, 7.99 mmol), the suspension turned white. The resulting suspension was refluxed for 3 hours. The colourless solid which deposited was filtered off, washed with water and ethanol, and then air-dried.

Yield: 0.73g, 61.19%

% Calc: 40.07%C, ; 2.69%H, ; 18.69%N,

% Found: 40.28%C, ; 2.27%H, ; 18.76%N,

IR (KBr): 3078.30, 1765.84, 1622.70, 1587.94, 1458.27, 1434.74, 1383.73, 1337.56, 1320.05, 1201.72, 1149.53, 1119.73, 1033.74, 1011.59, 992.09, 924.08, 902.63, 878.02, 860.95, 837.63, 813.42, 787.51, 762.25, 740.43, 635.81, 545.08, 433.51.

Solubility: insoluble in water, ethanol, methanol, acetone and DMSO

μ_{eff}: 6.09BM

E.5.2 [$TBZH_2NO_3$] (9)

To a solution of $Fe(NO_3)_3.9H_2O$(0.5 g, 1.24 mmol) in ethanol (100 cm^3) (yellow/orange solution), was added thiabendazole (0.5g, 2.47 mmol), the solution turned dark red. The resulting solution was refluxed for 3 hours. Upon standing colourless crystals of the product formed which were filtered and air dried.

Yield: 0.148g, 43.3%

% Calc: 45.62%C; 2.68%H; 21.28%N,

% Found: 45.45%C; 3.02%H; 21.18%N,

IR (KBr): 3406.67, 3112.58, 3084.15, 2928.07, 2345.12, 1637.48, 1597.84, 1467.55, 1421.96, 1384.90, 1311.94, 1232.33, 1162.53, 1119.95, 1040.16, 1013.65, 978.41, 903.93, 888.58, 873.43, 824.94, 744.35, 707.68, 634.78, 614.87, 527.39, 491.05, 432.78.

Solubility: partially soluble in ethanol and methanol, soluble in DMSO

E.5.3 [$Co(TBZH)_2(NO_3)](NO_3).H_2O$ (10)

To a solution of $CoNO_3.6H_2O$(0.5 g, 1.7 mmol) in ethanol (100 cm^3) (red solution), was added thiabendazole (0.7g, 3.4 mmol). The resulting orange solution was refluxed for 3 hours. The red/orange solution, upon standing for one month, yielded orange crystals of the product.

Yield: 0.1g, 9.75%

% Calc: 39.8%C; 2.67%H; 18.56%N,

% Found: 39.7%C; 2.6%H; 18.5%N,

IR (KBr): 3104.26, 1655.41, 1624.33, 1591.28, 1505.84, 1418.28, 1384.08, 1311.79, 1228.29, 1147.08, 1115.32, 1045.21, 1032.37, 1009.87, 993.54, 928.77, 902.65, 880.71, 837.94, 830.05, 817.84,

789.50, 766.32, 746.54, 652.24, 628.66, 571.58, 549.91, 492.90, 486.27, 434.92.

Solubility: soluble in ethanol, methanol

μ_{eff}: 4.82BM

Λ_M (EtOH): 202.73 cm^2mol^{-1}

λmax (EtOH): 313nm

E.5.3A $[Co(TBZH)_3](NO_3)_2.0.5EtOH.H_2O$ (11)

To a solution of $CoNO_3.6H_2O$(0.5 g, 1.7 mmol) in ethanol (100 cm^3) (red solution), was added thiabendazole (1.36g, 6.8 mmol). The resulting orange solution was refluxed for 3 hours. Upon standing for two weeks the resulting solution yielded red/orange crystals of the product.

Yield: 0.47g, 33.33%

% Calc: 44.98%C; 3.16%H; 18.61%N,

% Found: 44.86%C; 3.11%H; 18.33%N,

IR (KBr): 3362.69, 3142.21, 3092.17, 3064.47, 2967.58, 2911.82, 2824.49, 2753.89, 1623.29, 1591.53, 1507.98, 1477.72, 1454.02, 1428.91, 1383.61, 1323.63, 1298.78, 1278.41, 1228.66, 1195.39, 1148.81, 1113.99, 1041.52, 1010.61, 992.87, 928.11, 904.37, 875.19, 833.33, 744.72, 651.75, 626.91, 571.26, 550.70, 486.21, 431.95.

Solubility: soluble in ethanol, methanol

μ_{eff}: 4.98BM

Λ_M (EtOH): 122.83 cm^2mol^{-1}

λmax (EtOH): 322nm

E.5.4 $[Ni(TBZH)_2.(NO_3)_2](NO_3).H_2O$ (12)

To a green solution of $Ni(NO_3)_2.6H_2O$(0.5 g, 1.7 mmol) in ethanol (100 cm^3), was added thiabendazole (0.7g, 3.4 mmol). The resulting blue solution was refluxed for 3 hours. The clear blue solution upon standing for two weeks, yielded blue crystals of the product.

Yield: 0.35g, 34.13%

% Calc: 39.8%C; 2.67%H; 18.57%N,

% Found: 39.675%C; 2.625%H; 18.405%N,

IR (KBr): 3105.20, 2358.35, 4659.24, 1624.47, 1592.09, 1508.42, 1464.46, 1417.41, 1384.24, 1312.09, 1295.50, 1229.02, 1145.59, 1115.48, 1037.13, 1010.47, 994.61, 931.52, 903.81, 880.44, 878.40, 831.13, 818.33, 789.29, 765.77, 745.79, 652.67, 629.57, 572.41, 551.61, 486.24, 428.56.

Solubility: ethanol, methanol

μ_{eff}: 2.89BM

Λ_M **(EtOH):** 115.87cm^2mol^{-1}

λmax (EtOH): 307nm

E.5.5 $[Zn(TBZH)_2(NO_3)](NO_3)$ (13)

To a colourless solution of $Zn(NO_3)_2.6H_2O$(0.5 g, 2.6 mmol) in ethanol (100 cm^3), was added thiabendazole (1g, 5 mmol). The resulting colourless suspension was refluxed for 3 hours. The product was filtered off, washed with water and ethanol, and then air-dried. (The filtrate was left to stand for two weeks resulting in a small quantity of colourless crystals of the product forming.)

Yield: 0.6g, 38.98%

% Calc: 40.5%C; 2.38%H; 18.93%N,

% Found: 40.5%C; 2.33%H; 18.75%N,

IR (KBr): 3098.27, 1944.09, 1766.89, 1676.84, 1624.65, 1592.26, 1510.51, 1469.72, 1440.72, 1396.45, 1324.01, 1289.77, 1229.04, 1195.71, 1149.26, 1116.14, 1044.82, 1024.87, 1011.44, 995.07, 932.34, 877.49, 840.89, 814.17, 761.39, 745.27, 724.46, 649.89, 626.87, 569.86, 551.21, 485.79, 432.42.

Solubility: soluble in ethanol, methanol and DMSO

Λ_M (EtOH): 195.47 cm^2mol^{-1}

λmax (EtOH): 307nm

E.5.6 $[Ag_2(TBZ)(TBZH)](NO_3)$ (14)

To a colourless suspension of $AgNO_3$(0.5 g, 2 mmol) in ethanol (100 cm^3), was added, thiabendazole (0.6g, 4 mmol). The resulting solution was refluxed for 3 hours. The powder was filtered off, washed with water and ethanol, and then air-dried.

Yield: 0.7g, 51.5%

% Calc: 35.36%C; 1.92%H; 14.43%N,

% Found: 36.1%C; 1.98%H; 15.4%N,

IR (KBr): 3443.48, 3088.70, 2953.04, 2810.43, 2653.91, 2365.22, 2337.39, 1627.83, 1572.17, 1499.13, 1450.43, 1401.74, 1384.35, 1360.00, 1318.26, 1234.78, 1196.52, 1147.83, 1102.61, 1008.70, 987.83, 904.35, 886.96, 838.26, 730.43, 646.96, 629.57, 535.65, 431.30.

Solubility: insoluble in water, ethanol, methanol, acetone, trichloromethane and DMSO

E.5.6A [Ag(TBZH)$_2$](NO$_3$).0.5EtOH.0.5H$_2$O (15)

To a colourless suspension of $AgNO_3$(0.5 g, 2 mmol) in ethanol (100 cm^3), was added, thiabendazole (1.6g, 8 mmol). The resulting suspension was refluxed for 3 hours. The powder was filtered off, washed with water and ethanol, and then air-dried.

Yield: 0.84g, 70%

% Calc: 41.7%C; 2.97%H; 16.21%N,

% Found: 41.78%C; 2.38%H; 16.87%N,

IR (KBr): 3436.13, 3100.25, 2987.67, 2820.66, 2763.02, 2540.90, 2362.27, 1928.13, 1888.14, 1762.12, 1666.91, 1627.65, 1599.68, 1579.46, 1500.43, 1468.46, 1453.08, 1382.79, 1233.22, 1203.89, 1146.96, 1117.22, 1097.26, 1041.66, 1009.69, 995.57, 918.31, 897.45, 885.49, 823.19, 759.07, 739.26, 641.44, 573.17, 548.20, 486.34, 434.18.

Solubility: insoluble in water, ethanol, methanol, acetone, trichloromethane and DMSO

E.6 Reactions of Thiabendazole with Metal Sulpates

E.6.1 Attempted reaction of TBZH with Manganese(II)Sulphate

To a solution of $MnSO_4.H_2O$ (0.5 g, 2.95 mmol) in ethanol (100 cm^3) (clear/yellow solution), was added thiabendazole (1.19g, 5.9 mmol), the suspension turned white. The resulting suspension was refluxed for 3 hours. The colourless solid which deposited was filtered off, washed with water and ethanol, and then air-dried. IR spectroscopy confirmed this to be unreacted TBZH.

E.6.1A $[Mn(TBZH)_6](SO_4).0.5EtOH$ (16)

To a solution of $MnSO_4.H_2O$ (0.5 g, 2.95 mmol) in ethanol (100 cm^3) (clear/yellow solution), was added thiabendazole (2.37g, 11.8 mmol), the suspension turned white. The resulting suspension was refluxed for 3 hours. The colourless solid which deposited was filtered off, washed with water and ethanol, and then air-dried.

Yield: 1.24g, 31%

% Calc: 53.03%C; 3.28%H; 18.25%N,

% Found: 53.84%C; 3.18%H; 18.75%N,

IR (KBr): 3091.30, 2360.49, 1622.70, 1578.19, 1483.43, 1449.81, 1406.88, 1360.41, 1304.04, 1274.63, 1226.51, 1097.68, 1010.91, 985.95, 898.53, 872.78, 828.73, 739.76, 607.83, 531.31, 491.96.

Solubility: insoluble in water, ethanol, methanol, acetone and DMSO

μ_{eff}: 6.29BM

E.6.2 $[Fe(TBZH)](SO_4).8H_2O$ (17)

To a yellow solution of $Fe(II)SO_4$(0.5 g, 1.7 mmol) in ethanol (100 cm^3), was added thiabendazole (0.7g, 3.5 mmol) and the resulting solution was refluxed for 3 hours, afterwhich time a yellow powder precipitated. The product was filtered off, washed with water and ethanol, and then air-dried.

Yield: 0.5g, 59.14%

% Calc: 24.15%C; 4.62%H; 8.45%N,

% Found: 23.85%C; 2.565%H; 8.18%N,

IR (KBr): 3629.49, 3087.46, 2360.33, 2342.34, 1636.20, 1592.71, 1508.05, 1476.85, 1457.57, 1430.94, 1326.18, 1278.79, 1125.75, 1011.20, 992.32, 928.71, 877.69, 837.75, 748.28, 668.13, 603.35, 525.76, 487.73.

Solubility: insoluble in water, ethanol, methanol, acetone and trichloromethane, soluble in DMSO

μ_{eff}: 6.46BM

E.6.3 $[Co(TBZH)_2](SO_4).3H_2O$ (18)

To a pink solution of $CoSO_4.7H_2O$ (0.5 g, 1.77 mmol) in ethanol (100 cm^3),was added thiabendazole (0.5g, 2.47 mmol). The resulting pale pink solution was refluxed for 3 hours, after which time a pink powder precipitated. The product was filtered off, washed with water and ethanol, and then air-dried.

Yield: 0.9g, 83%

% Calc: 39.25%C; 3.27%H; 13.73%N,

% Found: 39.26%C; 2.745%H; 13.405%N,

IR (KBr): 3084.50, 2758.05, 1625.10, 1592.04, 1508.47, 1477.75, 1457.69, 1431.86, 1326.58, 1279.96, 1230.24, 1096.60, 1010.73, 992.73, 929.24, 876.83, 837.67, 765.50, 747.23610.68, 551.93, 487.99, 436.71.

Solubility: insoluble in water, ethanol, methanol, acetone, trichloromethane and DMSO

μ_{eff}:5.84BM

E.6.3A $[Co(TBZH)_3](SO_4).0.5EtOH.H_2O$ (19)

To a pink solution of $CoSO_4.7H_2O$ (0.5 g, 1.77 mmol) in ethanol (100 cm^3),was added thiabendazole (1.42g, 7.08 mmol). The resulting pale orange suspension was refluxed for 3 hours, after which time a pale orange powder precipitated. The product was filtered off, washed with water and ethanol, and then air-dried.

Yield: 0.86g, 60.56%

% Calc: 46.55%C; 3.27%H; 15.76%N,

% Found: 46.12%C; 2.96%H; 15.99%N,

IR (KBr): 3076.73, 2958.94, 2755.60, 2680.34, 1622.45, 1590.76, 1507.96, 1475.50, 1456.46, 1428.68, 1325.72, 1298.87, 1277.49, 1206.64, 1125.25, 1087.24, 1009.78, 990.98, 928.60, 877.92, 836.72, 766.76, 747.86, 653.45, 606.38, 570.81, 531.29, 487.70, 435.76.

Solubility: insoluble in water, ethanol, methanol, acetone, trichloromethane and DMSO

μ_{eff}: 4.89BM

E.6.4 $[Ni(TBZH)_2](SO_4).7H_2O$ (20)

To a pale green solution of $NiSO_4.6H_2O$(0.5 g, 1.9 mmol) in ethanol (100 cm^3), was added thiabendazole (0.7g, 3.8 mmol). The resulting pale blue solution was refluxed for 3 hours, afterwhich time a pale blue powder precipitated. The product was filtered off, washed with water and ethanol, and then air-dried.

Yield: 0.9g, 69.76%

% Calc: 35.15%C; 4.12%H; 12.29%N,

% Found: 34.98%C; 3.39%H; 12.39%N,

IR (KBr): 3082.20, 2360.84, 1624.56, 1591.99, 1509.42, 1478.49, 1458.45, 1433.69, 1327.02, 1301.11, 1280.23, 1230.03, 1092.80, 1011.50, 993.79, 931.45, 876.21, 838.05, 765.56, 746.29, 615.58, 554.84, 487.98, 435.11.

Solubility: Insoluble in water, ethanol, methanol, acetone, DMSO and trichloromethane

μ_{eff}: 4.28BM

E.6.5 $[Zn(TBZH)_2](SO_4).0.5EtOH.2H_2O$ (21)

To a colourless solution of $ZnSO_4.7H_2O$(0.5 g, 1.7 mmol) in ethanol (100 cm^3), was added thiabendazole (0.7g, 3.4 mmol). The resulting colourless suspension was refluxed for 3 hours. The product was filtered off, washed with water and ethanol, and then air-dried.

Yield: 0.8g, 75.5%

% Calc: 40.48%C; 3.39%H; 13.48%N,

% Found: 39.78%C; 3.11%H; 13.16%N,

IR (KBr): 3386.94, 3082.88, 2964.09, 2360.68, 2342.56, 1623.38, 1592.40, 1508.67, 1479.03, 1457.67, 1433.96, 1327.85, 1299.79, 1281.11, 1098.22, 1010.51, 993.76, 929.39, 876.68, 836.11, 765.16, 748.31, 650.92, 601.33, 571.46, 551.61, 485.43, 438.12.

Solubility: insoluble in ethanol, acetone, trichloromethane and DMSO

E.6.6 $[Ag_2(TBZH)_2](SO_4).EtOH$ (22)

To a colourless solution of Ag_2SO_4(0.5 g, 1.6 mmol) in ethanol (100 cm^3), was added thiabendazole (0.35g, 3.2 mmol). The resulting suspension was refluxed for 3 hours. The product was filtered off, washed with water and ethanol, and then air-dried.

Yield: 0.47g, 38.84%

% Calc: 34.75%C; 2.65%H; 11.05%N,

% Found: 35.64%C; 2.33% H; 12.02%N,

IR (KBr): 3415.89, 3086.80, 2957.32, 2866.74, 2810.85, 2757.04, 2677.98, 1664.72, 1625.21, 1597.59, 1575.33, 1520.55, 1501.15, 1452.56, 1423.46, 1326.17, 1296.42, 1230.64, 1136.05, 1095.07, 1047.45, 1007.10, 992.53, 917.46, 885.60, 835.22, 738.78, 600.98, 548.58, 524.92, 488.47, 434.76.

Solubility: insoluble in water, ethanol, methanol, acetone, trichloromethane and DMSO

E.6.6A $[Ag_2(TBZH)_2](SO_4).EtOH$ (23)

To a colourless solution of Ag_2SO_4(0.5 g, 1.6 mmol) in ethanol (100 cm^3), was added thiabendazole (1.28g, 6.4 mmol). The resulting suspension was refluxed for 3 hours. The product was filtered off, washed with water and ethanol, and then air-dried.

Yield: 0.59g, 48.76%

% Calc: 34.75%C; 2.65%H; 11.05%N,

% Found: 35.5%C; 2.27% H; 11.7%N,

IR (KBr): 3415.89, 3086.80, 2957.32, 2866.74, 2810.85, 2757.04, 2677.98, 1664.72, 1625.21, 1597.59, 1575.33, 1520.55, 1501.15, 1452.56, 1423.46, 1326.17, 1296.42, 1230.64, 1136.05, 1095.07, 1047.45, 1007.10, 992.53, 917.46, 885.60, 835.22, 738.78, 600.98, 548.58, 524.92, 488.47, 434.76.

Solubility: insoluble in water, ethanol, methanol, acetone, trichloromethane and DMSO

E.7 Reactions of Thiabendazole with Metal Acetates

E.7.1 [Mn(TBZ)(TBZH)CH_3COO]0.5H_2O (24)

To a solution of $Mn(CH_3COO)_2.4H_2O$ (0.5 g, 2.04 mmol) in ethanol (100 cm^3) (clear/yellow solution), was added thiabendazole (0.82g, 4.08 mmol), the suspension turned white. The resulting suspension was refluxed for 3 hours. The colourless solid which deposited was filtered off, washed with water and ethanol, and then air-dried.

Yield: 0.52g, 48.59%

% Calc: 50.38%C; 3.26%H; 16.02%N,

% Found: 50.67%C; 3.05%H; 15.74%N,

IR (KBr): 3079.52, 1890.77, 1529.00, 1469.79, 1404.91, 1324.92, 1296.28, 1274.22, 1227.67, 1160.95, 1111.25, 1044.71, 1010.37, 923.70, 878.72, 836.61, 770.26, 746.91, 654.37, 630.13, 613.00, 555.20, 491.11, 471.04, 439.81.

Solubility: insoluble in water, ethanol, methanol, acetone and DMSO

μ_{eff}: 5.47BM

E.7.1A [Mn(TBZ)$(TBZH)_2CH_3COO$] (25)

To a solution of $Mn(CH_3COO)_2.4H_2O$ (0.5 g, 2.04 mmol) in ethanol (100 cm^3) (clear/yellow solution), was added thiabendazole (1.6g, 8.16 mmol), the suspension turned white. The resulting suspension was refluxed for 3 hours. The colourless solid which deposited was filtered off, washed with water and ethanol, and then air-dried.

Yield: 1.19g, 81.5%

% Calc: 53.62%C; 3.23%H; 17.58%N,

% Found: 53.50%C; 3.26%H; 17.42%N,

IR (KBr): 3081.25, 2359.31, 1527.71, 1405.32, 1300.37, 1226.82, 1198.83, 1095.51, 1045.75, 1007.79, 874.72, 830.06, 742.99, 629.55, 562.67, 536.54, 485.03, 435.14, 489.50.

Solubility: insoluble in water, ethanol, methanol, acetone and DMSO

μ_{eff}: 5.78BM

E.7.2 [Co(TBZ)(TBZH)CH_3COO] (26)

To a pink solution of $(CH_3COO)_2Co.4H_2O$ (0.5 g, 2 mmol) in ethanol (100 cm^3), was added thiabendazole (0.8g, 4 mmol). The resulting orange suspension was refluxed for 3 hours, after which time a red solution formed. Upon cooling a pink solid formed. The product was filtered off, washed with water and ethanol, and then air-dried.

Yield: 0.39g, 37.5%

% Calc: 50.85%C; 3.08%H; 16.18%N,

% Found: 50.77%C; 2.97%H; 16.97%N,

IR (KBr): 3087.01, 2360.36, 1591.05, 1553.18, 1516.04, 1470.96, 1470.96, 1429.87, 1399.84, 1372.28, 1326.09, 1299.73, 1274.63, 1227.96, 1195.78, 1146.03, 1114.53, 1010.96, 983.18, 926.09, 909.35, 874.05, 829.45, 784.82, 754.58, 667.53, 655.35, 634.72, 625.08, 489.50.

Solubility: soluble in ethanol, methanol and DMSO

μ_{eff}: 4.45BM

Λ_M (EtOH): 53.64 cm^2mol^{-1}

λmax (EtOH): 337nm

E.7.2A [Co(TBZ)(TBZH)$_2$CH$_3$COO]H$_2$O (27)

To a pink solution of $(CH_3COO)_2Co.4H_2O$ (0.5 g, 2 mmol) in ethanol (100 cm^3), was added thiabendazole (1.6g, 8mmol). The resulting orange suspension was refluxed for 3 hours. Upon cooling an orange solid formed. The product was filtered off, washed with water and ethanol, and then air-dried.

Yield: 0.69g, 46.9%

% Calc: 52.02%C; 3.41%H; 17.06%N,

% Found: 52.14%C; 3.41%H; 17.95%N,

IR (KBr): 3085.33, 1590.61, 1552.32, 1511.33, 1470.92, 1429.80, 1399.38, 1367.79, 1324.86, 1299.35, 1273.88, 1227.88, 1195.79, 1146.35, 1114.04, 1048.54, 1010.29, 986.76, 925.95, 908.44, 873.84, 830.11, 784.87, 753.12, 654.80, 634.49, 574.18, 553.87, 489.18, 435.98.

Solubility: soluble in ethanol, methanol and DMSO

μ_{eff}: 4.82BM

Λ_M **(EtOH):** 39.62 cm^2mol^{-1}

λmax (EtOH): 304nm

E.7.3 [Ni (TBZH)$_2$(CH$_3$COO)$_2$]0.5EtOH.H$_2$O (28)

To a green solution of $(CH_3COO)_2Ni.4H_2O$ (0.5 g, 2 mmol) in ethanol (100 cm^3), was added thiabendazole (0.8g, 4 mmol). The resulting blue solution was refluxed for 3 hours, after which time a blue powder precipitated. The product was filtered off, washed with water and ethanol, and then air-dried.

Yield: 0.33g, 26.61%

% Calc: 48.4%C; 4.06%H; 13.54%N,

% Found: 48.29%C; 2.78%H; 13.97%N,

IR (KBr): 3386.28, 3086.27, 2950.22, 2750.22, 2345.39, 1685.87, 1655.02, 1618.71, 1589.06, 1560.59, 1546.54, 1508.48, 1477.70, 1458.12, 1432.92, 1385.10, 1299.03, 1279.21, 1228.11, 1147.92, 1011.13, 994.26, 929.90, 873.63, 787.60, 766.69, 743.24, 654.31, 626.99, 553.60, 486.95, 433.86.

Solubility: Insoluble in water, ethanol, methanol, acetone, trichloromethane and DMSO

μ_{eff}: 2.96 B.M.

E.7.4 $[Zn(TBZH)_2(CH_3COO)_2]$(29)

To a colourless solution of $(CH_3COO)_2Zn.2H_2O$ (0.5 g, 2.27 mmol) in ethanol (100 cm^3), was added thiabendazole (0.9g, 4.5 mmol). The resulting colourless suspension was refluxed for 3 hours. The product was filtered off, washed with water and ethanol, and then air-dried.

Yield: 1g, 72.99%

% Calc: 47.69%C; 3.64%H; 13.91%N,

% Found: 46.16%C; 2.96%H; 14.14%N,

IR (KBr): 3417.72, 3063.82, 1598.22, 1567.75, 1505.03, 1474.85, 1408.88, 1382.86, 1328.70, 1279.31, 1230.53, 1205.86, 1148.10, 1120.17, 1028.01, 1012.04, 995.47, 931.42, 920.38, 876.18, 834.33, 746.66, 665.05, 645.62, 615.45, 571.82, 533.95, 487.96, 439.59.

Solubility: soluble in ethanol, methanol, acetone and trichloromethane

Λ_M (EtOH): 41.39 cm^2mol^{-1}

λmax (EtOH): 337nm

E.7.5 Attempted reaction of TBZH with Silver(I)Acetate

To a colourless suspension of $(CH_3COO)Ag$ (0.5 g, 2.9 mmol) in ethanol (100 cm^3), was added thiabendazole (1.16g, 5.8 mmol). The resulting suspension was refluxed for 3 hours. The powder was filtered off, washed with water and ethanol, and then air-dried. IR spectroscopy confirmed the powder to be a mixture of unreacted starting materials.

E.7.5A $[Ag_2(TBZH)_2(CH_3COO)_2]$ H_2O (30)

To a colourless suspension of $(CH_3COO)Ag$ (0.5 g, 2.9 mmol) in ethanol (100 cm^3), was added thiabendazole (2.33g, 11.6 mmol). The resulting suspension was refluxed for 3 hours. The powder was filtered off, washed with water and ethanol, and then air-dried.

Yield: 0.5g, 22.93%

% Calc: 38.21%C; 2.93%H; 11.14%N,

% Found: 38.59%C; 1.74%H; 10.45%N,

IR (KBr): 3418.09, 3098.95, 3078.17, 3045.55, 1745.80, 1605.77, 1565.49, 1473.23, 1440.77, 1395.59, 1336.28, 1295.50, 1230.00, 1201.89, 1142.61, 1110.65, 1051.52, 1034.93, 1018.96, 999.26, 909.87, 883.09, 833.56, 803.80, 782.57, 750.44, 726.65, 671.70, 637.36, 620.08, 577.90, 484.94, 436.22.

Solubility: insoluble in water, ethanol, methanol, acetone, trichloromethane and DMSO

E.8 BIOLOGICAL PREPARATIONS AND METHODS

Fungal Isolates: An isolate of *Candida albicans* was obtained from Oxoid (ATCC 10231). *Candida* species were stored on Sabouraud dextrose agar (SDA) plates at 4 °C, and were subcultured monthly from the initial culture received.

Sterilisation was achieved by autoclaving at 121 °C and 100 kPa for 15 min. Alternatively, solutions that were susceptible to decomposition during autoclaving were sterilised by membrane filtration using 0.45 μm Millipore membrane filters.

Cell density was measured using McFarland standards.

Sabouraud dextrose agar (SDA) was obtained from Difco (0109-17-1) and made up according to the manufacturers instructions.

Minimal Media: 2% glucose, 0.17% yeast nitrogen base and 0.5% ammonium sulphate was dissolved in distilled water in a duran bottle. The resulting solution was autoclaved and stored at 4°C.

Phosphate buffered saline (PBS) was obtained from Oxoid (BR 14a) in tablet form and was prepared as follows:

1 tablet was dissolved in cold distilled water (100 cm^3) and the resulting solution autoclaved for 15 mins.

E.9 Preparation of complex solutions for antimicrobial susceptibility testing

Solutions or suspensions of test complexes were ground to a fine powder and dissolved the complex (0.1 g) in 0.1% DMSO (100 cm^3) to yield a stock solution at a concentration of 1000 $\mu g/cm^3$. Dilutions of the stock solution were prepared; 750$\mu g/cm^3$, 500$\mu g/cm^3$, 200$\mu g/cm^3$, 100$\mu g/cm^3$ and 50$\mu g/cm^3$. Yielding working solutions of the test complexes of concentrations 100$\mu g\ cm^{-3}$, 75 $\mu g\ cm^{-3}$, 50 $\mu g\ cm^{-3}$, 20 $\mu g\ cm^{-3}$, 10 $\mu g\ cm^{-3}$ and 5 $\mu g\ cm^{-3}$.

E.10 Antimicrobial Susceptibility testing methods

Yeast susceptibility testing: The broth microdilution reference method was used[69]. Prior to testing yeast cells were grown on SDA at 37°C for 24 h. Cell suspensions were prepared in sterile phosphate buffered saline (5cm^3) to a density of 0.5 McFarland standard. A 1:100 dilution of the 0.5 McFarland standard yeast suspension was made in minimal medium. The cell concentration of the final inoculum was $3.5x10^4$–$5.0x10^5$ cells cm^{-3}. The prepared cell suspension (90µl) was dispensed into microtitre plates and to this was added the test complex solutions (10µl) to yield working solutions of the test complexes of concentrations 100$\mu g\ cm^{-3}$, 75$\mu g\ cm^{-3}$, 50$\mu g\ cm^{-3}$, 20$\mu g\ cm^{-3}$, 10$\mu g\ cm^{-3}$ and 5$\mu g\ cm^{-3}$. Plates were then incubated for 24 h at 37°C with continuous shaking. Each complex was assessed in triplicate and three independent experiments were performed.

DISCUSSION

D.1 INTRODUCTION

Previous studies in this laboratory showed that Thiabendazole (TBZH), is a poor anti-*candida* agent[37]. Co-ordination of TBZH to a copper (II) centre resulted in a significant increase in its antifungal activity and also a significant increase in its chemotherapeutic potential was observed[37]. It was also shown that the nature of the counter ion in the complex could influence antimicrobial potency.

During the present study Thiabendazole was reacted with chloride, sulphate, nitrate and acetate salts of a range of transition metals (M=Mn^{+2}, Fe^{+2}, Fe^{+3}, Co^{+2}, Ni^{+2} and Ag^{+1}) in accordance with *Scheme 1*.

$$MX_n + yTBZH \xrightarrow[\text{REFLUX}]{\text{ETOH}} [MX_n(TBZH)_y]$$

where M = Mn^{+2}, Fe^{+2}, Fe^{+3}, Co^{+2}, Ni^{+2} , Zn^{+2} and Ag^{+1}

X = Cl^-, SO_4^-, NO_3^- and CH_3COO^-

n = 1,2,3

y = 1,2,3

Scheme 1: The synthetic pathway to the thiabendazole metal complexes

The anti-*candida* activity of these compounds was also studied.

D.2.1 Reaction of Thiabendazole with Metal Chlorides

Thiabendazole was reacted with the chloride salts of Manganese(II), Iron(III), Cobalt(II), Nickel(II) and Zn(II) in accordance with the general reaction equation shown in *Scheme 1* to yield complexes (**1**) – (**7**). The complexes were obtained as colourless {(**1**),(**2**) and (**7**)}, brown (**3**), purple (**4**), orange (**5**) and green (**6**) powders, respectively and they were formulated as shown below.

(1) **$[Mn(TBZH)_2Cl_2].3H_2O.0.5EtOH$**

% Calc: 41.62%C; 3.79%H; 13.87%N,

% Found: 41.14%C; 2.24%H; 14.04%N

(2) **$[Mn(TBZH)_3Cl_2].0.5EtOH$**

% Calc: 49.42%C; 3.18%H; 16.74%N,

% Found: 49.05%C; 2.79%H; 16.81%N

(3) **$[Fe(TBZH)_2Cl_3]H_2O.0.5EtOH$**

% Calc: 41.65%C; 3.14%H; 13.88%N,

% Found: 41.4%C; 2.925%H; 13.59%N

(4) **$[Co(TBZH)_2Cl_2]0.5H_2O.\ 0.5EtOH$**

% Calc: 44.65%C; 3.19%H; 14.88%N,

% Found: 44.43%C; 2.705%H; 14.7%N,

(5) **$[Co(TBZH)_3Cl_2]0.5EtOH$**

% Calc: 49.16%C; 3.17%H; 16.65%N,

% Found: 49.01%C; 3.33%H; 17.05%N,

(6) **$[Ni(TBZH)_2Cl_2]0.5EtOH$**

% Calc: 45.43%C; 3.07%H; 15.13%N,

% Found: 44.55%C; 2.985%H; 15.26%N,

(7) **$[Zn(TBZH)Cl_2]$**

% Calc: 35.54%C; 2.07%H; 12.44%N,

% Found: 35.475%C; 2.05%H; 12.62%N,

The room temperature magnetic moments of powdered samples of the complexes are shown in *Table 6*. The μ_{eff} value for (**2**) is close to the range expected (μ_{eff} =5.6-6.1 B.M.) for manganese complexes where there is no significant exchange interactions between adjacent metal centres[64]. That of complex (**1**) however falls significantly above the expected value and an interaction between the manganese atoms in this compound cannot be ruled out. Complex (**3**) has a room temperature magnetic moment value which falls in the range expected (μ_{eff} =5.7-6.0 B.M.)[64] for simple iron(III) species. The two cobalt complexes (**4**) and (**5**) both have μ_{eff} values that comply with the expected range (4.30-5.20 B.M.)[64] again indicating that no significant metal-metal interactions occur. Complex (**6**) was found to have a μ_{eff} value that was once again in the expected range (μ_{eff} =2.80-3.50 B.M.)[64] for a Nickel(II) complex in which no interactions between the metal centres occur. Whereas complexes (**1**) and (**2**) were totally insoluble in all solvents complex (**3**) –(**7**) were found to be extensively soluble in

a range of polar solvents. All attempts to grow crystals of the soluble compounds were unsuccessful.

Table 6: Magnetic Susceptibility and Molar Conductivity data for complexes (1) – (7)

Complex	μ_{eff} **(B.M.) {room T°}**	Λ_M **(S cm^2mol^{-1}) [in H_2O]**
$[Mn(TBZH)_2Cl_2].3H_2O.0.5EtOH$ (**1**)	6.87	-
$[Mn(TBZH)_3Cl_2].0.5EtOH$ (**2**)	5.56	-
$[Fe(TBZH)_2Cl_3.H_2O]0.5CH_3CH_2OH$ (**3**)	5.86	499.39
$[Co(TBZH)_2Cl_2]0.5H_2O.\ 0.5CH_3CH_2OH$ (**4**)	5.19	206.89
$[Co(TBZH)_3Cl_2]0.5CH_3CH_2OH$ (**5**)	4.51	120.56
$[Ni(TBZH)_2Cl_2]0.5CH_3CH_2OH$ (**6**)	3.29	215.55
$[Zn(TBZH)Cl_2]$ (**7**)	-	231.41

The molar conductivity values for the soluble complexes (**3**)-(**7**) are listed in *Table 6* and indicate that all of the complexes dissociate in aqueous solution. The molar conductivity value for an aqueous solution of (**3**) { Λ_M = 499.39 cm^2mol^{-1} } suggest that this complex probably forms a 1 : 3 electrolyte in water and dissociates in accordance to the equilibrium(the solvate molecules are omitted for clarity):

$$[Fe(TBZH)_2Cl_3] \rightleftharpoons [Fe(TBZH)_2]^{3+} + 3Cl^-$$

The molar conductivity values for aqueous solutions of (**4**), (**6**) and (**7**) { Λ_M = 206 - 231 cm^2mol^{-1} } suggests that these complexes probably form 1 : 2 electrolytes in water and dissociates in accordance to the following equilibria (the solvate molecules are omitted for clarity):

$$[Co(TBZH)_2Cl_2] \rightleftharpoons [Co(TBZH)_2]^{2+} + 2Cl^-$$

$$[Ni(TBZH)_2Cl_2] \rightleftharpoons [Ni(TBZH)_2]^{2+} + 2Cl^-$$

$$[Zn(TBZH)Cl_2] \rightleftharpoons [Zn(TBZH)]^{2+} + 2Cl^-$$

The molar conductivity of complex (**5**) in aqueous solution {Λ_M = 120.56 cm^2mol^{-1}} suggests that this complex probably forms a 1 : 1 electrolyte in water and may dissociates in accordance to the equilibrium(the solvate molecules are omitted for clarity):

$$[Co(TBZH)_3Cl_2] \rightleftharpoons [Co(TBZH)_3Cl]^{+} + Cl^-$$

The IR spectra of compounds (**1**)-(**7**) were compared to that of the free TBZH, and a number of differences were noted. The characteristic bands for free TBZH and the important IR spectral bands that provide evidence for the structure of the compounds are listed in *Table 7*.

Table 7: Characteristic IR bands of complexes (**1**)-(**7**) and free thiabendazole.

Band Assignment	**TBZH**	**(1)**	**(2)**	**(3)**	**(4)**	**(5)**	**(6)**	**(7)**
N-H stretch	3093	3089	3084	3092	3083	3063	3084	3095
N-H vibration	1093	1008	1008	1015	1009	1010	1010	1011
$\nu(C=N)_{imidazolic}$	1577	1587	1579	1593	1586	1590	1587	1590
$\nu(C=N)_{thiazolic}$	1480	1472	1473	1481	1473	1476	1474	1478
C-S stretch	1228	1224	1227		1224	1229	1224	1229
M-Cl (stretch)		545	545	553	550	552	553	548

Upon complexation the prominent bands at 3093 cm^{-1} (N-H stretching) and 1093cm^{-1} (N-H vibration) have remained in the spectra for compounds (**1**)-(**7**) but shifted slightly. The $\nu(C=N)_{imidazolic}$ and $\nu(C=N)_{thiazolic}$ bands (1577 cm^{-1} and 1480 cm^{-1} respectivley) in the free ligand are present in the spectra of all 7 compounds, but have shifted slightly indicating that the ligand is coordinated through the imidazolic and the thiazolic nitrogens. For compounds (**1**), (**2**), (**4**), (**6**) and (**7**) the C-S stretching band (at 1228cm^{-1} for the free ligand) remains essentially unchanged suggesting that the sulfur atom in the thiazole ring is uncoordinated. For the iron complex (**3**) the C-S band at 1228cm^{-1} is not present indicating that the sulfur atom in the thiazole ring may be bound to a metal centre. The presence of a new band in the range 545-555 cm^{-1} in the spectra of all of the complexes, which is not present in the spectrum of TBZH, may indicate that at least one of the chloride anions is bound to the central metal. The spectra of complexes (**1**) – (**6**) all have a new band at approximately 2970 cm^{-1} (Aliphatic C-H stretching) supporting the inclusion of the ethanol molecules of crystallization shown in their formulations. This band is not present for complex (**7**).

D.2.2 Reaction of Thiabendazole with Metal Nitrates

Thiabendazole was reacted with the Nitrate salts of Manganese(II), Iron(III), Cobalt(II), Nickel(II), Zinc(II) and Silver (I) in accordance with the general reaction equation shown in *Scheme 1* to yield compounds **(8)–(15)**. The compounds were obtained as colourless powders {**(8)**, **(13)**, **(14)** and **(15)**}, colourless crystals (**9**), orange microcrystals {**(10)**, **(11)**} and blue microcrystals (**12**), respectively and they were formulated as shown below. Attempts to react manganese(II) nitrate with TBZH in a 1:2 ratio were unsuccessful.

(8) **$[Mn(TBZH)_2(NO_3)]NO_3.H_2O$**

% Calc: 40.07%C; 2.69%H; 18.69%N,

% Found: 40.28%C; 2.27%H; 18.76%N,

(9) **$[TBZH_2NO_3]$**

% Calc: 45.62%C; 2.68%H; 21.28%N,

% Found: 45.45%C; 3.02%H; 21.18%N

(10) **$[Co(TBZH)_2(NO_3)]NO_3.H_2O$**

% Calc: 39.8%C; 2.67%H; 18.56%N

% Found: 39.7%C; 2.6%H; 18.5%N

(11) **$[Co(TBZH)_3](NO_3)_2.0.5EtOH.H_2O$**

% Calc: 44.98%C; 3.16%H; 18.61%N

% Found: 44.86%C; 3.11%H; 18.33%N

(12) **$[Ni(TBZH)_2.(NO_3)](NO_3).H_2O$**

% Calc: 39.8%C; 2.67%H; 18.57%N

% Found: 39.67%C; 2.62%H; 18.40%N

(13) **$[Zn(TBZH)_2(NO_3)](NO_3)$**

% Calc: 40.5%C; 2.38%H; 18.93%N,

% Found: 40.5%C; 2.33%H; 18.75%N,

(14) **$[Ag_2(TBZ)(TBZH)](NO_3)$**

% Calc: 35.36%C; 1.92%H; 14.43%N,

% Found: 36.1%C; 1.98%H; 15.4%N,

(15) **$[Ag(TBZH)_2](NO_3).0.5EtOH.0.5H_2O$**

% Calc: 41.7%C; 2.97%H; 16.21%N,

% Found: 41.78%C; 2.38%H; 16.87%N

The extremely novel non metal based nitrate salt $[TBZH_2NO_3]$ (**9**) was the major product (45% yield) of a reaction between TBZH and $Fe(III)(NO_3)_3.9H_2O$. Attempts to generate this salt using a direct method involving nitric acid and TBZH have so far been unsuccessful. Hydrated Fe(II) salts are known to act as aqua acids, a fact which could explain the protonation of the TBZH molecule during this reaction[65]. In aqueous solution the iron(III) nitrate dissociates to form $[Fe(H_2O)_6]^{3+}$ and it is this species which acts as the aqua acid. A possible mechanism for the formation of (**9**) is shown in *Scheme 2.*

$$[Fe(H_2O)_6]^{3+} + 3NO_3^- \xrightarrow{TBZH} [Fe(H_2O)_5(OH)]^{2+} + 2NO_3^- + [TBZH_2NO_3]$$

Scheme 2: A possible mechanism for the formation of (**9**)

Failure to isolate any Iron complex formed during this reaction may well be due its lack of stability.

The X-ray crytal structure of (**9**) is shown in *Figure 40* and selected bond lengths and angles are listed in *Table 8*. The asymmetric unit contains one protonated $TBZH_2$ cation and one nitrate anion (*Figure 40*). The TBZH is protonated on the benzimidazole imine nitrogen, resulting in delocalisation of the double bond over the N-C-N section (*Table 8*). The cations are hydrogen bonded (*Table 9*) to nitrate anions *via* each of the NH groups, resulting in a chain along which adjacent $TBZH_2$ units are oriented at approximately right angles to each other (*Figure 41*). There is significant π π-stacking between adjacent $TBZH_2$ cations with interplanar distance c.a. 3.3 Å (*Figure 43*).

Table 8. Bond lengths [Å] and angles [°] for $[TBZH_2NO_3]$ (**9**)

C(1)-C(3)	1.364(3)	C(5)-C(10)	1.398(3)
C(1)-S(1)	1.698(2)	C(6)-C(7)	1.379(3)
S(1)-C(2)	1.7209(19)	C(7)-C(8)	1.407(3)
C(2)-N(1)	1.303(3)	C(8)-C(9)	1.378(3)
N(1)-C(3)	1.379(2)	C(9)-C(10)	1.389(3)
C(3)-C(4)	1.441(3)	C(10)-N(3)	1.381(3)
C(4)-N(2)	1.338(2)	N(11)-O(13)	1.235(2)
C(4)-N(3)	1.341(2)	N(11)-O(11)	1.254(2)
N(2)-C(5)	1.385(3)	N(11)-O(12)	1.258(2)
C(5)-C(6)	1.390(3)		
C(3)-C(1)-S(1)	110.24(15)	C(6)-C(7)-C(8)	121.90(19)
C(1)-S(1)-C(2)	89.13(10)	C(9)-C(8)-C(7)	121.87(19)
N(1)-C(2)-S(1)	115.73(15)	C(8)-C(9)-C(10)	116.41(18)
C(2)-N(1)-C(3)	109.33(16)	N(3)-C(10)-C(9)	131.64(17)
C(1)-C(3)-N(1)	115.57(18)	N(3)-C(10)-C(5)	106.68(16)
C(1)-C(3)-C(4)	124.90(18)	C(9)-C(10)-C(5)	121.68(18)
N(1)-C(3)-C(4)	119.53(16)	C(4)-N(3)-C(10)	108.80(16)
N(2)-C(4)-N(3)	109.24(17)	O(13)-N(11)-O(11)	120.53(17)
N(2)-C(4)-C(3)	125.10(17)	O(13)-N(11)-O(12)	119.37(16)
N(3)-C(4)-C(3)	125.66(17)	O(11)-N(11)-O(12)	120.09(16)
C(4)-N(2)-C(5)	108.96(15)		
N(2)-C(5)-C(6)	131.75(17)		
N(2)-C(5)-C(10)	106.31(17)		
C(6)-C(5)-C(10)	121.94(18)		
C(7)-C(6)-C(5)	116.20(18)		

Table 9. Hydrogen bonds for [$TBZH_2NO_3$] (**9**) [Å and °].

D-H...A	d(D-H)	d(H...A)	d(D...A)	<(DHA)
N(2)-H(2A)...O(12)#1	0.88	1.91	2.785(2)	175.3
N(2)-H(2A)...O(13)#1	0.88	2.58	3.213(2)	129.7
N(3)-H(3)...O(11)#2	0.88	1.98	2.856(2)	170.9

Symmetry transformations used to generate equivalent atoms:
#1 -x+1/2, y+1/2, -z+3/2 and #2 -x, -y+1,-z +1.

Figure 40: The asymmetric unit of [$TBZH_2NO_3$] (**9**)

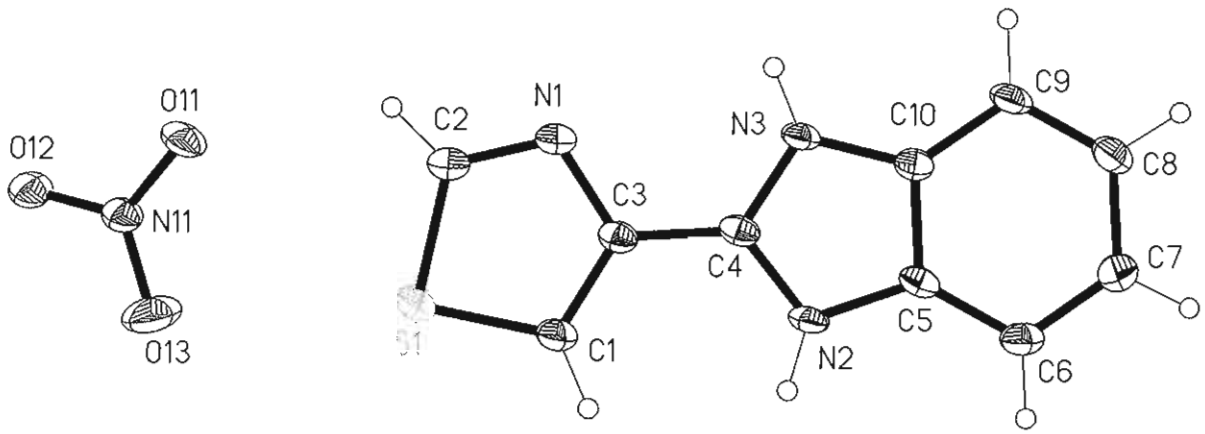

Figure 41: A view of the π-π stacking in [$TBZH_2NO_3$] (**9**)

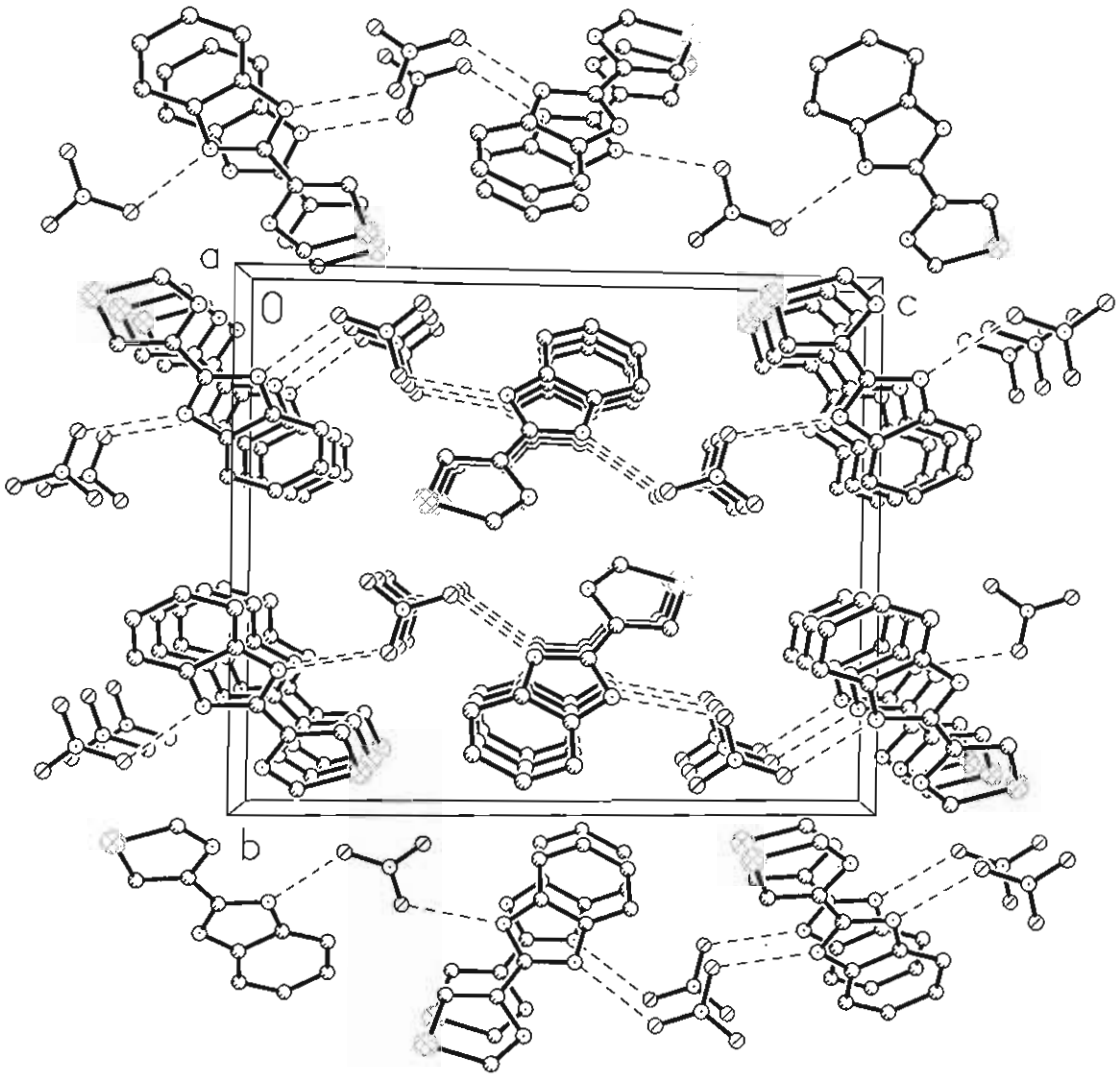

The room temperature magnetic moments of powdered samples of complexes (**8**), (**10**) – (**15**) are shown in *Table 10*. The μ_{eff} value for (**8**) is in the range expected (μ_{eff}=5.6-6.1 B.M.) for manganese complexes where there is no significant exchange interactions between adjacent metal centres[64]. The two cobalt complexes (**10**) and (**11**) both have μ_{eff} values that comply with the expected range (4.30-5.20 B.M.)[64] again indicating that no significant metal-metal interactions occur. Complex (**12**) was found to have a μ_{eff} value that was in the expected range (μ_{eff}=2.80-3.50 B.M.)[64] for a Nickel(II) complex in which no interactions between the metal centres occur. Complexes (**8**), (**9**), (**14**) and (**15**) were insoluble in all solvents, while, (**10**), (**11**), (**12**) and (**13**) were found to be insoluble in water, but soluble in ethanol or methanol or both.

The molar conductivity values for the soluble complexes (**10**)-(**13**) are listed in *Table 10*. The values for aqueous ethanol (10% EtOH) solutions of (**10**) and (**13**) { Λ_M = 202.73 and 195.47 cm^2mol^{-1} } suggest that these complexes probably form 1 : 2 electrolytes in that solvent and dissociate in accordance to the following equilibria (the solvate molecules are omitted for clarity):

$$[Co(TBZH)_2(NO_3)_2] \rightleftharpoons [Co(TBZH)_2]^{2+} + 2NO_3^-$$

$$[Zn(TBZH)_2(NO_3)_2] \rightleftharpoons [Zn(TBZH)_2]^{2+} + 2NO_3^-$$

The molar conductivity values (10% EtOH) for (**11**) and (**12**) {Λ_M = 122.83 and 115.87cm^2mol^{-1}} suggests that these complexes probably form 1 : 1 electrolytes and imply that one of the nitrate anions in the metal complexes may not dissociate from the

metal centre in both complexes. (**11**) and (**12**) may dissociate in accordance to the following equilibria (the solvate molecules are omitted for clarity):

$$[Co(TBZH)_3(NO_3)_2] \rightleftharpoons [Co(TBZH)_3(NO_3)]^+ + NO_3^-$$

$$[Ni(TBZH)_2(NO_3)_2] \rightleftharpoons [Ni(TBZH)_2(NO_3)]^+ + NO_3^-$$

Table 10 Magnetic Susceptibility and Molar Conductivity data for complexes (**8**) – (**15**)

Complex	μ_{eff} (B.M.) {room T°}	Λ_M (S cm^2mol^{-1}) [in EtOH]
$[Mn(TBZH)_2(NO_3)](NO_3).H_2O$ (**8**)	6.09	-
$[TBZH_2NO_3]$ (**9**)	-	-
$[Co(TBZH)_2(NO_3)](NO_3).H_2O$ (**10**)	4.82	202.73
$[Co(TBZH)_3](NO_3)_2.0.5EtOH.H_2O$ (**11**)	4.98	122.83
$[Ni(TBZH)_2.(NO_3)_2](NO_3).H_2O$ (**12**)	2.89	115.87
$[Zn(TBZH)_2(NO_3)](NO_3)$ (**13**)	-	195.47
$[Ag_2(TBZ)(TBZH)](NO_3)$(**14**)	-	-
$[Ag(TBZH)_2](NO_3).0.5EtOH.0.5H_2O$ (**15**)	-	-

Selected IR data for free TBZH, complexes (**8**), (**10**) -(**15**) and the nitrate salt (**9**) are shown in *Table 11*. The IR spectra of complexes (**8**)-(**15**) were compared to that of the free ligand and a number of differences were observed. The N-H stretch at 3093cm^{-1} for the free ligand has remained for all of the compounds, but has shifted slightly. For

compounds (**8**)-(**13**) and (**15**) the N-H vibration band at 1093cm^{-1} found in the free ligand is present but has shifted somewhat with the relative intensity remaining the same. The shift may be due to the proton being involved in hydrogen bonding[66] this band has shifted to approximately 1030cm^{-1}. In (**14**), this strong band at 1093cm^{-1} for the free ligand is observed, but has become much less intense indicating a loss of hydrogen from at least one TBZH ligand. This supports the presence of one deprotonated TBZ^- ligand in the formulation and indeed metal complexes containing such deprotonated thiabendazole ligands are known[67].

For compound (**9**) the band associated with ν(C=N) $_{imidazolic}$ at 1577cm^{-1} in the free ligand has completely disappeared in the cationic $TBZH^+_2$ due to protonation on the benzimidazole imine nitrogen, resulting in the delocalisation of the double bond over the N-C-N section. The ν(C=N) $_{imidazolic}$ and $\nu(C=N)_{thiazolic}$ bands (1577 cm^{-1} and 1480 cm^{-1} respectivley) in the free ligand have remained in spectra of (**8**) and (**10**)-(**15**) but have shifted slightly. For complexes (**10**)-(**15**) the C-S stretching band at 1228cm^{-1} for the free ligand remains essentially unchanged suggesting that the sulfur atom in the thiazole ring is uncoordinated. This band has shifted significantly in (**8**) (1201 cm^{-1}) suggesting that the sulpher atom is either associated with a metal or is involved in hydrogen bonding. New bands appear in the spectra of (**8**),(**10**),(**12**) and (**13**) which are indicative of the presence of coordinated (in the range 1310-1320cm^{-1}) and uncoordinated (in the range 1385-1395 cm^{-1}) nitrate groups. The spectra of complexes (**11**), (**14**) and (**15**) only possess bands due to the presence of uncoordinated nitrates (1383, 1383 and 1382 cm^{-1} respectively). The spectra of complexes (**11**) and (**15**) have a new band at approximately 2970 cm^{-1} (Aliphatic C-H stretching) supporting the

inclusion of the ethanol molecules of crystallization shown in their formulations. This band is not present for the other compounds.

Table 11: Characteristic IR bands of complexes (**8**)-(**15**) and free thiabendazole.

Band Assignment	**TBZH**	**(8)**	**(9)**	**(10)**	**(11)**	**(12)**	**(13)**	**(14)**	**(15)**
N-H stretch	3093	3078	3084	3103	3092	3105	3098	3091	3100
N-H vibration	1093	1011	1040	1032	1041	1037	1024	1096	1097
$\nu(C{=}N)_{imidazolic}$	1577	1587	1597	1591	1591	1592	1592	1578	1579
$\nu(C{=}N)_{thiazolic}$	1480	1458	1421	1468	1477	1464	1469	1452	1468
C-S stretch	1228	1201	1232	1228	1228	1229	1229	1229	1233
$NO_3^-{}_{(coord)}$		1320		1311		1326	1324		
$NO_3^-{}_{(uncoord)}$		1383	1385	1384	1383	1384	1393	1383	1382

D2.3 Reaction of Thiabendazole with Metal Sulfates

Thiabendazole was reacted with the Sulfate salts of Manganese(II) , Iron(II) , Cobalt(II) Nickel(II), Zinc(II) and Silver (I) in accordance with the general reaction equation shown in *Scheme 1* to yield complexes (**16**)–(**23**). The complexes were obtained as colourless {(**16**), (**21**), (**22**) and (**23**)}, yellow (**17**), pink (**18**), orange (**19**) and pale blue (**20**) powders, respectively, and they were formulated as shown below. Attempts to react manganese(II) sulfate with TBZH in a 1:2 ratio were unsuccessful.

(16) **$[Mn(TBZH)_6]$ (SO_4).0.5EtOH**

% Calc: 53.03%C; 3.28%H; 18.25%N

% Found: 53.84%C; 3.18%H; 18.75%N

(17) **$[Fe(TBZH)](SO_4).8H_2O$**

% Calc: 24.15%C; 4.62%H; 8.45%N

% Found: 23.85%C; 2.565%H; 8.18%N

(18) **$[Co(TBZH)_2](SO_4).3H_2O$**

% Calc: 39.25%C; 3.27%H; 13.73%N

% Found: 39.26%C; 2.745%H; 13.405%N

(19) **$[Co(TBZH)_3](SO_4).0.5EtOH.H_2O$**

% Calc: 46.55%C; 3.27%H; 15.76%N

% Found: 46.12%C; 2.96%H; 15.99%N

(20) **$[Ni(TBZH)_2](SO_4).7H_2O$**

% Calc: 35.15%C; 4.12%H; 12.29%N

% Found: 34.98%C; 3.39%H; 12.39%N

(21) **$[Zn(TBZH)_2](SO_4).0.5EtOH.2H_2O$**

% Calc: 40.48%C; 3.39%H; 13.48%N

% Found: 39.78%C; 3.11%H; 13.16%N

(22) **$[Ag_2(TBZH)_2](SO_4).EtOH$**

% Calc: 34.75%C; 2.65%H; 11.05%N

% Found: 35.64%C; 2.33% H; 12.02%N

(23) **$[Ag_2(TBZH)_2](SO_4).EtOH$**

% Calc: 34.75%C; 2.65%H; 11.05%N

% Found: 35.5%C; 2.27% H; 11.7%N

The room temperature magnetic moments of powdered samples of the complexes are shown in *Table 12*. The μ_{eff} value for (**16**) is close to the range expected (μ_{eff} =5.6-6.1 B.M.) for manganese complexes where there is no significant exchange interactions between adjacent metal centres[64]. The Iron (II) compound (**17**) falls significantly above the expected value and an interaction between the iron atoms in this compound cannot be ruled out. The cobalt complex (**18**) has a significantly higher value than expected, suggesting interactions between the metal centres, while (**19**) has a μ_{eff} value that complies with the expected range (4.30-5.20 B.M.)[64]. Complex (**20**) was found to have a μ_{eff} value that was considerably above the expected range (μ_{eff} =2.80-3.50 B.M.)[64]

indicating a metal-metal interaction between the nickel atoms. All of the complexes (**16**)-(**23**) were insoluble in all solvents.

Table 12 Magnetic Susceptibility data for complexes (**16**) – (**23**)

Complex	μ_{eff} **(B.M.) {room T°}**
$[Mn(TBZH)_6](SO_4).0.5EtOH$ (**16**)	6.29
$[Fe(TBZH)](SO_4).8H_2O$ (**17**)	6.46
$[Co(TBZH)_2](SO_4).3H_2O$ (**18**)	5.84
$[Co(TBZH)_3](SO_4).0.5EtOH.H_2O$ (**19**)	4.89
$[Ni(TBZH)_2](SO_4).7H_2O$ (**20**)	4.28
$[Zn(TBZH)_2](SO_4).0.5EtOH.2H_2O$ (**21**)	-
$[Ag_2(TBZH)_2](SO_4).EtOH$ (**22**)	-
$[Ag_2(TBZH)_2](SO_4).EtOH$ (**23**)	-

Characteristic IR bands of compounds (**16**)-(**23**) and of free TBZH are listed in *Table 13*. The N-H stretch at 3093cm^{-1} and N-H vibration at 1093cm^{-1} for the free ligand remains virtually unchanged in all spectra. The IR spectrum of TBZH presented two bands associated to the ν(C=N) $_{imidazolic}$ and $\nu(C=N)_{thiazolic}$ (1577cm^{-1}and 1480cm^{-1}, respectively). These bands have remained in the spectra of all complexes but have shifted slightly indicating that the ligand is coordinated through the imidazole and thiazole nitrogens. The C-S stretching band at 1228cm^{-1}appears to have remained in the spectra of a number of the complexes but proper assignment is not possible as the strong/broad sulphate band (1090-1280 cm^{-1}) overlaps and covers this region of the

spectrum. The presence of the sulphate anion is further evidenced by the appearance of a new characteristic band at approximately 600 cm^{-1} in the spectra of all of the complexes[68]. The spectra of complexes (**16**), (**19**), (**21**), (**22**) and (**23**) have a new band at approximately 2970 cm^{-1} (Aliphatic C-H stretching) supporting the inclusion of the ethanol molecules of crystallization shown in their formulations. This band is not present for the other compounds.

The formulation of complex (**16**) fits only for the presence of six TBZH ligands. It is unlikely that this is the case but it is worth noting that it is not unknown for potentially chelating ligands such as 1,10-phenanthroline and 1,1'-bipyridine to be present as molecules of crystallisation[53].

Table 13: Characteristic IR bands of complexes (**16**)-(**23**) and free thiabendazole.

Band Assignment	**TBZH**	**(16)**	**(17)**	**(18)**	**(19)**	**(20)**	**(21)**	**(22)**	**(23)**
N-H stretch	3093	3091	3087	3084	3076	3082	3082	3077	3086
N-H vibration	1093	1097	1011	1096	1087	1092	1098	1084	1095
$\nu(C{=}N)_{imidazolic}$	1577	1578	1592	1592	1590	1591	1592	1579	1575
$\nu(C{=}N)_{thiazolic}$	1480	1483	1476	1477	1476	1478	1479	1451	1452
C-S stretch	1228	*	*	*	*	*	*	*	*
SO_4^{2-}		1097	1125	1096	1087	1092	1098	1084	1095
		607	603	610	606	615	601	609	600

* Assignment was precluded because of the overlap of the sulphate bands

D2.4 Reaction of Thiabendazole with Metal Acetates

Thiabendazole was reacted with the Acetate salts of Manganese(II), Cobalt(II) Nickel(II), Zinc(II) and Silver (I) in accordance with the general reaction equation shown in *Scheme 1* to yield complexes (**24**)–(**30**). The complexes were obtained as colourless {(**24**),(**25**), (**29**) and (**30**)}, pink (**26**), orange (**27**) and blue (**28**) powders, respectively and they were formulated as shown below:

(24) **$[Mn(TBZ)(TBZH)CH_3COO]0.5H_2O$**

% Calc: 50.38%C; 3.26%H; 16.02%N,

% Found: 50.67%C; 3.05%H; 15.74%N,

(25) **$[Mn(TBZ)(TBZH)_2CH_3COO]$**

% Calc: 53.62%C; 3.23%H; 17.58%N,

% Found: 53.50%C; 3.26%H; 17.42%N,

(26) **$[Co(TBZ)(TBZH)CH_3COO]$**

% Calc: 50.85%C; 3.08%H; 16.18%N,

% Found: 50.77%C; 2.97%H; 16.97%N,

(27) **$[Co(TBZ)(TBZH)_2CH_3COO]H_2O$**

% Calc: 52.02%C; 3.41%H; 17.06%N,

% Found: 52.14%C; 3.41%H; 17.95%N,

(28) **[Ni (TBZH)$_2$(CH$_3$COO)$_2$]0.5EtOH.H$_2$O**

% Calc: 48.4%C; 4.06%H; 13.54%N,

% Found: 48.29%C; 2.78%H; 13.97%N,

(29) **[Zn(TBZH)$_2$(CH$_3$COO)$_2$]**

% Calc: 47.69%C; 3.64%H; 13.91%N,

% Found: 46.16%C; 2.96%H; 14.14%N,

(30) **[Ag$_2$(TBZH)$_2$(CH$_3$COO)$_2$] H$_2$O**

% Calc: 38.21%C; 2.93%H; 11.14%N,

% Found: 38.59%C; 1.74%H; 10.45%N,

The room temperature magnetic moments of powdered samples of the complexes are shown in *Table 14*. The μ_{eff} value for (**24**) and (**25**) is close to the range expected (μ_{eff} =5.6-6.1 B.M.) for manganese complexes where there is no significant exchange interactions between adjacent metal centres[64]. The two cobalt complexes, (**26**) and (**27**), give satisfactory μ_{eff} values compared to the expected range (4.30-5.20 B.M.)[64] for simplex cobalt(II) complexes[64]. (**28**) was found to have a μ_{eff} value within the expected range (μ_{eff} =2.80-3.50 B.M.)[64] signifying no metal-metal interactions between the nickel atoms in complex (**28**). All complexes were found to be insoluble, with the exception of the cobalt compounds (**26**) and (**27**), and the zinc compound (**29**), which were found to be soluble in a range of polar solvents.

Table 14 Magnetic Susceptibility and Molar Conductivity data for complexes (**24**) – (**30**)

Complex	μ_{eff} (B.M.) {room T°}	Λ_M (S cm^2mol^{-1}) [10%EtOH]
$[Mn(TBZ)(TBZH)CH_3COO]0.5H_2O$ (**24**)	5.47	-
$[Mn(TBZ)(TBZH)_2CH_3COO]$ (**25**)	5.78	-
$[Co(TBZ)(TBZH)CH_3COO]$ (**26**)	4.45	53.64
$[Co(TBZ)(TBZH)_2CH_3COO]H_2O$ (**27**)	4.82	39.62
$[Ni(TBZH)_2(CH_3COO)_2]0.5EtOH.H_2O$ (**28**)	2.96	-
$[Zn(TBZH)_2(CH_3COO)_2]$ (**29**)	-	41.39
$[Ag_2(TBZH)_2(CH_3COO)_2]\ H_2O$ (**30**)	-	-

The molar conductivity values for the soluble complexes (**26**), (**27**) and (**29**) are listed in *Table 14*. Their values of (10% EtOH solution) fall in the range of 39.62-53.64 cm^2mol^{-1} suggesting that they behave as poor electrolytes.

The IR spectra of compounds (**24**)-(**30**) were compared to that of the free TBZH, and a number of differences were noted. The characteristic bands for free TBZH and the important IR spectral bands that provide evidence for the structure of the compounds are listed in *Table 15*. The N-H stretching ($3093cm^{-1}$) and the N-H vibrational ($1093cm^{-1}$) bands are present for all of the complexes indicating the presence of at least one neutral TBZH group in their structures. However, in the spectra of complexes (**24**), (**26**) and (**27**) these N-H bands change shape and relative intensity supporting the inclusion

of anionic TBZ^- groups in their formulations. The presence of both neutral and anionic chelating benzimidazole ligands has recently been confirmed (by x-ray analysis) in this laboratory[69]. In the spectra of (**26**)-(**30**) the $\nu(C{=}N)_{imidazolic}$ and $\nu(C{=}N)_{thiazolic}$ bands (1577$cm^{-1}$and 1480cm^{-1}, respectively), have shifted, indicating that the ligand is coordinated through the imidazole and thiazole nitrogens. For (**24**) assignment of bands to these groups is precluded by the presence of broad carboxylate bands in these regions of the spectrum. For all complexes, (**24**)-(**30**), the C-S stretching band remains essentially in the same position in the spectra, suggesting that the sulfur atom in the thiazole ring is not involved in coordination. The IR spectra for all of the complexes contain bands attributable to νOCO_{asym} (1525-1600cm^{-1}) and νOCO_{sym} (1400-1435cm^{-1}), respectively. The ΔOCO values for complexes (**24**)-(**30**) all fall in the range of 120-190cm^{-1} and are well below the threshold (200cm^{-1}) which is indicative of monodentate acetate groups[65]. Complex (**24**) has a ΔOCO value of 125cm^{-1}which suggests that the acetate is chelating to the metal[66]. The others all have values in a region that is accepted as being untrustworthy but an ionic mode cannot be ruled out. A new band that appears in the range 553-557cm^{-1} in the spectra of all of the complexes is tentatively assigned to Metal-N vibration. The spectrum of complex (**28**) has a new band at approximately 2970 cm^{-1} (Aliphatic C-H stretching) supporting the inclusion of the ethanol molecules of crystallization shown in the formulation. This band is not present for the other compounds.

Complex (**25**) was generated by reacting four equivalents of TBZH with manganese(II) acetate. Although its microanalysis results fit for a formulation of $[Mn(TBZ)(TBZH)_2CH_3COO]$, the IR spectrum is quite similar to that of (**24**) and the possibility of an impure product cannot be ruled out.

Table 15: Characteristic IR bands of complexes (**24**)-(**30**) and free thiabendazole.

Band Assignment	**TBZH**	**(24)**	**(25)**	**(26)**	**(27)**	**(28)**	**(29)**	**(30)**
N-H stretch	3093	3079	3081	3087	3085	3086	3097	3089
N-H vibration	1093	1044	1095	1047	1048	1011	1028	1018
$\nu(C{=}N)_{imidazolic}$	1577			1553	1552	1560	1567	1565
$\nu(C{=}N)_{thiazolic}$	1480	1469		1470	1470	1477	1474	1473
C-S stretch	1228	1227	1226	1227	1227	1228	1230	1230
νOCO_{asym}		1529	1527	1591	1590	1589	1598	1565
νOCO_{sym}		1404	1405	1429	1429	1432	1408	1395
ΔOCO		125	122	162	161	157	190	170
M-N		555	562	554	553	553	554	577

D.3 ANTIFUNGAL ACTIVITY OF TBZH COMPLEXES AGAINST *CANDIDA ALBICANS*

TBZH is a poor anti-*Candida* agent. Previously this group has shown that upon coordination to a copper centre the biological activity of TBZH was significantly improved when tested against the pathogen in RPMI medium. The current study was seeking to establish if changing the type of metal centre in the complexes would alter the anti-*candida* potential of this class of compound. Also the affect of changing the nature of the counterion in the complexes was of interest. With these objectives in mind all of the complexes generated during this study were examined for their anti fungal activity towards *Candida albicans*. Because of problems that have recently occurred with respect to the quality of RPMI media being supplied to the group the current study was carried out in minimal media. Each transition metal complex was screened for its ability to inhibit the growth of an isolate of *Candida albicans* at concentrations of 100μg/cm^{-3}, 75 μg/cm^{-3}, 50 μg/cm^{-3}, 20 μg/cm^{-3}, 10 μg/cm^{-3} and 5 μg/cm^{-3} of minimal medium (*Table 16*). Furthermore the antifungal activity of these complexes was compared to the activity of their starting materials (*Table 17*) and the prescription drug Ketoconazole. At a concentration of 100μg/cm^{-3} all of the complexes exhibited moderate to good activity towards the pathogen with the silver compounds being exceptional. The activity, however, does not represent any significant improvement on that of the metal free TBZH and is only slightly better than that of the simple salts. As the concentration of the drug molecules is decreased their efficacy diminishes until finally at 5 μg/cm^{-3} none of the non-silver complexes possessed anti-*Candida* properties. The silver complexes showed percentage growth of between 6-7% at all concentrations, which compared favorably to that of the prescription drugs.

However it should be noted that the results for the silver complexes do not offer any significant improvement on those of the simple salts. This trend has been observed for other silver complexes previously studied in this laboratory[56]. It is possible that the lack of biological activity, for the majority of the complexes at the lower concentrations, may be related to the change in media employed, a factor which is quite common in microbiological assays. This hypothesis is currently being explored by another worker in the group.

Table 16: Percentage cell growth of *C.albicans* for the transition metal complexes of thiabendazole.

Test Compound	% Cell Growth					
	100μg	***75μg***	***50μg***	***20μg***	***10μg***	***5μg***
Control	100	100	100	100	100	100
$[Mn(TBZH)_2Cl_2].3H_2O.0.5EtOH$ (1)	53	64	76	92	94	99
$[Mn(TBZH)_3Cl_2].0.5EtOH$ (2)	53	61	74	90	94	96
$[Fe(TBZH)_2Cl_3]H_2O.0.5EtOH$ (3)	42	62	75	85	87	99
$[Co(TBZH)_2Cl_2]0.5H_2O.\ 0.5EtOH$ (4)	26	55	74	87	92	96
$[Co(TBZH)_3Cl_2]0.5EtOH$ (5)	29	57	75	88	92	96
$[Ni(TBZH)_2Cl_2]0.5EtOH$ (6)	38	60	75	89	90	94
$[Zn(TBZH)Cl_2]$ (7)	47	63	73	89	93	100
$[Mn(TBZH)_2(NO_3)](NO_3).H_2O$ (8)	45	63	76	91	92	99
$[TBZH_2NO_3]$ (9)	34	59	77	77	82	95
$[Co(TBZH)_2(NO_3)](NO_3).H_2O$ (10)	35	59	72	82	86	91
$[Co(TBZH)_3](NO_3)_2.0.5EtOH.H_2O$ (11)	33	55	70	82	84	91
$[Ni(TBZH)_2.(NO_3)_2](NO_3).H_2O$ (12)	41	61	73	89	89	94
$[Zn(TBZH)_2(NO_3)](NO_3)$ (13)	49	65	79	89	92	100
$[Ag_2(TBZ)(TBZH)](NO_3)$(14)	6	5	6	6	7	7
$[Ag(TBZH)_2\ ](NO_3).0.5EtOH.0.5H_2O$ (15)	7	5	7	6	7	7
$[Mn(TBZH)_6](SO_4).0.5EtOH$ (16)	46	62	76	92	94	98
$[Fe(TBZH)](SO_4).8H_2O$ (17)	43	61	83	90	93	97
$[Co(TBZH)_2](SO_4).3H_2O$ (18)	33	55	74	86	93	96
$[Co(TBZH)_3](SO_4).0.5EtOH.H_2O$ (19)	32	52	68	84	88	94
$[Ni(TBZH)_2](SO_4).7H_2O$ (20)	35	57	79	88	89	96
$[Zn(TBZH)_2](SO_4).0.5EtOH.2H_2O$ (21)	46	63	83	90	91	96
$[Ag_2(TBZH)_2](SO_4).EtOH$ (22)	7	5	6	6	7	7
$[Ag_2(TBZH)_2](SO_4).EtOH$ (23)	7	5	6	6	7	7
$[Mn(TBZ)(TBZH)CH_3COO]0.5H_2O$ (24)	49	61	81	90	90	101
$[Mn(TBZ)(TBZH)_2CH_3COO]$ (25)	45	60	76	88	91	98
$[Co(TBZ)(TBZH)CH_3COO]$ (26)	36	59	75	89	91	93
$[Co(TBZ)(TBZH)_2CH_3COO]H_2O$ (27)	37	57	72	88	91	94
$[Ni(TBZH)_2(CH_3COO)_2]0.5EtOH.H_2O$(28)	39	51	73	87	89	95
$[Zn(TBZH)_2(CH_3COO)_2]$ (29)	46	63	76	88	91	101
$[Ag_2(TBZH)_2(CH_3COO)_2]\ H_2O$ (30)	7	6	6	6	7	7

The compounds were tested at concentrations of 100μg/cm^{-3}, 75 μg/cm^{-3}, 50 μg/cm^{-3}, 20 μg/cm^{-3}, 10 μg/cm^{-3} and 5 μg/cm^{-3} of aqueous minimal medium. Yeast cells were grown for 24h at 37°C. Results are presented as % cell growth and the effectiveness of the compounds are compared to the growth of the control (no drug added).

Table 17: Percentage cell growth of *C.albicans* for the metal salts, thiabendazole and ketoconazole.

Test Compound	**% Cell Growth**					
	100µg	***75µg***	***50µg***	***20µg***	***10µg***	***5µg***
Control	100	100	100	100	100	100
Thiabendazole	47	56	71	81	88	97
Ketoconazole	5	7	14	20	23	25
$MnCl_2$	54	67	86	98	104	109
$Mn(NO_3)_2$	57	61	84	93	101	104
$MnSO_4.7H_2O$,	56	59	71	99	106	110
$Mn(CH_3COO)_2.4H_2O$	58	71	89	97	112	116
$Fe(NO_3)_3.9H_2O$	55	66	87	96	99	101
$FeCl_3$	51	63	82	94	96	100
$FeSO_4$	59	69	87	95	98	101
$CoCl_2.6H_2O$	61	72	91	98	101	103
$Co(NO_3)_2.6H_2O$	62	76	94	103	106	107
$CoSO_4.7H_2O$	59	71	88	95	97	99
$Co(CH_3COO)_2.4H_2O$	59	74	83	89	93	97
$NiCl_2.6H_2O$	58	69	87	97	99	103
$Ni(NO_3)_2.6H_2O$	63	72	86	100	102	103
$NiSO_4.6H_2O$	64	75	86	95	97	99
$Ni(CH_3COO)_2.4H_2O$	62	73	85	93	96	98
$ZnCl_2$	48	76	89	100	103	105
$Zn(NO_3)_2.6H_2O$	69	78	89	99	101	102
$ZnSO_4.7H_2O$	65	76	88	96	99	100
$Zn(CH_3COO)_2.2H_2O$	67	72	87	94	97	101
$AgNO_3$	5	5	5	6	6	6
Ag_2SO_4	5	5	5	6	6	6
$Ag(CH_3COO)$	5	5	5	6	6	6

The compounds were tested at concentrations of 100µg/cm^{-3}, 75 µg/cm^{-3}, 50 µg/cm^{-3}, 20 µg/cm^{-3}, 10 µg/cm^{-3} and 5 µg/cm^{-3} of aqueous minimal medium. Yeast cells were grown for 24h at 37°C. Results are presented as % cell growth and the effectiveness of the compounds are compared to the growth of the control (no drug added).

CONCLUSION

CONCLUSION

29 complexes {(**1**)-(**8**) and (**10**)-(**30**)} containing Thiabendazole(TBZH) were generated by reacting the Chloride, Nitrate, Sulphate and Acetate salts of Mn(II), Fe(II), Fe(III),Co(II), Ni(II), Zn(II) and Ag(I) with the N,N-donor ligand in aqueous ethanol. The majority of the complexes are thought to contain mononuclear metal centres as they have room temperature magnetic moments close to the values expected. However the magnetic data for some of the complexes did suggest that metal-metal interactions could not be ruled out. The TBZH is present in the complexes as either a neutral or anionic ligand. The IR data for all of the complexes {with the exception of $[Fe(TBZH)_2Cl_3]H_2O.0.5EtOH$(**3**)}indicate that the TBZH (or TBZ^-) ligand is coordinated through the imidazolic and the thiazolic nitrogens. For (**3**) there is evidence in the spectrum to support the possibility of the sulfur atom in the thiazole ring being involved in coordination. The chloride derivatives (**1**) and (**2**), the nitrate derivatives (**8**), (**14**) and (**15**), all of the sulfate derivatives (**16**)-(**23**) and the acetate derivatives (**24**), (**25**), (**28**) and (**30**) were insoluble and the possibility of polymeric structures for these complexes cannot be ruled out. The relative solubility of the remaining complexes may point to the possibility of them having monomeric structures.

TBZH reacted with $Fe(NO_3)_3.9H_2O$ to yield the unusual nitrate salt $[TBZH_2NO_3]$(**9**). All attempts to make this compound by reacting TBZH with nitric acid were unsuccessful. It is believed that the mechanism of its formation may involve the hydrated iron nitrate acting as an aqua acid. In the X-ray crystal structure of (**9**) the asymmetric unit contains one protonated $TBZH_2$ cation and one nitrate anion. The TBZH is protonated on the benzimidazole imine nitrogen, resulting in delocalisation of

the double bond over the N-C-N section. The cations are hydrogen bonded to nitrate anions *via* each of the NH groups, resulting in a chain along which adjacent $TBZH_2$ units are oriented at approximately right angles to each other. There is significant π π-stacking between adjacent $TBZH_2$ cations with interplanar distance c.a. 3.3 Å.

The complexes {(**1**)-(**8**) and (**10**)-(**30**)} and the nitrate salt (**9**) were tested for their ability to inhibit the growth of *Candida Albicans*. A comparative study of the fungitoxic activities of these compounds with that of the simple salt starting materials, TBZH and the prescription drug Ketoconazole was carried out. Only at the relatively high concentration of $100\mu g/cm^{-3}$ did the majority of the complexes show acceptable activity. However, all of the silver complexes were found to have superior biological activity to the Ketoconazole over the entire range of concentrations. The simple silver salts were also found to be highly active. In conclusion, with the exception of the silver compounds any changes in either metal or counterion type in the complexes yielded very little improvement in the anti-*Candida* activity of the TBZH derivatives.

REFERENCES

1 F. C. Odds, *Candida and Candidosis*, 2nd Ed., 1988, Bailliere Tindall London.

2 *Martindale*, 31st Ed., 1996, Royal Pharmaceutical Society London, 404.

3 Nature Reviews, *Genetics*, 2002, **3**, 918.

4 N. H. Georgapapadakou, T.J.Walsh, *Antimicrob.Agents Chemother.*, 1996, **40**, 279-291.

5 F.C.Odds, A.J.P. Brown, N.A.R.Gow, *TRENDS in Microbiology*, 2003, **11**, 272-279.

6 N. H. Georgapapadakou, *Current Opinion in Microbiology*, 1998, **1**, 547-557.

7 M. A. Viviani, S. De Marie, J. R.Graybiu, *Medical Mycology*, 1998, **36**, 194-206.

8 J.B.Wright, *The Chemistry of the Benzimidazoles*, 1951, 397-541.

9 Aldrich Structure Index, Published by Aldrich Chemical Company, INC., 1996-1997 Ed.

10 Wagner, Millett, *Org.Syn.coll.*, 1943, **2**, 65.

11 H.Dk. Brown, A.R. Matzuk, I.R.Ilvues, L.H.Peterson, S.A. Harris, L.H. Sarett, J.R.Edgerton, J.J Yaktis, W.C. Campell, and A.C.Cuckler, 1961, *J.Amer.Chem.Soc.* **83**,1764-1765.

12 B.L. Trust and R.E. Marsh, *Short Structural Papers*, 1973, **29**,2298-2301.

13 H.J. Roth, T. Beisswenger, 1988, John Wiley and sons., *Pharmaceutical Chemistry*, Vol.1: Drug Synthesis, **7**,234.

14 D. W. Woolley, *J. Biol. Chem.*, 1944, **152**, 225.

15 H. Goker, R. Ertan, H. Akgun and N. Yulug, *Arch. Pharm*, 1991, **324**, 283.

16 H. S. Gunes and G Cosar, *Arzneim.-Forsch./Drug Res*, 1992, **42 (II)**, 1045.

17 S. M. Rida, N. S. Habib, E. A. M. Badawey and H. T. Y. Fahmy, *Arch. Pharm.*,

1995, **328**, 325.

18 S. Demirayak and K. Guven, *Pharmazie*, 1995, **50**, 527.

19 H. Goker and C. Kus, *Arch. Pharm*, 1995, **328**, 425.

20 H. Goker and E. Tebrizli, *Il Farmaco*, 1996, **51**, 53.

21 H. Goker, G.Ayhan-Kýlcýgil, M.Tuncbilek, and N.Altanlar, *Il Farmaco,* 1999, **54**, 562–565.

22 S.Ersan, S.Nacak, N.Acar and T.Ozden, *Arzneim-Forsch./Drug Res.*, 1997, **47**, 773-775.

23 N. S. Habib, S. M.Rida, E. A. M. Badwey, H. T. Y. Fahmy and H. A. Ghozlan, *Pharmazie*, 1997, **52**, 346.

24 S. Ersan, S. Nacak, N. Acar and N. Noyanalpan, *Arzneim-Forsch./Drug Res.*, 1997, **47**, 410-412.

25 I. Oren, O. Temiz, I. Yalcin, E. Sener, A. Akin and N. Ucarturk, *Arzneim-Forsch./Drug Res.*, 1997, **47**, 1393.

26 S.Shallal, *Human Health Risk Assessment: Thiabendazole*, U.S. Environmental Protection Agency, 2001.

27 A.Baker, J. Hosp. *Pharm.*, 1972, **30**, 45.

28 T.Starton and C.Allard. *Phytiat. Phytopharm,* 1964, **13**,163.

29 P.M. Allen, and D.Gottlieb,. *J. Applied Micro*, 1970, **20**, 919-926.

30 H. Darpoux, T. Starton, A. Lebrun, and B. de la Tullaye, *Phytiat. Phytopharm.* 1966, **15**, 113-119.

31 H.F.Stallkercht, and G.L.Crane. *Phytopathology* 1969, **59**, 393.

32 H.Darpoux, T. Starton, E. Ventura, and J. Bouadin, 1966 *Phytiat. Phytopharm.* **15**, 121-128.

33 J. Gonaham, *Phytiat. Phytopharm,* 1966, **15**, 171-175.

34 D.C. Erwin, J.J. Sims, and J. Partridge, *Phytopathology* **58**, 860-865.

35 F.Cronin, *PhD.* Thesis, National University of Ireland, 1996.

36 M. Goodgame and L.I.B.Haing, *J.Chem. Soc.*, 1966, A, 174.

37 M. Devereux, M. McCann, D. O'Shea, R. Kelly, D. Egan, C. Deegan, K. Kavanagh, and V. McKee, *J. Inorg.Biochem*, 2004, **98**, 1023-1031.

38 C. Kowala, J.A.Wunderlich, *Inorg Chem.Acta*, 1972, 7, 331-338.

39 R.C. Van Landschoot, J.A.M, Van Hest, and J. Reedijk, *J. Inorg. Nucl.Chem.* 1976, **38,** 185-190.

40 J.M Grevy, F.Tellez, S.Bernes, H.Noth, R.Contreras, and N. Barba-Behrens, *Inorg. Chem. Acta.*, 2002, **339**, 532-542.

41 L. Mishra, M. K. Said and K. Takeya, *Bioorganic and medicinal Chemistry*, 1995, **3**, 1241.

42 C. J. Matthews, S. L. Heath, M. R. Elsegood, W. Clegg, T. A. Leese and J. C. Lockhart, *J. Chem. Soc. Dalton Trans.*, 1998, 1973.

43 C. J. Matthews, W. Clegg, S. L. Heath, N. C. Martin, M. N. Stuart Hill and J. C. Lockhart, *Inorg. Chem.*, 1998, **37**, 199.

44 M. J. Roman-Alpiste, J. D. Martin-Ramos, A. Castineiras-Campos, E. Bugella-Altamirano, A. G. Sicilia-Zafra, J. M. Gonzalez-Perez and J. Niclos-Gutierrez, *Polyhedron*, 1999, **18**, 3341.

45 L. Beyer, R. Richter, R. Wolf, J. Zaumseil, M. Lino-Pacheco and J. Angulo-Cornejo, *Inorg. Chem. Comm.*, 1999, **2**, 184.

46 P. A. M. Williams, E. G. Ferrer, K. A. Pasquevich and E. J. Baran, *Z. Anorg. Allg.*

Chem., 2000, **626**, 2509.

47 W. H. Kwok, H. Zhang, P. Payra, M. Duan, S. Hung, D. H. Johnston, J. Gallucci, E. Skrzypczak-Jankum and M. K. Chan, *Inorg. Chem.*, 2000, **39**, 2367.

48 Udupa , M.R., and Krebs, B., , *Inorg Chem.Acta*, 1979, 32, 1-5 .

49 M.Z.Wisniewski, T.Glowiak, A.Opolski, and J.Wietrzyk, *M.B.D.*, 2001, **8**, 189-194.

50 J.M Grevy, F Tellez, S.Bernes, H.Noth, R.Contreras, and N.Barba-Behrens, *Inorg. Chem. Acta.*, 2002, **339**, 532-542.

51 K.K.Mothilal, C.Karunakaran, A.Rajendran, and Murugesan, *J.Inorg Biochem.*,2004, **98**, 322-332.

52 M. McCann, B.Coyle, S.McKay, P.Mc Cormack, K.Kavanagh, M. Devereux, V.McKee, P.Kinsela, R.O'Gorman, M.Clynes, *Biometals*, in press, manuscript no.R-2-10-2003.

53 M. McCann, M. Devereux, M.Geraghty, D.O Shea, J.Mason and L.O Sullivan, *M.B.D.*, 2000, **7**, 185.

54 M. Devereux, M. McCann, V.Leon, R.Kelly, D.O Shea and V.McKee, *Polyhedron*, 2003, **22**, 3187-3194.

55 I.Druta, R.Dannac, M.Ungureanu, G.Grosu and G.Drochioiu, *Ann. Pharm.Fr.*, 2002, **60**, 348-351.

56 B.Coyle, K.Kavanagh, M. McCann, M. Devereux and M.Geraghty, *Biometals*, 2003, **16**, 321-329.

57 B.Coyle, P.Kinsella, M. McCann, M. Devereux, R.O Connor, M.Clynes and K.Kavanagh, *Toxicol. In Vitro*, 2004,**18**, 63–70.

58 D.O'Shea, *B.Sc.Hons.Thesis,* National University of Ireland, 1998.

59 N.S.Habib, S.M.Rida, E.A.M.Badawey, H.T.Y.Fahmy, H.A.Ghozlan, *Pharmazie*, 1997, **52**, 346-350.

60 H.J.Robins, H.C.Stoerk and O.E.Graesle, *Toxicol.Appl.Pharmacol*, 1965, **7**, 55-61.

61 M. Devereux, M. McCann, D.O'Shea, P.Murray, K.Kavanagh, unpublished results.

62 F.A. Cotton and G.Wilkinson, *Advanced Inorganic Chemistry*, 5th Ed., Wiley, New York, 1998.

63 National Committee for Clinical Laboratory Standards. *Reference method for broth dilution antifungal susceptibility testing of yeasts; proposed standard. NCCLS* document M27-P.Villanova.PA; NCCLS, **1992.**

64 J.E.Huheey, E.A. Keiter and R.L.Keiter, *Inorganic Chemistry*, 4th Ed., Harper Collins, 1993, 465.

65 D.F.Shriver, P.W.Atkins and C.H.Langford, *Inorganic Chemistry*, 2nd Ed., 1994, 191.

66 N.Nakamoto, *Infrared and Raman Spectra of Inorganic and Coordination Compounds,* 3rd Ed. , Wiley, New York, 1978.

67 M.Devereux and D.O'Shea, Unpublished results.

68 R.A. Nyquist and R.O. kagel, *Infrared Spectra of Inorganic Compounds*, Academic Press Inc., 1971.

69 M. Devereux, A. Kellett and V. McKee, personal communications.

APPENDIX

LIST OF INFRARED SPECTRA

TBZH	$C_{10}H_7N_3S$
(1)	$[Mn(TBZH)_2Cl_2].3H_2O.0.5EtOH$
(2)	$[Mn(TBZH)_3Cl_2].0.5EtOH$
(3)	$[Fe(TBZH)_2Cl_3]H_2O.0.5EtOH$
(4)	$[Co(TBZH)_2Cl_2]0.5H_2O.\ 0.5EtOH$
(5)	$[Co(TBZH)_3Cl_2]0.5EtOH$
(6)	$[Ni(TBZH)_2Cl_2]0.5EtOH$
(7)	$[Zn(TBZH)Cl_2]$
(8)	$[Mn(TBZH)_2(NO_3)]NO_3.H_2O$
(9)	$[TBZH_2NO_3]$
(10)	$[Co(TBZH)_2(NO_3)]NO_3.H_2O$
(11)	$[Co(TBZH)_3](NO_3)_2.0.5EtOH.H_2O$
(12)	$[Ni(TBZH)_2.(NO_3)](NO_3).H_2O$
(13)	$[Zn(TBZH)_2(NO_3)](NO_3)$
(14)	$[Ag_2(TBZ)(TBZH)](NO_3)$
(15)	$[Ag(TBZH)_2](NO_3).0.5EtOH.0.5H_2O$
(16)	$[Mn(TBZH)_6]\ (SO_4).0.5EtOH$
(17)	$[Fe(TBZH)](SO_4).8H_2O$
(18)	$[Co(TBZH)_2](SO_4).3H_2O$
(19)	$[Co(TBZH)_3](SO_4).0.5EtOH.H_2O$
(20)	$[Ni(TBZH)_2](SO_4)\ .7H_2O$
(21)	$[Zn(TBZH)_2](SO_4).0.5EtOH.2H_2O$
(22)	$[Ag_2(TBZH)_2](SO_4).EtOH$
(23)	$[Ag_2(TBZH)_2](SO_4).EtOH$

(24) **$[Mn(TBZ)(TBZH)CH_3COO]0.5H_2O$**

(25) **$[Mn(TBZ)(TBZH)_2CH_3COO]$**

(26) **$[Co(TBZ)(TBZH)CH_3COO]$**

(27) **$[Co(TBZ)(TBZH)_2CH_3COO]H_2O$**

(28) **$[Ni\,(TBZH)_2(CH_3COO)_2]0.5EtOH.H_2O$**

(29) **$[Zn(TBZH)_2(CH_3COO)_2]$**

(30) **$[Ag_2(TBZH)_2(CH_3COO)_2]\ H_2O$**

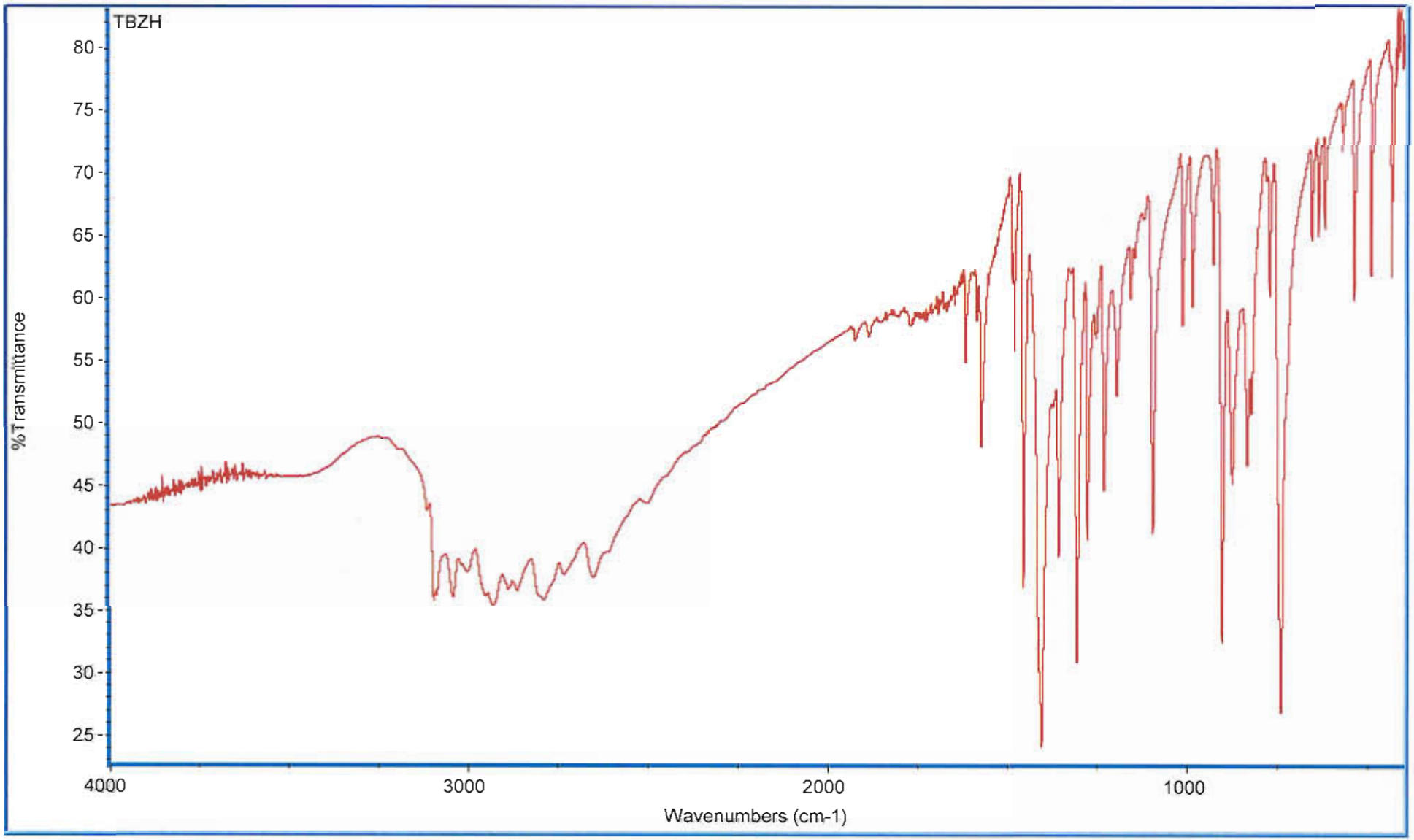
TBZH
%Transmittance
80
75
70
65
60
55
50
45
40
35
30
25
4000
3000
2000
1000
Wavenumbers (cm-1)

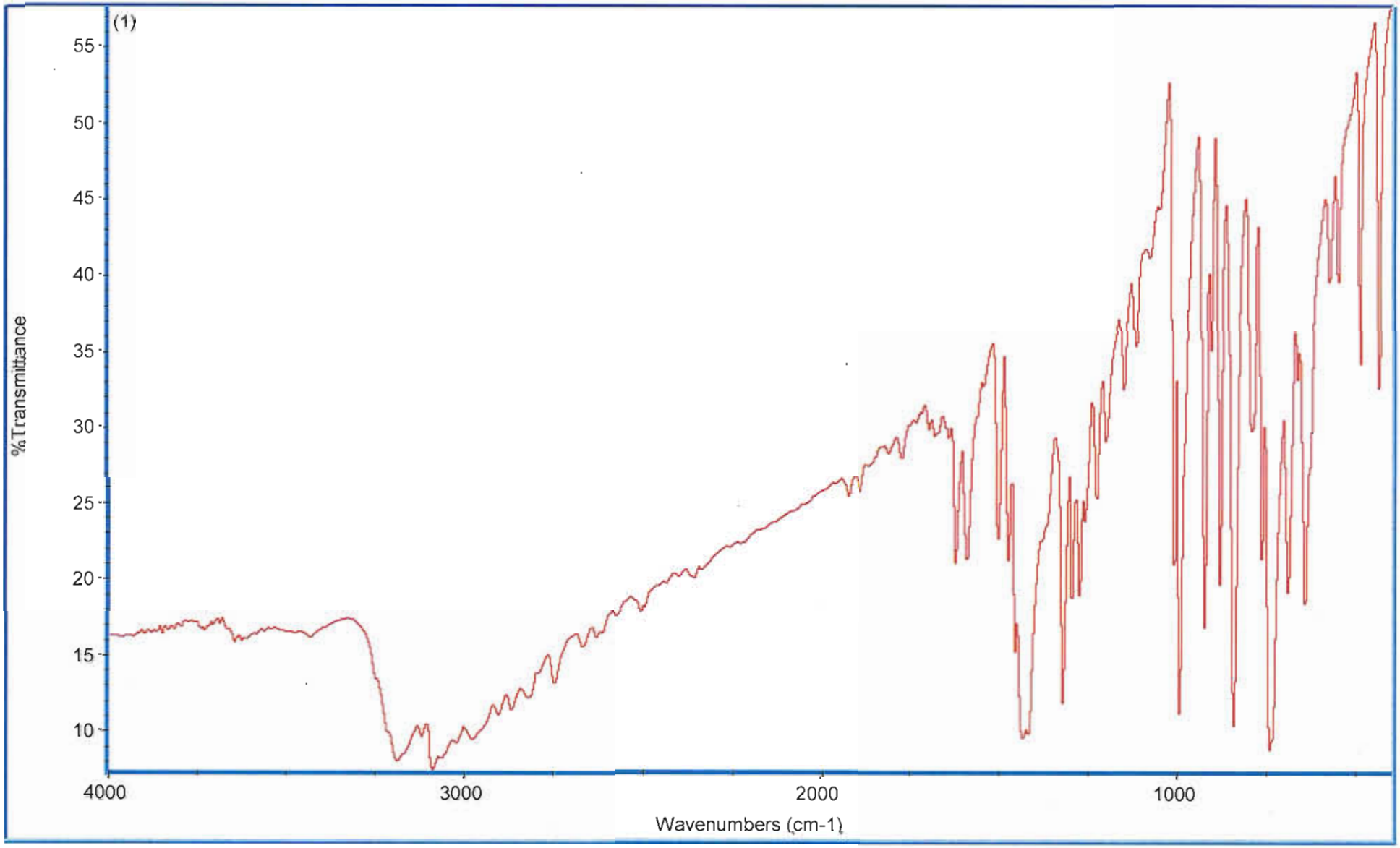
(1)
%Transmittance
55
50
45
40
35
30
25
20
15
10
4000
3000
2000
1000
Wavenumbers (cm-1)

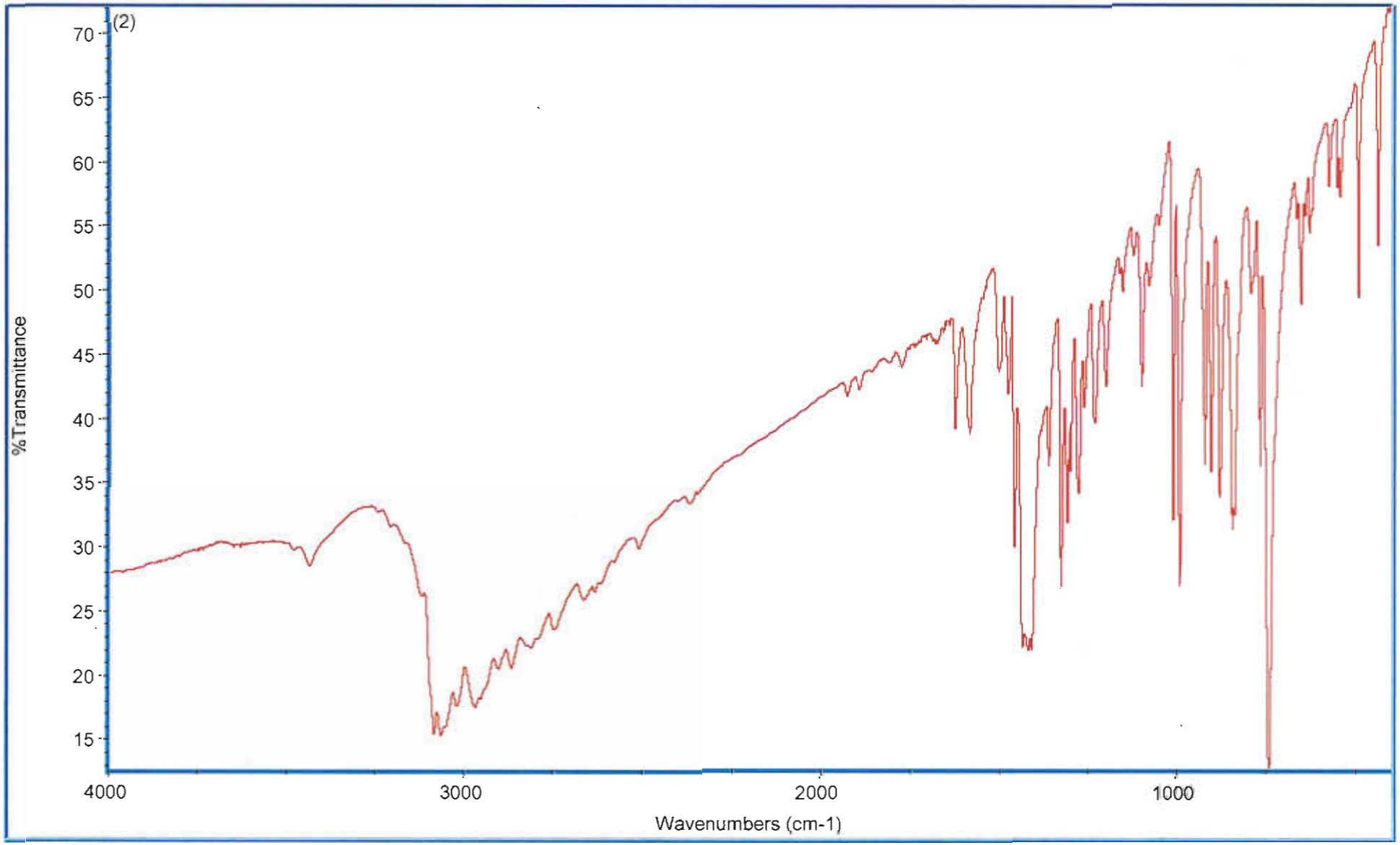
(2)
%Transmittance
70
65
60
55
50
45
40
35
30
25
20
15
4000
3000
2000
1000
Wavenumbers (cm-1)

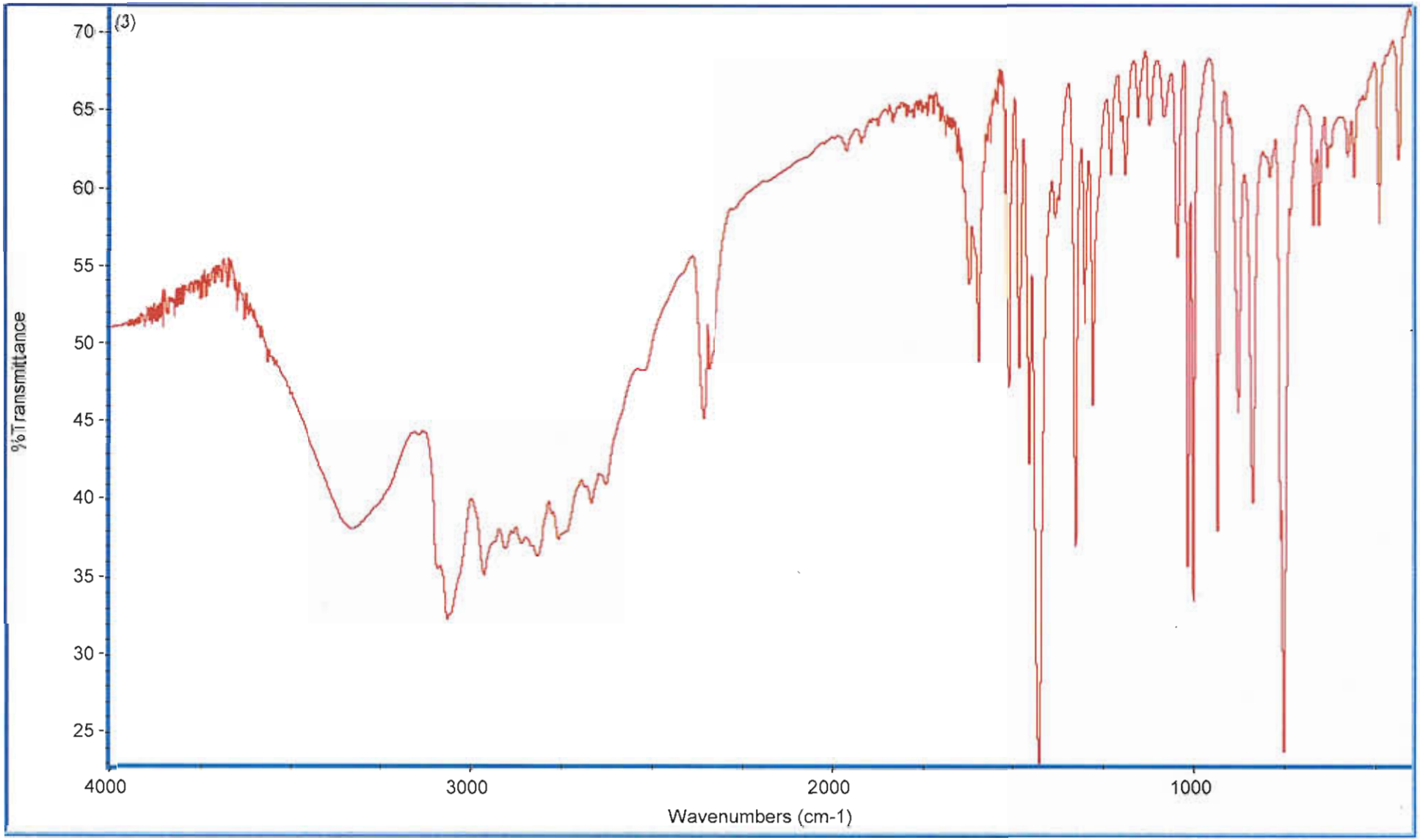
(3)
70
65
60
55
50
45
40
35
30
25
%Transmittance
4000
3000
2000
1000
Wavenumbers (cm-1)

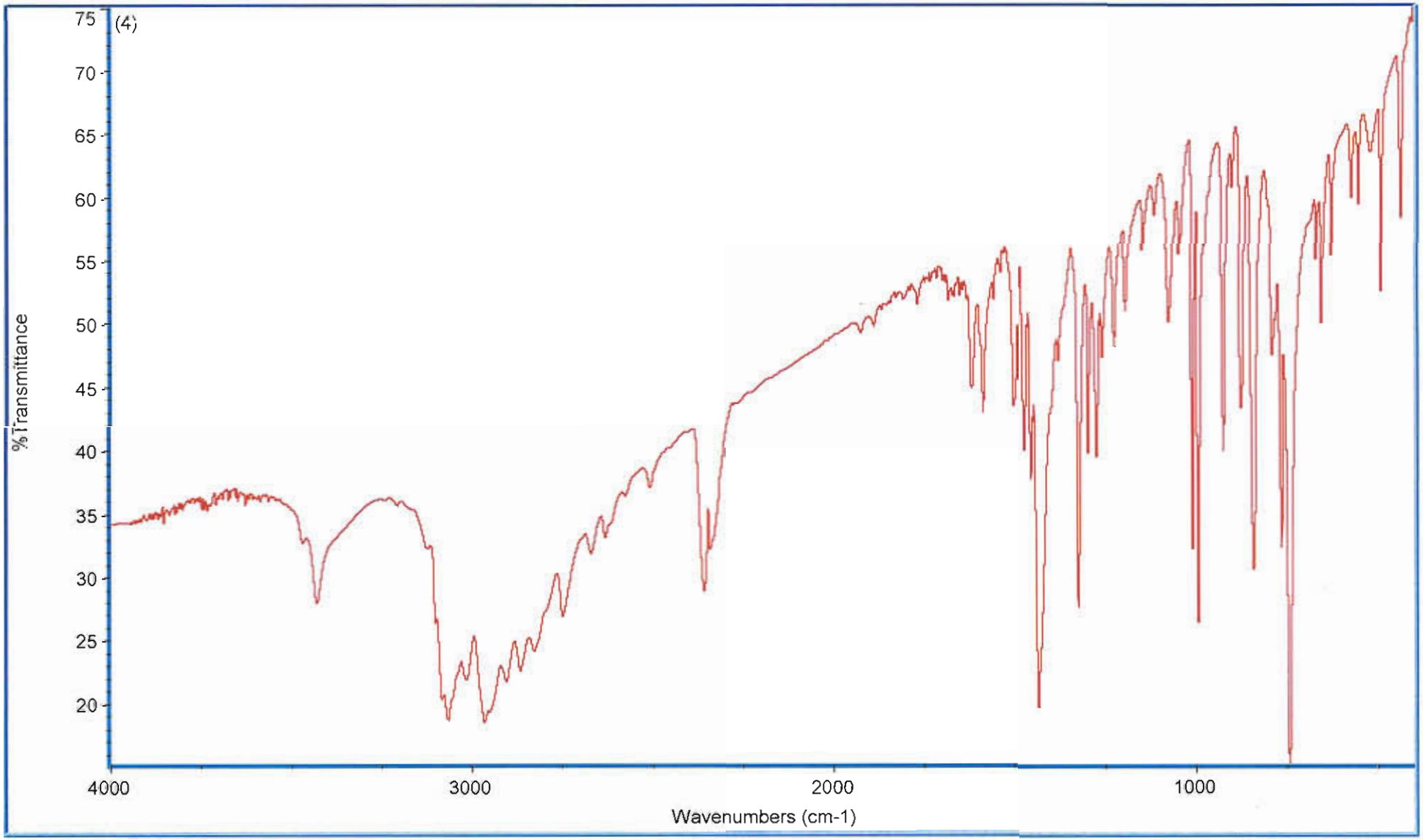
(4)
75
70
65
60
55
50
45
40
35
30
25
20
%Transmittance
4000
3000
2000
1000
Wavenumbers (cm-1)

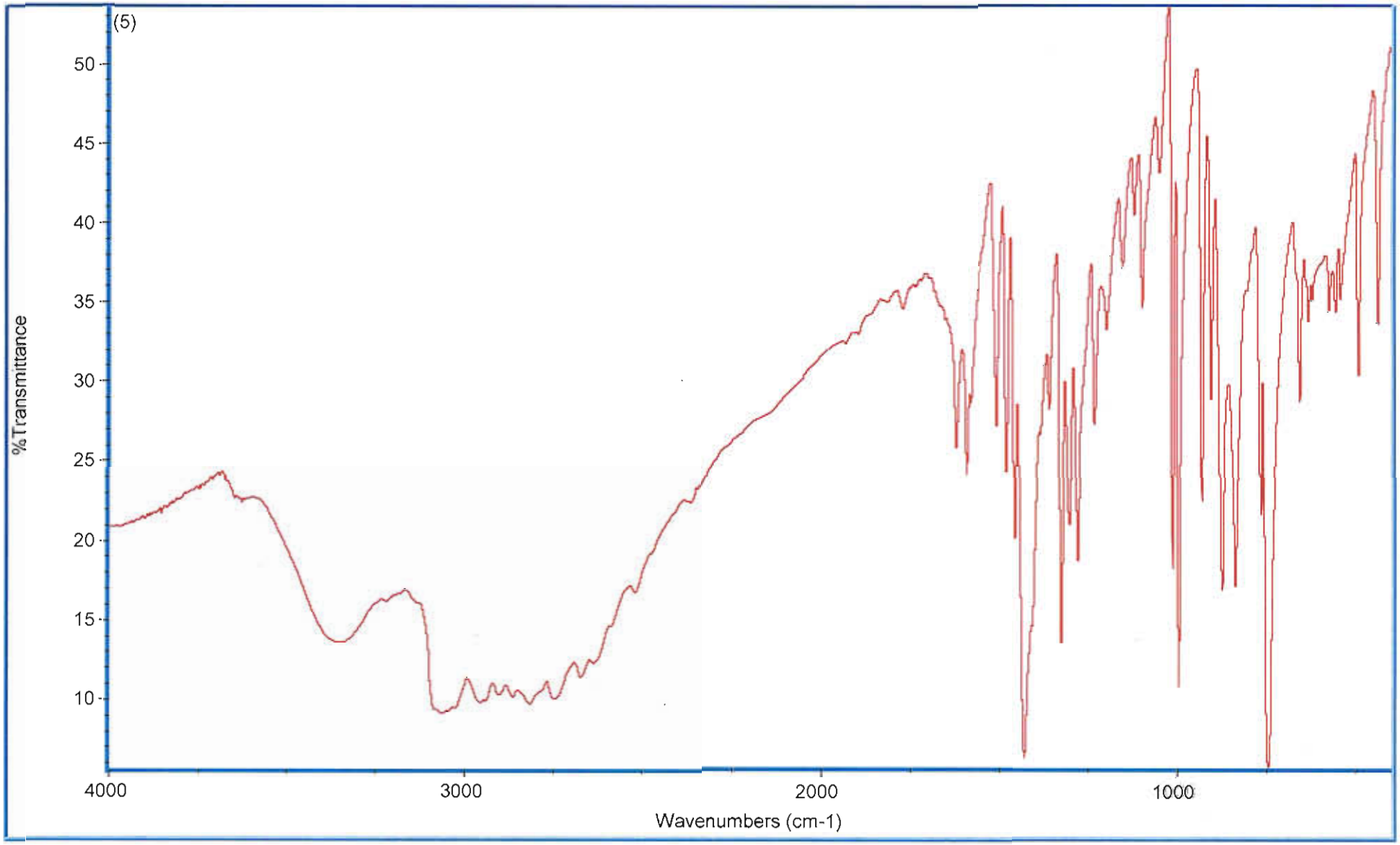
(5)
%Transmittance
50
45
40
35
30
25
20
15
10
4000
3000
2000
1000
Wavenumbers (cm-1)

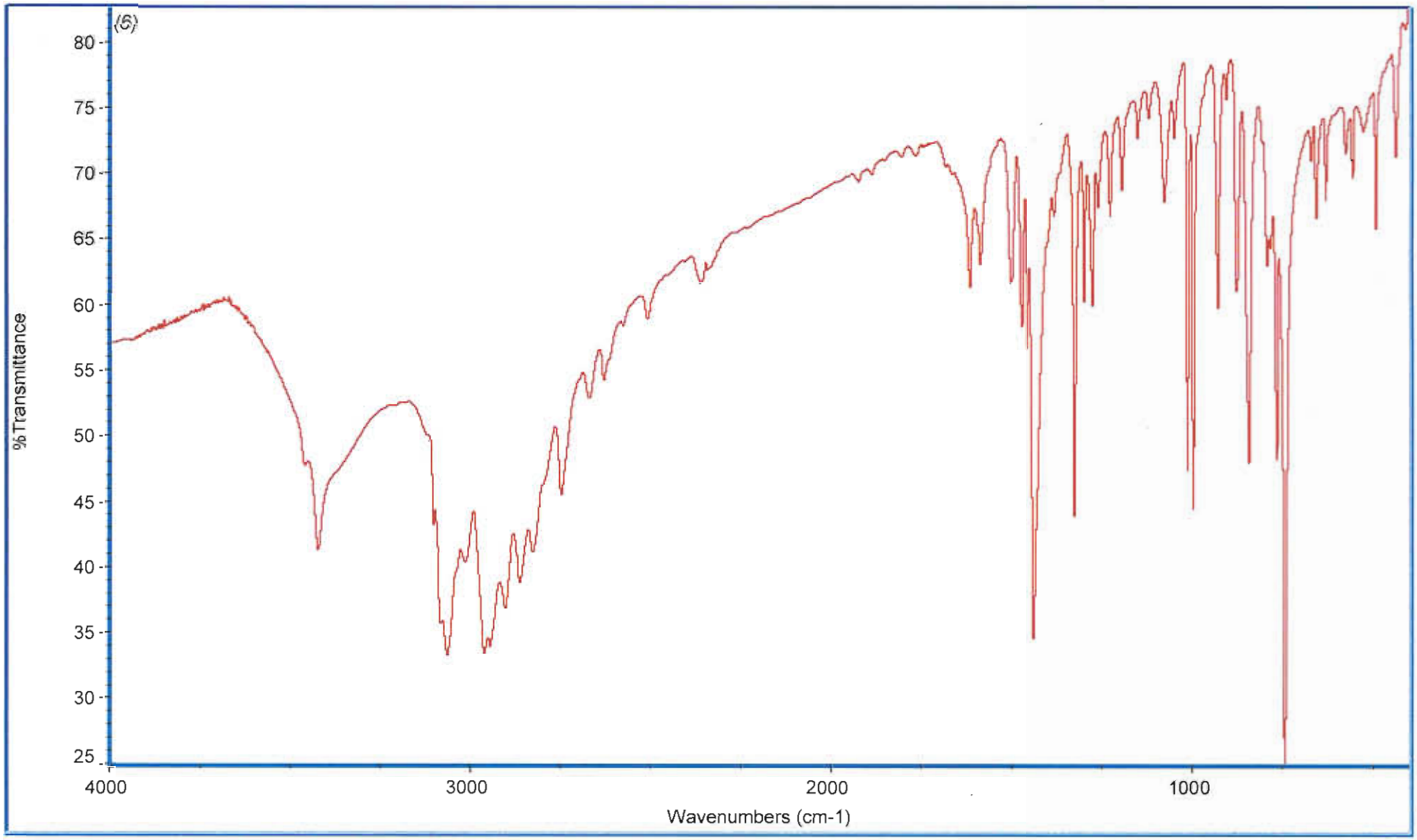
(5)
80
75
70
65
60
55
50
45
40
35
30
25
%Transmittance
4000
3000
2000
1000
Wavenumbers (cm-1)

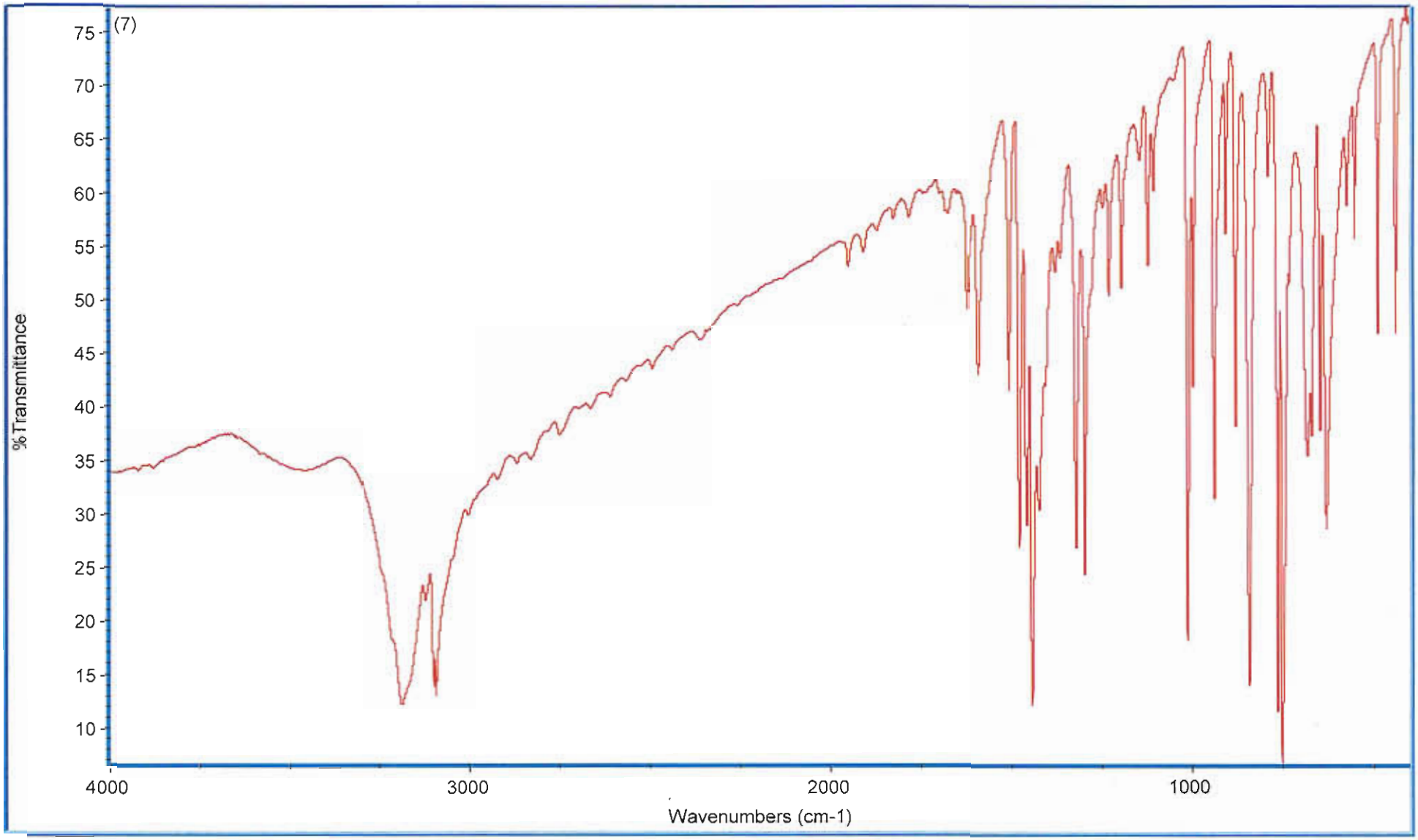
(7)
%Transmittance
75
70
65
60
55
50
45
40
35
30
25
20
15
10
4000
3000
2000
1000
Wavenumbers (cm-1)

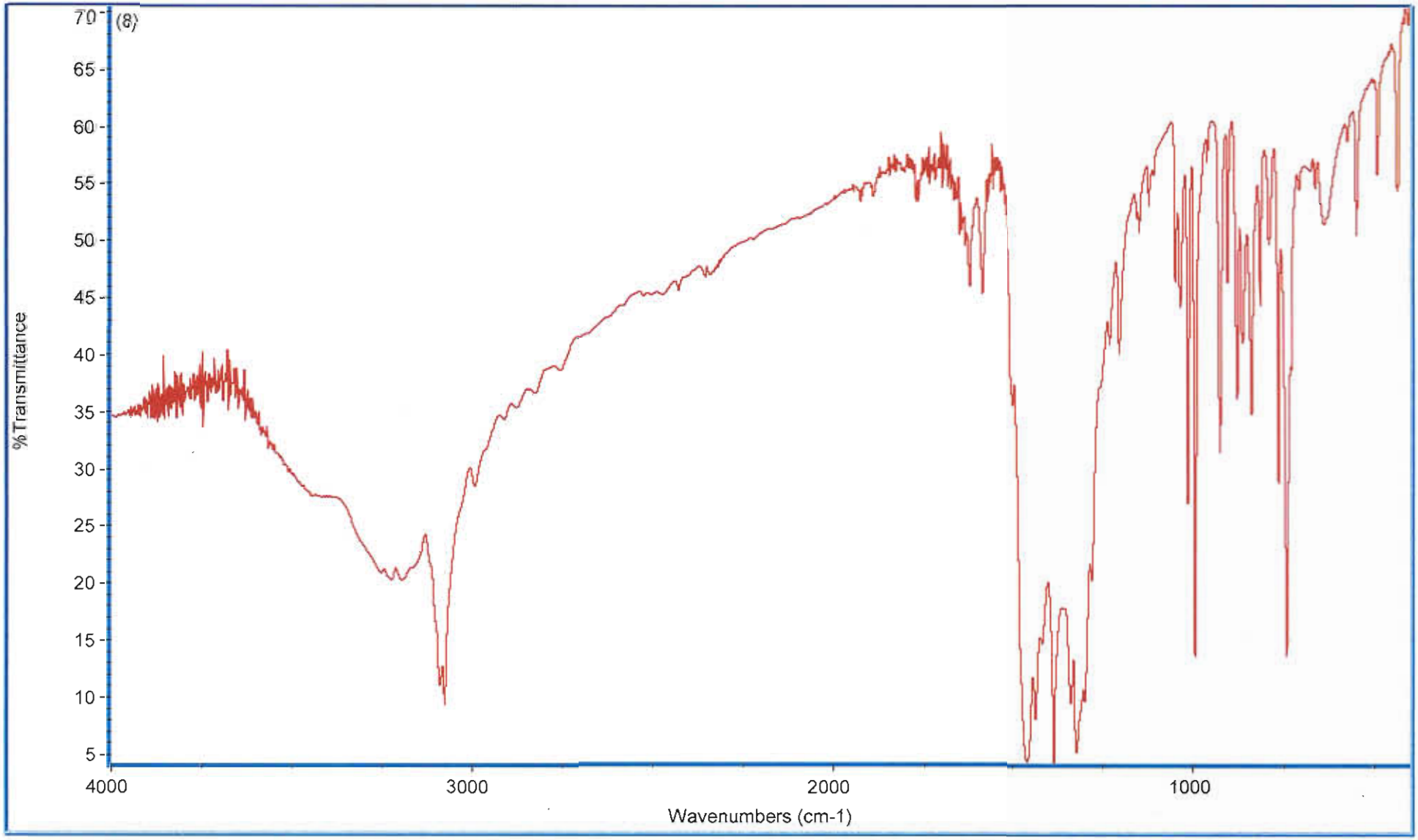
(8)
%Transmittance
70
65
60
55
50
45
40
35
30
25
20
15
10
5
4000
3000
2000
1000
Wavenumbers (cm-1)

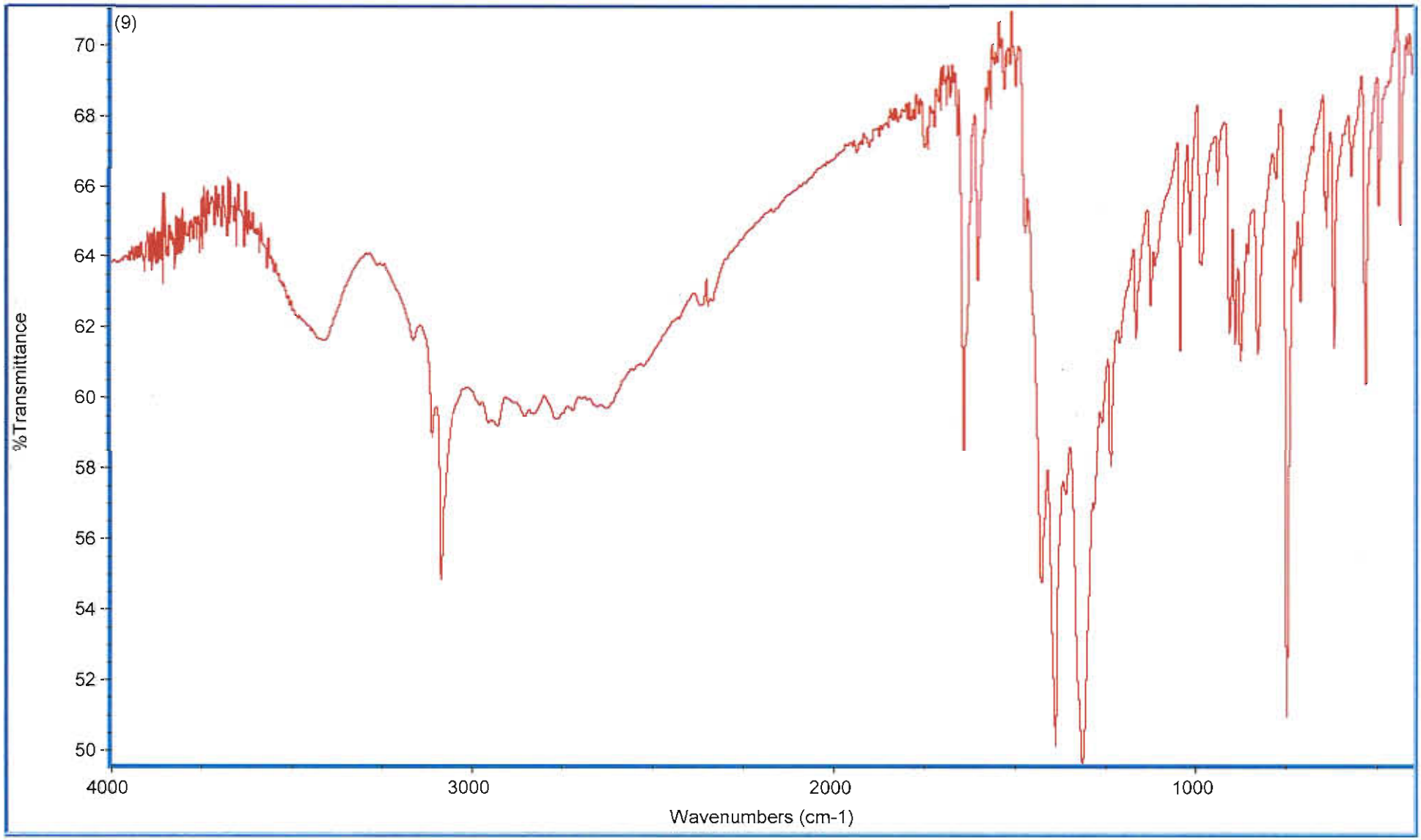
(9)
70
68
66
64
62
60
58
56
54
52
50
%Transmittance
4000
3000
2000
1000
Wavenumbers (cm-1)

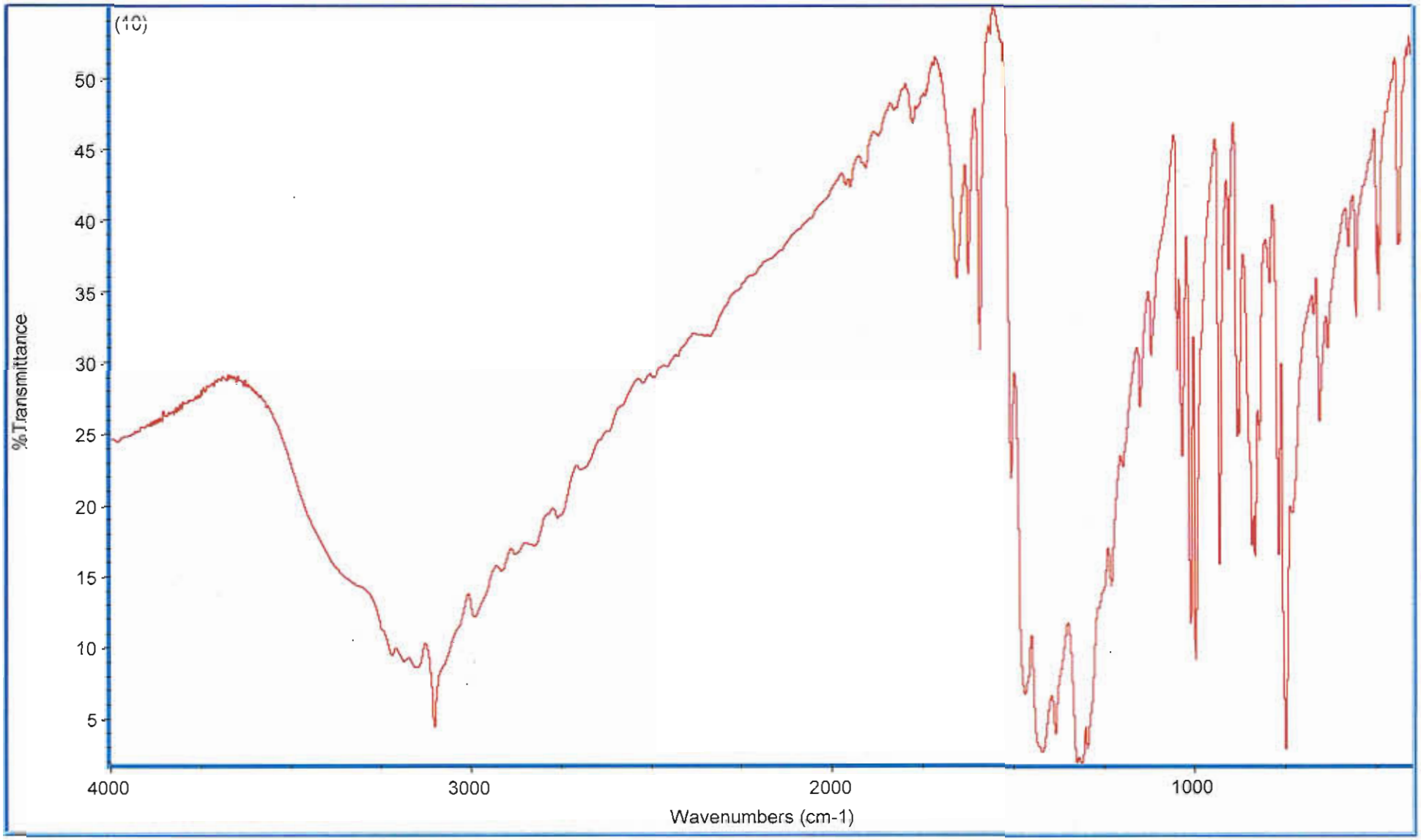
(10)
%Transmittance
50
45
40
35
30
25
20
15
10
5
4000
3000
2000
1000
Wavenumbers (cm-1)

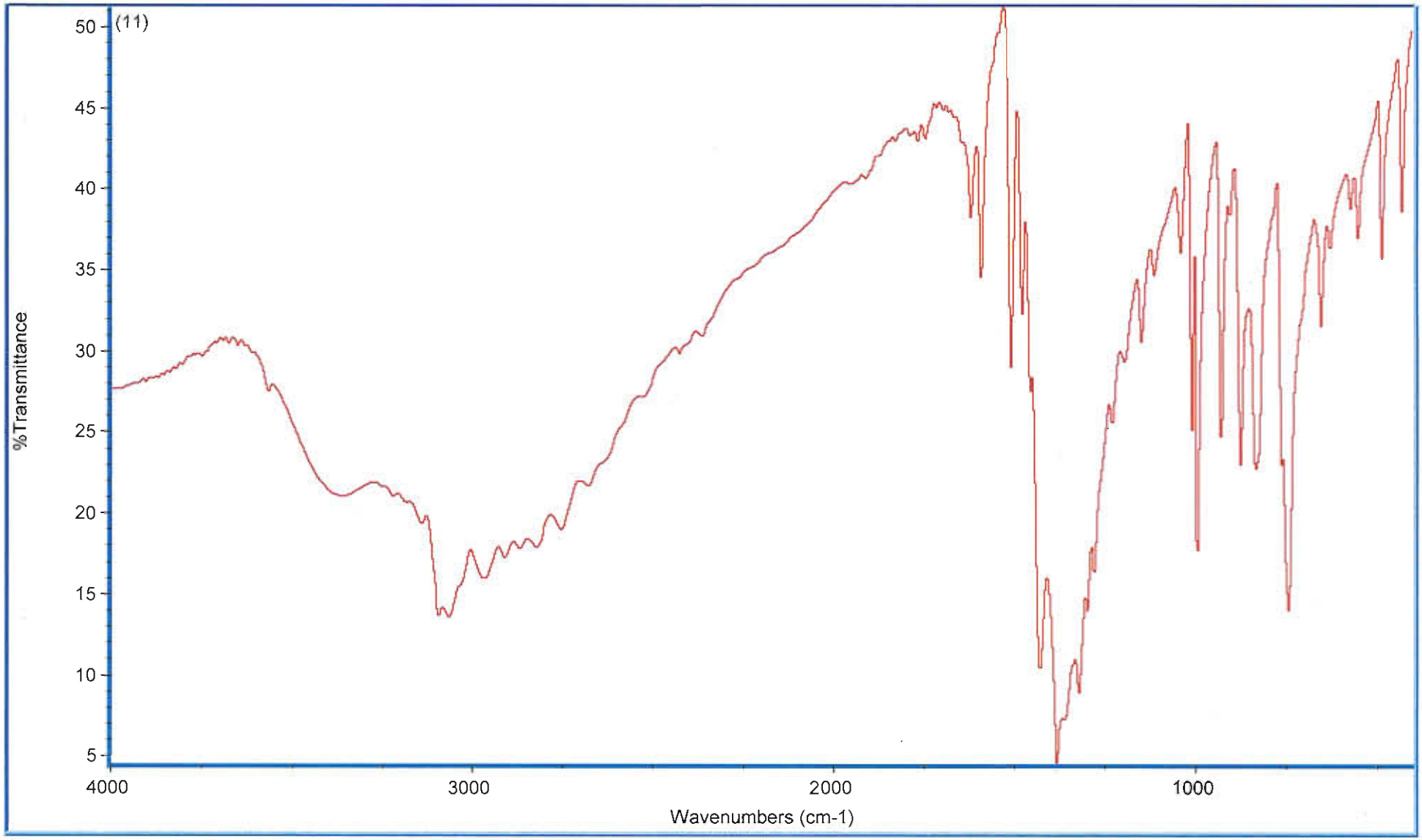
(11)
%Transmittance
50
45
40
35
30
25
20
15
10
5
4000
3000
2000
1000
Wavenumbers (cm-1)

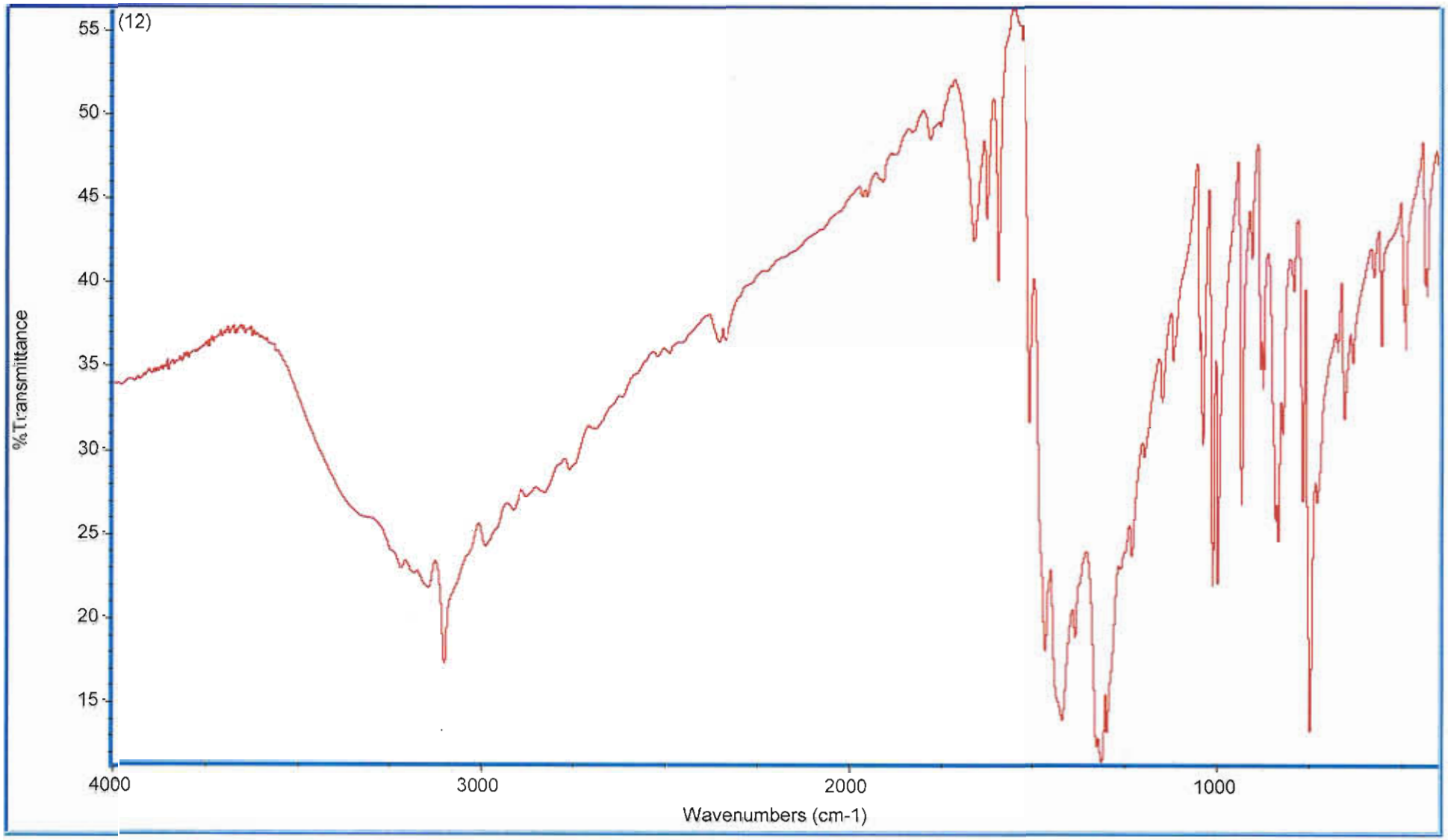
(12)
%Transmittance
55
50
45
40
35
30
25
20
15
4000
3000
2000
1000
Wavenumbers (cm-1)

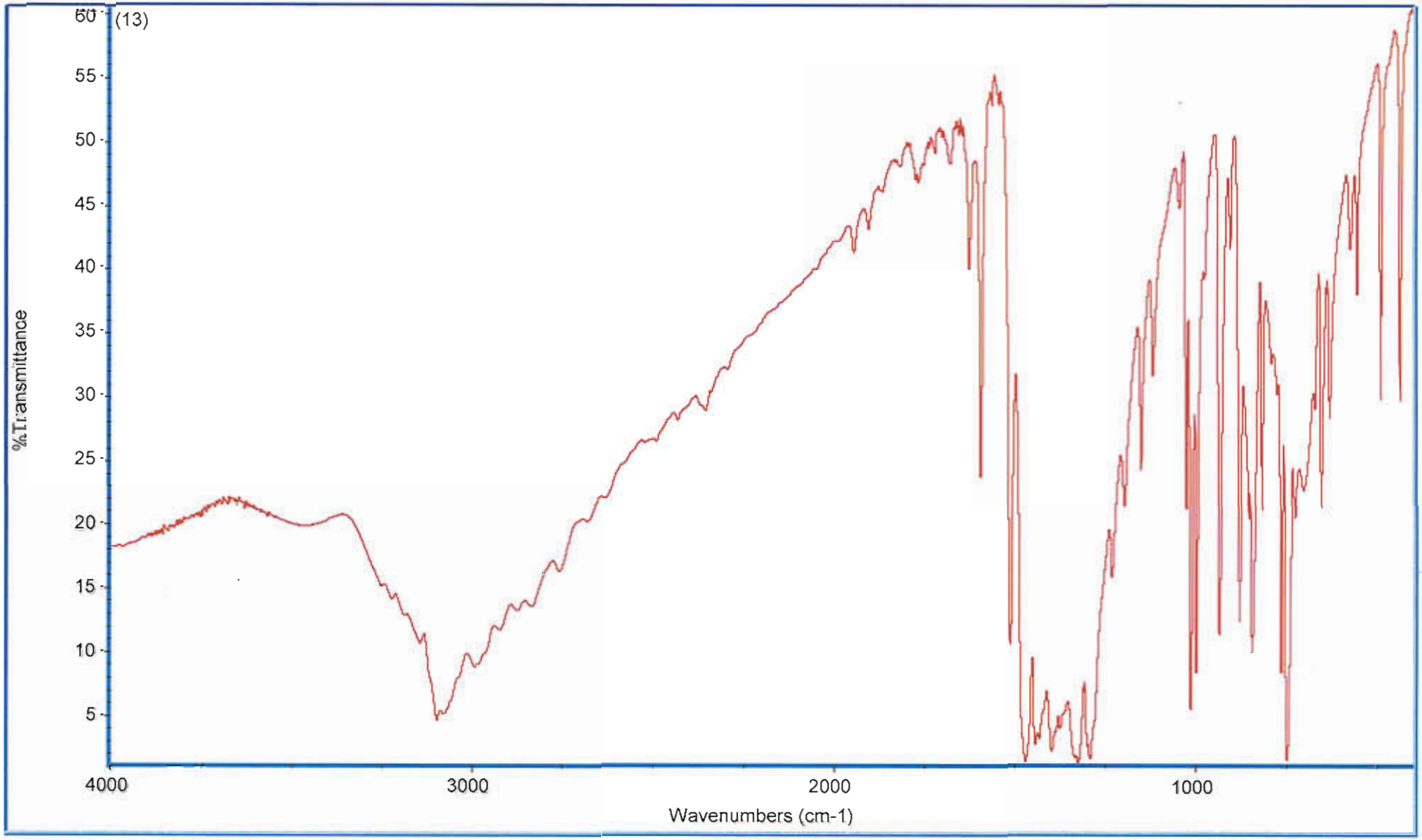
(13)
%Transmittance
60
55
50
45
40
35
30
25
20
15
10
5
4000
3000
2000
1000
Wavenumbers (cm-1)

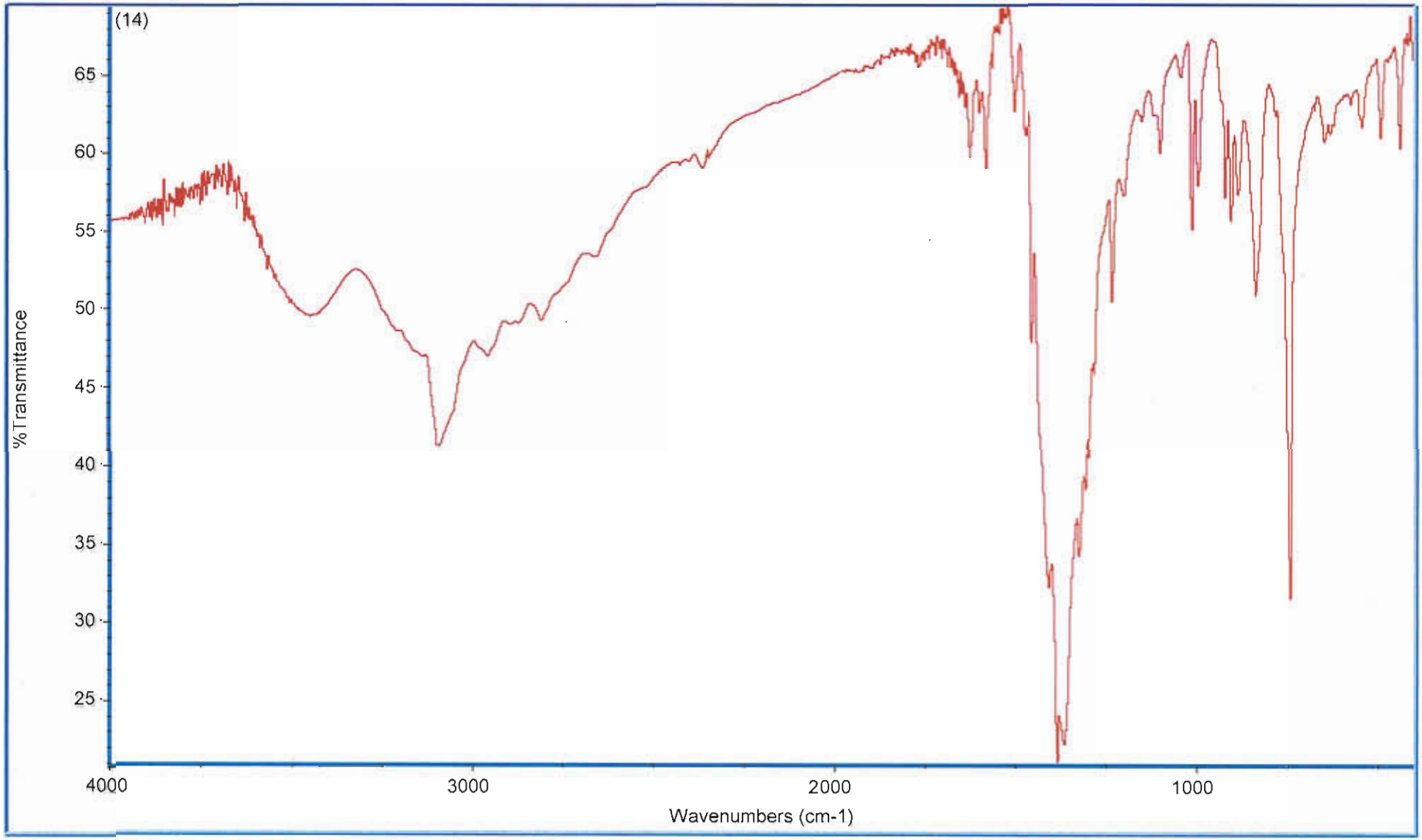
(14)
65
60
55
50
45
40
35
30
25
%Transmittance
4000
3000
2000
1000
Wavenumbers (cm-1)

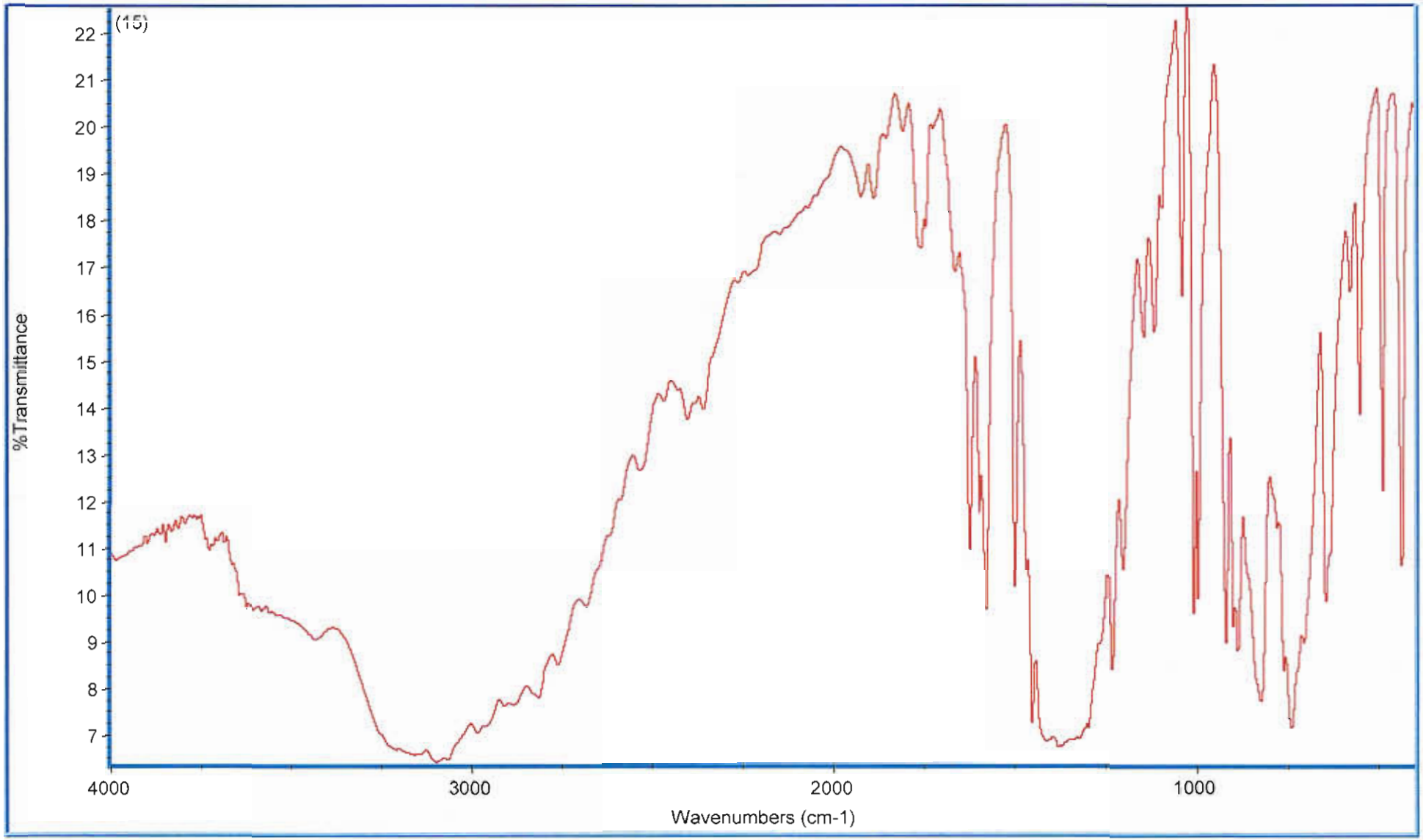
(15)
%Transmittance
22
21
20
19
18
17
16
15
14
13
12
11
10
9
8
7
4000
3000
2000
1000
Wavenumbers (cm-1)

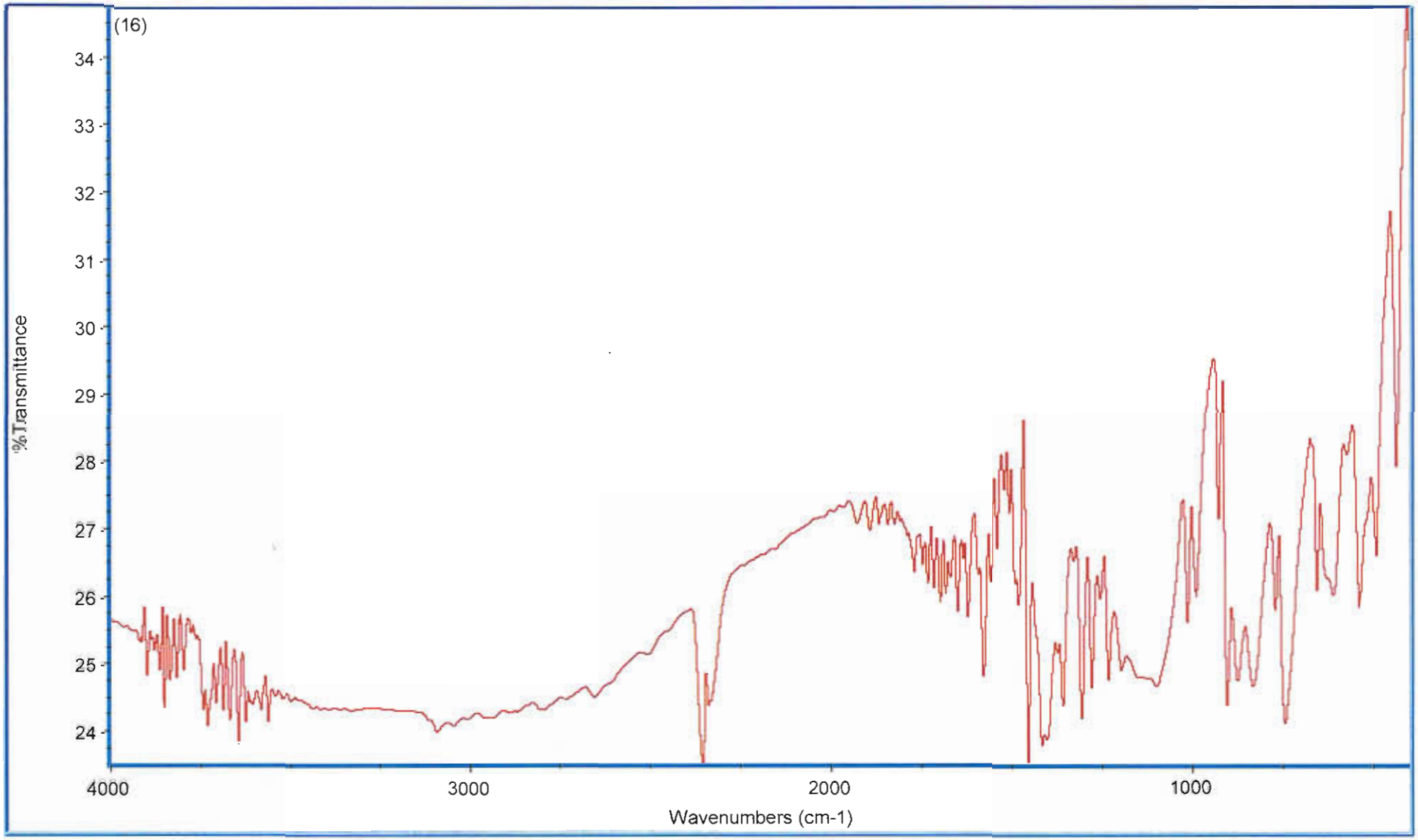
(16)
%Transmittance
34
33
32
31
30
29
28
27
26
25
24
4000
3000
2000
1000
Wavenumbers (cm-1)

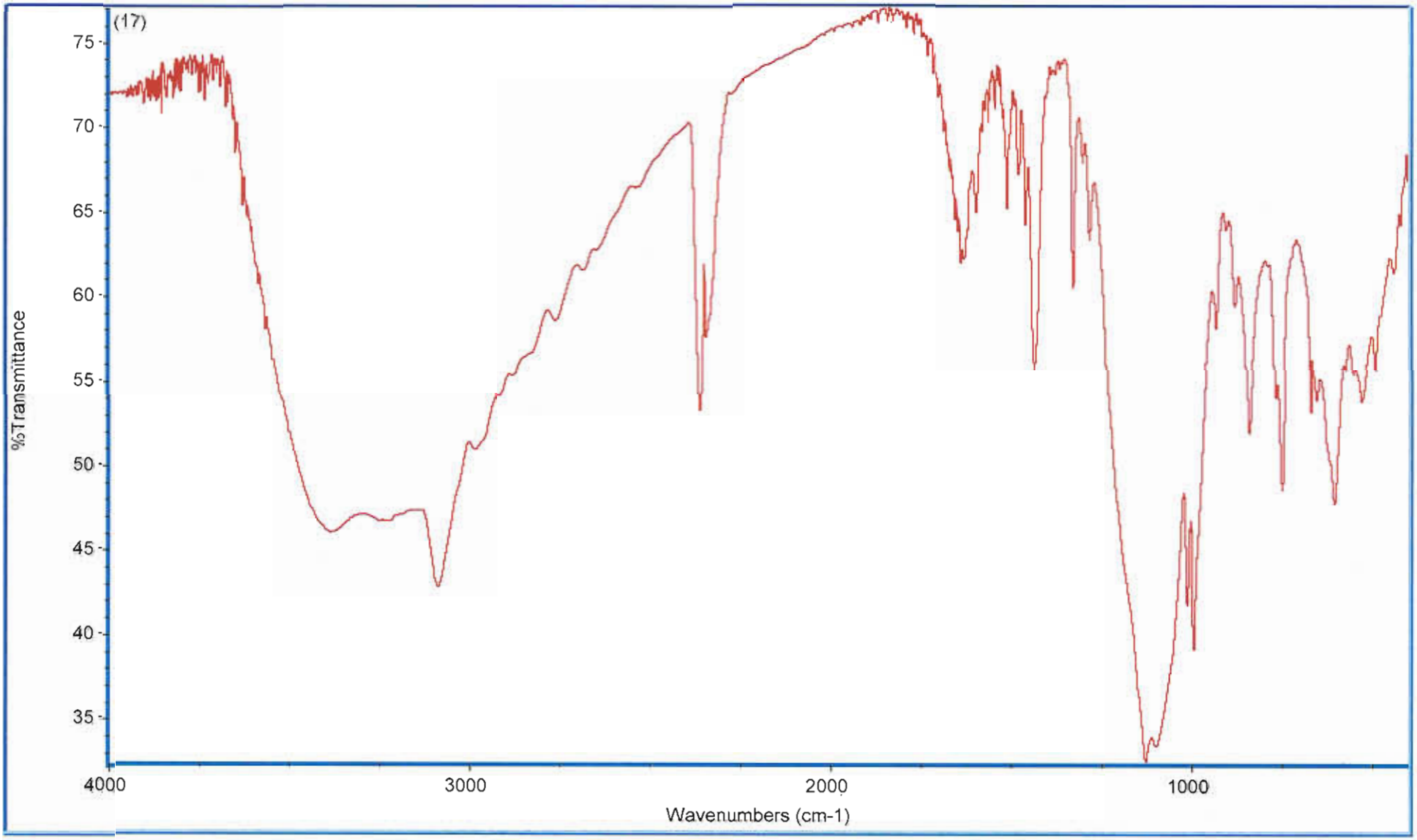
(17)
75
70
65
60
55
50
45
40
35
%Transmittance
4000
3000
2000
1000
Wavenumbers (cm-1)

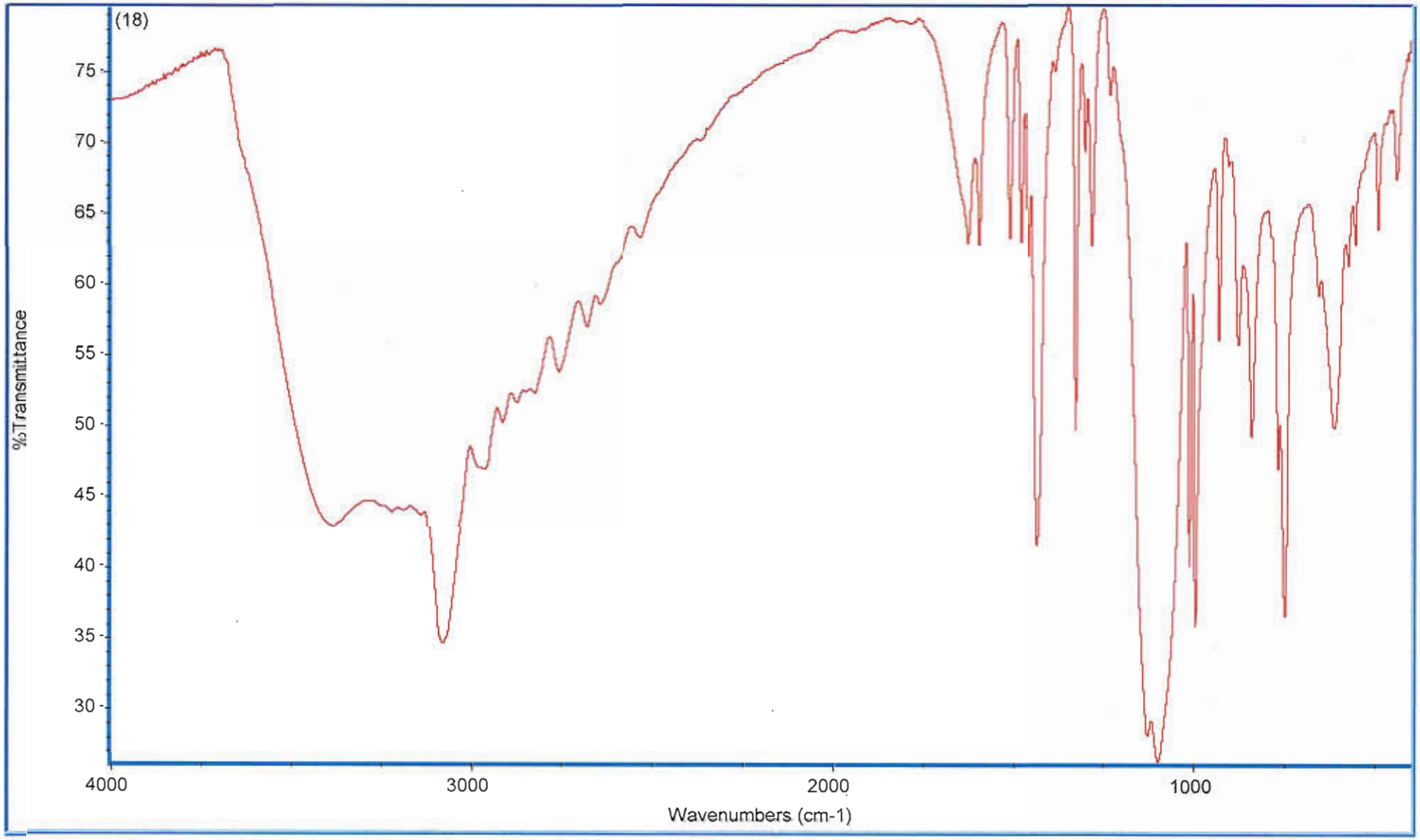
(18)
%Transmittance
75
70
65
60
55
50
45
40
35
30
4000
3000
2000
1000
Wavenumbers (cm-1)

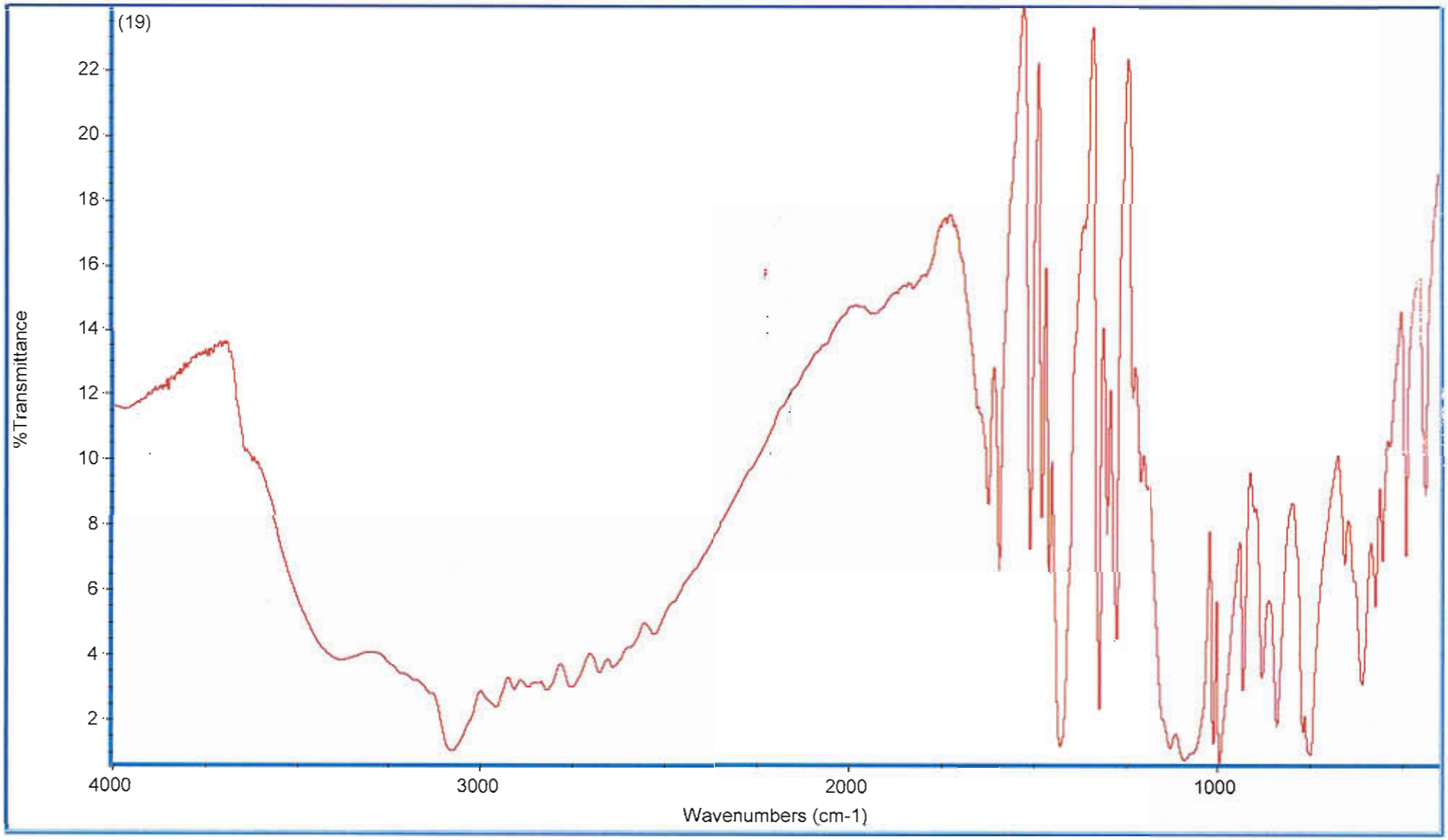
(19)
%Transmittance
22
20
18
16
14
12
10
8
6
4
2
4000
3000
2000
1000
Wavenumbers (cm-1)

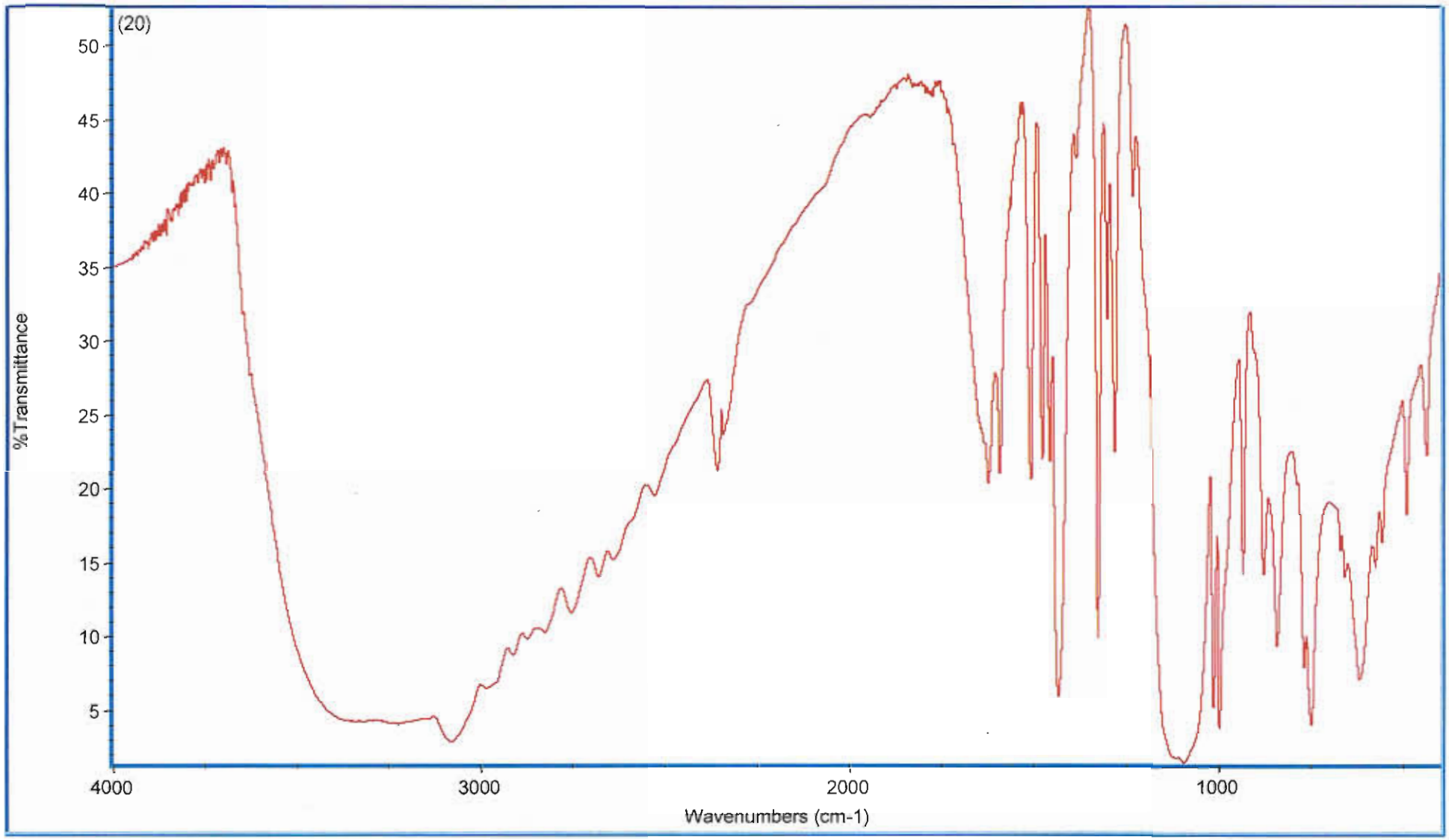
(20)
%Transmittance
50
45
40
35
30
25
20
15
10
5
4000
3000
2000
1000
Wavenumbers (cm-1)

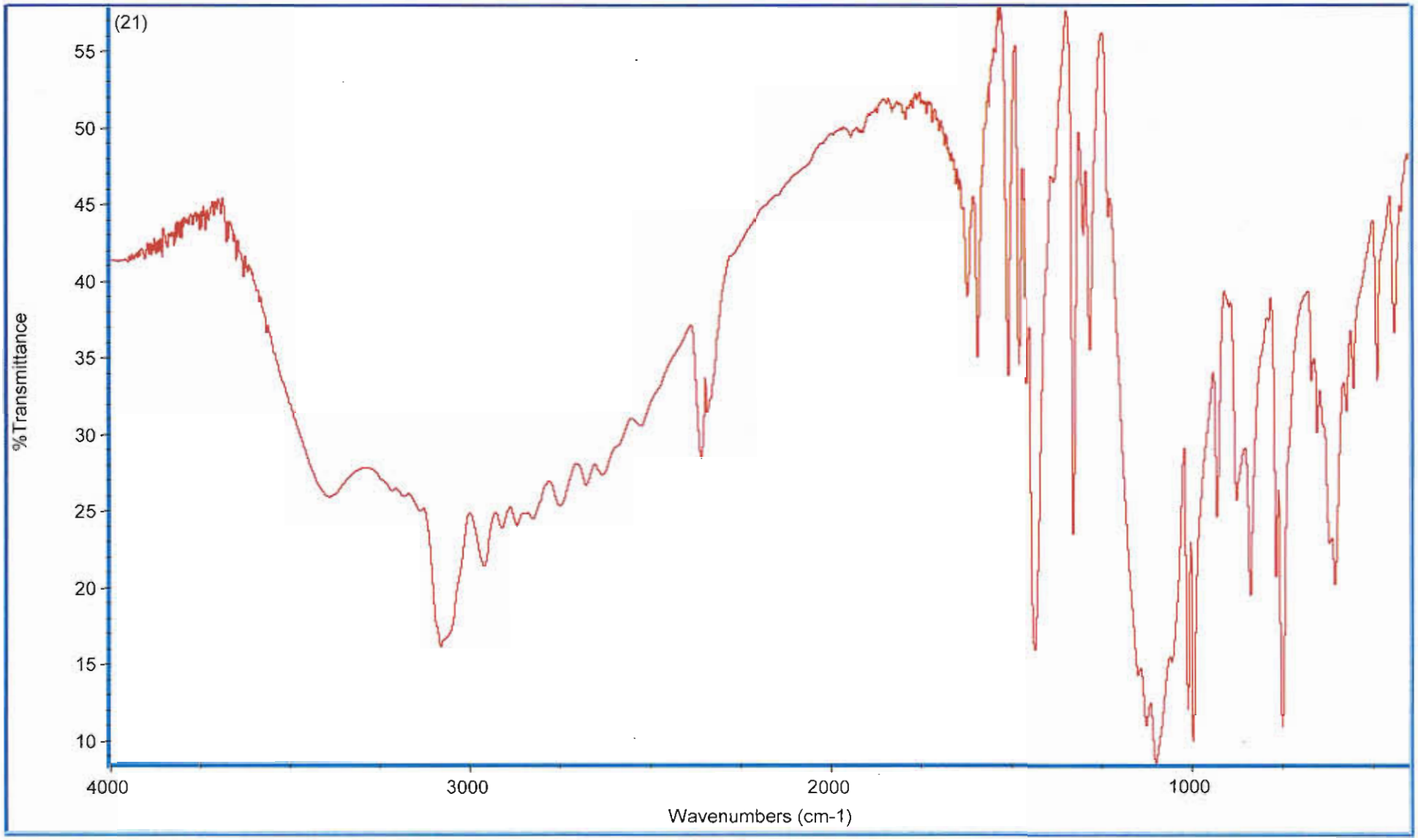
(21)
%Transmittance
55
50
45
40
35
30
25
20
15
10
4000
3000
2000
1000
Wavenumbers (cm-1)

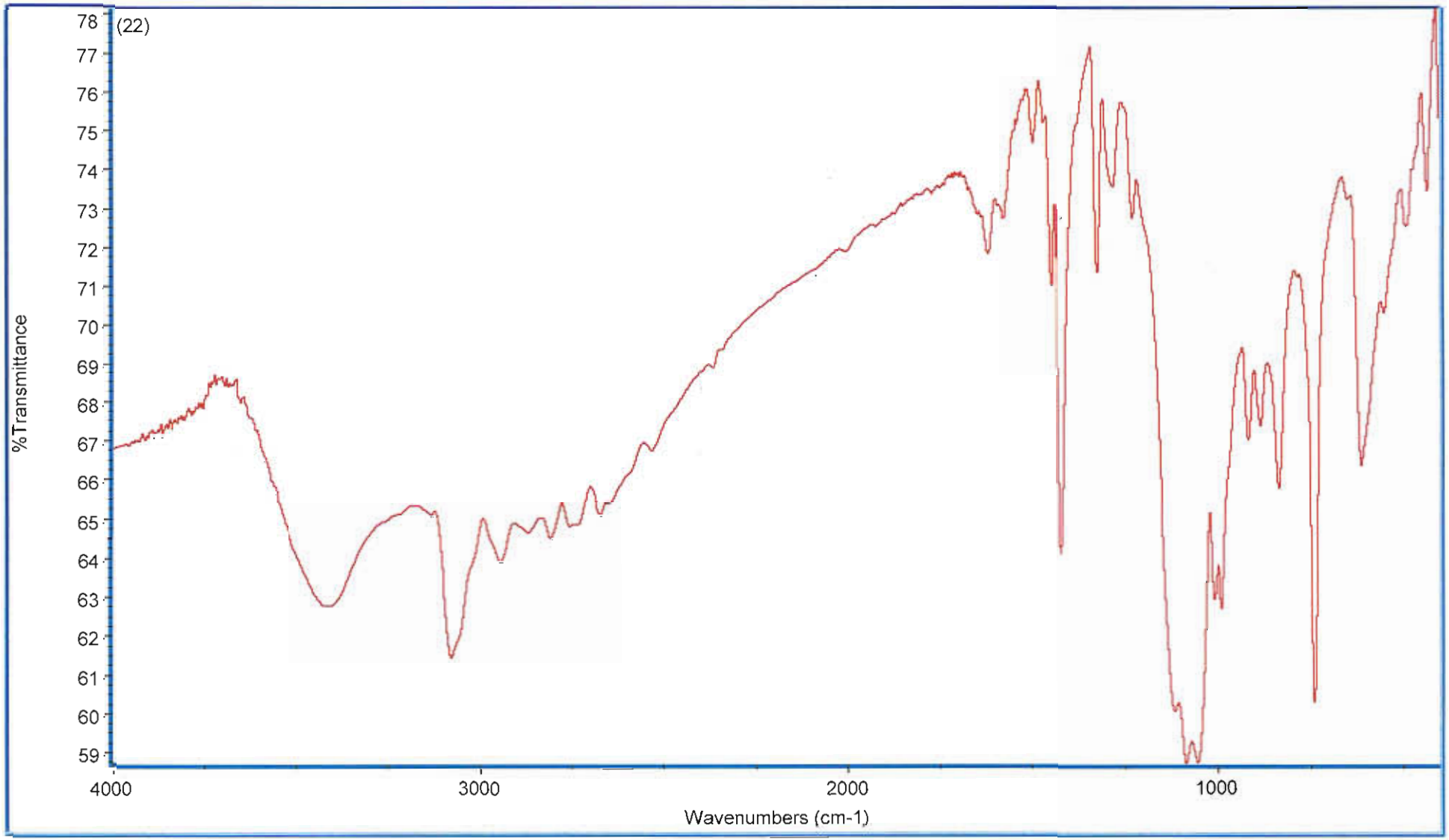
(22)
%Transmittance
78
77
76
75
74
73
72
71
70
69
68
67
66
65
64
63
62
61
60
59
4000
3000
2000
1000
Wavenumbers (cm-1)

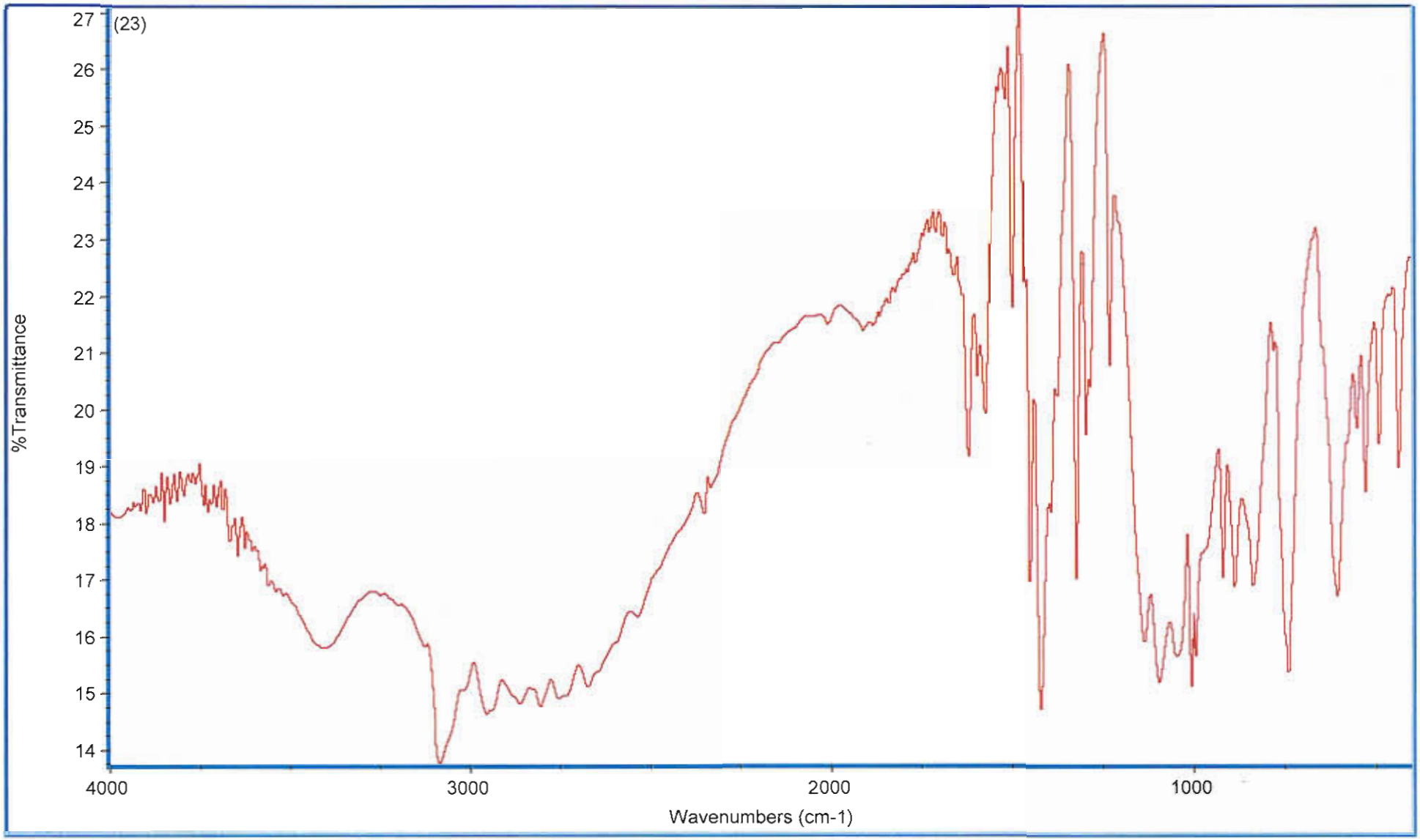
(23)
%Transmittance
27
26
25
24
23
22
21
20
19
18
17
16
15
14
4000
3000
2000
1000
Wavenumbers (cm-1)

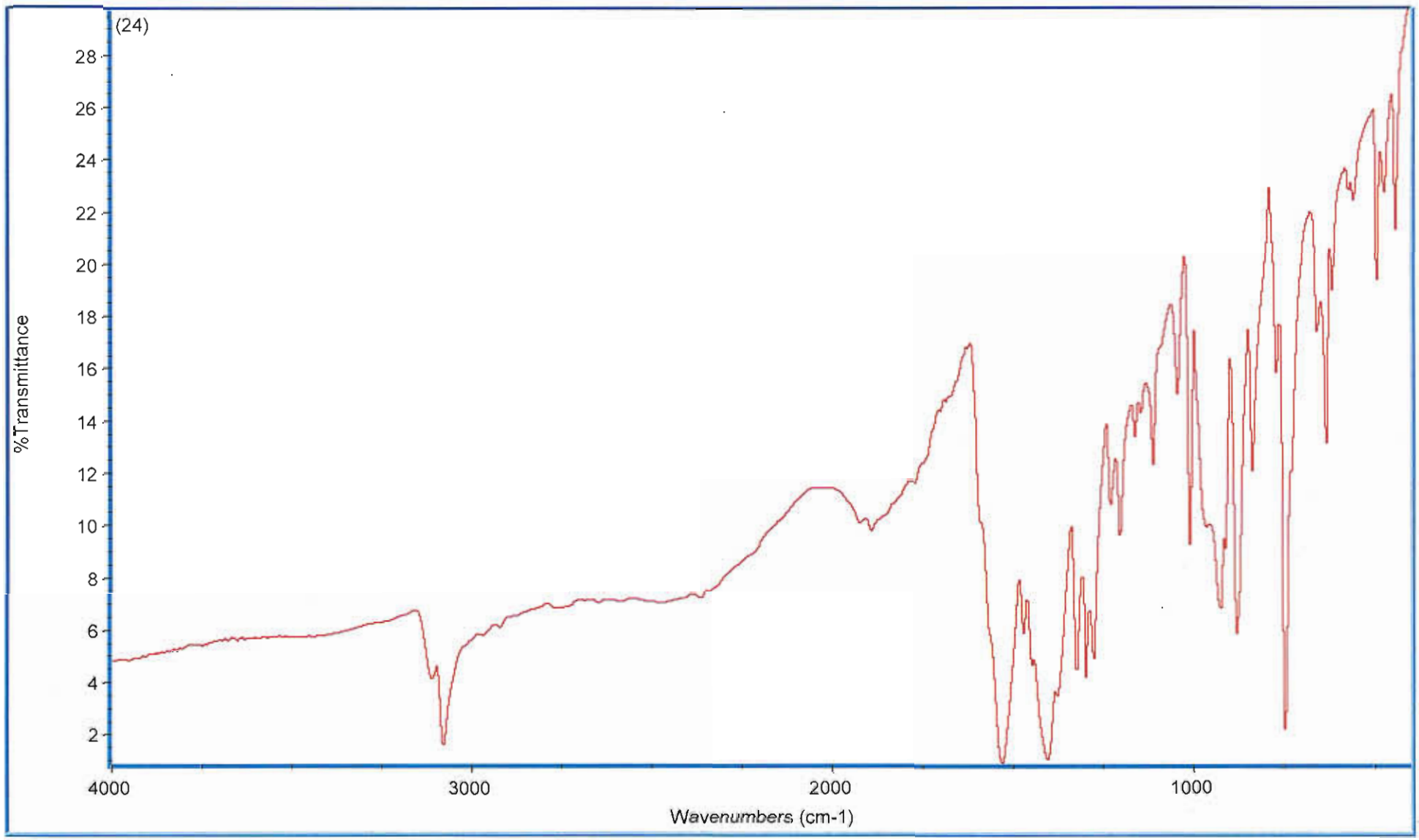
(24)
%Transmittance
28
26
24
22
20
18
16
14
12
10
8
6
4
2
4000
3000
2000
1000
Wavenumbers (cm-1)

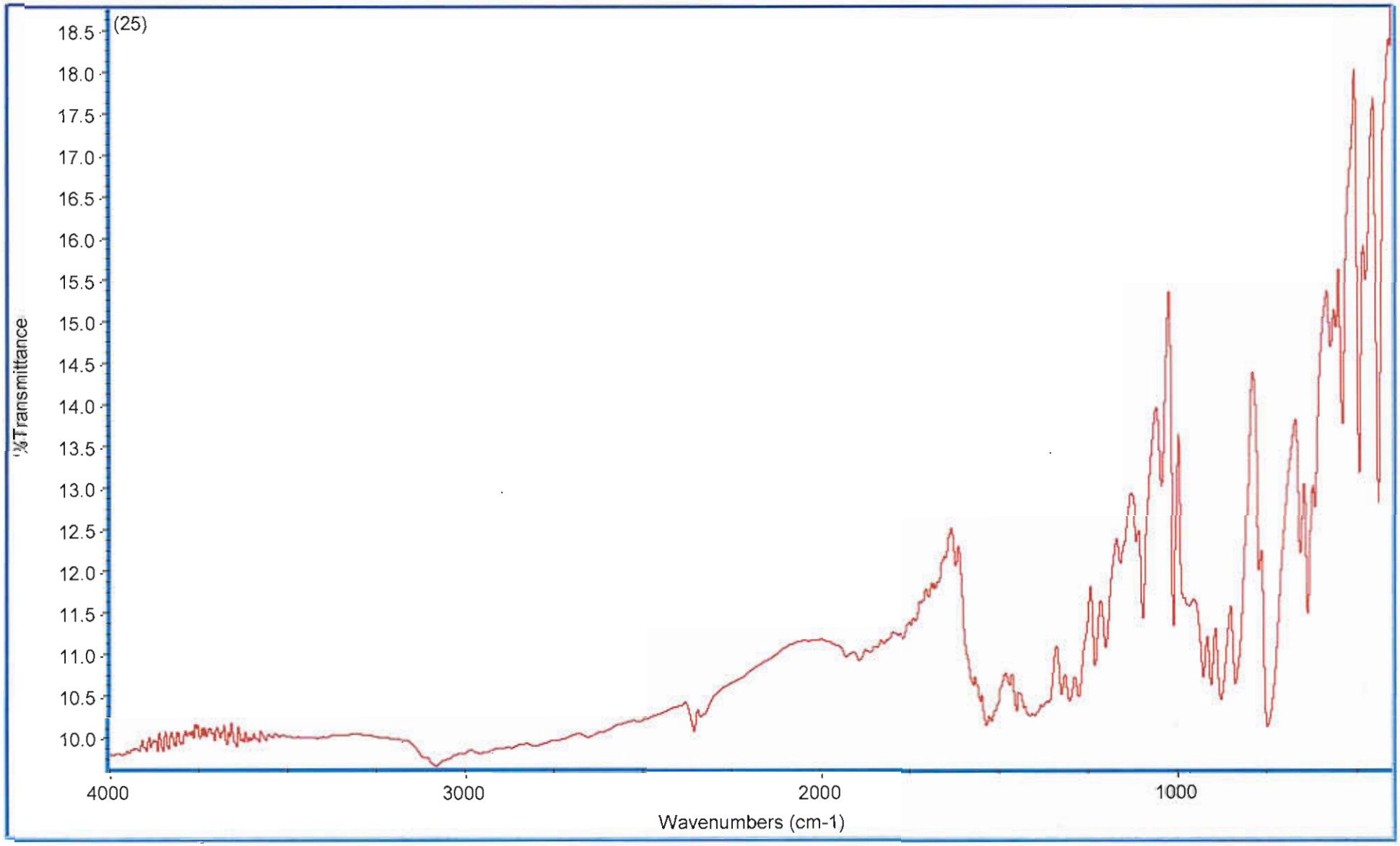
(25)
%Transmittance
18.5
18.0
17.5
17.0
16.5
16.0
15.5
15.0
14.5
14.0
13.5
13.0
12.5
12.0
11.5
11.0
10.5
10.0
4000
3000
2000
1000
Wavenumbers (cm-1)

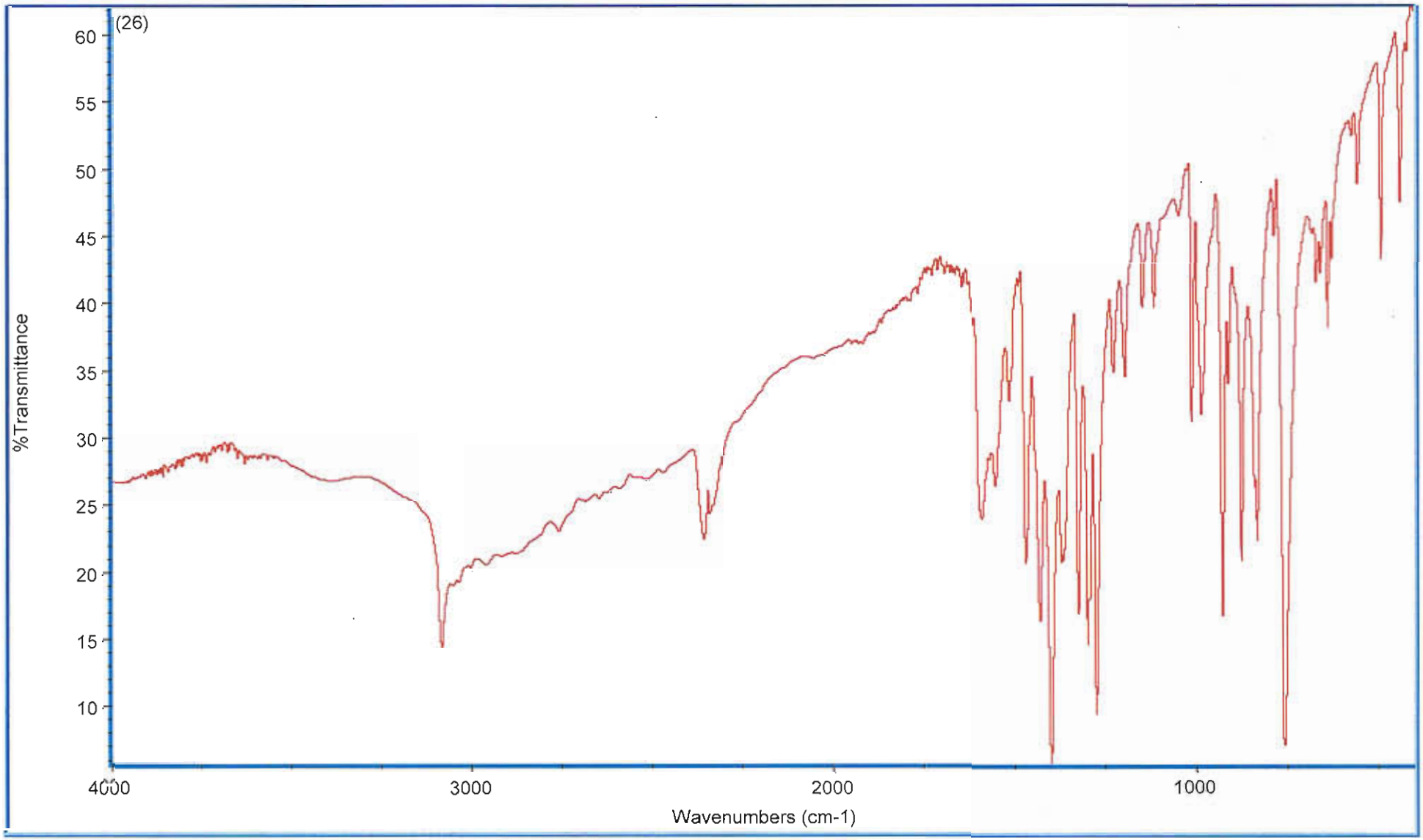
(26)
%Transmittance
60
55
50
45
40
35
30
25
20
15
10
4000
3000
2000
1000
Wavenumbers (cm-1)

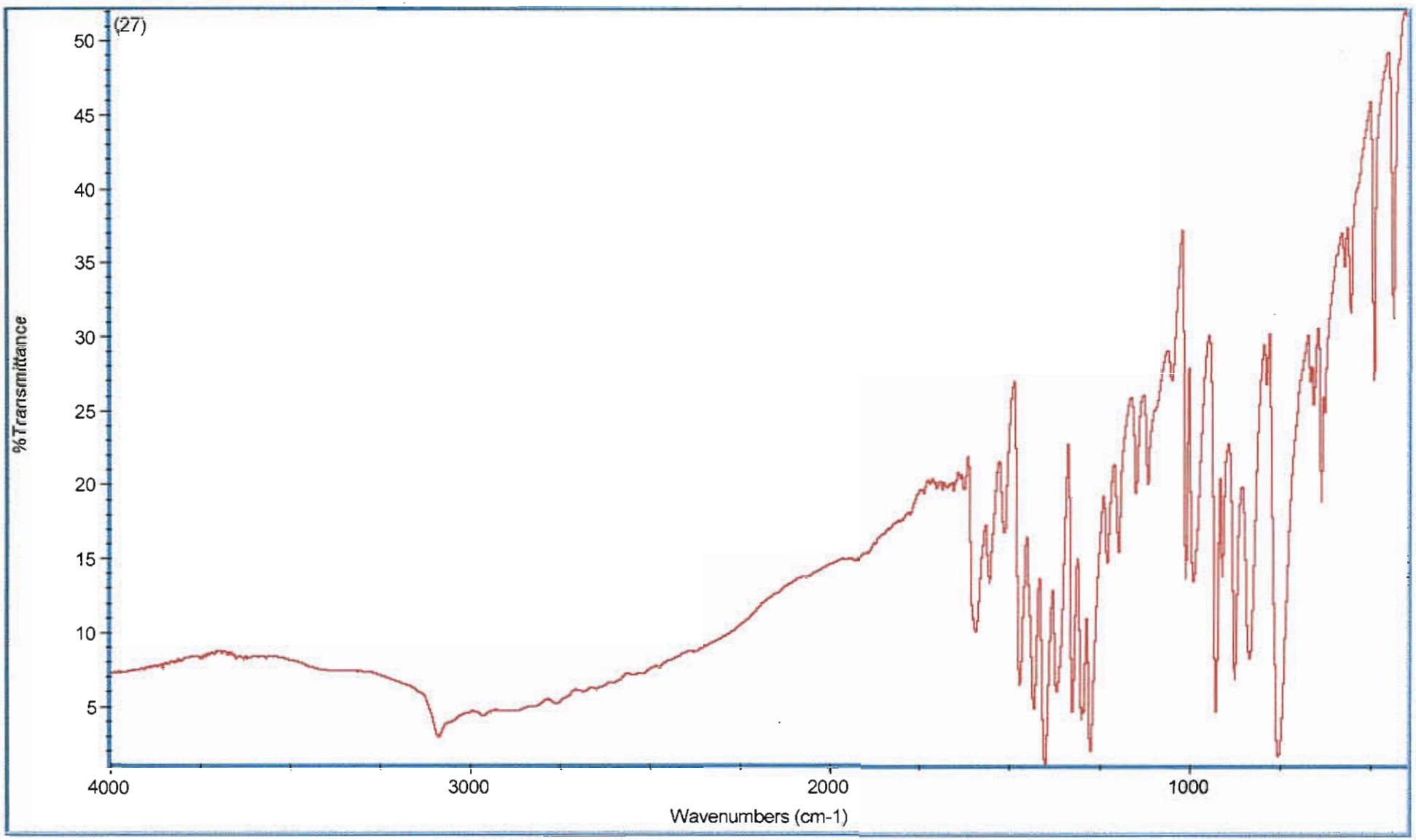
(27)
%Transmittance
50
45
40
35
30
25
20
15
10
5
4000
3000
2000
1000
Wavenumbers (cm-1)

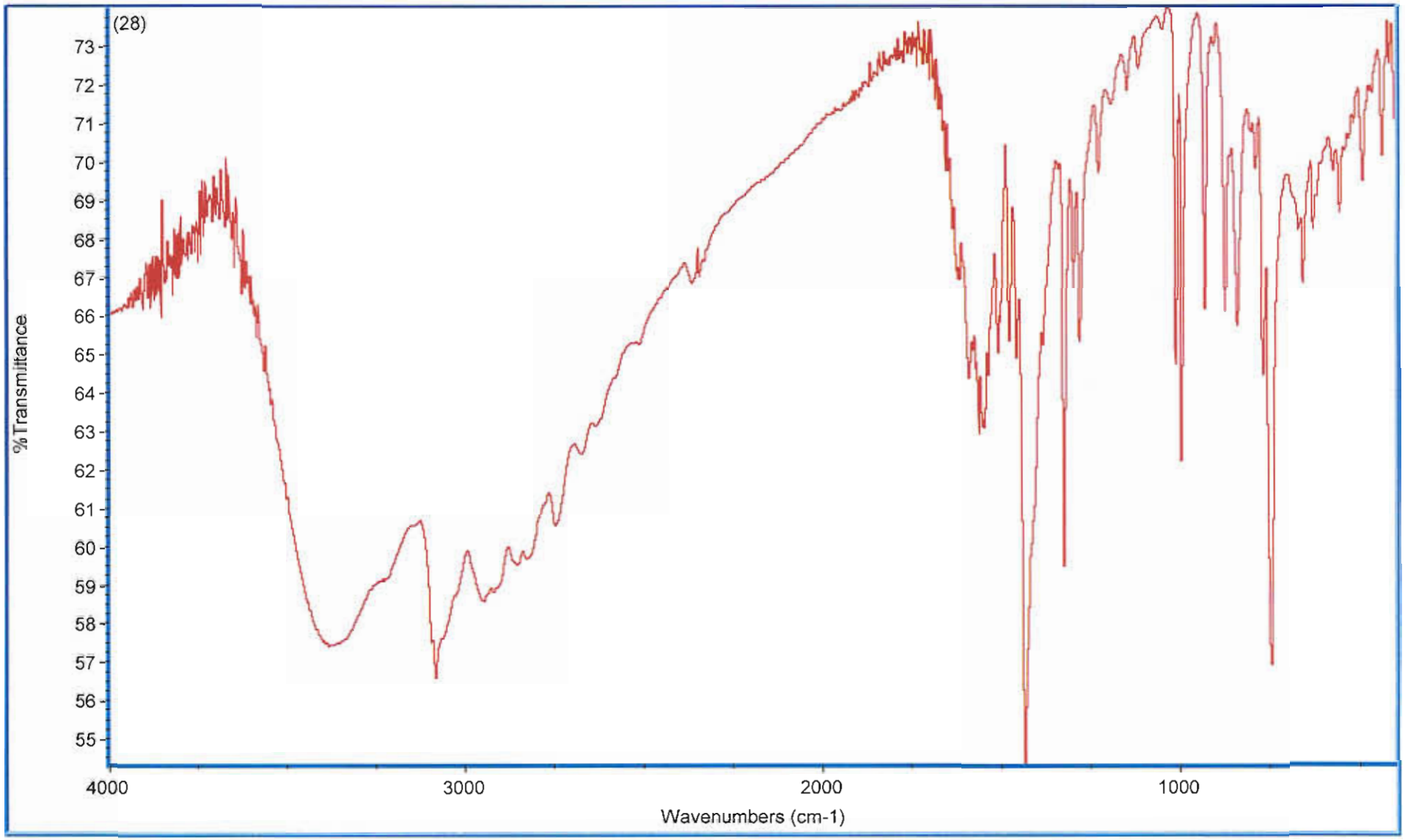
(28)
%Transmittance
73
72
71
70
69
68
67
66
65
64
63
62
61
60
59
58
57
56
55
4000
3000
2000
1000
Wavenumbers (cm-1)

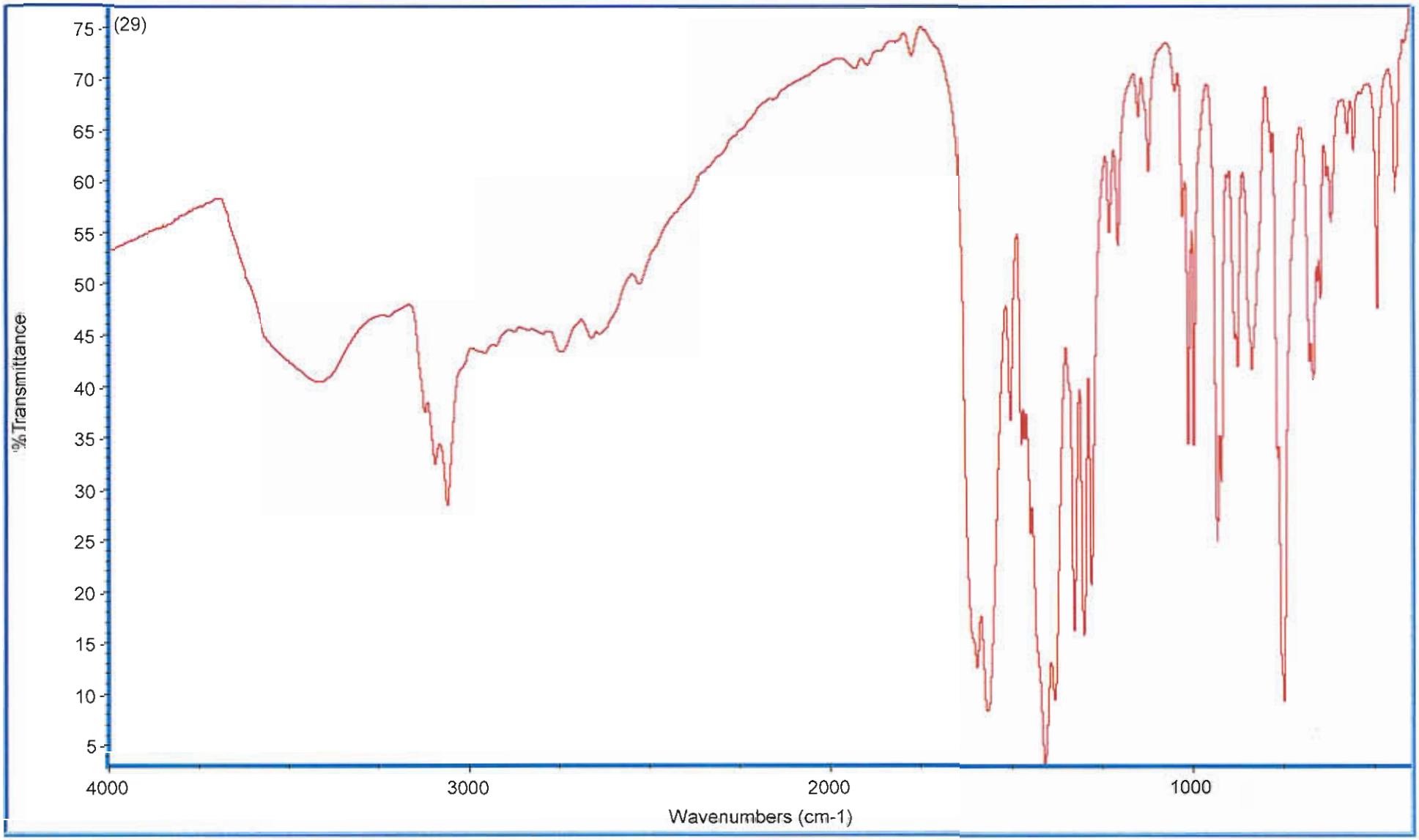
(29)
%Transmittance
75
70
65
60
55
50
45
40
35
30
25
20
15
10
5
4000
3000
2000
1000
Wavenumbers (cm-1)

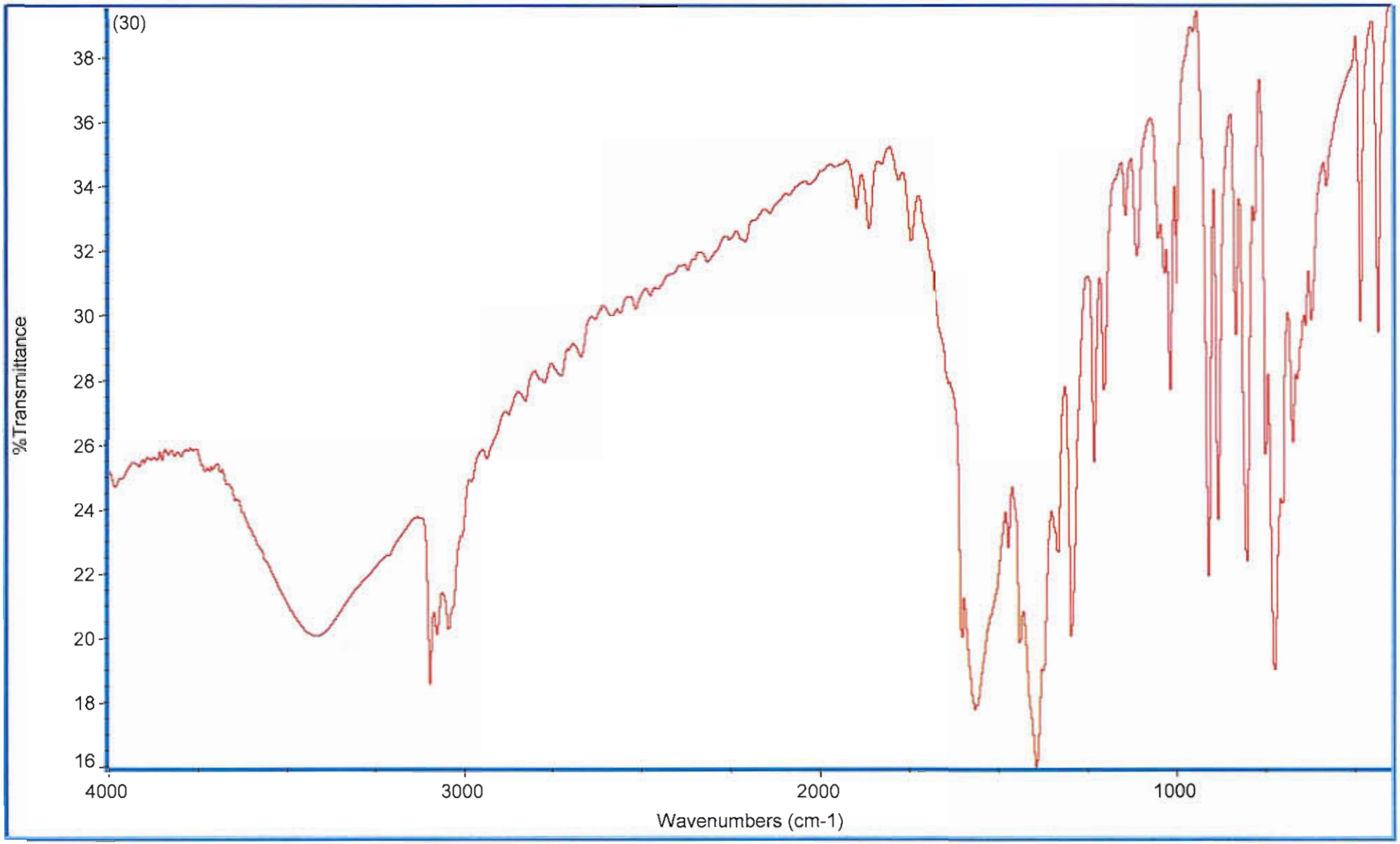
(30)
%Transmittance
38
36
34
32
30
28
26
24
22
20
18
16
4000
3000
2000
1000
Wavenumbers (cm-1)

RESEARCH PAPERS PUBLISHED DURING THIS STUDY

Available online at www.sciencedirect.com
SCIENCE DIRECT®
Polyhedron 22 (2003) 3187–3194
POLYHEDRON
www.elsevier.com/locate/po

Synthesis and in vitro anti-microbial activity of manganese (II) complexes of 2,2-dimethylpentanedioic and 3,3-dimethylpentanedioic acid: X-ray crystal structure of $[Mn(3dmepda)(phen)_2] \cdot 7.5H_2O$ ($3dmepdaH_2$ = 3,3-dimethylpentanedioic acid and phen = 1,10-phenanthroline)

Michael Devereux [a,*], Malachy McCann [b], Vanessa Leon [a], Rachel Kelly [a], Denis O Shea [a], Vickie McKee [c]

[a] *Dublin Institute of Technology, Cathal Brugha Street, Dublin, Ireland*
[b] *Chemistry Department, The National University of Ireland Maynooth, Maynooth, Co. Kildare, Ireland*
[c] *Chemistry Department, Loughborough University, Loughborough, Leics., England LE11 3TU, UK*

Received 10 April 2003; accepted 14 July 2003

Abstract

Reactions of 2,2-dimethylpentanedioic acid($2dmepdaH_2$) and 3,3-dimethylpentanedioic acid ($3dmepdaH_2$) with $Mn(CH_3COO)_2 \cdot 4H_2O$ yield the soluble complexes $[Mn(2dmepda)] \cdot 1.5H_2O$ (**1**) and $[Mn(3dmepda)] \cdot H_2O$ (**2**). Complex **1** reacts with ethanolic solutions of 2,2′-bipyridine or 1,10-phenanthroline to give $[Mn_2(2dmepda)_2(bipy)] \cdot H_2O$ (**3**) and [Mn(2dmepda)(phen)] (**4**), respectively. Similar reactions of **2** with these ligands generated $[Mn_2(3dmepda)_2(bipy)_3] \cdot 5H_2O$ (**5**) $[Mn(3dmepda)(phen)_2] \cdot 7.25H_2O$ (**6**). The molecular structure of **6** was determined by X-ray crystallography. The asymmetric unit contains two $[Mn(3dmepda)(phen)_2]$ units with 14.5 waters of crystallisation. The two manganese complexes are of very similar structure. In each case the manganese atom is ligated by four nitrogen atoms from two ehelating phen molecules and two oxygen atoms, one from each of the earboxylates moieties of the $3dmepda^{2-}$ ligand. Thus, the two carboxylate functions of the two $3dmepda^{2-}$ dianionic ligands are essentially monodentate. The 2,2- and the 3,3-dimethylpentanedioate complexes, the metal free ligands and a number of simple manganese salts were each tested for their ability to inhibit the growth of *Candida albicans*. Only the "metal free" 1,10-phenanthroline and its 2,2- and the 3,3-dimethylpentanedioate complexes exhibit fungitoxic activity.

Keywords: Manganese(II) complexes; 2,2-Dimethylpentanedioic acid; 3,3-Dimethylpentanedioic acid; 2,2′-Bipyridine; 1,10-Phenanthroline; Crystal structure; Anti-*Candida* activity

1. Introduction

The state-of-the-art Azole and Polyene drugs currently used to treat candidosis and other fungal infections are often ineffective because of problems with resistance or toxicity and thus the search for alternative anti-fungal agents has gathered momentum [1]. Furthermore, pharmaceutical manufacturers are intensively seeking cheaper and more effective anti-fungal therapeutic agents. A number of publications has appeared in the literature highlighting the fungicidal activity of novel transition metal carboxylate complexes [2].

Recently, this group has shown that a range of cobalt, copper, manganese and silver complexes containing carboxylic acid and 1,10-phenanthroline ligands inhibit the growth of *Candida albicans* [3–9]. The in vitro anti-fungal activity of the metal complexes that we

* Corresponding author. Tel.: +353-1-4024486; fax: +353-1-024495.
E-mail address: Michael.Devereux@dit.ie (M. Devereux).

0277-5387/$ - see front matter © 2003 Elsevier Ltd. All rights reserved.
doi:10.1016/S0277-5387(03)00469-8

studied was comparable to that of of a number of the commercial Azole drugs. Furthermore, we have shown that by changing the structural nature of the phenanthroline molecules it is possible to generate complexes that are active at much lower concentrations [10]. Early studies on the 1,10-phenanthroline complexes have revealed that these compounds appear to have a different mode of action to the prescription Azole and Polyene drugs [11]. Compounds that kill fungal cells in a different biochemical way to these drugs may not have the same resistance and toxicity problems.

As part of our ongoing studies into the synthesis and biological activity of metal complexes of α,ω-dicarboxcylic acids we have generated a number of new manganese(II) derivatives of 2,2-dimethylpentanedioic acid and 3,3-dimethylpentanedioic acid. In addition the in vitro anti-*Candida* activities of the metal free ligands and the metal complexes are discussed.

2. Results and discussion

Synthetic routes to the complexes **1–6** are shown in Scheme 1. Reaction of either 2,2-dimethylpentanedioic acid (2dmepdaH$_2$) or 3,3-dimethylpentanedioic acid (3dmepdaH$_2$) with manganese(II) acetate gave the complexes [Mn(2dmepda)]·1.5H$_2$O (**1**) and [Mn(3dmepda)]·H$_2$O (**2**), respectively. Reaction of **1** with either 2,2′-bipyridine or 1,10-phenanthroline resulted in the synthesis of [Mn$_2$(2dmepda)$_2$(bipy)]·H$_2$O (**3**) and [Mn(2dmepda)(phen)] (**4**). [Mn$_2$(3dmepda)$_2$ (bipy)$_3$]·5H$_2$O (**5**) and [Mn(3dmepda)(phen)$_2$]·7.25 H$_2$O (**6**) were obtained when **2** was treated similarly.

The X-ray crystal structure of [Mn(3dmepda)(phen)$_2$]·7.25H$_2$O (**6**) is shown in Figs. 1–3, and selected bond lengths and angles are listed in Table 1. The manganese atom is ligated by four nitrogen atoms [N(1A), N(2A), N(1B) and N(2B)] from two chelating phen molecules and two oxygen atoms [O(1) and O(3)], one from each of the carboxylates moieties of the 3dmepda^{2-} ligand (Fig. 1). Thus, the two carboxylate functions of the two 3dmepda^{2-} dianionic ligands are essentially monodentate with the two remaining carboxyl oxygens [O(2) and O(4)] uncoordinated. As a result of the bite of the phen ligands [N(2A)–Mn–N(1A) = 72.21(9)°, N(2B)–Mn–N(1B) = 72.90(9)°] the geometry of the complex is best described as irregular six-coordinate. The two manganese centres within the asymmetric unit (Fig. 2) differ in the conformation of the 3dmepda^{2-} dianion.

There is significant intermolecular association between the water solvate molecules, which are hydrogen-bonded to the uncoordinated carboxyl oxygens [O(2) and O(4)] of the 3dmepda^{2-} ligands (Table 2 and Fig. 3). Additionally, extensive π–π interactions involving all the phenanthroline groups are also present in the crystal structure.

The IR spectra of complexes (**1**)–(**6**) all contain prominent ν_{asym}(COO) stretching bands in the region 1560–1596 cm^{-1} and ν_{sym}(COO) stretching bands in the

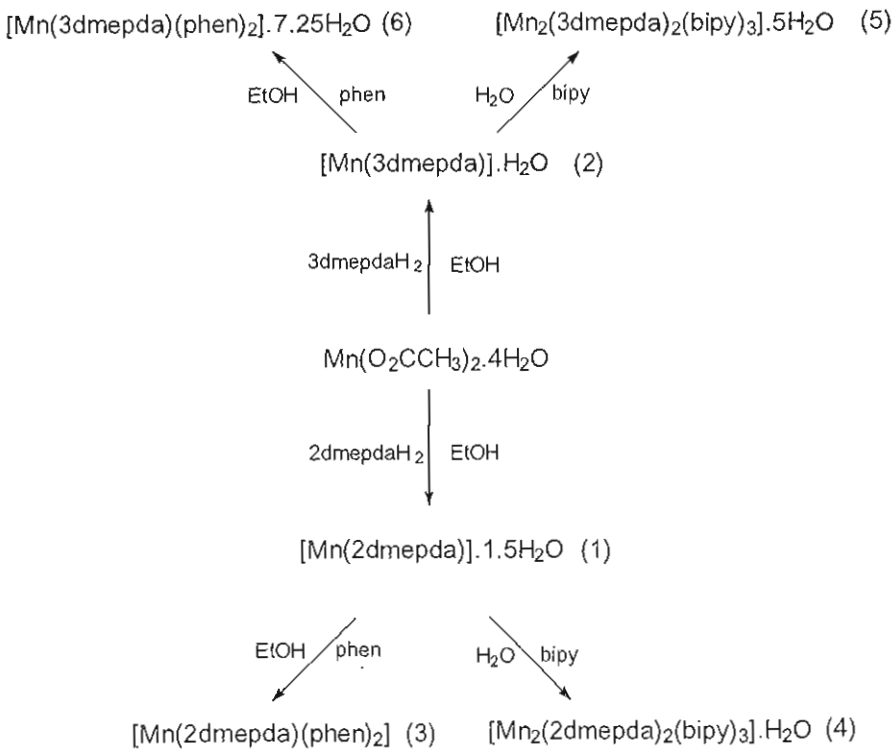

Scheme 1.

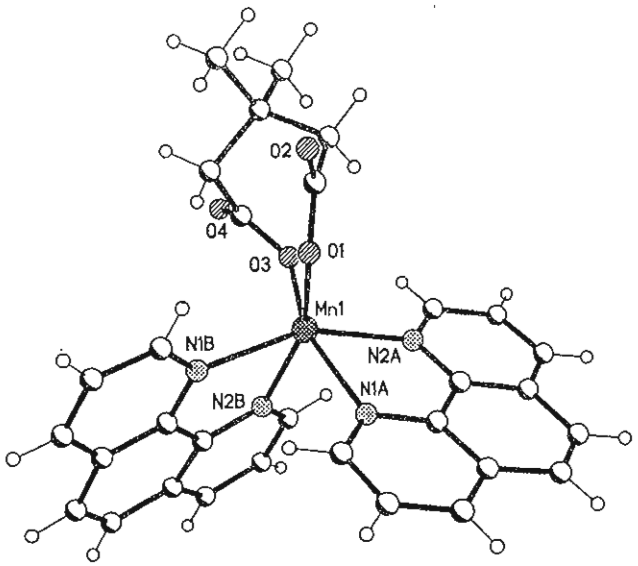

Fig. 1. The structure of one of the [Mn(3dmepda)(phen)$_2$] units in **6**.

region 1425–1385 cm^{-1} [$\Delta\nu$(COO) = 141–190 cm^{-1}]. The $\Delta\nu$(COO) values suggest that the coordination modes of the dicarboxylate ligands in these complexes may be similar [12].

The room temperature magnetic moments of powdered samples of complexes **1–6** (μ_{eff} = 5.6–6 BM) are consistent for manganese(II) complexes where there is no significant exchange interactions between adjacent metal centres [13]. Complexes **1–5** were found to be soluble in water suggesting that they are not polymeric. The molar conductivity values for aqueous solutions of complexes **1**, **2**, **4** and **6** (Λ_M = 87–143 S cm^2 mol^{-1}) suggest that these complexes probably form 1:1 electrolytes in water and may dissociate in accordance to the following equilibria:

$$[Mn(O_2C\text{–}R\text{–}CO_2)] \cdot nH_2O \overset{H_2O}{\rightleftharpoons} [Mn(H_2O)_n]^{2+} + (O_2C\text{–}R\text{–}CO_2)^{2-}$$

$$[Mn(O_2C\text{–}R\text{–}CO_2)](phen_m) \overset{H_2O}{\rightleftharpoons} [Mn(phen)_m]^{2+} + (O_2C\text{–}R\text{–}CO_2)^{2-}$$

The high molar conductivity values for complexes **3** and **5** (Λ_M = 198.16 and 355.29 S cm^2 mol^{-1}, respectively) suggest that they dissociate extensively in aqueous solution.

The complexes **1–6**, the metal free ligands and a number of simple manganese salts were each tested for their ability to inhibit the growth of *C. albicans* at a concentration of 10 μg cm^{-3} (Table 3). Both the 2,2- and the 3,3-dimethylpentanedioic acids, the simple manganese(II) salts, and the simple carboxylate complexes **1** and **2** are essentially devoid of anti-*Candida* activity. Both the uncoordinated 2,2′-bipyridine and its carboxylate derivatives (complexes **3** and **5**) are also ineffective against the pathogen. However the phenanthroline complexes **4** and **6** both exhibit discrete anti-Candida activity causing 68% and 70% inhibition of cell growth, respectively. Significantly the "metal free" 1,10-phenanthroline itself shows the greatest activity causing 89% inhibition of cell growth. However we believe that the so called metal free 1,10-phenanthroline is probably

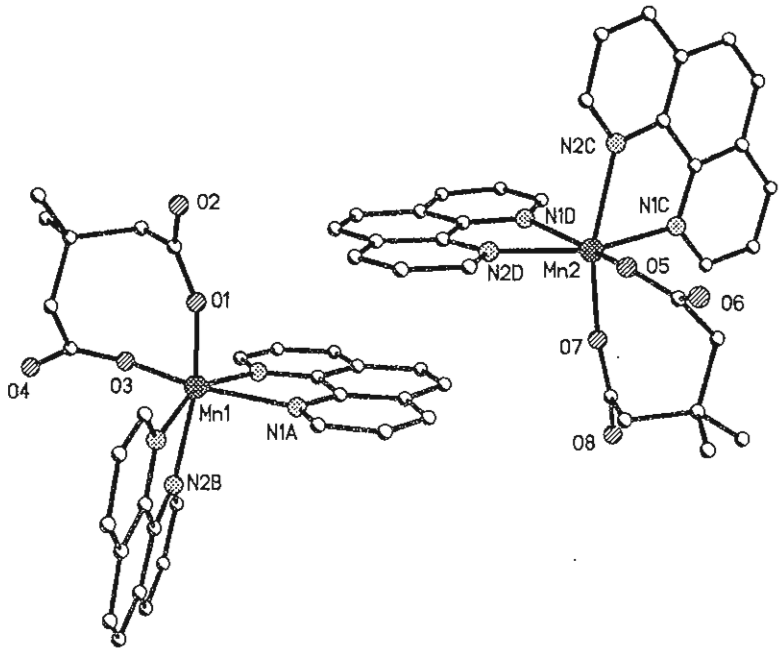

Fig. 2. Two independent [Mn(3dmepda)(phen)$_2$] units in **6** showing a π–π interaction between the phen groups.

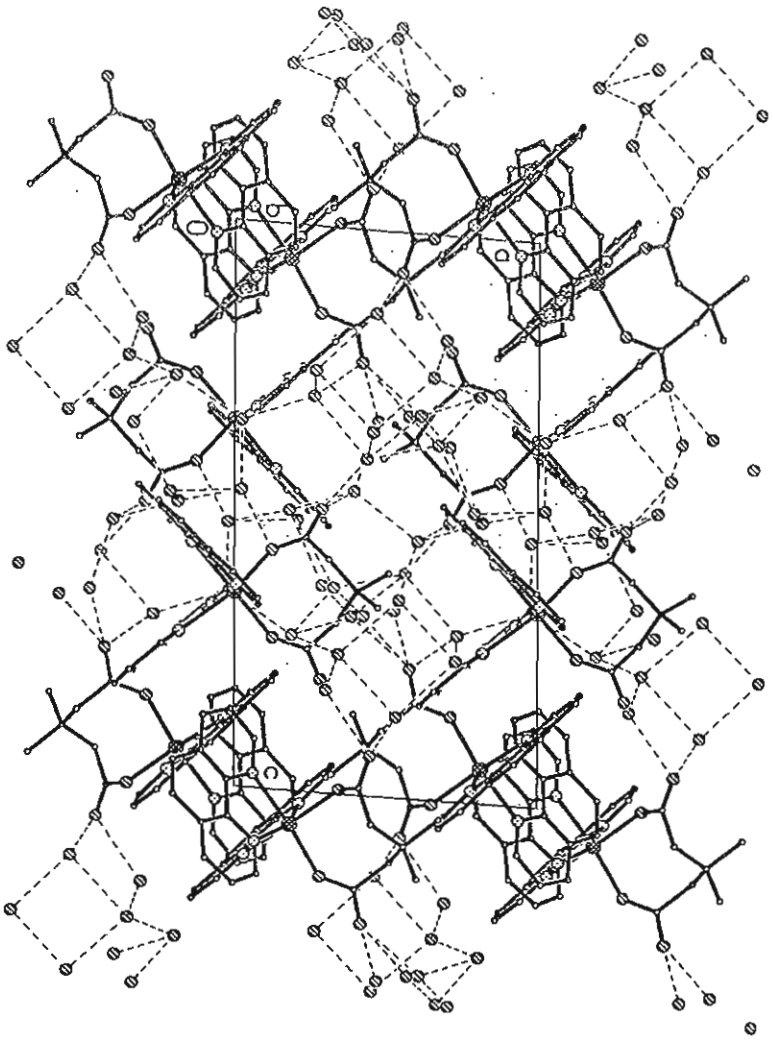

Fig. 3. The packing diagram for **6** viewed down the *b* axis, showing π–π stacking and hydrogen bonding.

coordinating to metal ions (other than the manganese) hat are present in trace amounts in the growth medium ınd that it is these resulting metal–phenanthroline :omplexes that are responsible for the high anti-*Candida* ıctivity. Studies are currently underway in our labora- ories to examine this theory. The efficacy of complexes l and **6** are comparable to the azole drug ketoconazole ıt 10 μg cm^{-3} (Table 3) and as the concentration is owered the anti-fungal activity decreases significantly.

In conclusion, it would appear that 2,2- and the 3,3- limethylpentanedioic acids, whether coordinated or ıncoordinated to manganese, do not possess any anti- *Candida* properties. Furthermore, the presence of the NN-donor 2,2′-bipyridine does not improve the activity of the complex. The 1,10-phenanthroline molecule is a potent anti-*Candida* agent and upon reaction with the manganese the 2,2- and the 3,3-dimethylpentanedioate complexes yields compounds with fungitoxic activity comparable to that of the state-of-the-art drug Keto- onazole.

3. Experimental

Chemicals were purchased from commercial sources and used without further purification. IR spectra were recorded as KBr discs in the region 4000–400 cm^{-1} on a Nicolet-400 Impact spectrometer. Magnetic susceptibility measurements were made using a Johnson Matthey Magnetic Susceptibility balance. $[HgCo(SCN)_4]$ was used as a reference. Conductivity readings were obtained using a Ciba Corning model check-mate 90 conductivity meter. Satisfactory microanalytical data for the complexes were reported by the Microanalytical Laboratory, University College Cork, Ireland.

3.1. [Mn(2dmepda)] · 1.5H_2O (1)

To a solution of 2,2-dimethylpentanedioic acid {2dmepdaH_2} (1.05 g, 6.57 mmol) in ethanol (100 cm^3) was added manganese(II) acetate tetrahydrate (1.15 g, 4.28 mmol), and the mixture was refluxed for 2 h. The

Table 1
Selected bond lengths [Å] and angles [°] for 6

Bond lengths			
Mn(1)–O(1)	2.091(2)	Mn(2)–O(5)	2.125(2)
Mn(1)–O(3)	2.108(2)	Mn(2)–N(2D)	2.281(3)
Mn(1)–N(2A)	2.262(3)	Mn(2)–N(2C)	2.293(3)
Mn(1)–N(2B)	2.265(3)	Mn(2)–N(1D)	2.302(2)
Mn(1)–N(1B)	2.265(3)	Mn(2)–N(1C)	2.312(3)
Mn(1)–N(1A)	2.329(3)	Mn(2)–O(7)	2.080(2)
Bond angles			
O(1)–Mn(1)–O(3)	95.98(9)	N(2B)–Mn(1)–N(1A)	96.18(9)
O(1)–Mn(1)–N(2A)	107.17(10)	N(1B)–Mn(1)–N(1A)	89.17(9)
O(3)–Mn(1)–N(2A)	86.85(9)	O(7)–Mn(2)–O(5)	99.97(9)
O(1)–Mn(1)–N(2B)	159.95(9)	O(7)–Mn(2)–N(2D)	101.23(9)
O(3)–Mn(1)–N(2B)	85.84(9)	O(5)–Mn(2)–N(2D)	86.73(9)
N(2A)–Mn(1)–N(2B)	92.86(9)	O(7)–Mn(2)–N(2C)	158.10(9)
O(1)–Mn(1)–N(1B)	87.94(9)	O(5)–Mn(2)–N(2C)	88.80(9)
O(3)–Mn(1)–N(1B)	111.25(9)	N(2D)–Mn(2)–N(2C)	99.26(9)
N(2A)–Mn(1)–N(1B)	155.44(9)	O(7)–Mn(2)–N(1D)	93.01(9)
N(2B)–Mn(1)–N(1B)	72.90(9)	O(5)–Mn(2)–N(1D)	157.30(9)
O(1)–Mn(1)–N(1A)	89.23(9)	N(2D)–Mn(2)–N(1D)	72.43(9)
O(3)–Mn(1)–N(1A)	159.02(9)	N(2C)–Mn(2)–N(1D)	85.85(9)
N(2A)–Mn(1)–N(1A)	72.21(9)	O(7)–Mn(2)–N(1C)	86.10(9)
O(5)–Mn(2)–N(1C)	108.49(9)		
N(2D)–Mn(2)–N(1C)	161.89(9)		
N(2C)–Mn(2)–N(1C)	72.07(9)		
N(1D)–Mn(2)–N(1C)	90.80(9)		

product formed as a colourless solid. The reaction mixture was allowed to cool to room temperature and then the product was filtered. The product was washed with two portions of ethanol and then dried in air. Yield: 0.63 g (39.93%). Complex **1** was soluble in H_2O, partially soluble in warm EtOH, and insoluble in MeOH, acetone, ether and chloroform. Found: C, 34.73; H, 5.45. Calc.: C, 35.01; H, 5.46. IR: 3382.09, 2979.10, 2925.37, 2871.64, 1561.94, 1474.63, 1414.18, 1300.00, 1138.81, 1051.49, 1031.34, 789.55, 668.66, 614.93 cm^{-1}. $\mu_{eff} = 5.99$ BM $\Lambda_M(H_2O) = 142.95$ S cm^2 mol^{-1}.

3.2. *[Mn(3dmepda)] · H_2O (2)*

To a solution of 3,3-dimethylpentanedioic acid 3dmepdaH_2 (2.00 g, 12.5 mmol) in ethanol (100 cm^3) was added manganese(II) acetate (3.03 g, 12.5 mmol), and the mixture was refluxed for 2 h. The product formed as a colourless solid. The mixture was allowed to cool to room temperature and then the product was filtered. The product was washed with two portions of ethanol and allowed to dry in air. Yield: 2.35 g (93.36%). Complex **2** was soluble in H_2O, partially soluble in warm EtOH and insoluble in MeOH, acetone, ether and chloroform. Found: C, 36.55; H, 5.15. Calc.: C, 36.38; H, 5.23. IR: 3402.24, 2972.39, 1561.94, 1454.48, 1407.46, 1313.43, 1252.99, 1145.52, 1118.66, 1038.06, 1011.19, 769.40, 735.82, 668.66 cm^{-1}. $\mu_{eff} = 5.88$ BM $\Lambda_M(H_2O) = 127.64$ S cm^2 mol^{-1}.

3.3. *[Mn_2(2dmepda)$_2$(bipy)] · H_2O (3)*

To a solution of [Mn(2dmepda)] · 1.5H_2O (**1**) (1.00 g, 4.16 mmol) in ethanol (100 cm^3) was added 2,2′-bipyridine (2.04 g, 13.06 mmol), and the mixture was refluxed for 3.5 h. The product formed as a yellow solid that was then filtered and dried in air. Yield: 0.96 g (37.01%). Complex **3** was soluble in H_2O and partially soluble in warm EtOH and ether, and insoluble in MeOH, acetone and chloroform. Found: C, 48.14; H, 4.79; N, 5.3. Calc.: C, 48.01; H, 5.03; N, 4.66. IR: 3422.39, 3106.72, 3066.42, 2992.54, 2952.24, 2905.22, 1582.09, 1474.63, 1441.04, 1407.46, 1373.88, 1340.30, 1259.70, 1158.96, 1064.93, 1017.91, 823.13, 769.40, 735.82, 655.22, 628.36 cm^{-1}. $\mu_{eff} = 5.65$ BM $\Lambda_M(H_2O) = 198.16$ S cm^2 mol^{-1}.

3.4. *[Mn(2dmepda)(phen)] (4)*

To a solution of [Mn(2dmepda)] · 1.5H_2O (**1**) (0.40 g, 1.66 mmol) in ethanol (50 cm^3) was added 1,10-phenanthroline (0.62 g, 3.46 mmol), and the mixture refluxed for 2 h. The product formed as a yellow solid that was then filtered off and dried in air. Yield: 0.47 g (69.07%). Complex **4** was soluble in H_2O, partially soluble in warm EtOH, ether and chloroform and insoluble in MeOH and acetone. Found: C, 58.63; H, 4.60; N, 7.02. Calc.: C, 58.02; H, 4.61; N, 7.12. IR: 3406.96, 3066.42, 2972.39, 2952.24, 2918.66, 2864.93, 1601.70,

Table 2
Hydrogen bond lengths [Å] and angles [°] for 6

D–H···A	d(D–H)	d(H···A)	d(D···A)	∠(DHA)
O(1W)–H(1WA)···O(8)#1	0.94	1.94	2.867(3)	169.9
O(1W)–H(1WB)···O(4)	0.89	1.92	2.803(3)	169.5
O(2W)–H(2WA)···O(4)	0.91	1.86	2.724(3)	158.5
O(2W)–H(2WB)···O(6W)	1.00	1.96	2.958(4)	175.7
O(3W)–H(3WA)···O(6)	0.93	1.79	2.707(3)	170.1
O(3W)–H(3WB)···O(15W)#2	0.85	1.91	2.700(6)	153.4
O(3W)–H(3WB)···O(12W)#2	0.85	2.00	2.845(6)	171.7
O(4W)–H(4WA)···O(3W)#3	0.90	1.94	2.841(4)	173.9
O(4W)–H(4WB)···O(5W)	0.92	2.02	2.885(4)	156.1
O(5W)–H(5WA)···O(7W)#3	0.93	1.98	2.877(4)	161.2
O(5W)–H(5WB)···O(2W)	0.95	1.85	2.791(4)	168.0
O(6W)–H(6WA)···O(4W)	0.94	1.84	2.768(4)	167.4
O(6W)–H(6WB)···O(1W)	0.99	1.82	2.785(4)	162.7
O(7W)–H(7WA)···O(3W)	1.08	1.78	2.810(4)	157.3
O(7W)–H(7WB)···O(2)#4	0.88	1.91	2.773(4)	168.2
O(8W)–H(8WA)···O(6W)#1	0.86	2.12	2.978(4)	178.4
O(8W)–H(8WB)···O(15W)#1	1.00	1.79	2.716(6)	152.4
O(8W)–H(8WB)···O(12W)#1	1.00	1.82	2.806(6)	165.8
O(9W)–H(9WA)···O(5)	0.87	2.01	2.879(3)	175.4
O(9W)–H(9WA)···O(6)	0.87	2.59	3.195(4)	128.0
O(9W)–H(9WB)···O(10W)#1	0.84	2.24	2.777(4)	121.6
O(11W)–H(1WE)···O(14W)	0.74	1.81	2.556(7)	177.5
O(11W)–H(1WE)···O(16W)	0.74	2.46	3.137(7)	151.2
O(10W)–H(1WC)···O(7W)#1	0.98	1.85	2.805(4)	162.5
O(10W)–H(1WD)···O(9W)#1	0.87	1.91	2.777(4)	178.0
O(11W)–H(1WF)···O(6)	0.99	1.87	2.826(4)	159.6
O(12W)·····O(13W)			2.698(7)	
O(12W)·····O(16W)#5			2.739(8)	
O(13W)·····O(2)#6			2.752(6)	
O(14W)·····O(9W)			2.925(7)	
O(14W)O·····(9W)#5			2.901(6)	
O(14W)·····O(18W)#5			2.834(8)	
O(15W)·····O(2)#6			2.914(6)	
O(15W)·····O(18W)			2.693(8)	
O(16W)·····O(18W)#5			2.802(9)	
O(17W)·····O(2)#6			2.776(7)	
O(17W)·····O(18W)			2.668(11)	

Symmetry transformations used to generate equivalent atoms: #1 $-x,-y,-z+1$; #2 $x-1,y,z$; #3 $x+1,y,z$; #4 $-x,-y,-z+2$; #5 $-x,1-y,1-z$; #6 $1-x,-y,2-z$.

Table 3
Anti-*Candida* (expressed as % growth of fungal cells)

Test compound	% Cell growth		
	10 μg cm^{-3}	5 μg cm^{-3}	2.5 μg cm^{-3}
Control	100	100	100
Ketoconazole	25 ± 3	26 ± 4	47 ± 10
[Mn(2dmepda) · 1.5H_2O] (1)	110 ± 13		
[[Mn(3dmpeda)] · H_2O (2)	112 ± 15		
[Mn_2(2dmpeda)$_2$(bipy)] · H_2O (3)	97 ± 7		
[Mn(2dmpeda)phen] (4)	32 ± 2	43 ± 12	60 ± 2
[Mn(3dmpeda)$_2$(bipy)$_3$] · 5H_2O (5)	95 ± 3		
[Mn(3dmpeda)(phen)$_2$] · 7.5H_2O (6)	30 ± 2	16 ± 2	72 ± 7
2dmpedaH_2	102 ± 3		
3dmpedaH_2	105 ± 10		
1,10 phen	11 ± 1	14 ± 2	22 ± 2
2,2 bipy	114 ± 6		
$MnCl_2$	110 ± 5		
$Mn(NO_3)_2$	118 ± 12		
$MnSO_4$	108 ± 9		

1534.52, 1474.63, 1420.32, 1360.45, 1300.00, 1232.84, 1138.16, 1104.57, 910.45, 856.01, 782.84, 728.37, 635.07 cm^{-1}. μ_{eff} = 5.97 BM $\Lambda_M(H_2O)$ = 125.86 S cm^2 mol^{-1}.

3.5. $[Mn_2(3dmepda)_2(bipy)_3]\cdot 5H_2O$ (5)

To a solution of Mn(3dmepda)·H_2O (**2**) (0.41 g, 1.77 mmol) in deionised water (50 cm^3) was added 2,2′-bipyridine (0.50 g, 3.20 mmol). The resulting green solution was left to stand for several days at room temperature to give yellow crystals. These were filtered, washed with deionised H_2O and dried in air. Yield: 0.13 g (7.63%). Complex **5** was soluble in H_2O, EtOH and MeOH and insoluble in acetone, ether and chloroform. Found: C, 53.34; H, 5.62; N, 9.18. Calc.: C, 53.66; H, 5.53; N, 8.53. IR: 3450.5, 3066.42, 2957.9, 2864.93, 1576.2, 1474.63, 1438.1, 1385.7, 1313.43, 1252.99, 1157.1, 1118.66, 1064.93, 957.46, 910.45, 774.7, 736.8, 648.51 cm^{-1}. μ_{eff} = 5.73 BM $\Lambda_M(H_2O)$ = 355.29 S cm^2 mol^{-1}.

3.6. $[Mn(3dmepda)(phen)_2]\cdot 7.25H_2O$ (6)

To a solution of [Mn(3dmepda)]·H_2O (**2**) (0.8 g, 3.46 mmol) in ethanol (100 cm^3) 1,10-phenanthroline (1.10 g, 6.92 mmol) was added, and the mixture was refluxed for 2 h. Upon standing for 1 week the solvent had evaporated leaving an impure looking product. The product was recrystallised from hot water to give yellow crystals plus a brown solution. The crystals were filtered off and dried at room temperature. Yield: 0.58 g (24.04%). Complex **6** was soluble in H_2O, EtOH, MeOH and acetone, and insoluble in ether and chloroform. Found: C, 53.37; H, 5.81; N, 8.09. Calc.: C, 53.22; H, 5.76; N, 8.01. IR: 3415.67, 3052.99, 2952.24, 2858.21, 1575.37, 1514.93, 1447.76, 1420.90, 1387.31, 1340.30, 1300.00, 1246.27, 1145.52, 1105.22, 850.00, 776.12, 729.10, 641.79 cm^{-1}. μ_{eff} = 6.03 BM $\Lambda_M(H_2O)$ = 116.53 S cm^2 mol^{-1}.

3.7. X-ray crystallography

Crystal data for [Mn(3dmepda)$(phen)_2$]·7.25H_2O (**6**) are summarised in Table 4. The data set for the complex was collected on a Siemens P4 diffractometer, solved by direct methods and refined on F^2 using SHELXTL 97 [14] and SHELXTL [15]. All the non-hydrogen atoms were refined with anisotropic atomic displacement parameters. Eleven lattice water molecules were refined with full occupancy and a further seven refined with 50% occupancy.

Hydrogen atoms bound to carbon were inserted at calculated positions; hydrogen atoms of full-occupancy

Table 4
Summary of crystal data, data collection, structure solution and refinement details for **6**

Empirical formula	$C_{31}H_{40}MnN_4O_{11.25}$
Formula weight	703.61
Temperature (K)	153(2)
Wavelength (Å)	0.71073
Crystal system	triclinic
Space group	$P\bar{1}$
Unit cell dimensions	a = 10.4292(16) (Å) b = 16.794(2) (Å) c = 19.893(4) (Å) α = 77.065(12)° β = 83.843(16)° γ = 81.133(9)°
Volume	3345.5(9)
Z	4
Density (calculated) (Mg/m^3)	1.397
Absorption coefficient (mm^{-1})	0.460
$F(000)$	1476
Crystal size (mm)	0.82 × 0.78 × 0.50
θ range for data collection	2.11° to 25.00°
Index ranges	$0 < h < 12$, $-19 < k < 19$, $-23 < l < 23$
Reflections collected	12,448
Independent reflections	11,743 [R_{int} = 0.0292]
Completeness to θ = 25.00° (%)	99.5
Absorption correction	empirical
Max. and min. transmission	0.8007 and 0.7558
Refinement method	full-matrix least-squares on F^2
Data/restraints/parameters	11,743/0/883
Goodness-of-fit on F^2	1.012
Final R indices [$I > 2\sigma(I)$]	R_1 = 0.0482, wR_2 = 0.0974
R indices (all data)	R_1 = 0.0853, wR_2 = 0.1112
Largest differential peak and hole (e $Å^{-3}$)	0.475 and −0.433

water molecules were located from difference maps and not further refined, those on 50% occupancy water molecules {O(12w)–O(18w)} were not included.

3.8. Anti-Candida testing

Candida albicans isolate was obtained commercially from Oxid Culti-loops (ATCC 10231). The isolate was stored on Sabouraud dextrose agar (SDA) plates at 4 °C. Culture conditions and measurement of drug minimum inhibitory concentrations (MICs) were as previously described [7].

4. Supplementary data

Crystallographic data have been deposited with the CCDC. Copies of this information may be obtained free of charge from the Director, CCDC, 12 Union Road, Cambridge CB2 1EZ, UK (fax +44-1223-336-033; e-mail: deposit@ccdc.cam.uk or www: http://www.ccdc.cam.ac.uk), quoting the deposition number CCDC206030.

Acknowledgements

M.D. acknowledges the late Noel O'Reilly (DIT) for technical assistance. V.L. and D.O.S. acknowledge the SRD and Seed funding schemes (DIT/EU) for financial support. This work has been carried out (in part) within the structures of the Facility for Optical Characterisation and Spectroscopy (FOCAS), funded by the Irish Government Programme for Research in Third Level Institutions. M.D. also acknowledges funding received through the Irish Technological Sector Research Strand III programme (Project No. CRS02-TA01).

References

[1] A.L. Barry, S.D. Brown, Antimicrob. Agents Chemother. 40 (1996) 1948.
[2] See for example: M. Petric, F. Pohleven, I. Turel, P. Segedin, A. White, D. Williams, Polyhedron 17 (1998) 255.
[3] M. Geraghty, M. McCann, M. Devereux, F. Cronin, M. Curan, V. McKee, Metal Based Drugs 6 (1999) 41.
[4] M. Geraghty, V. Sheridan, M. McCann, M. Devereux, V. McKee, Polyhedron 18 (1999) 2931.
[5] M. Geraghty, M. McCann, M. Devereux, V. McKee, Inorg. Chim. Acta 293 (1999) 160.
[6] M. Geraghty, M. Devereux, M. McCann, F. Cronin, Biometals 13 (2000) 1.
[7] M. Devereux, M. McCann, V. Leon, M. Geraghty, V. McKee, Polyhedron 19 (2000) 1205.
[8] M. Devereux, M. McCann, D.O. Shea, M. Geraghty, J. Mason, L.O. Sullivan, Metal Based Drugs 7 (2000) 185.
[9] M. Devereux, M. McCann, V. Leon, M. Geraghty, Vickie McKee, J. Wikaira, Metal Based Drugs 7 (2001) 275.
[10] B. Coyle, M. McCann, M. Devereux, M. Geraghty (unpublished results).
[11] B. Coyle, K. Kavanagh, M. McCann, M. Devereux, M. Geraghty, Biometals 16 (2003) 321.
[12] K. Nakamoto, Infrared and Raman Spectra of Inorganic and Coordination Compounds, 3rd ed., Wiley, New York, 1978.
[13] F.A. Cotton, G.K. Wilkinson, Advanced Inorganic Chemistry, 6th ed., Wiley, New York, 1999, p. 761.
[14] G.M. Sheldrick, SHELXTL 97, University of Göttingen.
[15] G.M. Sheldrick, SHELXTL, Version 5.1, Bruker Analytical X-ray Systems, Madison, WI, 1997.

Available online at www.sciencedirect.com
SCIENCE DIRECT®
Journal of Inorganic Biochemistry 98 (2004) 1023–1031
Journal of Inorganic Biochemistry
www.elsevier.com/locate/jinorgbio

Synthesis, antimicrobial activity and chemotherapeutic potential of inorganic derivatives of 2-(4′-thiazolyl)benzimidazole{thiabendazole}: X-ray crystal structures of $[Cu(TBZH)_2Cl]Cl \cdot H_2O \cdot EtOH$ and $TBZH_2NO_3$ (TBZH = thiabendazole)

Michael Devereux [a,*], Malachy McCann [b], Denis O Shea [a], Rachel Kelly [a], Denise Egan [c], Carol Deegan [c], Kevin Kavanagh [d], Vickie McKee [e], Gregory Finn [f]

[a] *Dublin Institute of Technology, Cathal Brugha St., Dublin 1, Ireland*
[b] *Chemistry Department, National University of Ireland Maynooth, Maynooth, Co. Kildare, Ireland*
[c] *Department of Applied Science, Institute of Technology, Tallaght, Dublin 24, Ireland*
[d] *Biology Department, National University of Ireland Maynooth, Maynooth, Co. Kildare, Ireland*
[e] *Chemistry Department, Loughborough University, Loughborough, Leics LE11 3TU, UK*
[f] *Cancer Research Programme, Beth Israel Deaconess Medical Centre, Harvard Institute of Medicine, Harvard Medical School, Boston, MA, USA*

Received 18 December 2003; received in revised form 19 February 2004; accepted 21 February 2004
Available online 18 March 2004

Abstract

Thiabendazole (TBZH) reacts with iron(III) nitrate causing protonation of the ligand to yield the nitrate salt $[TBZH_2NO_3]$ (**1**). Reaction of TBZH with copper(II) acetate results in the deprotonation of the ligand yielding $[Cu(TBZ)_2 \cdot (H_2O)_2]$ (**2**). Reactions of TBZH with the chloride, nitrate and butanedioate salts of copper(II) yields $[Cu(TBZH)_2Cl]Cl \cdot H_2O \cdot EtOH$ (**3**), $[Cu(TBZH)_2(NO_3)_2]$ (**4**) and $[Cu(TBZH)(O_2C{-}CH_2CH_2{-}CO_2)]$ (**5**), respectively. The TBZH acts as a neutral ehelating ligand in **3–5**. Molecular structures of **1** and **3** were determined crystallographically. In **1**, the asymmetric unit contains one $TBZH_2^+$ cation and one NO_3^- anion. The strueture of **3** comprises a five coordinate copper centre with the metal bound to two chelating TBZH ligands and one ehloride. The geometry is best described as trigonal bipyramidal. Hydrogen bonding connects the complex cation with the uncoordinated ehloride anion and the water and ethanol solvate molecules. Compound **1** and the copper complexes **2–5**, the metal free ligands and a number of simple copper(II) salts were each tested for their ability to inhibit the growth of *Candida albicans*. The metal free TBZH and its nitrate salt (**1**) exhibited very poor activity. Complex **2**, in whieh the TBZH is present as an anionic ligand (TBZ^-), exhibits moderate activity towards the pathogen. Chelation of the neutral TBZH to copper centres (complexes **3–5**) results in potent anti-*candida* activity. The dimethyl sulphoxide (DMSO) soluble complexes **3** and **4**, along with metal free TBZH were assessed for their cancer chemotherapeutic potential towards two human epithelial-derived cancer model cell lines. Complexes **3** and **4** displayed similar dose-dependent cytotoxicity in both cell lines with IC_{50} values of approximately 50 μM, which were found to be significantly lower than that for metal free TBZH.

Keywords: Anti-fungal; *Candida*; Chemotherapeutic potential; Metal complexes; Thiabendazole

1. Introduction

Candida albicans is a commensal of the human body and is considered to be an important fungal pathogen. Opportunistic infection can lead to the development of systemic candidosis which is often fatal in

* Corresponding author. Tel.: +353-1-4024486; fax: +353-1-4024495.
E-mail address: michael.devereux@dit.ie (M. Devereux).

0162-0134/$ - see front matter © 2004 Elsevier Inc. All rights reserved.
doi:10.1016/j.jinorgbio.2004.02.020

immunocompromised patients [1–4]. Existing therapies for systemic fungal infections rely on the use of polyene and azole anti-fungal drugs, such as nystatin and ketoconazole. Resistence to these drugs has been reported [5] and this reduces the efficacy of the therapy and can ultimately lead to the death of the patient. Mechanisms that confer antifungal drug resistence in yeast include an increase in the expression of drug efflux pumps which remove the drug from the cell before a toxic concentration can be reached [6], alterations in the target of the drug and variations in the ergosterol biosynthetic pathway [7]. The problems associated with the polyene and azole drugs have resulted in a search for possible alternative anti-fungal agents [8]. Reports have appeared in the literature describing the anti-fungal activity of metal complexes [9]. Due to the possibility of a differenee in mode of anti-fungal activity metal-based drugs may represent a novel group of anti-mycotic agents which could have potential applications as pharmaceuticals.

Recently, we have shown that a range of carboxylate and dicarboxylate complexes incorporating transition metal centres and including the *N,N′*-donor ligand 1,10-phenanthroline (phen) are potent in vitro inhibitors of the growth of *C. albicans* [10–16].

Furthermore, we have shown that by changing the structural nature of the chelating phenanthroline molecules it is possible to generate complexes that are very active at much lower concentrations [17]. Experiments with 1,7-phenanthroline and 4,7-phenanthroline demonstrated that ligands with chelating ability appeared to be desirable for anti-fungal activity [18]. However, when the 1,10-phenanthroline is replaced by the structurally similar *N,N′*-donor ligand 2,2′-bipyridine (bipy) complexes devoid of anti-*candida* activity are obtained [16]. Significantly, when the 1,10-phenanthroline itself is tested against the *candida* it generally exhibits superior activity to that of the metal complexes and activity comparable to the preseription drugs. Other workers have recently reported very good anti-*candida* activity for several new organic 1,10-phenanthroline derivatives [19]. We believe that the so-called "metal free" 1,10-phenanthroline is probably coordinating to metal ions that are present in trace amounts in the growth medium and that it is these resulting metal–phenanthroline complexes that are responsible for the high anti-*candida* activity.

The mode of action of 1,10-phenanthroline and a number of our potent anti-*candida* metal complexes {M = Cu(II), Mn(II) or Ag(I)} [20] was examined. The phen and its metal complexes had minimum inhibitory concentrations (MICs) in the range 1.25–5 μg/ml and at concentration of 10 μg/ml they displayed some fungidal activity.

Yeast cells exposed to these drugs showed a diminished ability to reduce 2,3,5-triphenyltetrazolium chloride (TTC), indicating a reduction in respiratory function. Treating exponential and stationary phase yeast cells with phen and the Cu(II) and Mn(II) complexes caused a dramatic increase in oxygen consumption. All of the drugs promoted reduction in levels of cytochrome *b* and *c* in the cells, whilst the Ag(I) complex also lowered the level of cytochrome *aa*. Cells treated with phen and the Cu(II) and Ag(I) species showed reduced levels of ergosterol whilst the Mn(II) complex induced an increase in the sterol concentration. The general conclusion was that phen and its Cu(II), Mn(II) and Ag(I) complexes damage mitochondrial function and uncouple respiration. The fact that these drugs were not uniformly active suggests that their biological activity has a degree of metal-ion dependency. The effect of these drugs on the structure of yeast and mammalian cell organelles and the integrity of cellular DNA was also studied [21]. The conclusion was that phen and the metal–phen complexes have the potential to induce apoptosis in fungal and mammalian cells. 1,10-Phenanthroline and its metal complexes represent a novel set of highly active anti-fungal agents whose mode of action is significantly different to that of the state-of-the-art polyene and azole prescription drugs. In an effort to extend this class of novel drug, we have been studying metal complexes containing benzimidazole-based ligands. Benzimidazole and many of its derivatives exhibit a variety of biological actions, including antibacterial, antiviral, anticancer and anti-fungal activity [22].

2-(4′-Thiazolyl)benzimidazole{thiabendazole (TBZH)} (Fig. 1) is a well-known anthelmintic which is non-toxic to humans [23] and it also has applications as a fungicide in agriculture [24]. Because of its structural similarity to the chelating agents 2,2′-bipyridine and 1,10-phenanthroline, we were prompted to try and generate metal complexes of it. Further interest is derived from TBZH as it can act as both an acid and a base making it possible to generate inorganic compounds in which it can be either neutral, anionic or cationic. Reports of the biological activity of metal complexes of this potential *N,N′*-donor chelating ligand are quite rare. In the present paper, we report the synthesis, characterisation and the fungitoxic activity of inorganic derivatives of TBZH. To date TBZH is the first *N,N′*-donor ligand we have studied that, in vitro, exhibits poor anti-*candida* activity on its own but when complexed to a copper(II) centre becomes a relatively potent drug. In light of the fact that

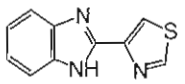

Thiabendazole

Fig. 1. The structure of thiabendazole.

very little is known about the biological properties of metal complexes of TBZH, we also investigated the chemotherapeutic potential of the free ligand and two of the novel complexes towards two tumourigenic human model cell lines.

2. Experimental

2.1. Chemistry

Chemicals were purchased from commercial sources and used without further purification. IR spectra were recorded in the region 4000–400 cm^{-1} on a Nicolet-400 Impact spectrometer. Magnetic susceptibility measurements were made using a Johnson Matthey Magnetic Susceptibility balance. $[HgCo(SCN)_4]$ was used as a reference. Satisfactory microanalytical data for the complexes were reported by the Microanalytical Laboratory, University College Cork, Ireland. $[Cu(O_2C–CH_2CH_2–CO_2)]\{HO_2C–CH_2CH_2–CO_2H$ = butanedioic acid} was synthesised using a method previously published [12].

2.1.1. $[TBZH_2NO_3]$ (1)

To a solution of $Fe(NO_3)_3 \cdot 9H_2O$ (0.5 g, 1.24×10^{-3} mmol) in ethanol (100 cm^3) was added thiabendazole (TBZH) (0.5 g, 2.47×10^{-3} mmol) and the resulting dark red solution was refluxed for 3 h. Upon standing colourless crystals of the product formed which were filtered and air-dried. Yield: 0.1478 g (45.3%). Calc: C, 45.62; H, 2.68; N, 21.28. Found: C, 45.45; H, 3.02; N, 21.18%. IR (KBr): 3408, 3084, 1635, 1586, 1385, 1347, 1304, 1043, 825, 739, 535 cm^{-1}. Solubility: soluble in ethanol and methanol.

2.1.2. $[Cu(TBZH)_2 \cdot (H_2O)_2]$ (2)

To a solution of thiabendazole (TBZH) (2.01 g, 10.00 mmol) in ethanol (100 cm^3) was added $[Cu_2(CH_3CO_2)_2 \cdot 2H_2O]$ (1.00 g, 5.00 mmol) and the resulting dark green solution was refluxed for 4 h. The dark green solid which deposited was filtered off, washed with water and ethanol, and then air-dried. Yield: 2.40 g (96%). Calc: C, 48.03; H, 3.22; N, 16.81. Found: C, 48.99; H, 2.60; N, 16.74%. IR (KBr): 3427, 3082, 1605, 1474, 1409, 1359, 1294, 1269, 1228, 1015, 933, 908, 875, 834, 744 cm^{-1}. μ_{eff}: 1.64 B.M. Solubility: insoluble in water, ethanol, methanol, acetone and trichloromethane.

2.1.3. $[Cu(TBZH)_2Cl]Cl \cdot H_2O \cdot EtOH$ (3)

To a solution of thiabendazole (TBZH) (3.14 g, 7.40 mmol) in ethanol (100 cm^3) was added $CuCl_2 \cdot 2H_2O$ (1 g, 7.40 mmol) and the resulting light green solution was refluxed for 4 h. The light green solid which deposited was filtered off, washed with water and ethanol, and then air-dried. Yield: 2.70 g (64%). Calc: C, 43.12; H, 3.17; N, 13.98. Found: C, 43.12; H, 3.28; N, 13.91%. IR (KBr): 3443, 3328, 3221, 3074, 2967, 2828, 2764, 1630, 1597, 1513, 1491, 1466, 1441, 1326, 1294, 1228, 1189, 1080, 1048, 1015, 998, 933, 875, 842, 744, 670 cm^{-1}. μ_{eff}: 1.57 B.M. Solubility: insoluble in water, ethanol, methanol, acetone and trichloromethane.

2.1.4. $[Cu(TBZH)_2(NO_3)_2]$ (4)

To a solution of thiabendazole (TBZH) (1.80 g, 9.02 mmol) in ethanol (100 cm^3) was added $Cu(NO_3)_2 \cdot 2H_2O$ (1.00 g, 4.29 mmol) and the resulting lime green solution was refluxed for 4 h. The lime green solid which deposited was filtered off, washed with water and ethanol, and then air-dried. Yield: 2.57 g (98%). Calc: C, 40.68; H, 2.37; N, 18.48. Found: C, 40.54; H, 2.39; N, 18.51%. IR (KBr): 3098, 2360, 1593, 1517, 1441, 1409, 1384, 1329, 1289, 1228, 1015, 998, 933, 875, 842, 769, 744 cm^{-1}. μ_{eff}: 1.71 B.M. Solubility: insoluble in water, ethanol, methanol, acetone and trichloromethane.

2.1.5. $[Cu(TBZH)(bda)]$ (5)

To a solution of thiabendazole (TBZH) (0.60 g, 3.00 mmol) in ethanol (50 cm^3) was added $[Cu(O_2C–CH_2CH_2–CO_2)]$ (0.50 g, 1.53 mmol) and the blue suspension was refluxed for 4 h. The resulting blue solid which deposited was filtered off, washed with water and ethanol, and then air-dried. Yield: 0.62 g (69%). Calc: C, 44.15; H, 2.91; N, 11.03. Found: C, 44.38; H, 2.85; N, 11.67%. IR (KBr): 3427, 3115, 2918, 2352, 1557, 1425,1409, 1285, 1228, 1187, 1015, 974, 941, 875, 834, 777, 637 cm^{-1}. μ_{eff}: 1.74 B.M. Solubility: insoluble in water, ethanol, methanol, acetone and trichloromethane.

2.2. X-ray crystallography

The two data sets were collected at 150°(2) K on a Bruker SMART 1000 diffractometer using Mo Kα radiation ($\lambda = 0.71073$ Å). Each was solved by direct methods and refined by full-matrix least-squares on F^2. All the non-hydrogen atoms were refined with anisotropic atomic displacement parameters and hydrogen atoms bonded to carbon were inserted at calculated positions using a riding model. In **1**, the hydrogen atoms bonded to nitrogen were located in the difference map but then inserted at calculated positions using a riding model. In **3**, the hydrogen atoms bonded to nitrogen were located from difference maps and not further refined; that bonded to the ethanol oxygen atom in **3** was treated in the same way. Hydrogen atoms bonded to water molecules were not included in the models. Details of the collection and refinement are given in Table 1 . All programmes used in the structure solution and refinement are contained in the SHELXTL package [25].

Table 1
Crystal data and structure refinement for 1 and 3

Compound	[TBZH$_2$NO$_3$] (1)	[Cu(TBZ)$_2$Cl]Cl · H$_2$O · EtOH (3)
Empirical formula	$C_{10}H_8N_4O_3S$	$C_{22}H_{22}Cl_2CuN_6O_2S_2$
Formula weight	264.26	601.02
Crystal system	Monoclinic	Monoclinic
Space group	$P2_1/n$	$P2/c$
a (Å)	4.8074(7)	16.2813(8)
b (Å)	13.812(2)	11.3482(6)
c (Å)	16.619(3)	15.6061(8)
β (°)	97.779(2)	118.075(1)
Volume (Å^3)	1093.4(3)	2544.1(2)
Z	4	4
Density (calc) (Mg/m^3)	1.605	1.569
Absorption coefficient (mm^{-1})	0.303	1.266
$F(000)$	544	1228
Crystal size (mm^3)	0.42 × 0.17 × 0.09	0.20 × 0.15 × 0.15
Crystal description	Yellow block	Green needle
θ range (°)	1.92–25.00	1.42–28.92
Index ranges	$-5 \leqslant h \leqslant 5$, $-16 \leqslant k \leqslant 15$, $-19 \leqslant l \leqslant 19$	$-21 \leqslant h \leqslant 22$, $-15 \leqslant k \leqslant 14$, $-20 \leqslant l \leqslant 20$
Reflections collected	7359	29,636
Independent reflections [R_{int}]	1926 [0.0275]	6164 [0.0484]
T_{max}, T_{min}	1.00000, 0.771000	0.928078, 0.762571
Data/restraints/parameters	1926/0/163	6164/0/316
Goodness-of-fit on F^2	1.060	1.013
Final R indices [$I > 2\sigma(I)$]	$R_1 = 0.0376$, $wR_2 = 0.0987$	$R_1 = 0.0484$, $wR_2 = 0.1321$
R indices (all data)	$R_1 = 0.0434$, $wR_2 = 0.1035$	$R_1 = 0.0820$, $wR_2 = 0.1534$
Largest difference peak and hole (e Å^{-3})	0.481 and −0.537	0.820 and −0.561

2.3. Anti-candida testing

Candida albicans isolate was obtained commercially from Oxid Culti-loops (ATCC 10241). The isolate was stored on Sabouraud dextrose agar (SDA) plates at 4 °C. Culture conditions and measurement of drug minimum inhibitory concentrations (MICs) were as previously described [11].

2.4. Cytotoxicity testing

Dimethyl sulphoxide (DMSO) and all cell culture reagents and media were purchased from Signa–Aldrich Ireland, Ltd, unless otherwise stated.

2.5. Cell lines and cell culture

Cytotoxicity assays were performed using two human model cell lines in order to assess the cancer chemotherapeutic potential of metal free TBZH and complexes **3** and **4** (the other complexes were not soluble in DMSO). The human malignant melanoma (melanocyte) skin cell line (SK-MEL-31) and squamous carcinoma tongue cell line (CAL-27) were purchased from the American Type Culture Collection, Manassas. SK-MEL-31 cells were grown as a monolayer in Eagle's minimum essential medium, supplemented with 2 mM L-glutamine and Earle's balanced salt solution, containing 1.5 g/L sodium bicarbonate, 0.1 mM non-essential amino acids, 1.0 mM sodium pyruvate, 100 U/ml penicillin and 100 μg/ml streptomycin supplemented to contain 15% (v/v) foetal bovine serum (Flow laboratories, Herts, UK). The CAL-27 cells were grown in Dulbecco's modified Eagle's medium, supplemented with 4 mM L-glutamine, containing 1.5 g/L sodium bicarbonate, 0.1 mM non-essential amino acids, 1.0 mM sodium pyruvate, 100 U/ml penicillin and 100 μg/ml streptomycin supplemented to contain 15% (v/v) foetal bovine serum. Both model cells were grown at 37 °C in a humidified atmosphere, in the presence of 5% CO_2 and were in the exponential phase of growth at the time of assay.

2.6. Assessment of cytotoxicity, using MTT assay

Test compounds were dissolved in DMSO, diluted in culture media and used to treat the two model cells over a drug concentration range 0.1–1000 μM for a period of 96 h. SK-MEL-31 and CAL-27 cells were seed at a density of 3.5×10^4 and 5×10^3 cells/well, respectively, into sterile 96 well flat-bottomed plates (Falcon Plastics, Decton Dickinson) and grown in 5% CO_2 at 37 °C. A miniaturised viability assay using 3-(4,5-dimethylthiazol-2-yl)-2,5-diphenyl tetrazolium bromide (MTT) was carried out according to the method described by Mosman [26]. The IC_{50} value was calculated for each drug and used as a means for comparing the toxicity of each of the derivatives tested. Consequently, IC_{50} was

defined as the drug concentration causing a 50% reduction in cellular viability. Each assay was carried out using five replicates and repeated on at least three separate occasions. Viability was calculated as a percentage of solvent treated control cells, and expressed as percentage of control. The significance of any reduction in cellular viability was determined using one-way ANOVA (analysis of variance). A probability of 0.05 or less was deemed statistically significant.

3. Results and discussion

3.1. Synthesis and characterisation of the compounds

Five inorganic derivatives of TBZH in which the ligand is protonated {$[TBZH_2NO_3]$ (**1**)}, deprotonated {$[Cu(TBZ)_2 \cdot (H_2O)_2]$ (**2**)} and neutral {$[Cu(TBZH)_2Cl]Cl \cdot H_2O \cdot EtOH$ (**3**), $[Cu(TBZH)_2(NO_3)_2]$ (**4**) and [Cu(TBZH)(bda)] (**5**)} were generated in moderate to good yield using the reactions shown in Scheme 1. The non-metal-based nitrate salt $[TBZH_2NO_3]$ (**1**) was the major product of a reaction between TBZH and $Fe(III)(NO_3)_3$. Attempts to generate this salt using a direct method involving nitric acid and TBZH have so far been unsuccessful and the mechanism of the formation of the salt is unknown. Hydrated Fe(III) salts are known to act as aqua acids, a fact which could explain the protonation of the TBZH molecule during this reaction. Failure to isolate any iron complex formed during the reaction may well be due to the fact that Fe(III) compounds are not particularly stable.

The formulation of the compounds was assigned on the basis of their elemental analysis, IR spectra and X-ray analysis (for **1** and **3**). In the respective IR spectra the majority of the ligand absorption bands, some of them with changed intensity, appear again in the compounds. In **1**, the N–H stretching band at 3093 cm^{-1} has shifted to 3084 cm^{-1} and has become more intense. Furthermore, the band associated to the imidazolic ν(C=N) at 1577 cm^{-1} in the free ligand has completely disappeared in the cationic $TBZH_2^+$ due to protonation on the benzimidazole imine nitrogen, resulting in delocalisation of the double bond over the N–C–N section. A strong absorption band at approximately 1385 cm^{-1} in the spectrum of **1** (which does not appear for the ligand) is characteristic of a nitrate group [27].

The anionic nature of the ligand in **2** is evident when its spectrum is compared to that of TBZH. The prominent bands at 3093 cm^{-1} (N–H stretching) and at 1093 cm^{-1} (N–H vibration) for the free ligand were absent in the spectrum of **2**. Also for **2**, the band associated to the imidazolic ν(C=N) at 1577 cm^{-1} in the free ligand has shifted to 1605 cm^{-1} due to deprotonation of the imidazolic nitrogen. In the spectra of complexes **3** and **4** the $\nu(C{=}N)_{imidazolic}$ and $\nu(C{=}N)_{thiazolic}$ bands (1577 and 1480 cm^{-1}, respectively) are shifted (to 1597 and 1513 cm^{-1} for **3**; 1593 and 1517 cm^{-1} for **4**) indicating that the ligand is coordinated through the imidazolic and the thiazolic nitrogens. The asymmetrical carboxylate stretching band precludes a similar assignment in the spectrum of **5**. For all four complexes **2**–**5** the C–S stretching band (at 1228 cm^{-1} for the free ligand) remains essentially unchanged suggesting that the sulphur atom in the thiazole ring is uncoordinated. New bands in the spectrum of **4** at approximately 1441 and 1289 cm^{-1} are assigned to an uncoordinated nitrate group whereas a new band at 1329 cm^{-1} is indicative of the presence of a coordinated nitrate. As well as the bands that have been assigned to chelating TBZH ligands the spectrum of **5** has bands that are characteristic of carboxylate anions {$\nu(OCO)_{assym}$ at 1557 cm^{-1} and $\nu(OCO)_{sym}$ at 1409}. The calculated Δ(OCO) value {$\nu(OCO)_{assym} - \nu(OCO)_{sym}$} of 148 cm^{-1} is typical for a carboxylate group bound to a metal in a chelating coordination mode [28]. Whereas the room temperature magnetic susceptibility values for **4** and **5** are close to those expected for simple copper(II) species (i.e., those lacking Cu–Cu interactions) the values for **2** and **3** are slightly lower and some form of antiferromagnetic interaction may be taking place in these complexes [29]. With the exception of the nitrate salt all of the complexes are effectively insoluble in common solvents. Complexes **3** and **4** were found to be soluble in DMSO.

Crystals suitable for X-ray analysis were isolated for compounds **1** and **3**. The structure of $[TBZH_2NO_3]$ (**1**) is shown in Figs. 2 and 3, and bond lengths and angles are

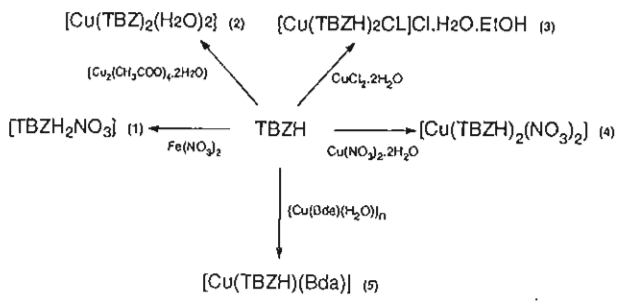

Scheme 1.

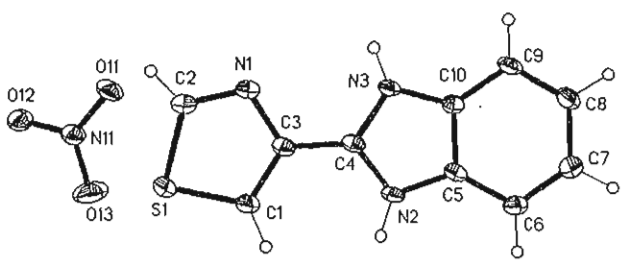

Fig. 2. The asymmetric unit of $[TBZH_2NO_3]$ (1).

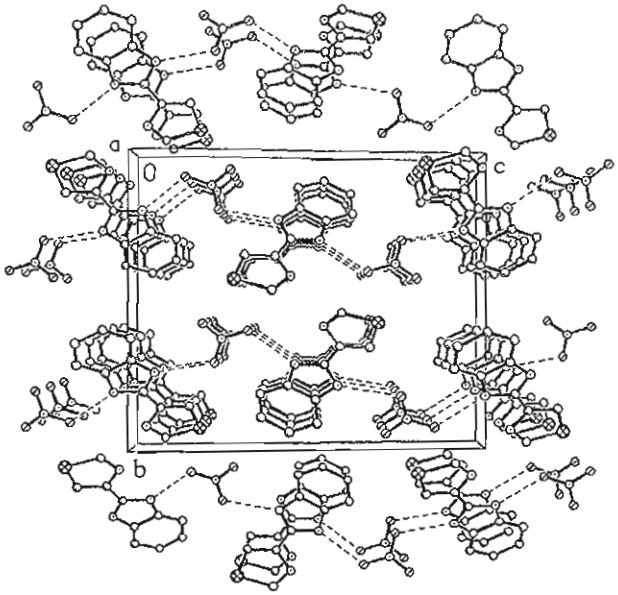

Fig. 3. A view of the π–π stacking in $[TBZH_2NO_3]$ (1).

listed in Table 2. The asymmetric unit contains one protonated $TBZH_2$ cation and one nitrate anion. The TBZH is protonated on the benzimidazole imine nitrogen, resulting in delocalisation of the double bond over the N–C–N section (Table 2). The cations are hydrogen bonded (Table 3) to nitrate anions via each of the NH groups, resulting in a chain along which adjacent $TBZH_2$ units are oriented at approximately right angles to each other. There is significant ππ-stacking between adjacent $TBZH_2$ cations with an interplanar distance ca. 3.3 Å.

The structure for $[Cu(TBZH)_2Cl]Cl \cdot H_2O \cdot EtOH$ (3) is shown in Figs. 4–6 and selected bond lengths and angles are listed in Table 4. The copper ion is five-coordinate, bound to two TBZH ligands via α-dümine units and to one chloride anion (Fig. 4). The geometry at copper is irregular but perhaps best described as trigonal bipyramidal with the benzimidazole nitrogen atoms N2 and N12 as apieal donors (N2–Cu–N12 171.9(1)°). The benzimidazole NH groups N1 and N11 are hydrogen bonded to Cl1 of a neighbouring cation and to Cl2, respectively (Table 5 and Fig. 5). The OH protons of the solvate water and ethanol molecules are also involved in hydrogen bonding (Fig. 4), resulting in a 3D network of hydrogen bonding extending through the lattice and supported by π–π-interactions (Fig. 6).

3.2. Biological activities

The nitrate salt of TBZH (1), all of the copper complexes {2–5 and $[Cu(O_2C–CH_2CH_2–CO_2)]$}, the free ligands and a selection of simple copper salts were each tested for their ability to inhibit the growth of *C. albicans*

Table 2
Bond lengths (Å) and angles (°) for $[TBZH_2NO_3]$ (1)

C(1)–C(3)	1.364(3)
C(1)–S(1)	1.698(2)
S(1)–C(2)	1.7209(19)
C(2)–N(1)	1.303(3)
N(1)–C(3)	1.379(2)
C(3)–C(4)	1.441(3)
C(4)–N(2)	1.338(2)
C(4)–N(3)	1.341(2)
N(2)–C(5)	1.385(3)
C(5)–C(6)	1.390(3)
C(5)–C(10)	1.398(3)
C(6)–C(7)	1.379(3)
C(7)–C(8)	1.407(3)
C(8)–C(9)	1.378(3)
C(9)–C(10)	1.389(3)
C(10)–N(3)	1.381(3)
N(11)–O(13)	1.235(2)
N(11)–O(11)	1.254(2)
N(11)–O(12)	1.258(2)
C(3)–C(1)–S(1)	110.24(15)
C(1)–S(1)–C(2)	89.13(10)
N(1)–C(2)–S(1)	115.73(15)
C(2)–N(1)–C(3)	109.33(16)
C(1)–C(3)–N(1)	115.57(18)
C(1)–C(3)–C(4)	124.90(18)
N(1)–C(3)–C(4)	119.53(16)
N(2)–C(4)–N(3)	109.24(17)
N(2)–C(4)–C(3)	125.10(17)
N(3)–C(4)–C(3)	125.66(17)
C(4)–N(2)–C(5)	108.96(15)
N(2)–C(5)–C(6)	131.75(17)
N(2)–C(5)–C(10)	106.31(17)
C(6)–C(5)–C(10)	121.94(18)
C(7)–C(6)–C(5)	116.20(18)
C(6)–C(7)–C(8)	121.90(19)
C(9)–C(8)–C(7)	121.87(19)
C(8)–C(9)–C(10)	116.41(18)
N(3)–C(10)–C(9)	131.64(17)
N(3)–C(10)–C(5)	106.68(16)
C(9)–C(10)–C(5)	121.68(18)
C(4)–N(3)–C(10)	108.80(16)
O(13)–N(11)–O(11)	120.53(17)
O(13)–N(11)–O(12)	119.37(16)
O(11)–N(11)–O(12)	120.09(16)

Table 3
Hydrogen bonds for $[TBZH_2NO_3]$ (1) (Å and °)

D–H···A	d(D–H)	d(H···A)	d(D···A)	∠(DHA)
N(2)–H(2A)···O(12)#1	0.88	1.91	2.785(2)	175.3
N(2)–H(2A)···O(13)#1	0.88	2.58	3.213(2)	129.7
N(3)–H(3)···O(11)#2	0.88	1.98	2.856(2)	170.9

Symmetry transformations used to generate equivalent atoms: #1 $-x+1/2, y+1/2, -z+3/2$ and #2 $-x, -y+1, -z+1$.

(Table 6). Butanedioic acid ($HO_2C–CH_2CH_2–CO_2H$) and the simple copper salts are essentially inactive against the pathogen. Furthermore, coordination of butanedioic acid to a copper center {$[Cu(O_2C–CH_2CH_2–CO_2)]$} does not result in any significant improvement in the activity

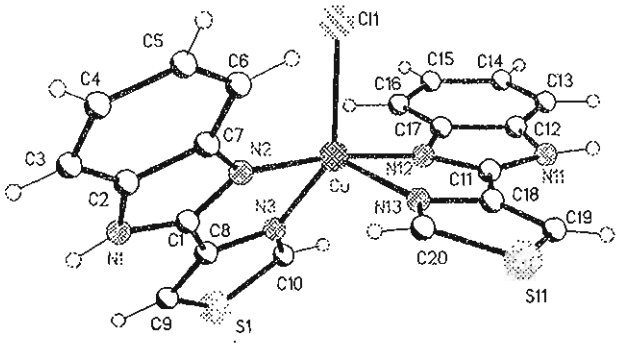

Fig. 4. The structure of the cation in $[Cu(TBZH)_2Cl]Cl \cdot H_2O \cdot EtOH$ (3).

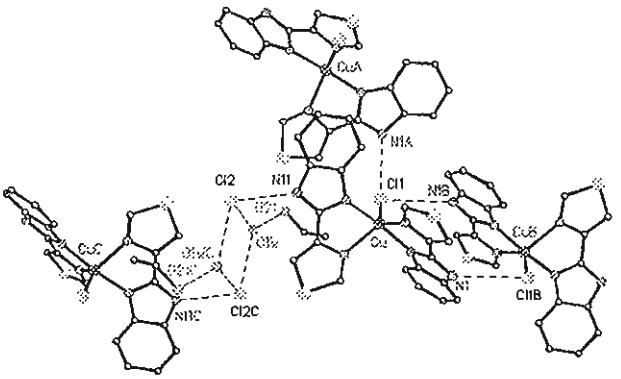

Fig. 5. Hydrogen bonding in $[Cu(TBZH)_2Cl]Cl \cdot H_2O \cdot EtOH$ (3).

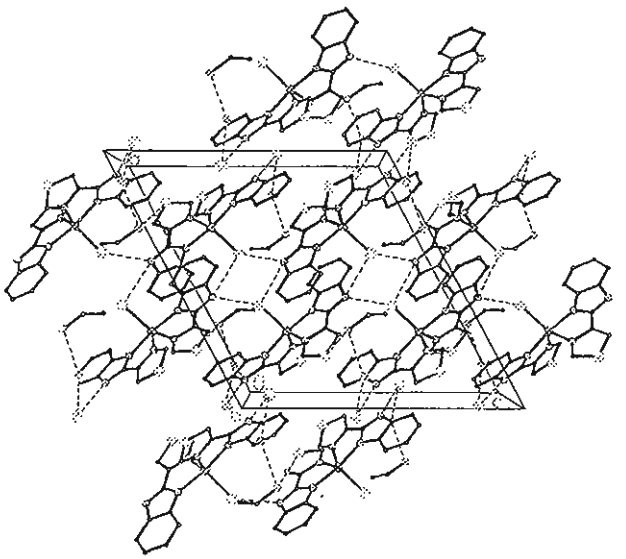

Fig. 6. The packing diagram in $[Cu(TBZH)_2Cl]Cl \cdot H_2O \cdot EtOH$ (3).

Table 4
Selected bond lengths (Å) and angles (°) for $[Cu(TBZ)_2Cl]Cl \cdot H_2O \cdot EtOH$ (3)

Cu–N(2)	1.972(3)
Cu–N(12)	1.975(3)
Cu–N(3)	2.076(3)
Cu–N(13)	2.153(3)
Cu–Cl(1)	2.3050(11)
N(2)–Cu–N(12)	171.91(13)
N(2)–Cu–N(3)	80.75(12)
N(12)–Cu–N(3)	95.98(12)
N(2)–Cu–N(13)	95.27(11)
N(12)–Cu–N(13)	79.98(11)
N(3)–Cu–N(13)	120.82(12)
N(2)–Cu–Cl(1)	95.22(9)
N(12)–Cu–Cl(1)	92.34(10)
N(3)–Cu–Cl(1)	134.35(9)
N(13)–Cu–Cl(1)	104.82(9)

Table 5
Hydrogen bonds for $[Cu(TBZ)_2Cl]Cl \cdot H_2O \cdot EtOH$ (3) (Å and °)

D–H···A	d(D–H)	d(H···A)	d(D···A)	∠(DHA)
N(1)–H(1)···Cl(1)#1	0.91	2.37	3.209(3)	152.2
N(11)–H(11)···Cl(2)#2	0.88	2.18	3.050(3)	168.3
O(21)–H(21)···O(1W)	0.88	1.89	2.732(7)	161.4
N(1)–H(1)···Cl(1)#5	0.91	2.77	3.398(3)	126.6
O1W···Cl2#3			3.187(5)	
O1W···Cl2#4			3.158(4)	

Symmetry transformations used to generate equivalent atoms: #1 $x, -y+1, z+1/2$, #2 $-x, -y, -z$, #3 $x, -y, z+1/2$, #4 $-x, y, -z+1/2$ and #5 $-x+1, -y+1, -z+1$.

Table 6
Anti-*candida* activity[a]

Test compound	% Cell growth
Control	100
Ketoconazole	20
1,10-Phenanthroline	15
$CuCl_2$	95
$CuNO_3$	98
Cu(OAc)2	94
$HO_2C–CH_2CH_2–CO_2H$	98
$[Cu(O_2C–CH_2CH_2–CO_2)]$	95
TBZH	76
$[TBZH_2NO_3]$ (1)	60
$[Cu(TBZ)_2(H_2O)_2]$ (2)	54
$[Cu(TBZH)_2Cl]Cl \cdot H_2O \cdot EtOH$ (3)	29
$[Cu(NO_3)_2(TBZH)_2]$ (4)	30
$[Cu(TBZH)(O_2C–CH_2CH_2–CO_2)]$ (5)	19

[a] The compounds were tested at concentrations of 10 μg/ml of aqueous RPMI medium. Complexes 2–5 were insoluble in water and were used as suspensions. Yeast cells were grown for 24 h at 37 °C. Results are presented as % cell growth and the effectiveness of the compounds are compared to the growth of the control (no drug added).

of the dicarboxylic acid. The metal free neutral TBZH is a very poor inhibitor of the growth of the pathogen. Compound **1** and complex **2** (in which the ligand is found in its cationic and anionic states, respectively) are both moderate anti-*candida* agents. Significantly when the neutral TBZH is coordinated to a copper center

(complexes 3–5) very potent anti-*candida* drugs are produced. Complex 5 exhibits the greatest fungitoxic activity and indeed is comparable to the prescription drug ketoconazole at this concentration. Preliminary studies on the mode of action of the copper TBZH complexes have revealed that they cause a reduction in the ergosterol content of the fungal cells [30] which was also found to be the case for the phenanthroline complexes previously reported [20].

The chemotherapeutic potential of TBZH and the DMSO soluble complexes 3 and 4 was determined by calculation of IC_{50}. Calculation of this value allows a direct comparison of the cytotoxicity of each of the test agents. The IC_{50} values were calculated using the data presented in Figs. 7 and 8. The values were obtained for each compound and in each cell line (Table 7). TBZH was capable of killing both cancer-derived cell lines only at higher concentrations with IC_{50} value of 453 and 677 μM (equivalent to 91.7 and 136.9 μg/ml), for the tongue and skin cell line, respectively. In the case of compounds 3 and 4, the IC_{50} values were very similar across the two human model cell lines. They had almost identical IC_{50} values of 55 and 54 μM (equivalent to 33.1 and 31.9 μg/ml), respectively, in the CAL-27 cell line and 50 and 47 μM (equivalent to 39.1 and 30.7 μg/ml), respectively in the SK-MEL-31 cell line. Although the activities of 3 and 4 do not fall within the accepted activity parameters adopted for in vitro screening (i.e., IC_{50} values not exceeding 4 μg/ml) [31] the results suggest the chemotherapeutic potential of TBZH is significantly enhanced upon coordination to a metal centre. Furthermore, the cytotoxic activity of all three compounds is concentration dependent for both cell lines (Figs. 7 and 8).

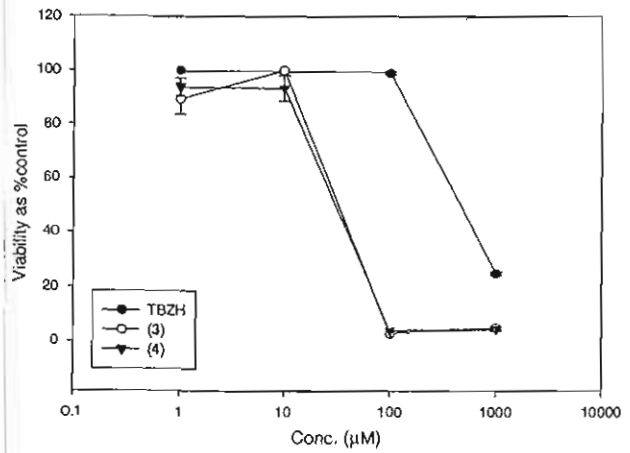

Fig. 7. Effects of TBZH, 3 and 4 on the viability of CAL-27 cells following continuous incubation with increasing drug concentration (0.1–1000 μM) for 96 h. Bars indicate standard error of the mean (SEM) and results were statistically significant from control at $p < 0.05$.

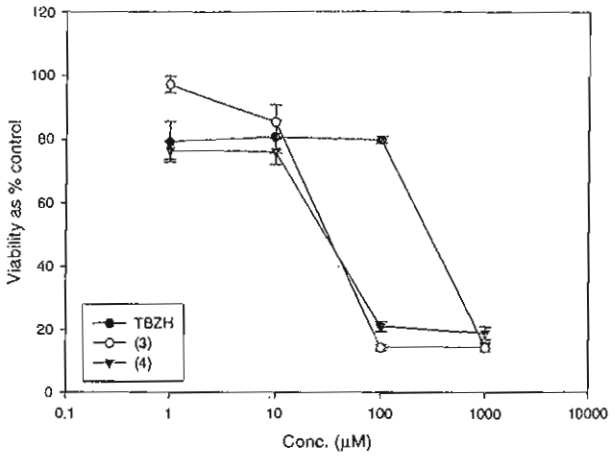

Fig. 8. Effects of TBZH, 3 and 4 on the viability of SK-MEL-31 cells following continuous incubation with increasing drug concentration (0.1–1000 μM) for 96 h. Bars indicate standard error of the mean (SEM) and results were statistically significant from control at $p < 0.05$.

Table 7
The chemotherapeutic potential of TBZH 3 and 4

Test compound	Toxicities (IC_{50}, μM)	
	CAL-27 (means ± SD)	SK-MEL-31 (means ± SD)
TBZH	676.7 ± 12.0	453.3 ± 66.0
$[Cu(TBZH)_2Cl]Cl \cdot H_2O \cdot EtOH$ (3)	55.0 ± 0.0	49.5 ± 7.7
$[Cu(NO_3)_2(TBZH)_2]$ (4)	54.0 ± 2.5	46.7 ± 5.0

Cancer chemotherapeutic potential of complexes 3 and 4 along with metal free TBZH in CAL-27 and SK-MEL-31, following continuous incubation for 96 h in the concentration range 0.1–1000 μM, using MTT assay. A graph of viability as % of solvent treated control verses drug concentration was used to calculate IC_{50} values (μM), (means ± SD; $n = 5$).

4. Conclusion

Neutral thiabendazole (TBZH) when uncoordinated to a metal centre is a poor anti-*Candida* agent and has very little chemotherapeutic potential. Protonation of TBZH to form the nitrate salt 1 and its deprotonation to yield the complex 2 results in only moderate improvement in its anti-*candida* activity. Complexes 3–5, in which the TBZH is present as a neutral chelating ligand, are all potent anti-*candida* agents with five possessing activity comparable to the prescription drug ketoconazole. Coordination of neutral TBZH to a copper centre in complexes 3 and 4 resulted in a significant increase in its chemotherapeutic potential.

5. Supplementary data

Crystallographic data have been deposited with the CCDC (12 Union Road, Cambridge, CB2 1EZ, UK)

and are available on request quoting the deposition numbers 219675 and 219676, respectively.

Acknowledgements

D.O.S. acknowledges the SRD and Seed funding schemes (DIT/EU) for financial support. This work has been carried out (in part) within the structures of the Facility for Optical Characterisation and Spectroscopy (FOCAS), funded by the Irish Government Programme for Research in Third Level Institutions. The authors also acknowledge funding received through the Irish Technological Sector Research Strand III programme 2002 (project No. CRS02-TA01).

References

[1] T.J. Walsh, J.W. Hiemenz, E. Anaissie, Infect. Dis. Clin. North Am. 29 (1996) 365–400.
[2] A.H. Groll, P.M. Shah, C. Mentzel, M. Schneider, G. Just-Neubling, G. Heubling, K. Huebner, J. Infect. 33 (1996) 23–32.
[3] G.Y. Minamoto, A.S. Rosenberg, Med. Clin. North Am. 81 (1997) 381–409.
[4] A.H. Groll, A.J. De lucca, T.J. Walsh, Trends Microbiol. 6 (1998) 117–124.
[5] M.E. Klepser, E.J. Ernst, M.A. Pfaller, Trends Microbiol. 5 (1997) 372–375.
[6] S. Wirsching, S. Michel, G. Kohler, J. Morschhauser, J. Bacteriol. 182 (2000) 400–404.
[7] G.P. Moran, D. Sanglard, S.M. Donnelly, D. Shanley, D.J. Sulivan, D.C. Colemen, Antimicrob. Agent Chemother. 42 (1998) 1819–1830.
[8] F.C. Odds, Int. J. Antimicrob. Agents 6 (1996) 145–147.
[9] See for example: M. Petric, F. Pohleven, I. Turel, P. Segedin, A. White, D. Williams, Polyhedron 17 (1998) 255–260.
[10] M. Geraghty, V. Sheridan, M. McCann, M. Devereux, V. McKee, Polyhedron 18 (1999) 2931–2939.
[11] M. Devereux, G.M. McCann, V. Leon, M. Geraghty, V. McKee Jan Wikaira, Polyhedron 19 (2000) 1205–1211.
[12] M. Geraghty, M. McCann, M. Devereux, F. Cronin, M. Curran, V. McKee, Metal Based Drugs 6 (1999) 41–48.
[13] M. Geraghty, M. McCann, M. Devereux, V. McKee, Inorg. Chim. Acta 293 (1999) 160–166.
[14] M. Geraghty, F. Cronin, M. Devereux, M. McCann, Biometals 13 (2000) 1–8.
[15] M. McCann, B. Coyle, J. Briody, F. Bass, N.O. Gorman, M. Devereux, K. Kavanagh, V. McKee, Polyhedron 22 (2003) 1595–1601.
[16] M. Devereux, M. McCann, V. Leon, R. Kelly, D.O. Shea, V. McKee, Polyhedron 22 (2003) 3187–3194.
[17] M. McCann, B. Coyle, S. McKay, P. McCormack, K. Kavanagh, M. Devereux, V. McKee, P. Kinsela, R.O. Gorman, M. Clynes, Biometals, manuscript No. R-2-10-2003, in press.
[18] M. McCann, M. Devereux, M. Geraghty, D.O. Shea, J. Mason, L.O. Sulivan, Metal Based Drugs 7 (2000) 185–193.
[19] I. Druta, R. Danuac, M. Ungureanu, G. Grosu, G. Drochioiu, Ann. Pharm. Fr. 60 (2002) 348–351.
[20] B. Coyle, K. Kavanagh, M. McCann, M. Devereux, M. Geraghty, Biometals 16 (2003) 321–329.
[21] B. Coyle, P. Kinsella, M. McCann, M. Devereux, R.O Connor, M. Clynes, K. Kavanagh, Toxicol. In Vitro 18 (2004) 63–70.
[22] N.S. Habib, S.M. Rida, E.A.M. Badawey, H.T.Y. Fahmy, H.A. Ghozlan, Pharmazie 52 (1997) 346–350.
[23] H.J. Robins, H.C. Stoerk, O.E. Graesle, Toxicol. Appl. Pharmacol. 7 (1965) 55–61.
[24] C. Tomlin (Ed.), The Pesticide Manual, 10th ed., Crop Protection Publications The Royal Society of Chemistry, 1994, pp. 972–973.
[25] G.M. Sheldrick, SHELXTL (V5.1), Bruker AXS, Madison, WI, 1998.
[26] T. Mosmann, J. Immunol. 65 (1983) 55–63.
[27] R. Nyquist, R. Kagel, Infrared Spectra of Inorganic Compounds, Academic Press Inc., 1971, pp. 113–147.
[28] G.B. Deacon, R.J. Philips, Coord. Chem. Rev. 33 (1980) 227–250.
[29] F.A. Cotton, G. Wilkinson (Eds.), Advanced Inorganic Chemistry, fifth ed., Wiley, New York, 1998, p. 768.
[30] M. Devereux, M. McCann, D.O Shea, P. Murray, K. Kavanagh, unpublished results.
[31] R.S. So, A.A. Adjei, J. Clin. Oncol. 17 (1999) 409–418.